Departament de Genètica i Microbiologia
Facultat de Biociències
Universitat Autònoma de Barcelona

# A comprehensive functional study of *Caenorhabditis elegans rsr-2* uncovers a new link between splicing and transcription

# L'estudi funcional complet del gen *rsr-2* de *Caenorhabditis elegans* revela un nou nexe entre *splicing* i transcripció

Memòria de tesi doctoral presentada per na

**Laura Fontrodona Montals**

per optar al Grau de Doctor

Treball realitzat sota la direcció del Dr. Julián Cerón Madrigal a la Unitat de Genètica Molecular de l'Institut d'Investigació Biomèdica de Bellvitge (IDIBELL)

Barcelona, 2012

| Julián Cerón Madrigal<br>(Director) | Antonio Barbadilla Prados<br>(Tutor) | Laura Fontrodona Montals<br>(Doctoranda) |
|---|---|---|

IDIBELL
Institut d'Investigació Biomèdica de Bellvitge

UAB
Universitat Autònoma de Barcelona

A qui sempre em guardava els retalls de ciència del diari.
A qui més trobo a faltar en aquest món.
Al meu avi.

# Table of contents

**Figure index** ______ v

**Table index** ______ xiii

**Abbreviations and acronyms index** ______ ix

**Introduction** ______ 1

**I.1. *Caenorhabditis elegans* as a model organism** ______ **3**

I.1.1. Silencing gene expression in *C. elegans*: the RNA-mediated interference method ______ 5

I.1.1.1. RNA interference by feeding ______ 5

I.1.1.2. RNA interference by injection ______ 6

**I.2. The germ line** ______ **6**

I.2.1. Gonadogenesis and germ line proliferation ______ 6

I.2.2. The germ line sex determination pathway ______ 8

I.2.1.1. *mog* genes ______ 9

**I.3. Novel roles for a subset of splicing components in *lin-35* Rb-controlled processes** ______ **11**

I.3.1. *rsr-2* genetically interacts with *lin-35* Retinoblastoma ______ 11

I.3.2. *rsr-2* is a synMuv B gene ______ 12

**I.4. Pre-mRNA splicing** ______ **14**

**I.5. *rsr-2* through evolution** ______ **16**

I.5.1. *rsr-2* is a member of the SR-like proteins subfamily ______ 16

I.5.2. *rsr-2* is orthologous to the yeast Cwc21 and the human SRm300/SRMM2 splicing factors ______ 17

I.5.2.1. The human SRm300/SRRM2: a co-activator of splicing ______ 18

I.5.2.2. Cwc21, the *rsr-2* yeast ortholog, has been proposed to function at the catalytic core of the spliceosome ______ 19

**I.6. Shades and lights of co-transcriptional splicing** ______ **22**

**Aims** ______________________________________________ **25**

**Results** ____________________________________________ **29**

**R.1. *rsr-2* is an essential gene for the development of *C. elegans*** _________________ **31**

R.1.1. Deletion mutants in *rsr-2* ____________________________________________ 31

R.1.2. *rsr-2(tm2625)* mutants show defects in intestinal cell differentiation___________ 33

**R.2. *rsr-2* regulates the germ line sex determination** ____________________________ **34**

R.2.1. *rsr-2(RNAi)* animals develop masculinized germ lines _______________________ 34

R.2.2. *rsr-2* cooperates with *fbf* genes and *nos-3* to control the sperm/oocyte switch___ 36

R.2.3. *rsr-2* is necessary for *fem-3* 3'UTR-mediated repression in somatic cells ________ 39

**R.3. *rsr-2* RNAi does not affect constitutive splicing in intestinal cells** ______________ **41**

**R.4. The mitosis/meiosis switch is not affected in *rsr-2(RNAi)* animals**______________ **42**

**R.5. RSR-2 is ubiquitously expressed in somatic cells but presents a restricted pattern in the germ line**___________________________________ **44**

**R.6. *rsr-2*(*RNAi*) animals have a global decrease in transcript levels but the splicing mechanism seems not to be affected**_____________________ **48**

R.6.1. Tiling arrays reveal a general decrease in transcript levels of *rsr-2(RNAi)* L4 animals 48

R.6.2. Germ line and spermatogenesis genes are enriched among downregulated genes in *rsr-2(RNAi)* worms _______________________ 49

R.6.3. Germ line sex determination genes do not present aberrant splicing isoforms in *rsr-2(RNAi)* worms _________________________________ 52

**R.7. *rsr-2(tm2625)* arrested larvae do not show an altered pattern of alternative splicing** _____________________________________________ **53**

**R.8. Functional links between RSR-2 and transcription** __________________________ **55**

R.8.1. Specificity of a novel antibody against RSR-2 ______________________________ 55

R.8.2. RSR-2 location is nuclear ______________________________________________ 56

R.8.3. ChIP-seq experiments reveal that RSR-2 co-immunoprecipitates with chromatin similarly to RNA polymerase II__________________________ 59

R.8.3.1. Anti-RSR-2 immunoprecipitates chromatin _______________________ 60

R.8.3.2 RSR-2 presents a chromatin-binding pattern similar to the RNAP II _____ 60

R.8.4. RSR-2 regulates RNA polymerase II distribution along genes__________________ 62

R.8.5. Hyperphosphorylated RNAP II accumulates in *rsr-2(RNAi)* worms _____________ 63

R.8.6. RSR-2 is splicing-independently recruited to transcriptionally active genes 64

**R.9. Transcriptome analysis exposes a functional link between *rsr-2* and *prp-8* 67**

R.9.1. Common targets of RSR-2 and PRP-8 67

R.9.2. *rsr-2(RNAi)* animals do not accumulate introns 70

**Discussion 73**

**D.1. *rsr-2* and germ line development 75**

D.1.1. *rsr-2*-mediated regulation of sex determination 75

D.1.2. *rsr-2* & *mogs*: find the 4 differences 77

**D.2. *rsr-2* expression pattern 79**

**D.3. Tools to study transcriptomes 81**

**D.4. RSR-2 is not a protagonist within the spliceosome, just a team player 82**

**D.5. RSR-2, a novel link between transcription and splicing 83**

**D.6. How is *rsr-2* regulated? 86**

D.6.1. *rsr-2* and *lin-35* Rb 86

D.6.2. *rsr-2* is the first gene of the operon CEOP2720 87

**D.7. Our model: RSR-2 is a multitask protein that regulates development through transcription and splicing 89**

**Conclusions 92**

**Materials & methods 96**

**MM.1. Strains and general methods 98**

**MM.2. RNA-mediated interference (RNAi) 100**

MM.2.1. By feeding 100

MM.2.2. By microinjection 100

**MM.3. Sodium hypochlorite treatment 102**

**MM.4. Semiquantitative RT-PCR 103**

**MM.5. Dissection of gonads** 105

**MM.6. *In situ* hybridization of mRNA** 106

**MM.7. Immunostaining** 107
MM.7.1. Of dissected gonads 107
MM.7.2. Of larvae (Freeze–cracking protocol) 107

**MM.8. Generation of DNA constructs** 109
MM.8.1. PCR-fusion approach 109
MM.8.2. Gateway Three-fragment Cloning System 109

**MM.9. Generation of GFP reporters and transgenic animals** 113
MM.9.1. Complex arrays 113
MM.9.2. DNA transformation by gene bombardment 113

**MM.10. β-galactosidase reporter assays** 115

**MM.11. Genomic tiling microarrays** 116

**MM.12. Quantitative PCR (qPCR)** 117

**MM.13. Protein extraction and analysis** 119

**MM.14. Chromatin Immunoprecipitation - Sequencing (ChIP-Seq)** 121

**MM.15. Transcriptome sequencing (RNA-Seq)** 124

**MM.16. Computational tools** 125

**References** 126

**Annex** 139
**Article 1** 141
**Article 2** 153

# Figure Index

## Introduction

Figure I.1. Life cycle of *C. elegans* at 22°C______________________________________ 4

Figure I.2. Protocols for performing RNAi in *C. elegans* ___________________________ 5

Figure I.3. Scheme of the germ line generation process through *C. elegans* development 7

Figure I.4. Genetic regulatory network of the sex determination pathway in the germ line 9

Figure I.5. Color code representation of the strenght of RNAi phenotypes
of candidate genes in different genetic backgrounds ____________________ 11

Figure I.6. Inactivation of *rsr-2* resembles the extra intestinal cell phenotype
of synMuv B genes ________________________________________________ 12

Figure I.7. Novel roles of specific spliceosome components in the synMuv B pathway __ 13

Figure I.8. Schematic diagram showing the assembly and recycling
of the spliceosome components ____________________________________ 15

Figure I.9. Schematic representation of 2 different types of SR proteins______________ 16

Figure I.10. Schematic representation of RSR-2 _________________________________ 16

Figure I.11. Phylogenetic tree of RSR-2 and its orthologs___________________________ 17

Figure I.12. Multiple alignments of sequences homologous to the N-terminal
150 aminoacid of RSR-2____________________________________________ 18

Figure I.13. Splicing coactivator model for the function of SRm160/300______________ 19

Figure I.14. Deletion strains of Cwc21 and Isy1 do not present aberrant
splicing in *S. Cerevisiae* ______________________________________________ 21

Figure I.15. Prp8 contains an intramolecular fold that can be cross-linked
to the conserved cwf21 domain in Cwc21 _____________________________ 21

Figure I.16. Positioned nucleosomes obstruct RNA polymerase II transcription
elongation across internal exons_____________________________________ 23

Figure I.17. Proposed model for the network of splicing regulatory interactions _______ 24

## Results

Figure R.1. Scale scheme of *rsr-2* gene ________________________________________ 31

Figure R.2. Genomic context of *rsr-2* alelles ____________________________________ 31

Figure R.3. *rsr-2(tm2625)/mIn1* animals segregate a mixed population of
heterozygous and homozygous animals that can be distinguished _________ 32

Figure R.4. *rsr-2(tm2625)* homozygous worms arrest at early larval stage ____________ 33

Figure R.5. *rsr-2(tm2625)* homozygous animals show defects in intestinal
cell differentiation ________________________________________________ 33

Figure R.6. *rsr-2(RNAi)* animals are Mog ________________________________________ 35

Figure R.7. Microinjection of *rsr-2* dsRNA produces Mog animals ____________________ 36

Figure R.8. *rsr-2* is downstream of *gld-3* in the germ line sex determination pathway ___ 37

Figure R.9. *rsr-2* is upstream of *fog-1* in the germ line sex determination pathway _____ 37

Figure R.10. *fem-3* expression is translationally repressed by *rsr-2* in intestinal cells ____ 39

Figure R.11. Schematics of the transgene expressed in BL3466______________________ 41

Figure R.12. Constitutive splicing is not affected in BL3466 reporter animals upon *rsr-2* RNAi ________________________________________________ 41

Figure R.13. Mitosis-to-meiosis switch and meiotic progression in *rsr-2(RNAi)* animals __ 42

Figure R.14. *rsr-2* expression in the soma _______________________________________ 45

Figure R.15. *rsr-2* is broadly expressed in somatic tissues __________________________ 45

Figure R.16. *rsr-2* expression in the germ line____________________________________ 46

Figure R.17. RSR-2::GFP forms nuclear speckles__________________________________ 47

Figure R.18. Gene expression changes in *rsr-2(RNAi)* animals _______________________ 49

Figure R.19. Changes in mRNA levels of several sex determination genes after *rsr-2* RNAi assayed by qRT-PCR _____________________________________ 51

Figure R.20. A subset of germ line related genes are being correctely spliced upon reduction of *rsr-2* expresion levels________________________________ 52

Figure R.21. *rsr-2(tm2625)* homozygotes do not present AS altered patterns __________ 53

Figure R.22. Semiquantitative RT-PCR of regulated AS events across L1, L2, L3, L4 and adult stages _______________________________________ 53

Figure R.23. RSR-2 protein sequence ____________________________________________ 55

Figure R.24. Detection of protein levels in L4440*(RNAi)* and *rsr-2(RNAi)* animals ________ 56

Figure R.25. RSR-2 expression is low in mitotic cells and absent in sperm cells__________ 56

Figure R.26. RSR-2 in not detected by Ab Q5092 in *rsr-2(tm2625)/mIn1; rsr-2(RNAi)* gonads _______________________________ 57

Figure R.27. RSR-2 co-localizes with chromatin in germ cells________________________ 57

Figure R.28. RSR-2 is not expressed in homozygous *tm2625* arrested larvae in contrast to the expression detected in heterozygous *tm2625* larvae _______ 58

Figure R.29. RSR-2 overlaps with chromatin in intestinal nuclei of adult worms_________ 58

Figure R.30. ChIP-seq workflow_________________________________________________ 59

Figure R.31. Chromatin used to generate the four barcoded Illumina multiplexed libraries 60

Figure R.32. Chromatin-binding profiles of RNAP II and RSR-2 are similar______________ 60

Figure R.33. RSR-2 and RNAP II are similarly enriched at TSS________________________ 61

Figure R.34. Distribution of RNAP II and RSR-2 along an averaged gene _______________ 62

Figure R.35. RNAP II accumulates at the genes 5′ regions upon RNA interference of *rsr-2* 62

Figure R.36. Hyperphosphorylated RNAP II accumulates in *rsr-2(RNAi)* worms _________ 63

Figure R.37. $\alpha$-RSR-2 IP chromatin of intronless genes______________________________ 64

Figure R.38. Chromatin-binding profiles of RNAP II and RSR-2, and RNA-seq reads for the set of intronless genes chosen for ChIP-seq validation ____________ 65

Figure R.39. RNAP II and RSR-2 ChIP peaks locate at promoters and CDS of intronless genes ____________ 66

Figure R.40. Differential gene expression analysis in *rsr-2(RNAi)* and *prp-8(RNAi)* animals 67

Figure R.41. *rsr-2* and *prp-8* share target genes ____________ 68

Figure R.42. Several common downregulated genes in *rsr-2* and *prp-8(RNAi)* worms are genes highly expressed at L3 stage ____________ 68

Figure R.43. A subset of L3 highly expressed genes are correctly spliced upon reduction of *rsr-2* expression levels ____________ 69

Figure R.44. Differential intron expression analysis of *rsr-2(RNAi)* versus control *gfp(RNAi)* 70

Figure R.45. Differential intron expression of *prp-8(RNAi)* versus control *gfp(RNAi)* ____ 70

Figure R.46. *rsr-2(RNAi)* animals do not retain introns____________ 71

## Discussion

Figure D.1. Proposed model for *rsr-2* in controlling the sperm-to-oocyte switch in *C. elegans* ____________ 76

Figure D.2. *rsr-2* mRNA distribution in the germ line presents a region-specific pattern where levels are lower at mitotic cells than at the rest of the germ line cells_ 79

Figure D.3. *prp-8* and F53B7.3*(RNAi)* worms display Mog phenotypes ____________ 82

Figure D.4. Changes in *rsr-2* mRNA accumulation in *lin-35(n745)* mutants ____________ 86

Figure D.5. *rsr-2* is predicted as the first gene of the operon CEOP2720____________ 88

Figure D.6. Proposed model for RSR-2 molecular functions____________ 91

## Materials & Methods

Figure MM.1. Generating a reporter transgene by PCR fusion ____________ 110

Figure MM.2. Schematics of the Three-fragment Gateway Cloning System ____________ 112

Figure MM.3. Schematic representation of the probe distribution in different array types 117

# Table Index

## Introduction

Table I.1. Orthologs of *C. elegans mog* genes in yeast and human and their known roles in splicing 10

Table I.2. Proteins detected by mass spectrometry of TAP-tagged affinity-purified Cwc21 complexes 20

## Results

Table R.1. Temperature-dependent phenotypes in *rsr-2(RNAi)* animals 35

Table R.2. Sperm-to-oocyte switch defects in *rsr-2(RNAi)* animals 38

Table R.3. β-galactosidase activity scoring in lacZ transgene reporters 40

Table R.4. Transgenes and transformation methods used to study the expression and distribution of *rsr-2* 44

Table R.5. Gene expression group analysis in *rsr-2(RNAi)* animals 50

Table R.6. Germ line gene expression in L4 *rsr-2(RNAi)* animals versus the control *gfp(RNAi)* animals 51

Table R.7. Percentage of differential intron expression in *rsr-2* and *prp-8(RNAi)* animals versus the control *gfp(RNAi)* 71

## Discussion

Table D.1. *mog* mutants in *C. elegans* do not show significant splicing defects 78

## Materials & Methods

Table MM.1. Mutant and transgenic strains used during the development of this study and some of their characteristics 99

Table MM.2. Antibodies and dilutions used in immunostainings of this study 109

Table MM.3. List of plasmids used to generate *rsr-2* reporter constructs 113

Table MM.4. List of plasmids generated in our lab to study *rsr-2* expression *in vivo* in *C. elegans* 113

Table MM.5. Antibodies and dilutions used in western blots of this study 120

# Abbreviations and acronyms Index

**Ab:** Antibody
**AS:** Alternative Splicing
**CDS:** Coding DNA Sequence
**ChIP-Seq:** Chromatin Immunoprecipitation-sequencing
**CTD:** RNA polymerase II large subunit Carboxy-terminal Domain
**C-ter:** Carboxy-terminal
**DAPI:** 4',6-diamidino-2-phenylindole
**DIC:** Differential Interference Contrast
**Dpy:** Dumpy phenotype
**dsRNA:** double stranded RNA
**Emo:** Endomitotic oocytes phenotype
**F1:** First generation
**Fem:** Feminization of germ line phenotype
**FBF:** *fem-3* Binding Factors
**GFP:** Green Fluorescent Protein
**H2B:** Histone 2B
**H3:** Histone 3
**IgG:** Immunoglobulin G
**IP:** Immunoprecipitation
**IPTG:** Isopropyl β-D-1-thiogalactopyranoside
**L1-L4:** Larval stages from 1 to 4
**Lva:** Larval arrest phenotype
**modENCODE:** model organisms Encyclopedia of DNA Elements
**Mog:** Masculinization of germ line phenotype
**mRNA:** messenger RNA
**ncRNA:** non-coding RNA
**NBP:** National Bioresource Project for the Experimental Animal Nematode *C. elegans*
**NMD:** Nonsense Mediated Decay
**NTC:** NineTeen Complex
**N-ter:** Amino-terminal
**Oo:** Oocytes
**ORF:** Open Reading Frame
**$P_0$:** Parental generation
**POL $II_0$:** active hyperphosphorylated form of RNAP II
**POL $II_a$:** hypophosphorylated form of RNAP II
**PTC:** Premature Termination Codon
**PUF:** Pumilio and FBF
**qRT-PCR:** quantitative Real Time-Polymerase Chain Reaction
**Rb:** Retinoblastoma
**RISC:** RNA-induced Silencing Complex
**RNAi:** RNA-mediated interference
**RNAP II or POL-II:** RNA polymerase II
**RNA-seq:** Transcriptome sequencing
**RRM:** RNA Recognition Motif
**rRNA:** ribosomal RNA
**RT-PCR:** Reverse Transcriptase-Polymerase Chain Reaction
**SGA:** Synthetic Genetic Array

**siRNA:** small interfering RNA
**snRNP:** small nuclear Ribonucleoprotein
**Sp:** Sperm
**sqRT-PCR:** semiquantitative Reverse Transcriptase-Polymerase Chain Reaction
**SR or RS:** Serine and Arginine-rich domains
**SRm160:** SR-related nuclear matrix protein of 160 kDa
**SRm300:** SR-related matrix antigen of 300 kDa
**ss:** splice site
**SynMuv:** Synthetic Multivulva
**TAP:** Tandem Affinity Purification
**TAS:** Tiling Analyses Software (Affymetrix)
**TMP/UV:** Trimethyl Psoralen/Ultraviolet
**ts:** temperature sensitive
**TSS:** Transcription Start Site
**UTR:** Untranslated Region
**WT:** Wild Type
**X-gal:** 5-bromo-4-chloro-indolyl-β-D-galactopyranoside
**YA:** Young Adult

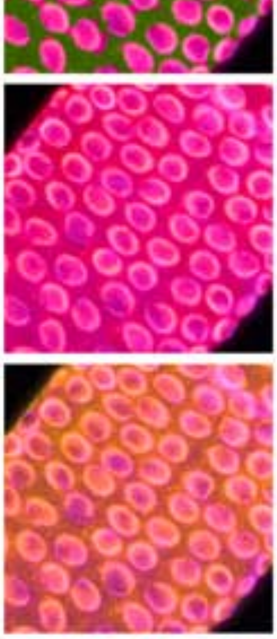

# Introduction

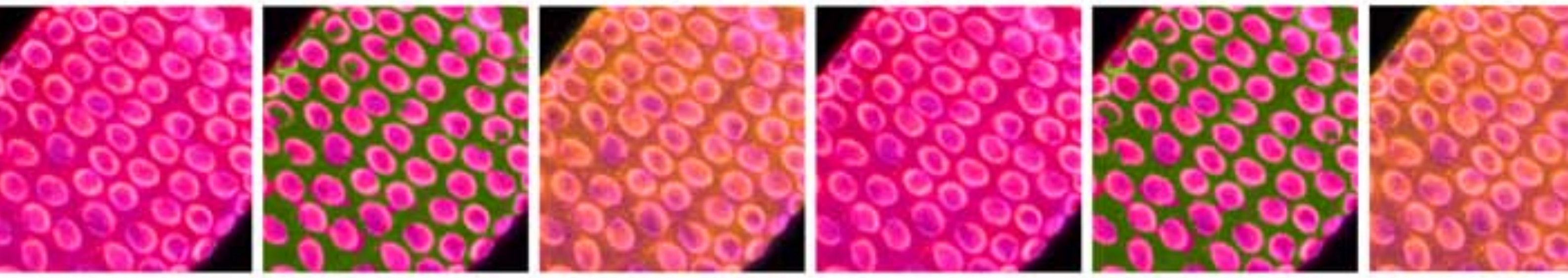

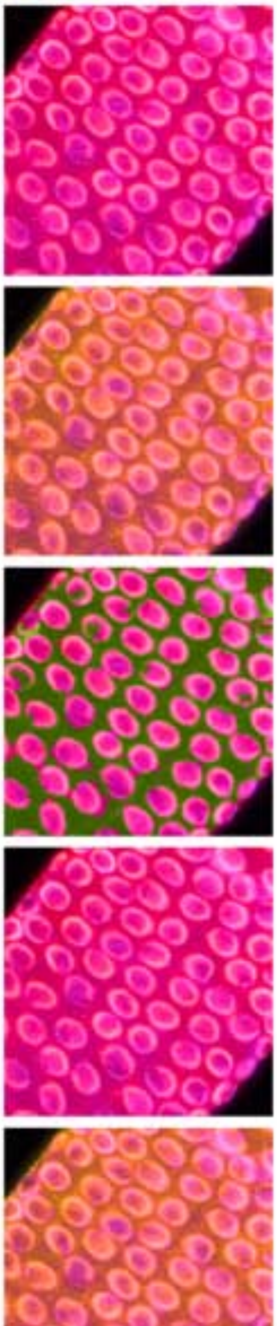

" La chispa adecuada"
Héroes del Silencio

# I.1. *Caenorhabditis elegans* as a model organism

*Caenorhabditis elegans* is a small nematode, which lives in the soil and feeds on microorganisms. This specie was first used in research by Sydney Brenner, who wrote the first manuscript about the genetics of *C. elegans* (Brenner, 1974). In 2002, Brenner shared the Nobel Prize of Physiology and Medicine with H. Robert Horvitz and John E. Sulston in recognition of their studies about genetic regulation of developmental processes and apoptosis in this animal model.

*Caenorhabditis elegans* is a powerful model for research in many fields including genomics, cell biology, aging and neuroscience. Among the features that make *C.elegans* an important tool for biological research these are the most relevant ones:

- It has a short life cycle.

  *C. elegans* has two sexes: self-fertilizing hermaphrodites (XX) and males (XO). Individuals are almost all hermaphrodites and males appear just in a 0.1% of the total progeny of an hermaphrodite. The *C. elegans* life cycle consists in an embryonic stage, followed by four larval stages (from L1 to L4) and adulthood (Figure I.1.). In the lab worms are cultured between 15 and 25°C and the duration of their life cycle is temperature-dependent. For instance, 4 days and a half are needed to complete the cycle at 15°C and only 2 days at 25°C.

- It is easy to maintain.

  Strains are cheap and can be kept as frozen stocks for a long-term storage. When thawed, most of the worms frozen as starving L1 are viable.

- It is a transparent animal.

  Body parts can be studied at cellular level in living worms by differential interference contrast (DIC) microscopy.

- The easiness of generating mutations in *C. elegans* together with its hermaphrodite self-fertilization mode of reproduction emerges this animal as a convenient tool for genetic analysis.

  *C. elegans* is a diploid animal what implies that detrimental mutations can be induced and propagated without killing the animal. Moreover, the effect of

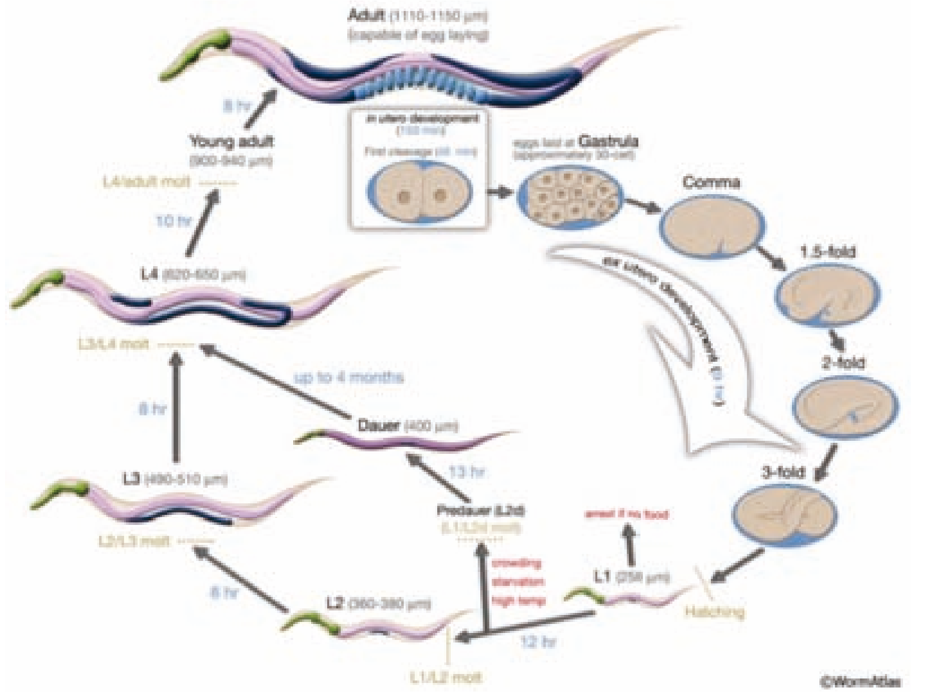
Adult (1110-1150 µm)
(capable of egg laying)
8 hr
Young adult
(900-940 µm)
L4/adult molt
10 hr
L4 (620-650 µm)
L3/L4 molt
8 hr
up to 4 months
Dauer (400 µm)
L3 (490-510 µm)
L2/L3 molt
8 hr
13 hr
Predauer (L2d)
(L1/L2d molt)
crowding
starvation
high temp
arrest if no food
L1 (250 µm)
L2 (360-380 µm)
12 hr
L1/L2 molt
Hatching
in utero development
(150 min)
First cleavage (40 min)
eggs laid at Gastrula
(approximately 30-cell)
Comma
1.5-fold
2-fold
3-fold
ex utero development (9 hr)
©WormAtlas

ui t c 3 u F s 1 F . I TT° J m e ht n w, 4z. . . ). t hn v c) h3 E) 5 h se sc 2 hvlsu vst e) i l e3vi t 2vi esn l v i cv3 sc T, h cc 1 se n s ht n v hc) f n hc lt e3vi ht . c e1s v vi 1f h vst e t 2 i tv 3 )

n f v vst ec se i t n t up3t csvp e 1sh v lp cvf 1s 1 se vi t 22c, hse3 t 2 i v h up3t f c c l2M hvlsu 1 n t vi h 2t llt . se3 h e1 ls e c 3h 3 vst e t 2vi n f v vst e) e 11svst e9 h l h vse3 t 22 hc h t h g hc vsvp se vi sct l vst e e1 n sev e e t 2n f v ev tvh sec c ll c se h nse3 e . t e c)

e 7 be i g n f v vst ec e 22s s evlp 3 e h v 1 p f cse3 i n s l n f v 3 ec e1 t esuse3 h 1s vst e n t e3 t vi hc t h3 ec e1 e3t 9W55W)

- 7 be i g, h c evc e eg hs l llf l h se 3 )

    i 1 g lt , n ev l 2v t 2 g hp cse3l ct n vs llJ“8“ 2t h hn , i ht 1sv c e1 C5DC 2t h h l cE c e cv lsci 1 e1 vi se 3 c t 2vi c llc h seg hs ev n t e3 e1sgs1f lc h ee h C“’ qE)

- vc 3 et n sc t n , v)

    7 be i g . c vi 2shcv n f lvs llf l h t h3 escn vt 2f llp c wf e 1 J 7 be i g wf e se3 t ect hvsf n 9C““/E) vc 3 et n t n , hsc c n t h vi e W5555 , ht v se M t 1se3 3 e c e1 n t h vi e C6555 3 e c se vt v l t 2 C55 J t hn c l c WDC9 hf hp W5CW9 e1 vi sc t n , ve cc , hn svc e 1g e 1 eet v vst e t 2vi t hn Oc3 et n t wf e t n , h 1 vt t vi h f n hpt vs 3 et n c)

- The disruption of the function of a specific gene by RNA-mediated interference (RNAi) is a straightforward tecnique in *C. elegans*.

  RNAi is a technique used to study the phenotypic effects of knocking down the expression of a gene. RNAi produces a mRNA sequence-specific degradation thus, providing information to infer the function of the gene of interest. To perform RNAi, worms can be fed on genetically transformed bacteria expressing the double stranded RNA (dsRNA) of interest. Alternatively, worms can be soaked in or injected with a solution containing the dsRNA (Figure I.2.).

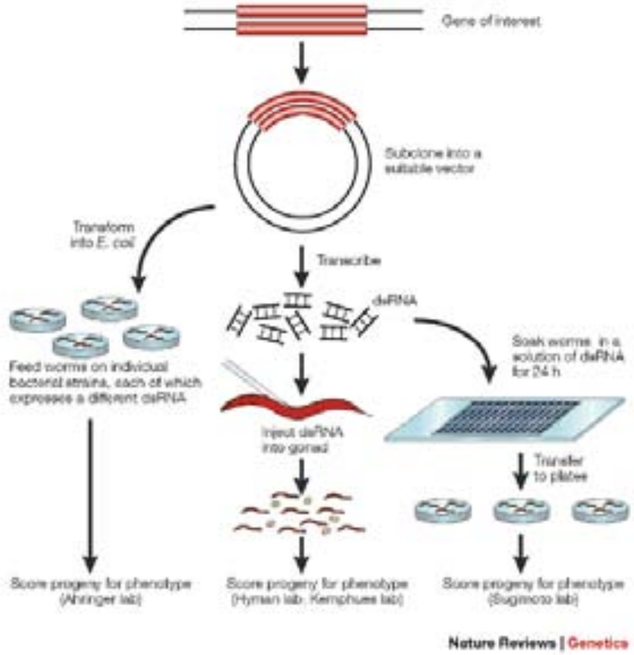
Gene of interest
Subclone into a suitable vector
Transform into E. coli
Transcribe
dsRNA
Feed worms on individual bacterial strains, each of which expresses a different dsRNA
Soak worms in a solution of dsRNA for 24 h
Inject dsRNA into gonad
Transfer to plates
Score progeny for phenotype (Ahringer lab)
Score progeny for phenotype (Hyman lab, Kemphues lab)
Score progeny for phenotype (Sugimoto lab)
Nature Reviews | Genetics

**Figure I.2. Protocols for performing RNAi in *C. elegans*.** Left, RNAi by feeding; middle, RNAi by injection; right, RNAi by soaking (Taken from Kim, 2001).

### I.1.1. Silencing gene expression in *C. elegans*: the RNA-mediated interference method

Eventhough natural RNAi targets include double stranded RNA from “parasitic genes” like viruses and transposons, the RNAi molecular machinery has also an important role in directing development as well as gene expression.

In 2006, the *C. elegans* researchers Andrew Fire and Craig Mello were awarded with the Nobel Prize of Physiology and Medicine for discovering that introduction of double stranded RNA in the worm resulted in a specific and dramatic knockdown of the corresponding endogenous RNA sequence (Fire, 1998). Remarkably, this silencing effect is not only efficient in the parental generation but also can be heritable.

Briefly, introduced dsRNA is recognized by the enzymatic Dicer-RDE complex which cleaves the dsRNA molecules into small 21-23 bp RNA fragments known as small interfering RNAs (siRNAs).

The multiple siRNA molecules will trigger the target messenger RNA (mRNA) degradation. The siRNA-Dicer complex then joins the RNA-induced silencing complex (RISC) so that the siRNA molecules can base-pair with the complementary endogenous mRNA and eventually the target is degradated into small fragments not translatable to protein.

As mentioned above, there are three methods to carry out RNAi in *C.elegans*: feeding, soaking and injection (Figure I.2).

### I.1.1.1. RNA interference by feeding

There are two RNAi feeding libraries in *C. elegans* that together cover more that 94% of the worm genome (Ahringer, 2006).

- Julie Ahringer's group developed an RNAi library (Timmons and Fire, 1998) by using PCR-amplified genomic DNA fragments as a template. Gene-specific genomic DNA fragments were cloned into the EcoRV site of vector L4440 (between two T7 inverted promoters which are inducible by IPTG) and transformed into bacterial strain HT115 (Fraser et al., 2000). This strain bears a transposon into the RNAse III gene (also named dsRNAase), which abrogates its function allowing massive dsRNA accumulation into the cell. The whole library comprises 16757 clones.
- Marc Vidal and collaborators have generated another library. In this case, the PCR template was cDNA, so this library targets expressed genes only (Rual et al., 2004). The "ORFeome" library clones have been produced by using the Invitrogen Gateway recombinatorial system. The host bacterial strain is also HT115 and about 12000 clones have been generated.

### I.1.1.2. RNA interference by injection

In this case, dsRNA is produced *in vitro* and a solution at a concentration of 0.2–1.0 $\mu g/\mu l$ is injected into young adult hermaphrodite germ lines (see MM2.2). Next, the progeny is scored for mutant phenotypes (Ahringer, 2006).

All three methods efficiently inactivate gene expression. Which method to use depends on the type of experiment you desire to perform. For instance, RNAi by feeding and by soaking permit to work with big populations of worms in contrast to the more laborious method of microinjecting single animals. However, RNAi by injection gives a stronger gene inhibition compared to the other two approaches.

Independently of the method, observation of a phenotype is a candid indication of a positive RNAi result since false positives are less than 1% (Kamath and Ahringer, 2003). Eventhough, mRNA levels and/or protein levels should be checked to further validate your result.

## [illegible]

### [illegible]

[illegible]

[illegible]

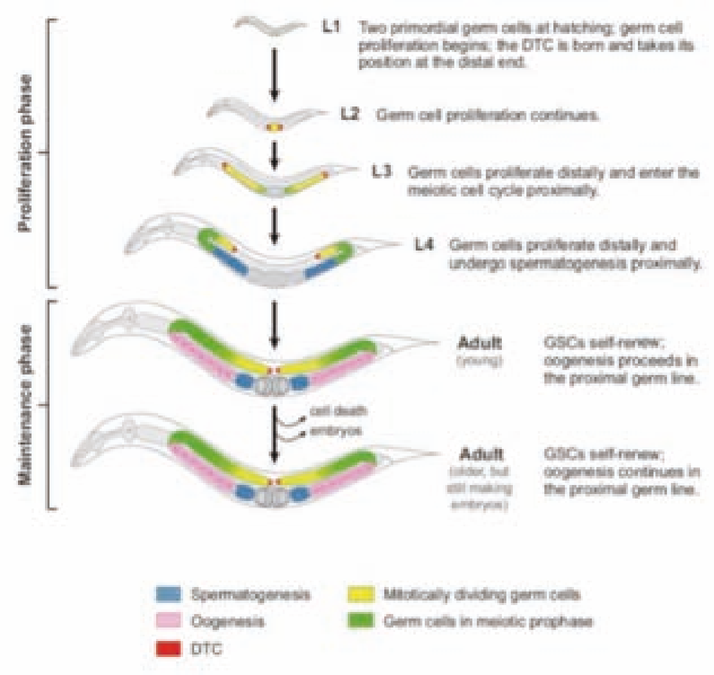
Proliferation phase
Maintenance phase
L1
Two primordial germ cells at hatching; germ cell proliferation begins; the DTC is born and takes its position at the distal end.
L2
Germ cell proliferation continues.
L3
Germ cells proliferate distally and enter the meiotic cell cycle proximally.
L4
Germ cells proliferate distally and undergo spermatogenesis proximally.
Adult
(young)
GSCs self-renew; oogenesis proceeds in the proximal germ line.
cell death
embryos
Adult
(older, but still making embryos)
GSCs self-renew; oogenesis continues in the proximal germ line.
Spermatogenesis
Oogenesis
DTC
Mitotically dividing germ cells
Germ cells in meiotic prophase

[illegible]

A pool of stem cells at the distal end of each gonad arm is maintained by the somatic distal tip cell (DTC), which signals to the germ line via the Notch-signalling pathway and controls a network of RNA regulators. More specifically, the GLP-1 receptor, which is preferentially expressed in the distal germ line, recieves the LAG-2 signal from the distal tip cell and promotes mitosis at the expense of meiosis (Crittenden et al., 1994).

The choice between keep dividing cells mitotically or entering into the meiotic cell cycle is coordinated by a network of RNA regulatory proteins, most of them transcriptionaly regulated by the Notch signaling pathway. These RNA regulatory factors are FBF-1 and FBF-2 and are in conjunction named FBF proteins (*fem-3* Binding Factor). They belong to the PUF protein family (Pumilio and FBF).

FBF proteins are required for continued mitotic divisions and maintenance of adult germ line stem cells. In *fbf-1; fbf-2* double mutants, all proliferating cells enter in meiosis and differentiate to sperm (Crittenden et al., 2002). FBF bind regulatory elements in the 3' untranslated regions (3'UTRs) of target mRNAs thus, blocking their translation. Some of these targets are known, as *gld-1* and *gld-3*, which encode factors that promote meiosis (Eckmann et al., 2004).

Importantly, many of the regulators controlling the mitosis/meiosis switch also control the sperm/oocyte decision indicating that these two processes are coupled.

### I.2.2. The germ line sex determination pathway

The regulatory network that rules the sex determination in the germ line of *C. elegans* has been well characterized in the last two decades. Sexual fate of germ cells is, in part, determined by several regulators that also participate in the sex determination pathway in somatic cells. However, in order to produce sperm and oocytes, there must be some specific regulators that act exclusively in the germ line. As proof of this principle, two of the *fog* genes (*fog-1* and *fog-3*) are present only in germ cells. *fog* genes together with the three *fem* genes (*fem-1, fem-2* and *fem-3*) are necessary to promote sperm production.

Genetic analyses evidence that *fog-1* and *fog-3* act downstream of all other genes in the pathway and probably they are directly implicated in initiating spermatogenesis (Ellis and Schedl, 2007) (Figure I.4.).

[illegible]

[illegible]

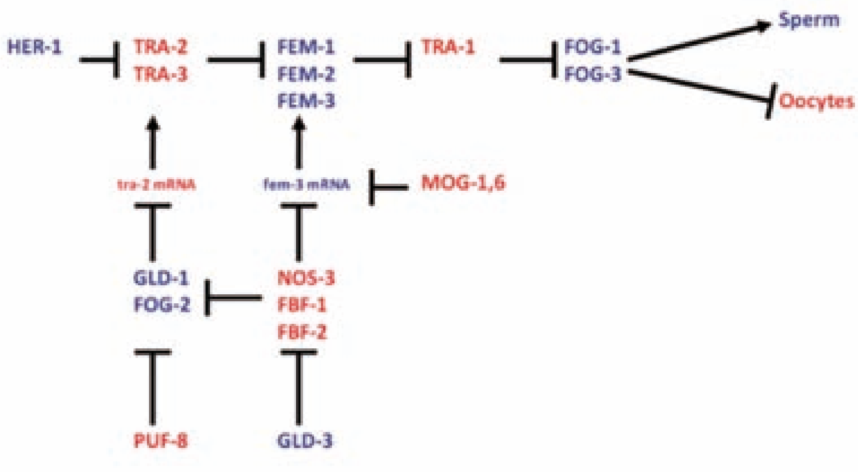
HER-1
TRA-2
TRA-3
FEM-1
FEM-2
FEM-3
TRA-1
FOG-1
FOG-3
Sperm
Oocytes
tra-2 mRNA
fem-3 mRNA
MOG-1,6
GLD-1
FOG-2
NOS-3
FBF-1
FBF-2
PUF-8
GLD-3

[illegible]

[illegible]

[illegible]

[illegible]

[illegible]

Screens in search for genes that disrupt the potential to switch from sperm to oocyte production had identified the *mog* genes (masculinization of the germ line) (Graham and Kimble, 1993). MOG proteins repress *fem-3* through its 3'UTR (Gallegos et al., 1998). Even so, differently to FBF proteins, their action on *fem-3* might be indirect.

Intriguingly, all MOG proteins are homologous to splicing factors (Table I.1) (Puoti and Kimble, 2000; Konishi et al., 2008). Some of their roles within the splicing process are summarized on Table I.1. Despite the involvement of *mog* genes in splicing, none of their corresponding mutant animals in *C. elegans* showed any splicing defect (see D.1.2).

| ***C. elegans mog* gene** | **Yeast ortholog** | **Human ortholog** | **Splicing step/general process** |
|---|---|---|---|
| *mog-1* | Prp16 | PRP16 | Second step |
| *mog-2* | Lea1 | U2A' | Probably first catalytic reaction |
| *mog-3* | Cwc25 | CWC25 | Probably first catalytic reaction |
| *mog-4* | Prp2 | PRP2 | Before first step |
| *mog-5* | Prp22 | PRP22 | Second step, spliceosome disassembly |
| *mog-6* | - | CYP60 | Role in splicing yet not determined |

**Table I.1. Orthologs of *C. elegans mog* genes in yeast and human and their known roles in splicing.**

Kerins and co-workers found *prp-17* as a factor functioning downstream of GLP-1 in the mitotic/meiotic switch and also playing a role in the sperm/oocyte switch. *prp-17* is the ortholog of the yeast and human PRP17/CDC4 splicing factor. They performed an RNAi screen against splicing factors and searched for phenotypes that alter these two important decisions during germ line development. Several splicing-related genes were involved in the two critical germ line decisions (Kerins et al., 2009). Importantly, *rsr-2*, the gene of study in this thesis, was not among the tested genes. Why mutations in the splicing machinery are specifically associated with the proliferation/meiosis switch and/or with sex determination is reviewed and contrasted in the discussion of this thesis.

## [illegible]

### [illegible]

[illegible]

[illegible]

[illegible]

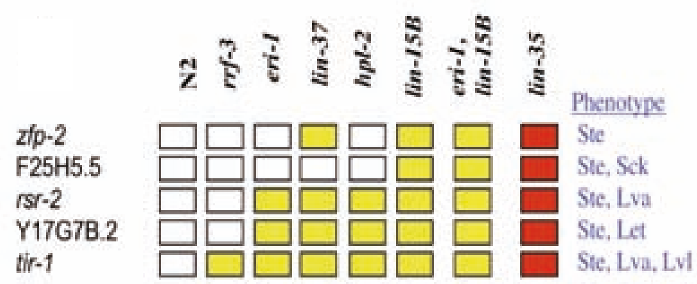

|  | N2 | rrf-3 | eri-1 | lin-37 | hpl-2 | lin-15B | eri-1, lin-15B | lin-35 | Phenotype |
|---|---|---|---|---|---|---|---|---|---|
| zfp-2 | ☐ | ☐ | ☐ | 🟨 | ☐ | 🟨 | 🟨 | 🟥 | Ste |
| F25H5.5 | ☐ | ☐ | ☐ | 🟨 | ☐ | 🟨 | 🟨 | 🟥 | Ste, Sck |
| rsr-2 | ☐ | ☐ | 🟨 | 🟨 | 🟨 | 🟨 | 🟨 | 🟥 | Ste, Lva |
| Y17G7B.2 | ☐ | ☐ | 🟨 | 🟨 | 🟨 | 🟨 | 🟨 | 🟥 | Ste, Let |
| tir-1 | ☐ | 🟨 | 🟨 | 🟨 | 🟨 | 🟨 | 🟨 | 🟥 | Ste, Lva, Lvl |

[illegible]

[illegible]

[illegible]

[illegible]

[illegible]

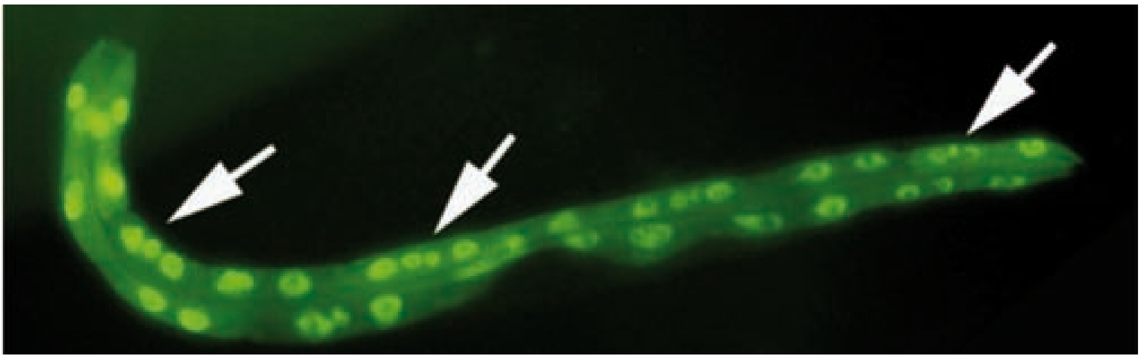

[illegible]

[illegible]

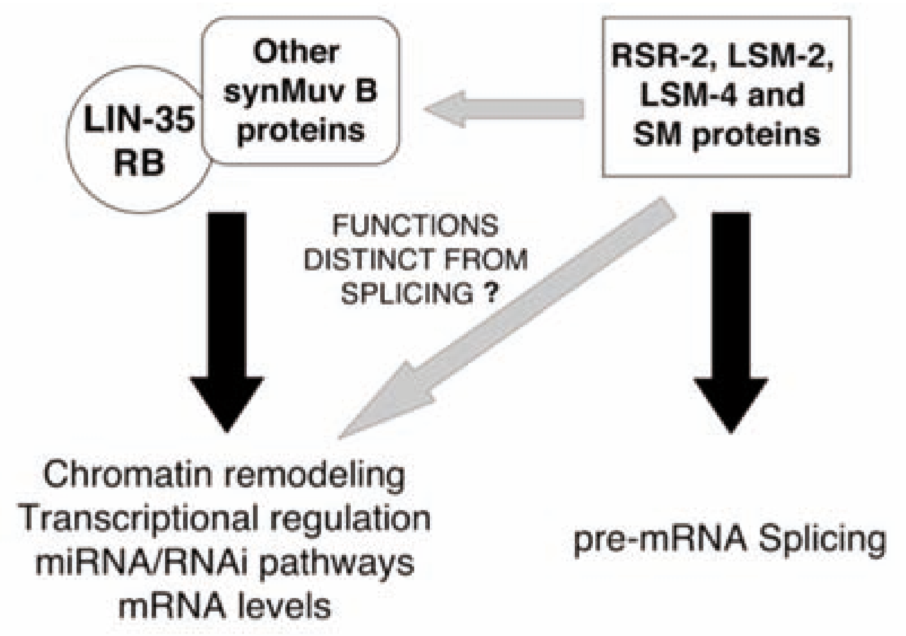
LIN-35
RB
Other
synMuv B
proteins
RSR-2, LSM-2,
LSM-4 and
SM proteins
FUNCTIONS
DISTINCT FROM
SPLICING ?
Chromatin remodeling
Transcriptional regulation
miRNA/RNAi pathways
mRNA levels
pre-mRNA Splicing

[illegible]

# I.4. Pre-mRNA splicing

Pre-messenger RNA (pre-mRNA) splicing is a central step in gene expression through which noncoding intron sequences are accurately removed from a precursor mRNA molecule and exons are spliced together (Grainger and Beggs, 2005). Alternative splicing (AS) occurs when exons are spliced in different combinations leading to multiple distinct messenger RNAs from a single gene. By this mechanism, expansion of the genome coding potential allows the enlargement of the proteome (Nilsen and Graveley, 2010). Furthermore, the process of AS also serves to shut off gene expression. This post-transcriptional regulatory mechanism happens when by AS, a premature termination codon (PTC) is generated in one of the isoforms and that specific messenger is degraded by the Nonsense Mediated Decay pathway (NMD) (Barberan-Soler et al., 2009).

Splicing is essentially identical in *C. elegans* and in vertebrates. Nevertheless, there are some differences such as shorter introns, or a not yet identified consensus branch-point sequence (Blumenthal and Steward, 1997).

To ensure the proper removal of introns, a stepwise assembly of the spliceosome components is needed. The spliceosome is a massive complex. The molecular nature of its members consists of 5 small nuclear RNA-Protein (sn-RNP) complexes and over 150 proteins. After splicing is performed, the assembled machinery disassembles, and its components are recycled for the next round of pre-mRNA maturation (Wahl, Will and Lührmann, 2009).

After many years of research trying to enlight the steps that build the splicing reaction, the general layout of spliceosomal assembly and disassembly has been depicted. Still, the understanding of how the events are arranged at the molecular level is very limited (Newman and Nagai, 2010).

What we know to date is that the snRNP complexes, named as U1, U2, U4, U5 and U6 snRNPs, together with several non-snRNP proteins play key roles in this process. Nuclear pre-mRNA entails 2 transesterification reactions. The first snRNP that interacts with the immature messenger RNA is U1 snRNP. It does it by base-pairing with the intron 5' splice site creating the early ATP-independent “E complex”. Then, an ATP-dependent reaction occurs when U2 snRNP binds to the intronic branch-point and the “A complex” is formed. U4/U6 di-snRNP and U5 snRNP associates as a tri-snRNP to give rise to the “B complex”. The B complex will be activated and primed for catalysis after assotiation of the NineTeen protein Complex (NTC in yeast; Prp19-CDC5 complex in humans). The formation of the catalytic spliceosome “C complex” is achieved by subsequent ATP-dependent rearrangements that involve multiple protein-protein and protein-RNA connections which eventually lead to the release of U1 and U4 snRNPs (Madhani and Guthrie, 1994). Hence, this complex consists of U2, U5, U6 and a set of conserved proteins such as eight DexD/H box helicases (Rocak and Linder, 2004), which permit the 2-transesterification reactions and the final liberation of the spliced intronic lariat (Figure I.8).

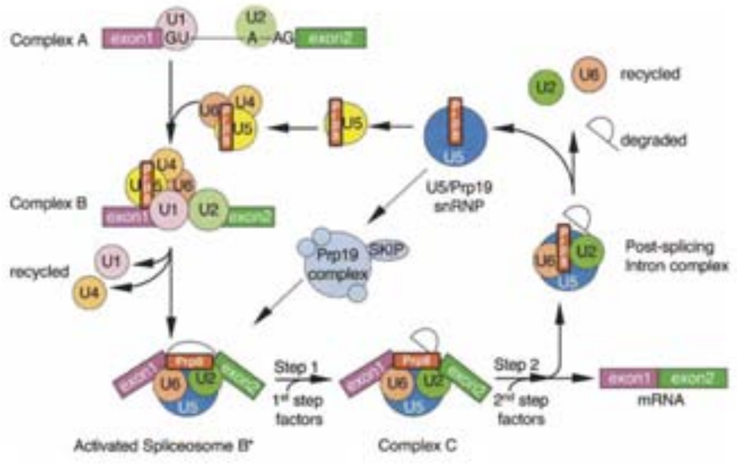
Complex A
exon1
U1
GU
U2
A
AG
exon2
U2
U6
recycled
degraded
U6
U4
U5
U5
U5
Complex B
U4
U5
U6
exon1
U1
U2
exon2
U5/Prp19
snRNP
Prp19
complex
SKIP
recycled
U1
U4
U6
U2
U5
Post-splicing
Intron complex
exon1
Prp8
U6
U2
U5
exon2
Step 1
1st step
factors
exon1
Prp8
U6
U2
U5
exon2
Step 2
2nd step
factors
exon1
exon2
mRNA
Activated Spliceosome B*
Complex C

**Figure I.8. Schematic diagram showing the assembly and recycling of the spliceosome components** (from Grainger and Beggs, 2005). The conserved 5' and 3' splice sites represent the U2 *cis*-spliceosomal GU and AG residues, respectively.

The easiness in performing RNA-Seq of a whole organism to identify and quantify alternative splicing extension events, and the opportunity to perform genetic screenings that uses transgenic worms expressing fluorescent reporters convert *C. elegans* an atractive model for studies about splicing.

Protein components of the splicing machinery are well conserved in eukaryotes and several of these components have been identified as essential for metazoan spliceosome assembly (Blencowe, 2000; Kramer, 1996). A good example of such essential spliceosomal components are the members of the SR protein family.

## [illegible]

### [illegible]

[illegible]

[illegible]

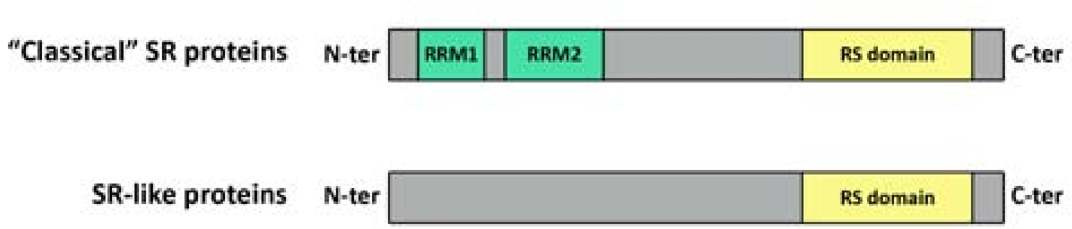
"Classical" SR proteins
N-ter
RRM1
RRM2
RS domain
C-ter
SR-like proteins
N-ter
RS domain
C-ter

[illegible]

[illegible]

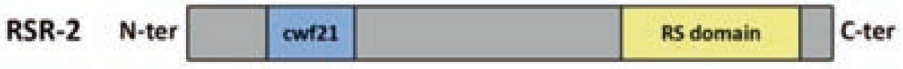
RSR-2
N-ter
cwf21
RS domain
C-ter

[illegible]

There are many splicing factors containing RS domains that are important for protein-protein interactions within the spliceosome, but the RS domain is not exclusive for splicing related genes being also present in other types of proteins such as chromatin modifiers or transcriptional regulators (Boucher et al., 2001). There is an increasing number of *cis*-acting and *trans*-acting splicing mutations affecting RNA processing that are implicated in human diseases (Wang and Cooper, 2007). Particularly, modification of SR protein sequences or alteration of their target motifs may lead to diseases including cancer (Long and Caceres, 2009).

### I.5.2. *rsr*-2 is orthologous to the yeast Cwc21 and the human SRm300/SRMM2 splicing factors

SR proteins have been greatly conserved in metazoans but, with few exceptions, some of them are absent in *Saccaromyces cerevisiae*. This is not the case of *rsr-2*, which is present from yeast to humans (Figure I.11).

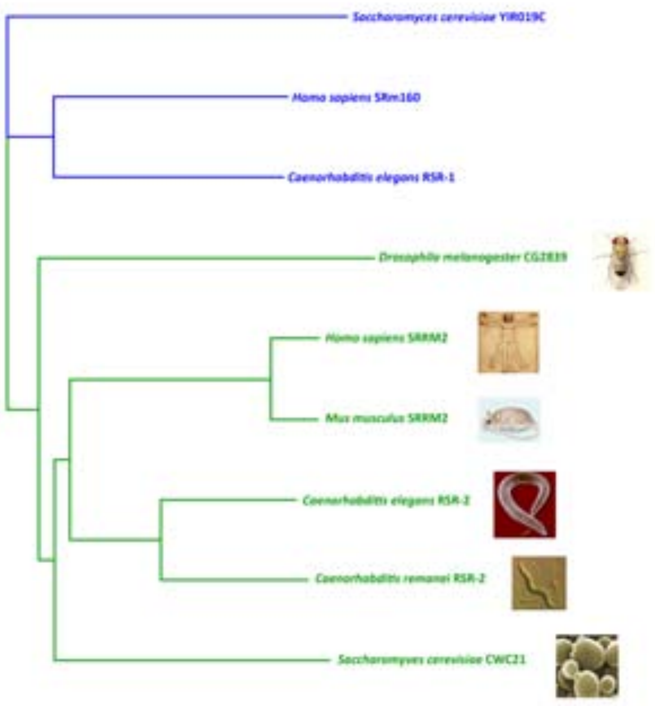
Saccharomyces cerevisiae YIR019C
Homo sapiens SRm160
Caenorhabditis elegans RSR-1
Drosophila melanogaster CG2839
Homo sapiens SRRM2
Mus musculus SRRM2
Caenorhabditis elegans RSR-2
Caenorhabditis remanei RSR-2
Saccharomyces cerevisiae CWC21

**Figure I.11. Phylogenetic tree of RSR-2 and its orthologs.** RSR-2 ortholog sequences were aligned using ClustalW and CLC sequence Viewer was used to generate the tree using the Neighbor Joining algorithm. The output group has to be a group of proteins close enough to allow inference from sequence data, but far enough to be a clear outgroup. In this case, the chosen output is formed by the proteins RSR-1 and its orthologs in yeast (YIR019C) and human (SRm160) (represented in blue).

The *Saccharomyces cerevisiae* protein Cwc21 is a 135 aminoacid protein that presents high homology to the N-terminal region of the *C. elegans* RSR-2 and human SRm300/SRRM2 proteins (Figure I.12).

Human SRm300/SRRM2, although is a much larger protein than its yeast and worm orthologs (2296 versus 135 and 425 aminoacids respectively) contains a highly conserved N-terminal region. In this N-terminal region, like in RSR-2, there is also present a cwf21 motif. Regarding the homology of this N-terminal part of the protein, the first 150 aminoacids of

[illegible]

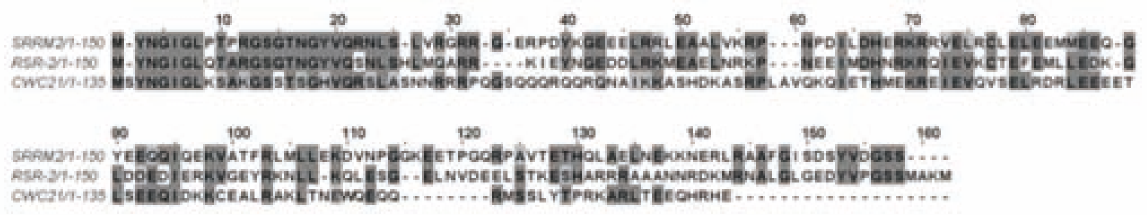
SRRM2/1-150
RSR-2/1-150
CWC21/1-135

[illegible]

[illegible]

[illegible]

[illegible]

[illegible]

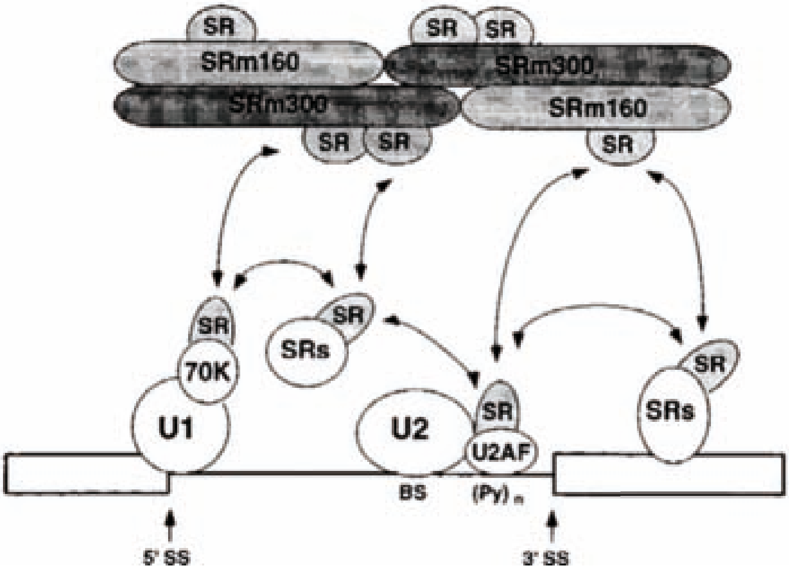
SR
SRm160
SRm300
SR SR
SR SR
SRm300
SRm160
SR
SR
70K
U1
SRs
SR
U2
SR
U2AF
SRs
SR
BS
(Py)n
5' SS
3' SS

[illegible]

## [illegible]

[illegible]

[illegible]

[illegible]

[illegible]

Another insight into the function of Cwc21 was given by the results of the TAP, where both protein and RNA composition of the Cwc21-purified complexes were analyzed. Through mass spectrometry analysis, the data obtained concerning the proteic part of the complexes was consistent with the previous genetic data showing that Cwc21 physically interacts with multiple spliceosomal components (Table I.2). Proteins detected in a parallel affinity purification of Prp8 complexes are shown for comparison, since Prp8 is a conserved splicing factor involved in the catalytic core of the spliceosome (Valadkhan and Jaladat, 2010). Notably, Cwc21 interacts with Prp8 and viceversa (Table I.2, rows 1 and 6), suggesting that Cwc21 could be functionally located at the core of the spliceosome.

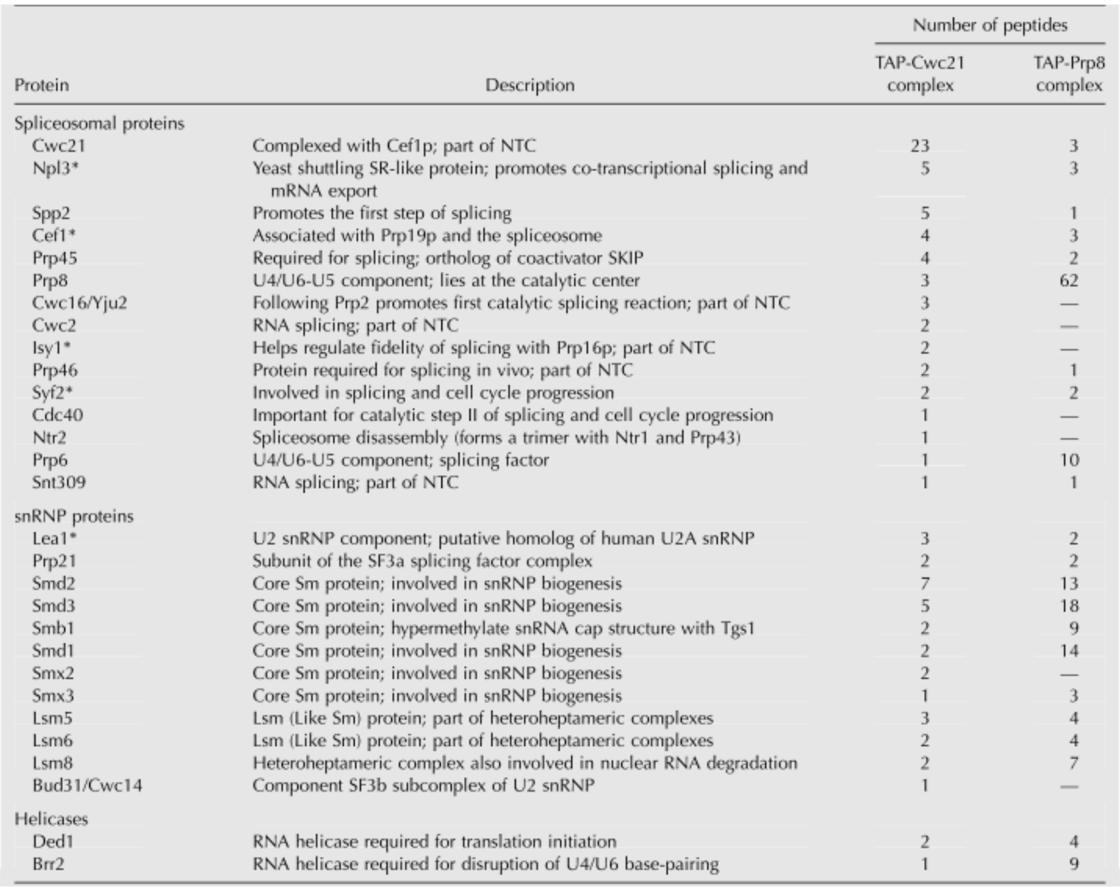

| Protein | Description | Number of peptides<br>TAP-Cwc21 complex | <br>TAP-Prp8 complex |
|---|---|---|---|
| Spliceosomal proteins | | | |
| Cwc21 | Complexed with Cef1p; part of NTC | 23 | 3 |
| Npl3* | Yeast shuttling SR-like protein; promotes co-transcriptional splicing and mRNA export | 5 | 3 |
| Spp2 | Promotes the first step of splicing | 5 | 1 |
| Cef1* | Associated with Prp19p and the spliceosome | 4 | 3 |
| Prp45 | Required for splicing; ortholog of coactivator SKIP | 4 | 2 |
| Prp8 | U4/U6-U5 component; lies at the catalytic center | 3 | 62 |
| Cwc16/Yju2 | Following Prp2 promotes first catalytic splicing reaction; part of NTC | 3 | — |
| Cwc2 | RNA splicing; part of NTC | 2 | — |
| Isy1* | Helps regulate fidelity of splicing with Prp16p; part of NTC | 2 | — |
| Prp46 | Protein required for splicing in vivo; part of NTC | 2 | 1 |
| Syf2* | Involved in splicing and cell cycle progression | 2 | 2 |
| Cdc40 | Important for catalytic step II of splicing and cell cycle progression | 1 | — |
| Ntr2 | Spliceosome disassembly (forms a trimer with Ntr1 and Prp43) | 1 | — |
| Prp6 | U4/U6-U5 component; splicing factor | 1 | 10 |
| Snt309 | RNA splicing; part of NTC | 1 | 1 |
| snRNP proteins | | | |
| Lea1* | U2 snRNP component; putative homolog of human U2A snRNP | 3 | 2 |
| Prp21 | Subunit of the SF3a splicing factor complex | 2 | 2 |
| Smd2 | Core Sm protein; involved in snRNP biogenesis | 7 | 13 |
| Smd3 | Core Sm protein; involved in snRNP biogenesis | 5 | 18 |
| Smb1 | Core Sm protein; hypermethylate snRNA cap structure with Tgs1 | 2 | 9 |
| Smd1 | Core Sm protein; involved in snRNP biogenesis | 2 | 14 |
| Smx2 | Core Sm protein; involved in snRNP biogenesis | 2 | — |
| Smx3 | Core Sm protein; involved in snRNP biogenesis | 1 | 3 |
| Lsm5 | Lsm (Like Sm) protein; part of heteroheptameric complexes | 3 | 4 |
| Lsm6 | Lsm (Like Sm) protein; part of heteroheptameric complexes | 2 | 4 |
| Lsm8 | Heteroheptameric complex also involved in nuclear RNA degradation | 2 | 7 |
| Bud31/Cwc14 | Component SF3b subcomplex of U2 snRNP | 1 | — |
| Helicases | | | |
| Ded1 | RNA helicase required for translation initiation | 2 | 4 |
| Brr2 | RNA helicase required for disruption of U4/U6 base-pairing | 1 | 9 |

**Table I.2. Proteins detected by mass spectrometry of TAP-tagged affinity-purified Cwc21 complexes** (from Khanna et al., 2009). An asterisk indicates a protein detected as having a genetic interaction with Cwc21 in the SGA screen. All peptides for listed proteins were detected at a confidence of at least 99.6%.

Besides, RNA from Cwc21-complexes was hybridized to a tiled yeast ncRNA microarray and Cwc21 was preferentially found in association with snRNAs of step I spliceosomes (predominantly U2 snRNA but also U5 and U6 snRNAs).

Interestingly, Cwc21 is not essential for viability in contrast to the observations made in *C. elegans,* where *rsr-2* inactivation by dsRNA microinjection gave rise to arrested animals

J te3n e v l) W55CE) i p cv 1 l vst e cvh se m y S M 1 t c et v ci t . 1 2 vc se , h M c, ls se 3 cse vi sevht eM t ev se se 3 3 e c . h e lpc 1 e 1 sevht e h v evst e . c et v , , h s l J s3f h )CqE) t . g h e 1 n t h sn , t hv ev9 vi t g h ll Vh ec hs, v l g lc . h 2t f e 1 vt tls3i vlp h 1f 1 i ee v l) 9W55“E)

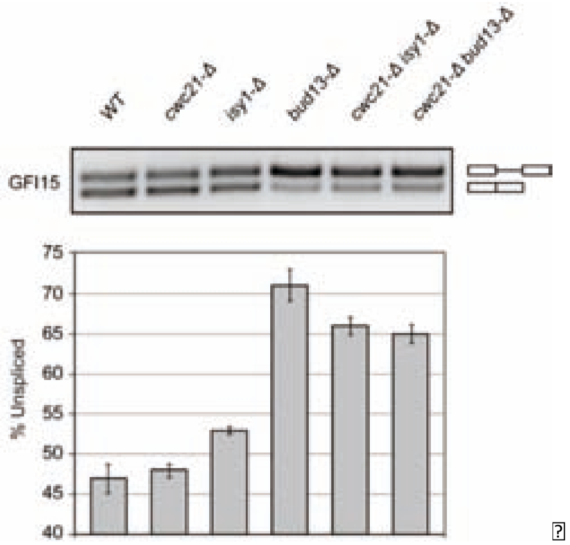

ui t c /O8 lu1. yl c u y 1 F C T/ . ys / 1 . 1l L c y . l cc . l yL u u i u . J m e 2ht n i ee v l) 9W55“E) , h c ev vsg M cc p t 2c, ls 1 e 1 f ec, ls 1 Vh ec hs, vc 2ht n vi 3 e C8 se vi n f v ev cvh sec e lpu 1 p vlse 3 n s ht hh pc)

e tev n , t h hp . t hm9 h se 3 h e 1 t ll t h vt hc 1 c hs 1 i t . . WC , ht v se 1sh Vlp sev h vc svi vi v. t t h c, ls se 3 2 vt hc h, / e 1 ef CCq J h se 3 h v l) 9W55“E9 1 2se se 3 vi 1t n sec vi ht f 3i vi c sev h vst ec V m , l s3f h )C8E)

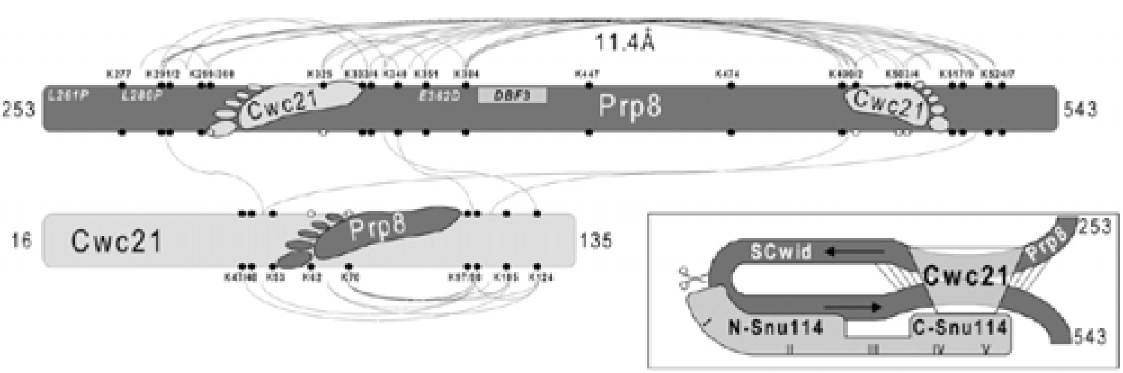
11.4Å
K277
K291/2
K299/309
K325
K333/4
K348
K351
K364
K447
K474
K498/2
K503/4
K517/9
K524/7
253
L261P
L280P
Cwc21
E362D
DBF3
Prp8
Cwc21
543
16
Cwc21
Prp8
135
K41/80
K53
K62
K70
K97/98
K105
K124
SCwid
Cwc21
Prp8
253
N-Snu114
C-Snu114
543
II
III
IV
V

ui t c /53 cL B 1. l u y . u l c l 1 t c F1 l g l . c1 yyvu e 1 g 1 . y c2 C FT/ 1 l u u C T/ J m e 2ht n h se 3 h v l) 9W55“E) i n vs 1s 3h n ci t . se 3 vi sevh n t l f l h $^{D}$ ht ccNs emc s1 ev s2s 1 p h cc t, vht n vhp t h h t n se ev h, / $^{V8DN8qD}$ e 1 . WC $^{C6NCD8}$ 9 svi ll lpcse c se 1s v 1 p sh l c) ht ccNs emc tee vse 3 lpcse c t h , vs1 c t ev se se 3 v. t lpcse c h ci t . e p se )

t h t g h9 vi p 1 n tecvh v 1 vi v vi i f n e M l v 1 , ht v se n D55z W sc se 2 V9 2f e vst e l t hvi t lt 3 t 2 vi p cv . WC e 1 c lct 1sh Vlp se 1se 3 vt h, / e 1 ef CCq)

# I.6. Shades and lights of co-transcriptional splicing

Classically, attemps to understand the mechanism and regulation of splicing relied on the study of *cis*- and *trans*- acting factors within the molecule of RNA. However, these signals are not sufficient to explain how introns and exons are distinguished by the spliceosome to eventually achieve a proper maturation of a messenger pre-mRNA, indicating that other layers of regulation may exist (Schwartz et al., 2010).

One of these regulatory layers could be that splicing occurs co-transcriptionally. RNA polymerases seem to be evolutionary selected to support co-transcriptional events. In *E. Coli,* ribosome assembly is only achieved if the rDNA is transcribed by its own polymerase, but not if the enzyme is substitute by the bacteriophage T7 polymerase (Lewicki et al., 1993). Similarly, in yeast rRNA processing is abrogated if RNA polymerase I is mutated (Schneider et al., 2007).

In fact, the general pre-mRNA processing events of 5’ end capping, splicing and 3’ end formation by cleavage/polyadenylation also occur co-transcriptionally. In eukaryotes, intron removal is tightly linked to transcription by RNA Polymerase II (RNAP II) as it moves along the gene (Bentley et al., 2005). Why is important whether introns are eliminated in a co-transcriptional manner? Some *in vitro* studies suggest that post-transcriptional splicing would be less efficient (Das et al., 2007; Yu et al., 2010).

The most dominant factor implicated in the cross-talk bewteen transcription and splicing is the RNAP II (Hicks et al., 2006). How does RNAP II facilitate splicing? There are evidences that support two mechanisms. First, RNAP II presents an exclusive C-terminal domain (CTD) that bears a large number of heptad repeats. The CTD serves as a “landing pad” to recruit RNA processing factors to the nascent transcript (Phatnani and Greenleaf, 2006). In particular, splicing is functionally dependent on phosphorilation of the heptad serines 2 and 5 of the CTD. In addition, U1 snRNP components immunoprecipitate with RNAP II (Das et al., 2007) and the presence of U1 snRNP at a 5’ss can promote recruitment of RNAP II and transcription factors to the promoter of the genes (Damgaard et al., 2008). SR proteins, which interact with U1 and U2 to regulate splicing assembly, have also been found to immunoprecipitate with RNAP II (Das et al., 2007). Secondly, RNAP II kinetics can also control the splicing process. In agreement with this model, when RNAP II elongation rate is fast, weak splice sites are not recognized and a putative alternative exon would be excluded from the final transcript. However, if the RNAP II elongation rate is slow, it would give time to the splicing machinery for recognition of weak splice sites thus, including the anternative exon to the matured transcript. Hence, RNAP II elongation rate impacts in the splicing efficiency (Oesterreich et al., 2011).

[illegible]

[illegible]

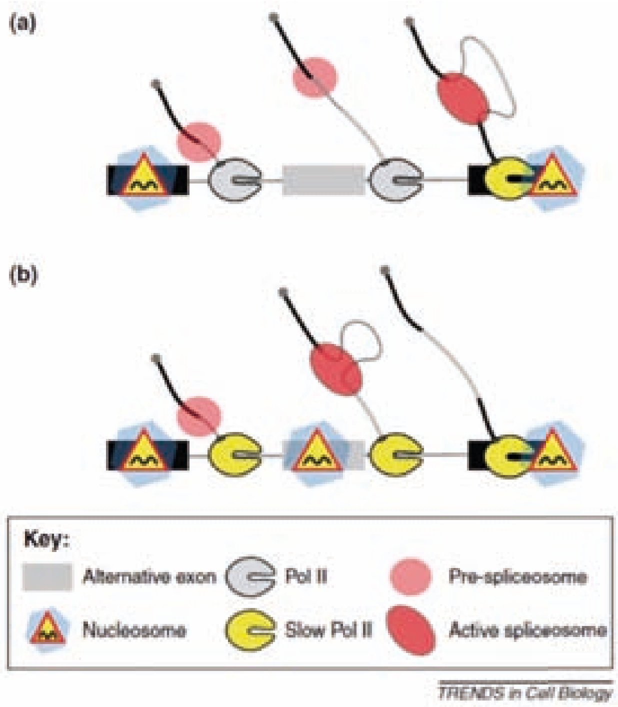
(a)
(b)
Key:
Alternative exon
Pol II
Pre-spliceosome
Nucleosome
Slow Pol II
Active spliceosome
TRENDS in Cell Biology

[illegible]

[illegible]

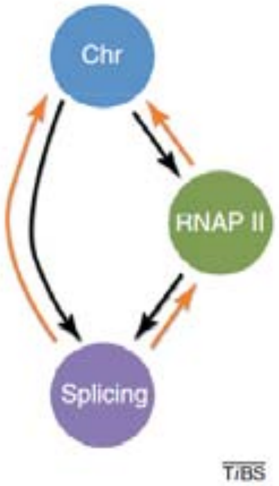

**Figure I.17. Proposed model for the network of splicing regulatory interactions** (Modified from Almeida and Carmo-Fonseca, 2012). In the splicing regulatory model, the feedforward loop consists of a chromatin structure (Chr) that directely controls the RNAP II transcription rate and pre-mRNA splicing, so that both chromatin and RNP II jointly regulate the splicing outcome (black curves). In this model, RNAP II feeds back to reassemble chromatin, and splicing stimulates both transcription and histone modification (orange curves).

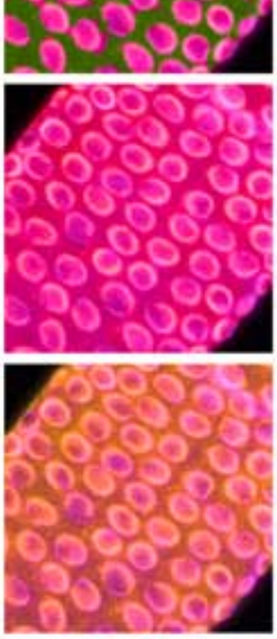

# Aims

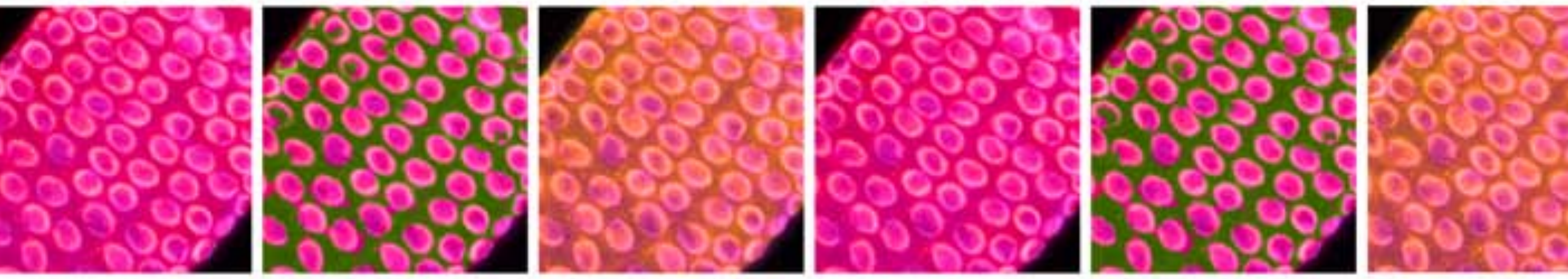

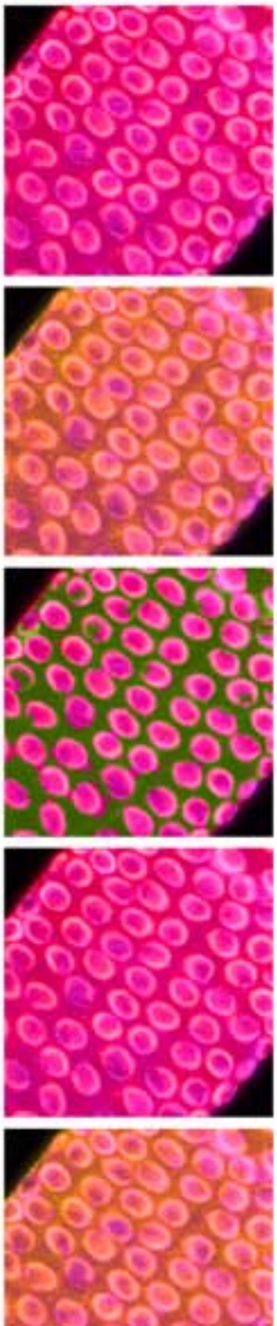

"Soul meets body"
Death Cab for Cutie

The general aims of this thesis are:

- To characterize the role of *rsr-2*, the ortholog of the SRm300/SRRM2 human splicing co-activator, in *Caenorhabditis elegans* development.
- To uncover the molecular functions of RSR-2 within the gene expression machinery.

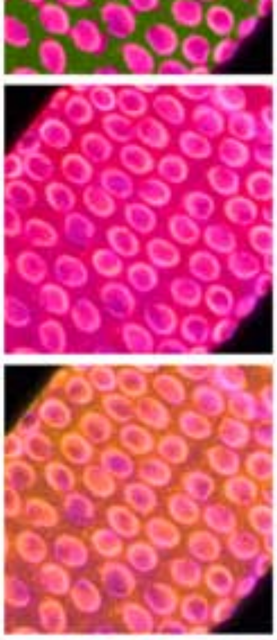

# Results

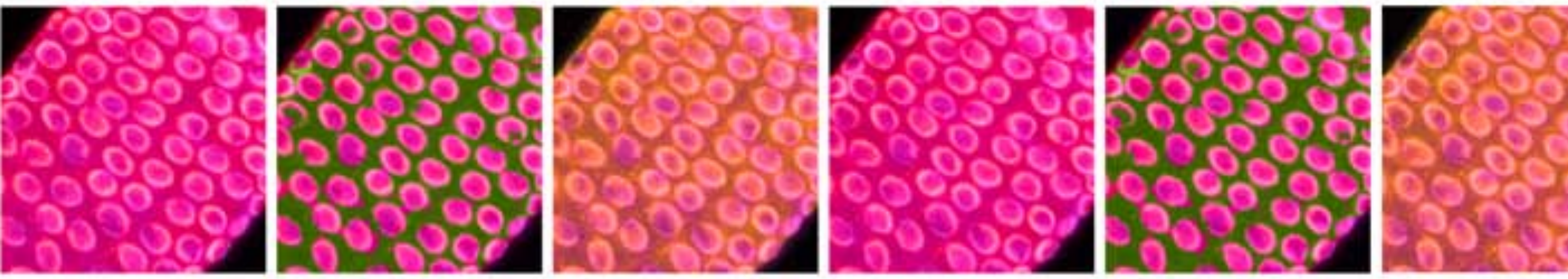

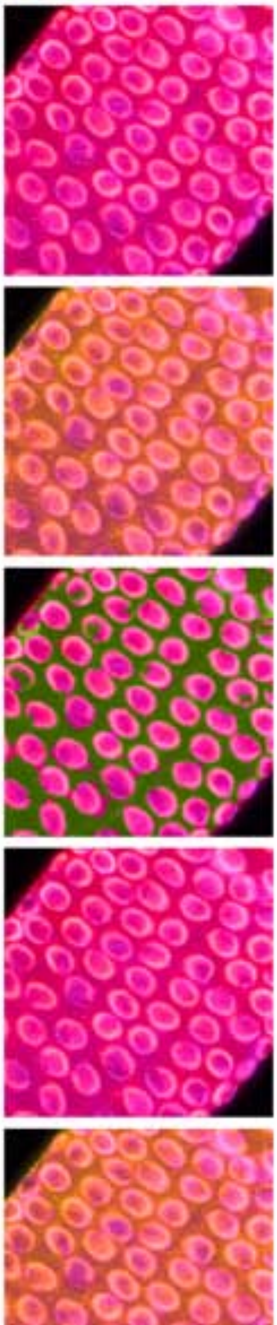

> "I can't stop this feeling I've got"
>
> Razorlight

# R.1. *rsr-2* is an essential gene for the development of *C. elegans*

## R.1.1. Deletion mutants in *rsr-2*

*rsr-2* is a gene located at the chromosome II and encodes a 1934-nucleotide transcript which contains three exons and a 3'UTR (Figure R.1).

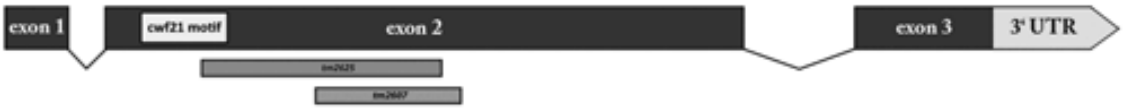

**Figure R.1. Scale scheme of *rsr-2* gene.** Connecting lines, introns; inner box, cwf21 motif; outer boxes, regions affected in *rsr-2* alelles.

Upon our request, the Japanese consortium "National Bioresource Project for the Experimental Animal Nematode *C. elegans* (NBP)" (http://www.shigen.nig.ac.jp/c.elegans/index.jsp) generated two deletion alleles of this gene. Aforementioned consortium uses a random mutagenesis method with TMP/UV (Trimethyl Psoralen/Ultraviolet) and gene-specific primers to identify deletion alleles (Gengyo-Ando and Mitani, 2000).

In *rsr-2*, the allele *tm2607* presents a 196 bp deletion plus 1 bp insertion while the allele *tm2625* lacks 337 bp and has an insertion of 2 bp (Figure R.1 and R.2).

***tm2607* allele**

```
...ccgggaagctcgatggcca -[196 BP DELETION] aagaaggagaagaagcagaa... -- WT
...ccgggaagctcgatggcca C----------------- aagaaggagaagaagcagaa... -- tm2607
```

***tm2625* allele**

```
...tagaggacaagggcctcga --[337 BP DELETION] gtagcagtagctcatcaga... -- WT
...tagaggacaagggcctcga GT----------------- gtagcagtagctcatcaga... -- tm2625
```

**Figure R.2. Genomic context of *rsr-2* alelles.**

Once we received these alleles, *rsr-2(tm2607)* and *rsr-2(tm2625)* animals were backcrossed 3 and 5 times respectively. The backcross strategy consists in repeated crossing of the mutant genome of interest with a wild type genome to get rid of other probable mutations generated during the mutagenesis process.

Moreover, the allele *tm2625* was balanced with an inversion carrying a *dpy* mutation and a GFP marker under the control of a pharynx specific promoter to make the strain CER004 (*rsr-2(tm2625)/mIn1* [*dpy-10(e128) mIs14(myo-2::GFP)*] II) (Edgley and Riddle, 2001). Such type of balancer allows the researcher to discern from wild type, heterozygous and homozygous animals by simply observing the animals under a fluorescence stereomicroscope to check the GFP expression in the pharynx and the dumpy (Dpy) phenotype (Figure R.3).

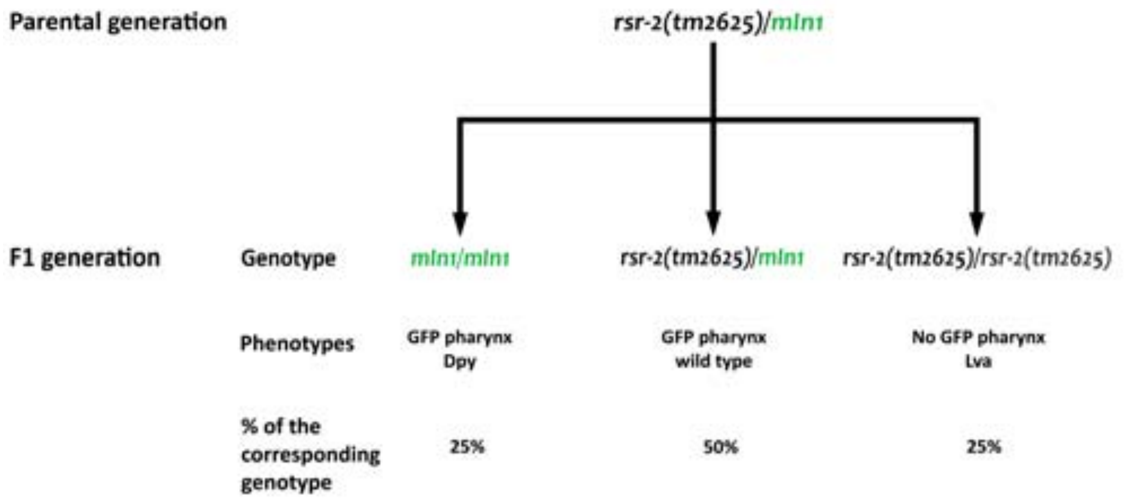
Parental generation
rsr-2(tm2625)/mIn1
F1 generation
Genotype
mIn1/mIn1
rsr-2(tm2625)/mIn1
rsr-2(tm2625)/rsr-2(tm2625)
Phenotypes
GFP pharynx
Dpy
GFP pharynx
wild type
No GFP pharynx
Lva
% of the corresponding genotype
25%
50%
25%

**Figure R.3.** ***rsr-2(tm2625)/mIn1*** **animals segregate a mixed population of heterozygous and homozygous animals that can be distinguished.**

The genomic fragment removed in *rsr-2(tm2607)* animals is not essential for the gene function since mutant animals do not display any phenotype and the deletion/insertion is not affecting the open reading frame. Thus, a fully functional truncated protein may be produced in these worms.

However, the *tm2625* deletion/insertion eliminates part of the cwf21 motif (mRNA splicing-related motif) and also changes the frameshift, producing animals arrested in early larval stages (Larval arrest (Lva) phenotype) (Figure R.4A). To further analyze these mutants, CER004 animals were grown at 25°C for 114 hours (approximately 5 days) and sizes for wild type, heterozygous and homozygous *rsr-2(tm2625)* worms were measured using the NIS-Elements Software.

We observed that the Lva phenotype was not temperature dependent. After 5 days of post-embryonic development, either at 15 or at 25 °C, animals homozygous for the *tm2625* mutation were about 0.3 mm large, the corresponding size for an L1 animals, while heterozygous *rsr-2(tm2625)* or homozygous *rsr-2(tm2607)* worms reached the standard adult size of 1 mm (Figure R.4B)

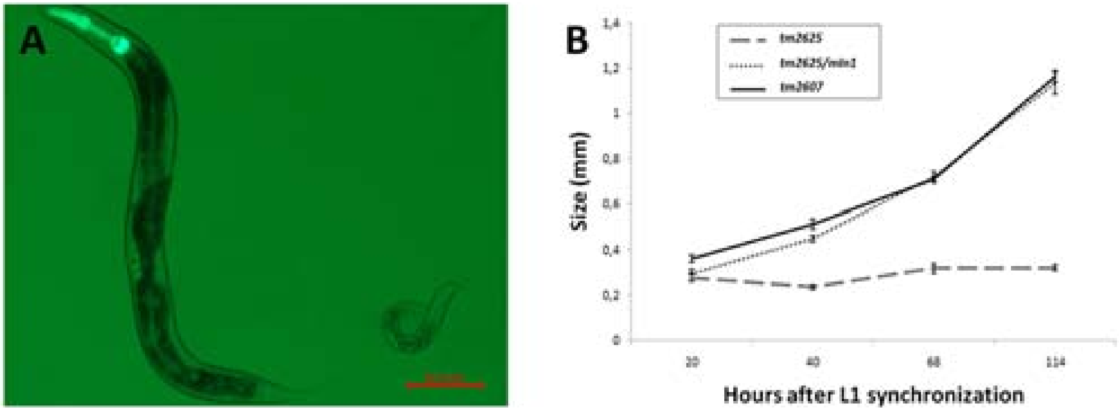
A
B
tm2625
tm2625/mIn1
tm2607
Size (mm)
1,4
1,2
1
0,8
0,6
0,4
0,2
0
20
40
68
114
Hours after L1 synchronization

[illegible]

[illegible]

[illegible]

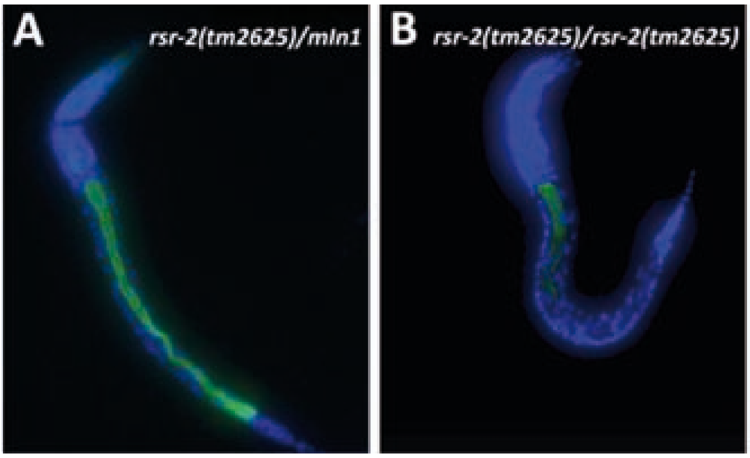
A
rsr-2(tm2625)/mIn1
B
rsr-2(tm2625)/rsr-2(tm2625)

[illegible]

[illegible]

# R.2. *rsr-2* regulates the germ line sex determination

## R.2.1. *rsr-2(RNAi)* animals develop masculinized germ lines

The severe larval arrest phenotype of *rsr-2(tm2625)* animals does not allow studies at other developmental stages where genetic pathways are better described. Moreover, the fact that this non-viable mutation needs to be kept in a balanced strain hampers the harvesting of a large pure population of mutant worms that is necessary for certain assays.

The RNA interference is an alternative approach to mutations and its effect on gene silencing could be milder allowing to track and dissect genetically the role of the gene of interest. Previous RNAi assays have shown that *rsr-2* is essential for *C. elegans* development. *rsr-2* RNAi by feeding and by microinjection produces a variety of phenotypes from larval or embryonic lethality to reduced brood size or sterility (Longman et al., 2001; J. F. Rual et al., 2004; Ceron et al., 2007).

A RNA interference by feeding protocol was established in order to get a population with homogeneous but weaker phenotype than that observed in null mutants of *rsr-2*. Wild type N2 worms were synchronized following the sodium hypochloride treatment (Porta-de-la-Riva et al., 2012) and L1 animals grown at 25°C and fed with bacteria producing *gfp* dsRNA (control) and *rsr-2* dsRNA (see MM.2). Indeed, we verified by semiquantitative Reverse Transcription-PCR (sqRT-PCR) that silencing the *rsr-2* expression through this technique led to a partial reduction of the *rsr-2* mRNA levels (Figure R.6A) (see MM.4). Quantification of this reduction was also carried out through Real Time PCR (Figure R.19 in section R.6.2). *rsr-2(tm2607)* viable mutants were included in this experiment and we observed that *tm2607* insertion/deletion is in frame and these mutants produce a shorter transcript (195 nucleotides less than the wild type), which should generate a funtional truncated protein.

Although *rsr-2(RNAi)* worms could reach the adulthood stage, similarly to control *gfp(RNAi)* worms, they were sterile. After 3 days post-L1 animals were harvested, their gonads dissected, fixed with paraformaldehyde 4% and stained with DAPI (see MM.5). We observed that such sterility was due to a defect in the sperm/oocyte switch that produces a masculinized germline.

The Mog phenotype (M̲asculinization o̲f the g̲erm line) that *rsr-2(RNAi)* animals displayed results in the lack of oogenesis and an excess of sperm production (Figure R.6B). The same phenotype was observed in *rsr-2(RNAi); rsr-2(tm2607)* animals (not shown).

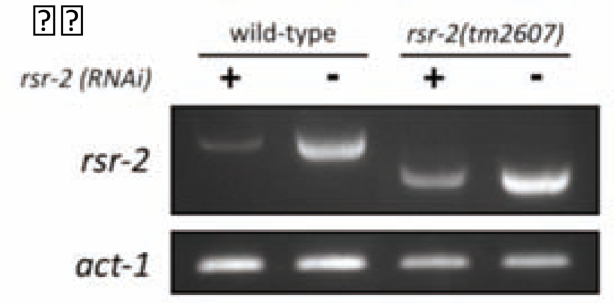

[illegible]

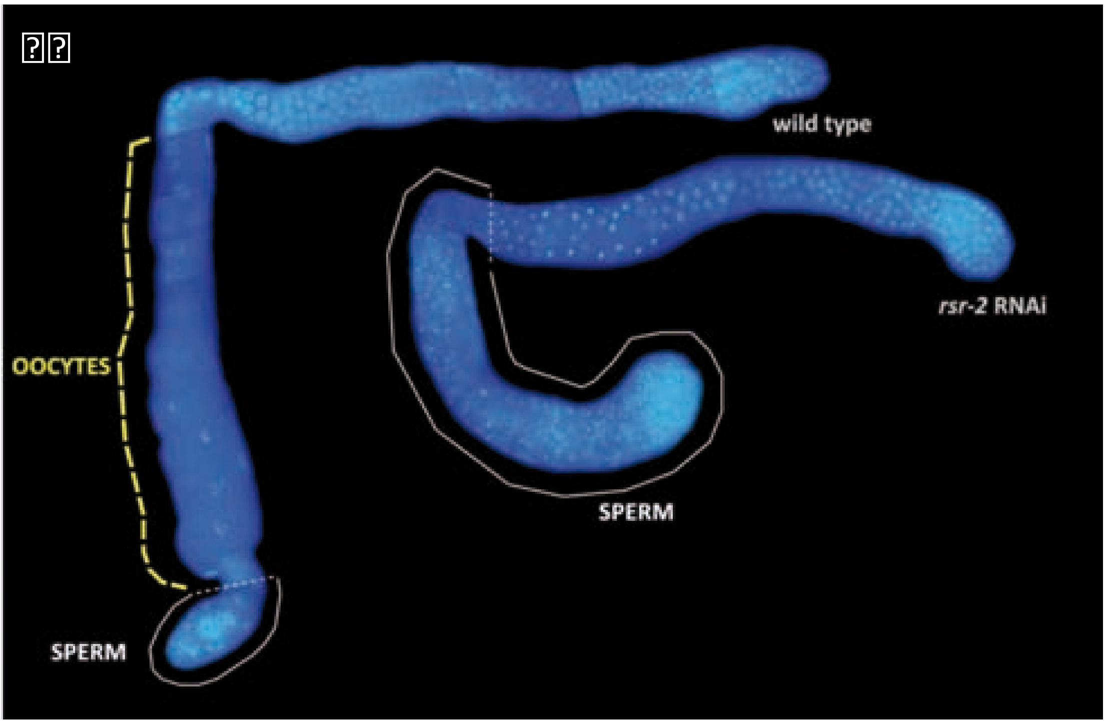
wild type
rsr-2 RNAi
OOCYTES
SPERM
SPERM

[illegible]

| [illegible] | [illegible] | | |
|---|---|---|---|
| | [illegible] | [illegible] | [illegible] |
| C8° | D5K | 5K | ' D |
| W8° | /“K | CCK | ~C55 |

[illegible]

[illegible]

[illegible]

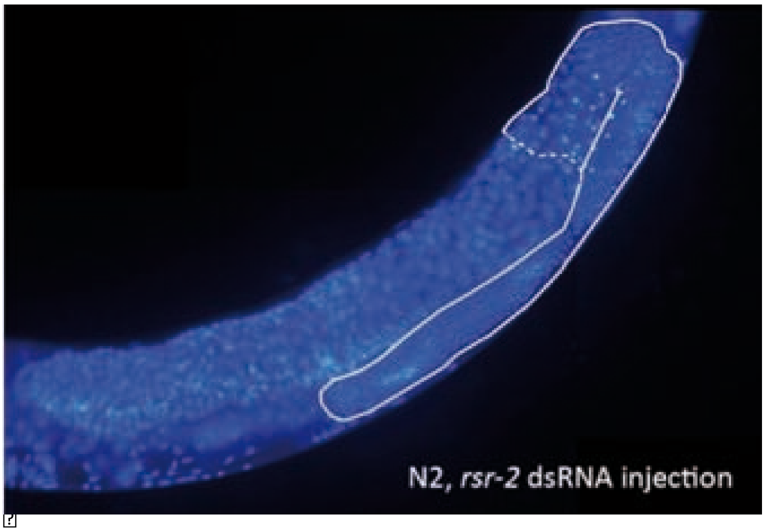
N2, rsr-2 dsRNA injection

[illegible]

[illegible]

## [illegible]

[illegible]

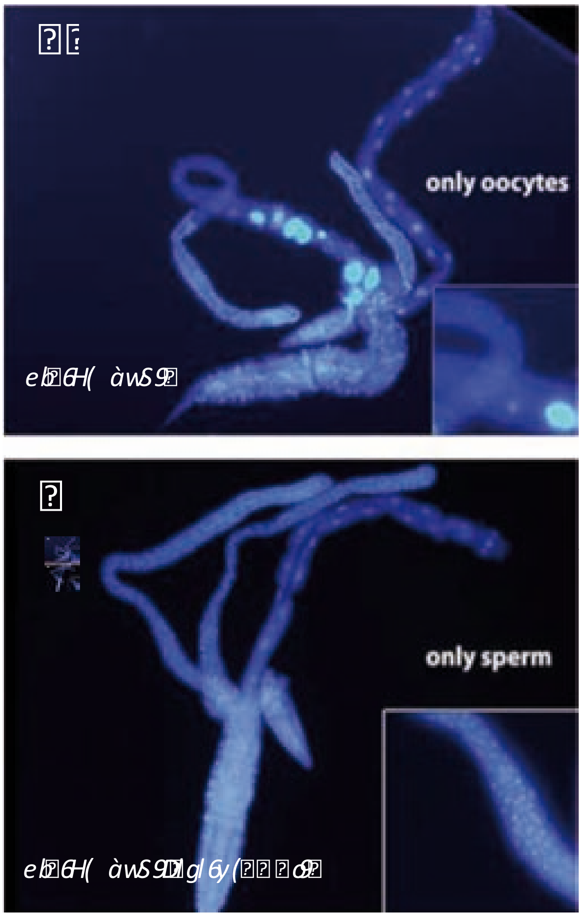
only oocytes
only sperm

[illegible]

[illegible]

[illegible]

[illegible]

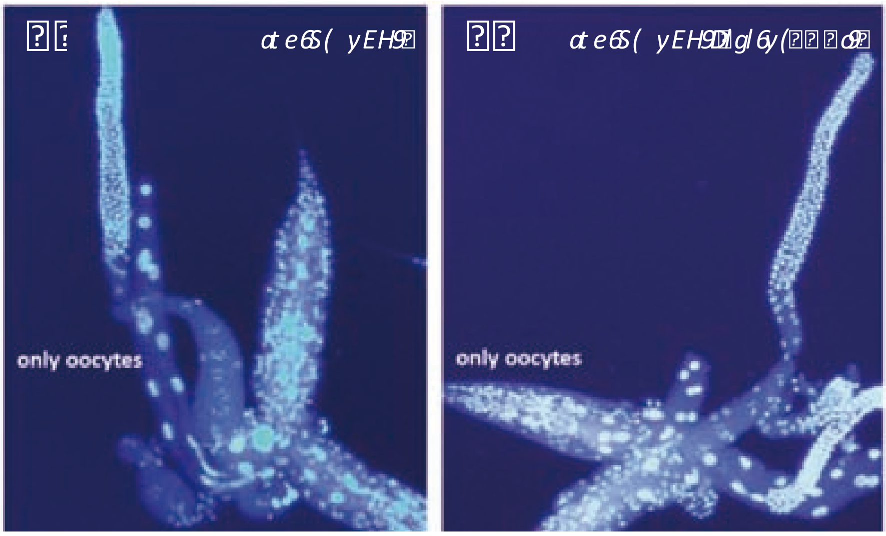
only oocytes
only oocytes

[illegible]

| Genotype[1] | Sp[2]+Oo[2] | Sp[2] only | Oo[2] only | n[3] |
|---|---|---|---|---|
| Wild type | 100% | 0% | 0% | >100 |
| Wild type, *rsr-2(RNAi)* | 11% | 89% | 0% | >100 |
| *gld-3(q741)* | 0% | 0% | 100% | >100 |
| *gld-3(q741); rsr-2(RNAi)* | 0% | 100% | 0% | >100 |
| *fog-1(q253)* | 0% | 0% | 100% | >100 |
| *fog-1(q253); rsr-2(RNAi)* | 0% | 0% | 100% | >100 |
| *fog-2(q71)* | 0% | 0% | 100% | 91 |
| *fog-2(q71); rsr-2(RNAi)* | 0% | 0% | 100% | 111 |
| *fog-2(oz40)* | 0% | 0% | 100% | 21 |
| *fog-2(oz40); rsr-2(RNAi)* | 0% | 0% | 100% | 93 |
| *fem-3(e2006)* | 0% | 0% | 100% | >100 |
| *fem-3(e2006); rsr-2(RNAi)* | 16% | 2% | 82% | 81 |
| *fbf-1(ok91)* | 100% | 0% | 0% | >100 |
| *fbf-1(ok91); rsr-2(RNAi)* | 72% | 28% | 0% | 72 |
| *fbf-2(q738)* | 99% | 0% | 1% | >100 |
| *fbf-2(q738); rsr-2(RNAi)* | 31% | 50% | 19% | 121 |
| *nos-3(q650)* | 100% | 0% | 0% | >100 |
| *nos-3(q650); rsr-2(RNAi)* | 72% | 28% | 0% | 130 |
| *puf-8(ok302)* | 93% | 3.5% | 3.5% | 54 |
| *puf-8(ok302); rsr-2(RNAi)* | 16% | 74% | 10% | 125 |
| *puf-8(q725)* | 90% | 10% | 0% | 56 |
| *puf-8(q725); rsr-2(RNAi)* | 25% | 66% | 9% | 110 |

**Table R.2. Sperm-to-oocyte switch defects in *rsr-2(RNAi)* animals.** [1]animals grown at 25°C except *puf-8(ok302),* which were grown at 20°C. [2]Sp, sperm; Oo, oocytes. [3]total number of germlines scored.

Once the involvement of *rsr-2* in the germ line sex determination pathway was confirmed, other germ line genes were epistatically assessed.

Concerning the analysis of *fem-3*, a central gene of this network, *fem-3*(*e2006*) worms produce only oocytes (Table R.2) and *rsr-2* RNAi barely rescues that phenotype (only 16% of animals with oocytes and sperm), locating *rsr-2* mostly upstream of *fem-3*, although it may act partially downstream. Such an ambiguous location is frequent for genes within this germ line sex determination genetic network, hampering the establishment of a linear genetic pathway (Ellis and Schedl, 2007).

*fem-3* is a key gene in the germ line sex determination pathway and hermaphrodites cannot switch from the production of sperm to oogenesis unless FEM-3 activity is reduced. In the germline, FEM-3 levels are downregulated by repression of *fem-3* translation through its 3'UTR (Ahringer and Kimble, 1991). Cytoplasmic FBF-1, FBF-2 and NOS-3, members of the Pumilio family of translational repressors, have been implicated in this repression (Kraemer et al., 1999).

*fbf-1*, *fbf-2* and *nos-3* are redundant and strong inactivation of two of these genes is required to observe an "only sperm" phenotype (Kraemer et al., 1999; Lamont et al., 2004).

To investigate the genetic interaction of *rsr-2* with these three genes, *fbf-1*(*ok91*), *fbf-2*(*q738*) and *nos-3*(*q650*) mutants, which produce both sperm and oocytes, were treated with *rsr-2* RNAi. As a result, 30 to 50% of the animals made only sperm (Table R.2). Another RNA binding protein, PUF-8, controls redundantly with FBF-1 the sperm/oocyte switch (Bachorik & J Kimble 2005). We used two *puf-8* mutations with a wild type aspect to perform *rsr-2* RNAi. Similarly to the effect observed on *fbf-1, fbf-2* and *nos-3* mutants, *rsr-2* RNAi produced just a partial "sperm only" phenotype in *puf-8* mutants (Table R.2). We conclude that *rsr-2* cooperates with *fbf-1*, *fbf-2*, *nos-3* and *puf-8* in the sperm/oocyte switch.

To further study the possible role of *rsr-2* upstream of *fem-3*, we took advantage of a transgenic reporter of *fem-3* translational inhibition in intestinal cells.

### R.2.3. *rsr-2* is necessary for *fem-3* 3'UTR-mediated repression in somatic cells

The gene *fem-3* is regulating both the germ line and the somatic sex determination in *C. elegans* (Zarkower, 2006). The somatic expression of a lacZ reporter transgene that was controlled by the *fem-3* 3' UTR (Gallegos et al., 1998) was used as a tool to explore the possibility of *rsr-2* being a regulator of *fem-3* expression in somatic cells.

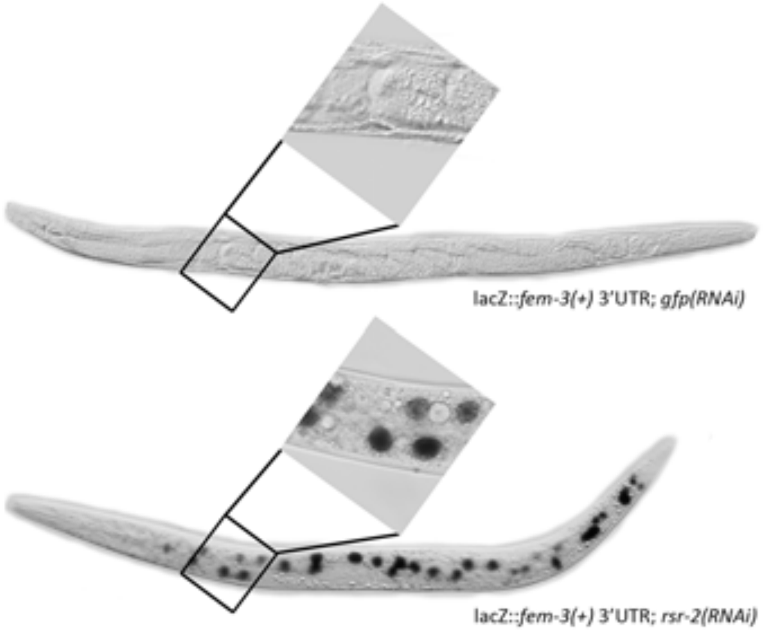
lacZ::fem-3(+) 3'UTR; gfp(RNAi)
lacZ::fem-3(+) 3'UTR; rsr-2(RNAi)

**Figure R.10. *fem-3* expression is translationally repressed by *rsr-2* in intestinal cells.** Transgenic line *qIS43* [lacZ::*fem-3(+)* 3'UTR] fed with control *gfp (RNAi)* (top) and *rsr-2 (RNAi)* (bottom) showing the amount of X-gal staining in the intestinal nuclei.

Whereas animals carrying the lacZ::*fem-3* 3’ UTR did not show expression of the reporter, *rsr-2(RNAi)* worms showed a strong lacZ expression (Figure R.10). Thus, *rsr-2* functions, either directly or indirectly, as a translational repressor of *fem-3* through its 3’ UTR. Importantly, *rsr-2* RNAi did not allow the lacZ expression on lacZ::*tra-2* 3’ UTR transgenic animals, indicating the molecular specificity of RSR-2 when regulating 3’UTRs (Table R.3).

**Table R.3. β-galactosidase activity scoring in lacZ transgene reporters.** Strains used as a staining control and specificity control are [lacZ::*fem-3(q96gf)* 3’UTR] and [lacZ::*tra-2(+)* 3’UTR] respectively. For each condition n>100 animals were scored in 3 biological replicates. +, more than 80% of animals had > 20 intestinal nuclei with X-gal staining; -, less than 20% of the animals had >10 intestinal nuclei with X-gal staining.

| **Genotype** | ***gfp(RNAi)*** | ***rsr-2(RNAi)*** |
|---|---|---|
| lacZ::*fem-3(q96) 3’UTR* | **+** | **+** |
| lacZ::*fem-3(+) 3’UTR* | **-** | **+** |
| lacZ::*tra-2(+) 3’UTR* | **-** | **-** |

## [illegible]

[illegible]

gfp

[illegible]

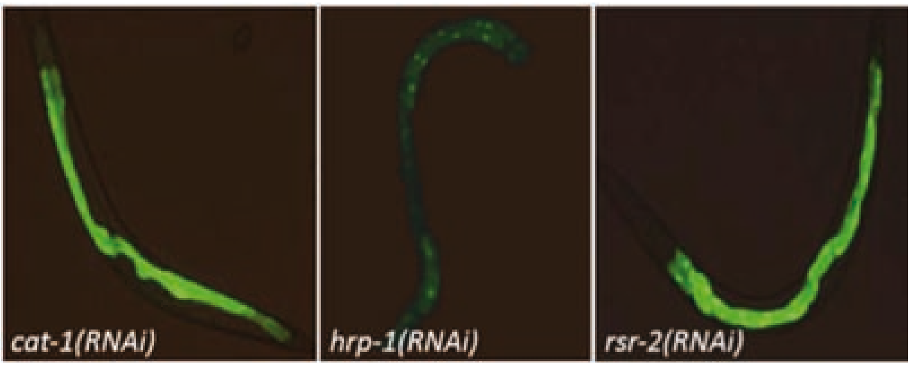
cat-1(RNAi)
hrp-1(RNAi)
rsr-2(RNAi)

[illegible]

[illegible]

# R.4. The mitosis/meiosis switch is not affected in *rsr-2(RNAi)* animals

There are two main cell fate decisions during the *C. elegans* germ line development. The first is the above-mentioned switch from spermatogenesis to oogenesis, and the second is the transformation of proliferating cells into meiotic cells. If this mitosis/meiosis switch, which is regulated by the GLP-1/Notch signaling pathway, fails, cells do not enter meiosis and keep proliferating forming a tumorous germ line. A recent report has identified splicing factors affecting the mitosis versus meiosis decision and the sperm/oocyte switch in the germ line (Kerins et al., 2010). 47 out of 114 splicing factors inactivated by RNAi in a sensitized background displayed at least one of the scored phenotypes (defect in the proliferation/meiotic entry decision or in the germ line sex determination). Since *rsr-2* was not among the tested genes we analyzed the phenotype of *rsr-2*(*RNAi*) in the same strains suitable to detect the implication of genes in the mitosis/meiosis switch.

In *rrf-1(pk1417)*; *glp-1(oz264)* animals grown at 20°C, negative control *gfp*(*RNAi*), positive control *lsm-2*(*RNAi*) and *rsr-2*(*RNAi*) presented tumorous germ line in 14.5%, 31.5%, and 15.6% of the gonads respectively (Figure R.13). These results indicate that *rsr-2*(*RNAi*) does not alter the meiotic entry decision. Since overproliferation in the germ line could be also a consequence of a defect in meiotic progression, similar RNAi assays were performed with the strain *rrf-1(pk1417)*; *gld-3 (q730)*. These experiments excluded a major role of *rsr-2* in meiotic progression (Figure R.13). According to our observations described at the end of the section R.2.1, strong inactivation of *rsr-2* by microinjection implicated that *rsr-2* is irrelevant to the mitosis-meiosis switch. Importantly, we observed the Mog phenotype (~ 40% at 20 ˚C) among the non-tumorous *rsr-2*(*RNAi*) animals, confirming the effectiveness in interfering the expression of *rsr-2*.

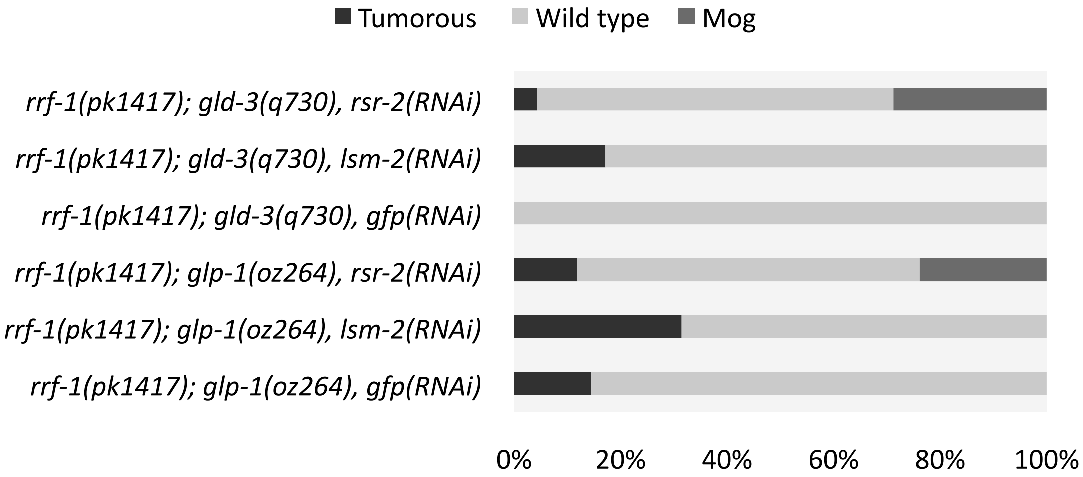

**Figure R.13. Mitosis-to-meiosis switch and meiotic progression in *rsr-2(RNAi)* animals.** *rrf-1(pk1417); glp-1(oz264)* and *rrf-1(pk1417); gld-3(q730)* mutants subjected to L1-feeding RNAi specific for *gfp*, *lsm-2* and *rsr-2* were grown and scored as described by Kerins et al., 2010. More than 70 germlines for each condition were scored. Vertical axis indicates the percentage of the animals that showed each phenotype.

In addition, we detected phosphorylation of Histone 3 by inmunofluorescence and calculated the mitotic index of *gfp(RNAi)* and *rsr-2(RNAi)* germ lines at two conditions. Neither one-day adults grown at 15 ˚C nor L4 grown at 25˚C showed increased mitotic index in *rsr-2(RNAi)* animals (data not shown). Finally, microinjection of *rsr-2* dsRNA produced diverse phenotypes like embryonic lethality, larval arrest and sterility (data not shown). Importantly, among the microinjected worms that reached the adult stage and became sterile, we detected the Mog phenotype but did not observe tumorous germ lines. Thus, inactivation of *rsr-2* by diverse RNAi protocols does not affect the mitosis/meiosis decision. Therefore, the reason for the absence of a tumorous phenotype in *rsr-2(RNAi)* worms is because *rsr-2* is not implicated in such process rather than due to an inefficient inactivation of *rsr-2*.

# R.5. RSR-2 is ubiquitously expressed in somatic cells but presents a restricted pattern in the germ line

## R.5.1. Generating *rsr-2* transgenics

There are three methods described to avoid transgene silencing in the germ line: complex arrays (Kelly et al., 1997); low-copy transgenics by gene-gun transformation (Praitis et al., 2001) and Mos1-mediated Single Copy Insertion (MosSCI) (Frøkjaer-Jensen et al., 2008) (see MM.9).

The germ line of *C. elegans* exhibits an exceptional ability to silence exogenous DNA. Besides this difficulty, gene expression studies in the germ line also present two other issues. First, most part of the germ line development takes place in a syncitium, which means that transgene products can be detected far away from the place they had been initially expressed (Hubbard & Greenstein, 2005). Second, not only promoters are important regulatory elements, but also 3'UTRs play a crucial role in germ line gene regulation (Merritt et al. 2008).

These considerations must be carefully taken together when designing transgenes whose expression will be studied in this peculiar tissue. For these reasons, several transgenic animals were generated in the laboratory to report either cellular expression of *rsr-2* or subcellular location of RSR-2 (Table R.4).

| Genotype (Extrachromosomal/Integrated) | Transformation method | Characteristics |
|---|---|---|
| *sEX20394* (*prsr-2*::GFP); *dpy-5(e907) I*<br>(Extrachromosomal) | Microinjected | GFP diffuse pattern under the control of the promoter |
| *cerEX01* (*prsr-2*::GFP::H2B::*rsr-2 3'UTR*)<br>(Extrachromosomal) | Complex arrays (Microinjected) | Silenced in one or two generations |
| *cerEX04* (*prsr-2*::GFP::RSR-2::*rsr-2 3'UTR*)<br>(Extrachromosomal) | Gene-gun | Includes all regulatory elements and the protein tagged with GFP |

**Table R.4. Transgenes and transformation methods used to study the expression and distribution of *rsr-2*.**

The *promoter rsr-2*::GFP transgene was created by fusion of PCR products (see MM.8.1). In particular, a *rsr-2* upstream region of 1.5 kb was fused in frame upstream to the GFP ORF. The PCR fragment was microinjected in *dpy-5(e907)* mutants together with the rescue vector pCeh361 [*dpy-5(+)*] (see MM.9.2). Next, phenotypically no-Dpy worms were scored for GFP expression, as described in Hunt-Newbury et al., 2007. Because small reporter proteins such as GFP diffuse inside the cell, this type of transgene facilitates the observation of cellular expression in certain structures like the vulva or the nervous system. In fact, *rsr-2* expression was clearly found in various types of neurons and vulva muscles (Figure R.14).

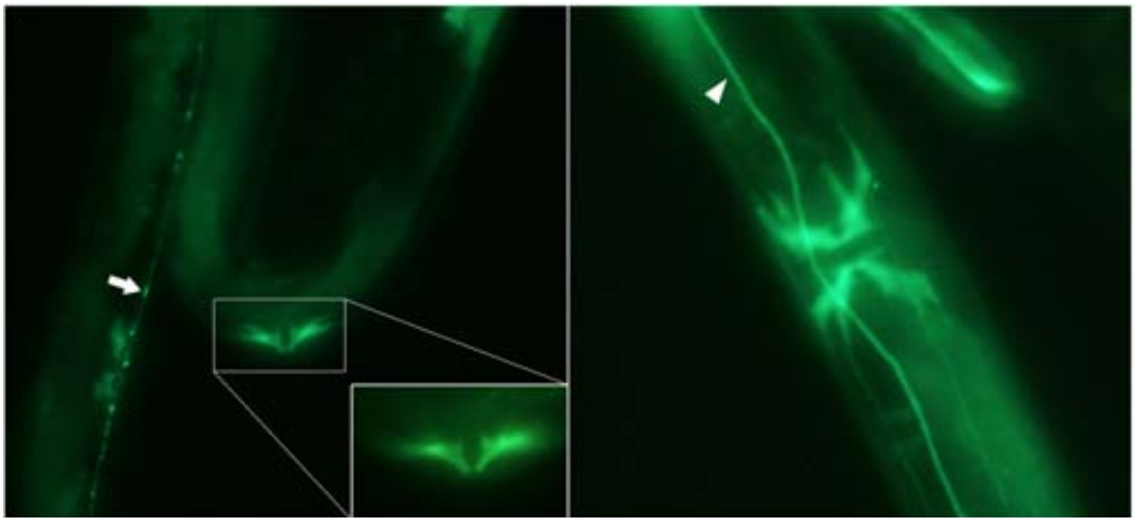

**Figure R.14. *rsr-2* expression in the soma.** Two transgenic animals expressing GFP under the control of *rsr-2* promoter. Left panel: arrow points to the nucleus of one ventral cord neuron. Magnified area shows GFP expression in vulva muscles defining the vulva structure. Right panel: ventral vision of the vulva. Arrowhead points to the axon of one ventral chord neuron.

Because this GFP-alone-fusion transgene gives a diffuse pattern, a GFP::H2B fusion was constructed and expressed under the control of 5’ and 3’ regulatory regions of *rsr-2*. The transgene *rsr-2* promoter::GFP::Histone2B::*rsr-2* 3’UTR was microinjected linearized together with digested genomic DNA to make complex arrays, what allowed germ line expression at least for one or two generations.

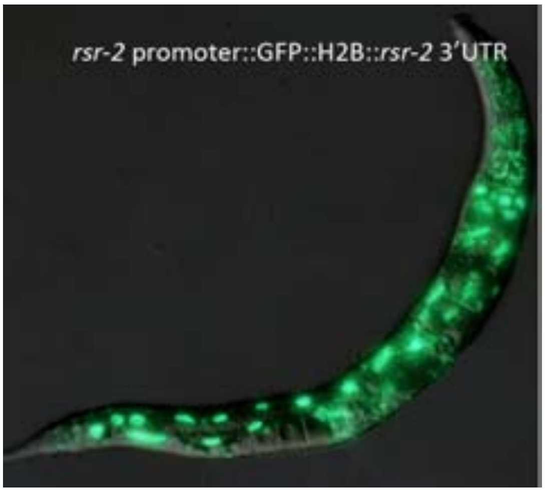

**Figure R.15. *rsr-2* is broadly expressed in somatic tissues.**

In the study of the resulting transgenics, *rsr-2* was broadly expressed in somatic tissues. It was detected in intestinal cells, hypodermal cells, muscle cells, neurons, amongst other types (Figure R.15). Interestingly, a restricted pattern was observed in the germ line since expression was low or absent in the most distal part, where mitosis takes place (Figure R.16). We corroborated this *rsr-2* expression pattern absent in the most distal part of the gonad through *in situ* hybridization experiments (Figure R.16).

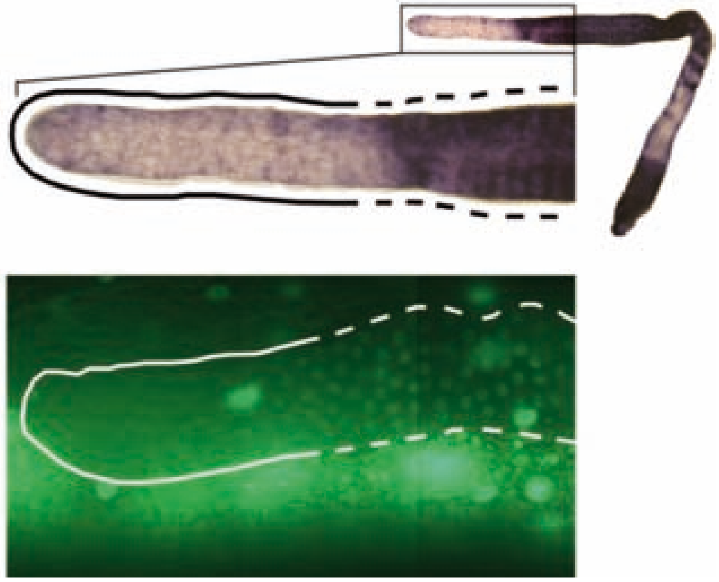

[illegible]

[illegible]

[illegible]

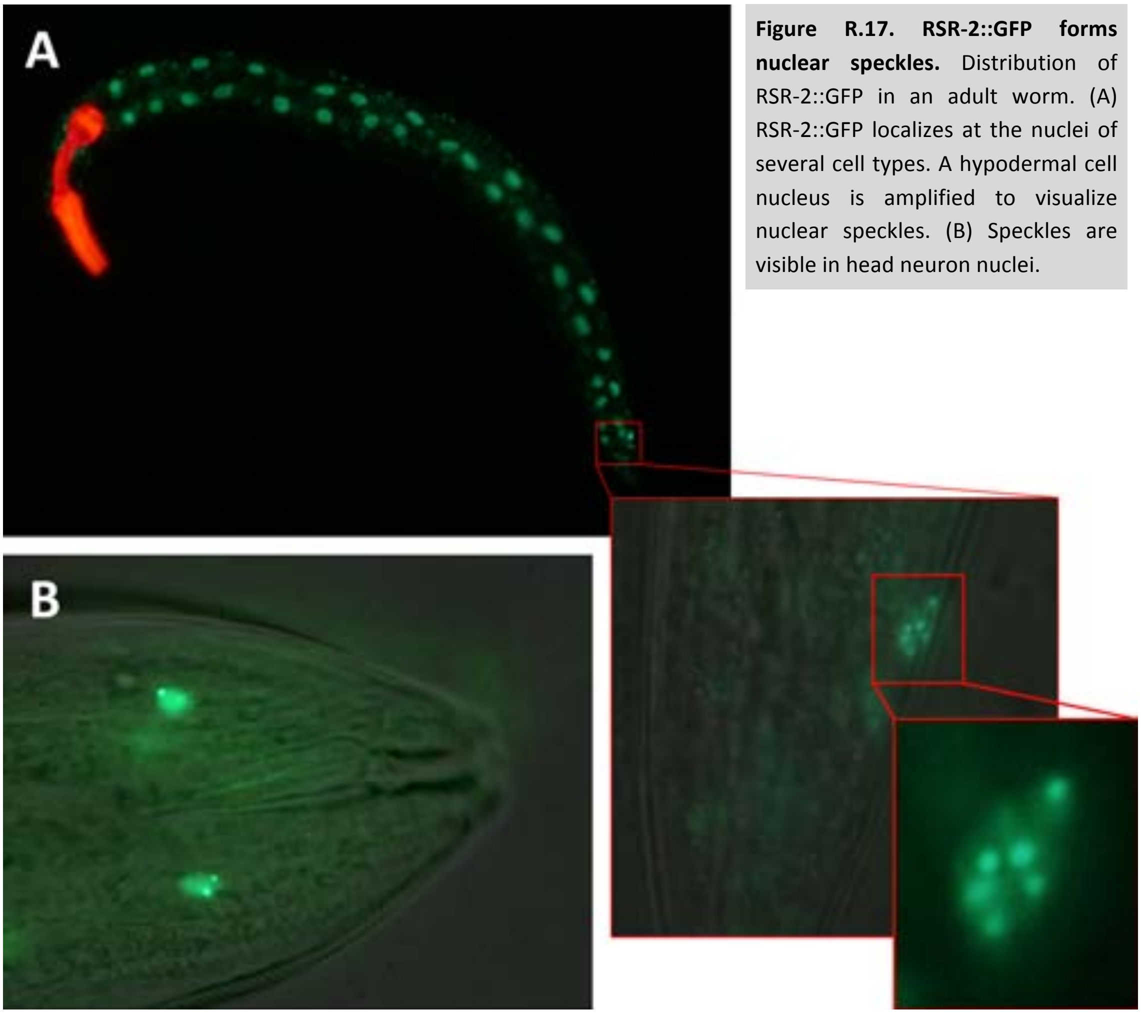

**Figure R.17. RSR-2::GFP forms nuclear speckles.** Distribution of RSR-2::GFP in an adult worm. (A) RSR-2::GFP localizes at the nuclei of several cell types. A hypodermal cell nucleus is amplified to visualize nuclear speckles. (B) Speckles are visible in head neuron nuclei.

Putting together *rsr-2* expression data, *rsr-2* is expressed ubiquitously in somatic cells and RSR-2 locates in the nucleus where it accumulates forming speckles. However, the restricted *rsr-2* expression in the germ line where different cellular processes occur at different locations is intriguing.

## R.6. *rsr-2*(*RNAi*) animals have a global decrease in transcript levels but the splicing mechanism seems not to be affected

### R.6.1. Tiling arrays reveal a general decrease in transcript levels of *rsr-2(RNAi)* L4 animals

As it has been shown in the previous R.3 section of this thesis, constitutive splicing is not affected in *rsr-2(RNAi)* animals in a somatic lineage as the intestine at least. Still, these are the questions that need to be answered:

- Does *rsr-2* RNAi affect constitutive splicing in other lineages?
- Does rsr-2 RNAi affect constitutive splicing of other transcripts?

To answer these questions and shed light into the molecular functions of *rsr-2* during *C. elegans* development Affymetrix tiling arrays 1.0 (ref 900935) were used to examine not only transcript levels but also intron retention and alternative splicing events.

Total RNA was extracted and purified from L4 synchronized animals grown at 25°C (36 hours after L1) in *gfp* and *rsr-2* RNAi plates. Under these conditions, harvested worms are in late L4 stage, when the germ line switches permanently to oogenesis. This protocol matches one of the conditions followed by the modENCODE consortium for transcriptome analysis of different strains done by tilling arrays and RNA-Seq (Celniker et al., 2009; Gerstein et al., 2010).

We used two experimental replicates for each condition and raw data (CEL files) was analyzed using the Affymetrix® Tiling Analyses Software (TAS) V. 1.1.02. This analysis provided information about the levels of 30431 transcripts. To estimate gene expression in control *gfp*(*RNAi*) and *rsr-2*(*RNAi*) animals, we used bioinformatics tools to plot mean signal intensities for transcripts, exons and introns by chromosomes (Figure R.18). Using the tools implemented in the Galaxy platform (Goecks et al., 2010; Blankenberg et al., 2011) and based on the information contained in the worm genome assembly WS180, the array signal values were used to infer the mean signal intensity for each gene in control and *rsr-2(RNAi)* worms as an indirect estimation of whole gene expression. These estimates were used to recognize up and down regulated genes in the *rsr-2(RNAi)* population, and also to characterize the transcriptional patterns of each chromosome.

i sc e lpcsc, t sev 1 t f v vi v lgl6y s sc f cse3 cls3i v t g h ll h 1f vst e svi h se vh ec hs, v9 Tt e9 e1 sevht e g lc 2t h ll vi i ht n t ct n c) lvi t f 3i vi 1s22 h e c h et v cv vscvs llp cs3es2 ev9 vi v e1 e p vt. h1c 1sn sesci 1 l g lc t 2 vh ec hs, vc sc l h h se f vt ct n c vi e se i ht n t ct n )

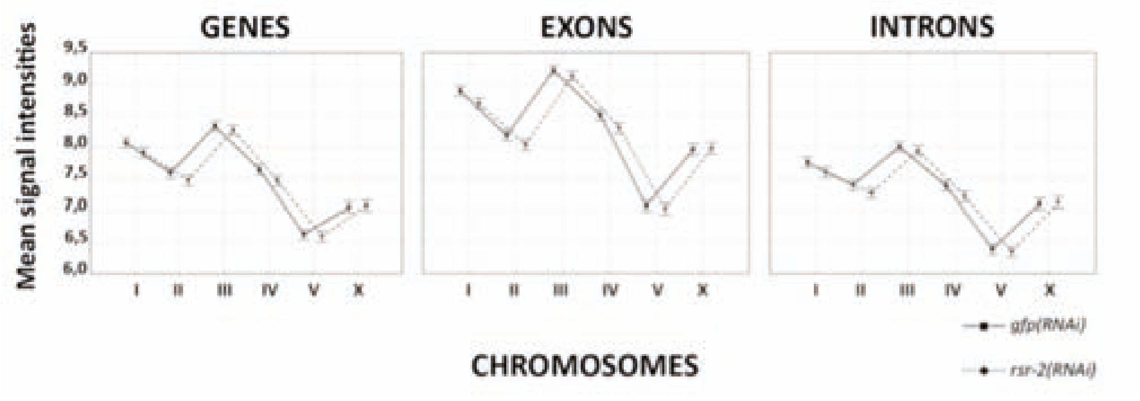

**ui t c 3/B3 . PL c yyu1. g . i yu lrg . u y3** t n, hsct e v. e eos( o c t evht l e1 lgl6y( o esn lc t 2 vi g h3 cs3e l sev ecsvs c vh ec hs, vst e t 2 3 e c9 Tt ec e1 sevht ec t 1 1 p i ht n t ct n c) ht h hc t f ev 2t h tv e1 h1 1 gs vst e v. e vi v. t st lt 3s l h, ls v c)

se Tt ec e1 sevht ec 1sc, l p csn sl h g lf c se v hn c t 2 h e cs3e l sev ecsvs c vi ht f 3i vi 3 et n t e lf 1 vi v9 t g h ll9 vh ec hs, vst e sc 22 v 1 i sl c, ls se3 sc e t v)

## t3tj t d1 a a em d1 ls a e e a e d ad 1 s a sn ad r. l a e a h s d1 e

e t h1 h vt 3 v h t h se 2t hn vst e t f v 1t. eh 3f l v 1 3 e c 1se3 vt vi ll t 2 vh ec hs, v sev ecsvp cs3e lc se lgl6y J d esn lc9 c l v 1 3 e c i t c T, h ccst e g lc h W5K i s3i h t h t. h vi e vi t evht l) i f c9 lscv t 2 C' W/ f, h 3f l v 1 vh ec hs, vc JC65“ 3 e c e1 Wq8D 1t. eh 3f l v 1 vh ec hs, vc JWD5/ 3 e c. c t v se 1) i c v. t 3 e lscvc . h f, lt 1 1 vt h t 1 se i vv, 4zzsev hn se )n t 1 e t 1 )t h3E9 i s i sc h ct f h vi v ll t. c sev hc vst e t 23 e c t 2 sev h cv svi 3 e t ll vst ec 3 e h v 1 p 1sg hc , f ls vst ec)

ev h cvse3lp9 3 hn se 3 e c h t f e1 t g hh, h c ev 1 n t e3 vi 1t. eh 3f l v 1 J l )8E) t n a t h 1s22 h e c. h 1 c hs 1 t e hese3 ct n M, s2s 3 e c e1 lv he vsg c, ls se3M 3f l v 1 3 e c p sevht e h v evst e) c h n hm h cf lv9 vi n a t hsvp t 2 c, hn vt 3 e csc 3 e c. h 1t. eh 3f l v 1 e1 t elp t e c, hn M, s2s 3 e . c t g h T, h cc 1 e vi lgl6y( o m3ht f e14 t e6S)

| Gene clasess | Upregulated > 1,2<br>1609 | Downregulated < 0,8<br>2308 |
|---|---|---|
| 169 germ line-specific genes[1] | 0 | **28** |
| 844 spermatogenesis genes[2] | 1 | **298** |
| 1177 soma specific genes[3] | 36 | 26 |
| 2215 germ line-enriched genes[4] | 34 | **133** |
| 4678 germ line-expressed[5] | 38 | **138** |
| 545 intron-retention AS[6] | 10 | 16 |
| 3339 genes in operons[7] | 35 | 41 |
| 551 intronless genes[8] | 48 | 64 |

**Table R.5. Gene expression group analysis in *rsr-2(RNAi)* animals.**

[1] Germline-specific genes. Union of germ line-enriched and germ line SAGE (tag > 0) (Reinke et al., 2004), intersected with SMD (Strictly Maternal Degradation) class genes (Baugh et al., 2003), subtracted any gene also expressed (tag > 0) in muscle, gut or neuron SAGE (Wang et al., 2009; Meissner et al., 2009). Compiled by Andreas Rechtsteiner & Susan Strome.

[2] Spermatogenesis genes. (Reinke et al., 2004). Compiled by Andreas Rechtsteiner & Susan Strome.

[3] Soma-specific genes (gut, muscle or neuron). Expressed in gut, muscle, or neuron SAGE (tag > 8) minus any gene germ line-enriched or germ line-expressed (germline SAGE tag > 0) (Meissner et al., 2009; Reinke et al., 2004; Wang et al., 2009). Compiled by Andreas Rechtsteiner & Susan Strome.

[4] Germ line-enriched genes, not including spermatogenesis-related genes (Reinke et al., 2004). Compiled by Andreas Rechtsteiner & Susan Strome.

[5] Germ line-expressed genes based on SAGE data (Wang et al., 2009). Compiled by Andreas Rechtsteiner & Susan Strome.

[6] Intron Retention in Alternative Splicing events (Ramani et al., 2011).

[7] (Allen et al. 2011)

[8] Extracted from www.wormbase.org (WS220)

Such a decrease in transcripts required for spermatogenesis suggests that, although *rsr-2*(*RNAi*) animals are able to make sperm but not oocytes, sperm may not be properly differentiated.

Sperm-enriched and germ line intrinsic genes are nearly absent from the X chromosome (Reinke et al., 2000). Thus, the differential effect that we observed in expression levels of the X-chromosome (Figure R.18) could be due to the strong downregulation of sperm-related genes in *rsr-2(RNAi)* animals. Since most sperm-enriched genes are located in autosomes, *rsr-2(RNAi)* worms with less expression of sperm genes should have a higher ratio of X chromosome/autosomal gene expression.

To validate the tiling array data quantitative Real Time PCR (qRT-PCR) was performed to study expression levels of a chosen subset of germ line sex determination genes. In terms of gene expression, qRT-PCR is more sensitive than tiling arrays. In both methods, a reference value of 1 was set in the control *gfp(RNAi)* sample to be compared with the *rsr-2(RNAi)* sample. In general accordance with results from tiling arrays (Table R.6), qRT-PCRs of three independent experimental samples revealed that all the tested genes except *fog-1* (enriched in sperm) (Lamont & Kimble, 2008) had reduced levels of mRNA in *rsr-2*(*RNAi*) versus *gfp(RNAi*) animals (Figure R.19).

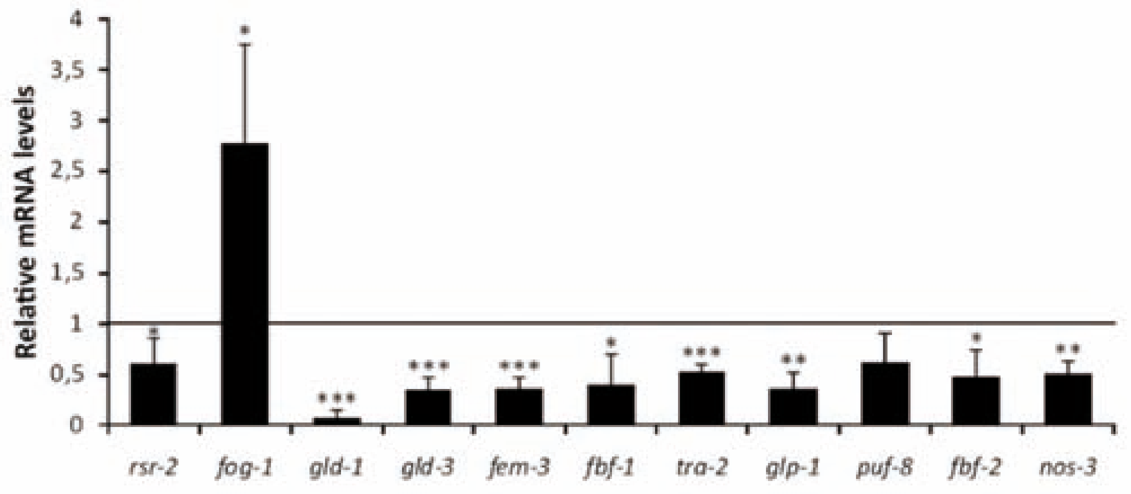
Relative mRNA levels
4
3,5
3
2,5
2
1,5
1
0,5
0
*
*
***
***
***
*
***
**
*
**
rsr-2
fog-1
gld-1
gld-3
fem-3
fbf-1
tra-2
glp-1
puf-8
fbf-2
nos-3

[illegible]

| [illegible] | [illegible] | [illegible] |
|---|---|---|
| [illegible] | [illegible] | [illegible] |
| | [illegible] | [illegible] |
| [illegible] | [illegible] | [illegible] |
| [illegible] | [illegible] | [illegible] |
| | [illegible] | [illegible] |
| [illegible] | [illegible] | [illegible] |
| [illegible] | [illegible] | [illegible] |
| [illegible] | [illegible] | [illegible] |
| | [illegible] | [illegible] |
| [illegible] | [illegible] | [illegible] |
| [illegible] | [illegible] | [illegible] |
| [illegible] | [illegible] | [illegible] |
| [illegible] | [illegible] | [illegible] |
| | [illegible] | [illegible] |

[illegible]

[illegible]

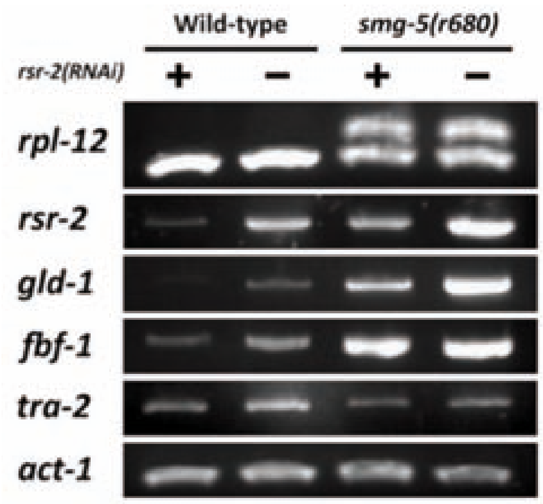
Wild-type
smg-5(r680)
rsr-2(RNAi)
+
−
+
−
rpl-12
rsr-2
gld-1
fbf-1
tra-2
act-1

## [illegible]

[illegible]

[illegible]

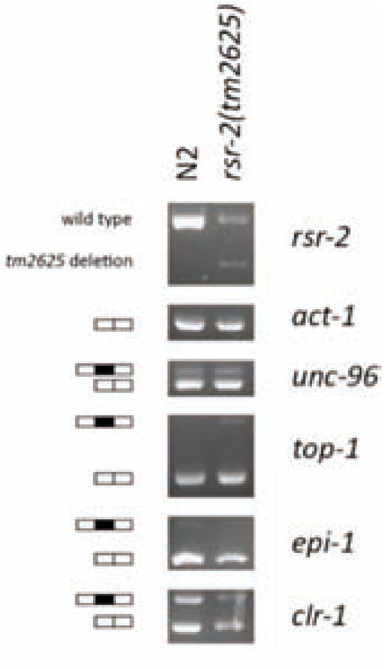
N2
rsr-2(tm2625)
wild type
tm2625 deletion
rsr-2
act-1
unc-96
top-1
epi-1
clr-1

[illegible]

[illegible]

[illegible]

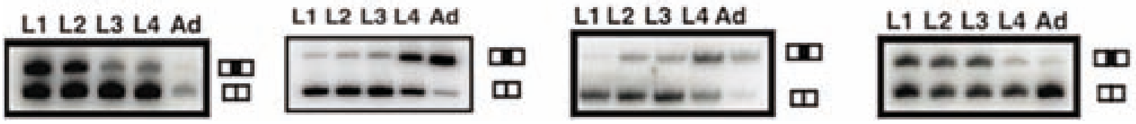
unc-96
top-1
epi-1
clr-1
L1 L2 L3 L4 Ad
L1 L2 L3 L4 Ad
L1 L2 L3 L4 Ad
L1 L2 L3 L4 Ad

[illegible]

No obvious differences were observed between the regulated expression of the two splice variants of *unc-96*, *top-1*, *epi-1* and *clr-1* in *tm2625* enriched population versus the wild type.

Altogether, although we cannot discard that RSR-2 may participate in specific AS events, our data suggests that RSR-2 does not have a key role in AS.

# R.8. Functional links between RSR-2 and transcription

## R.8.1. Specificity of a novel antibody against RSR-2

Upon our request, the SDIX company generated a rabbit polyclonal antibody (Ab) against RSR-2 in two different animals. Among the 425-aminoacid sequence of the protein, the epitope recognized by these antibodies comprises aminoacids from positions 39 to 138 (Figure R.23).

MYNGIGLQTARGSGTNGYVQSNLSHLMQARRKIEYNGE**DDLRKMEAELNRKPNEEIMDHNRKRQIEVKC**
**TEFEMLLEDKGLDDEDIERKVGEYRKNLLKQLESGELNVDEELSTKESHARRRAAANNRDKMRNALGLG**
EDYVPGSSMAKMNKSDVVGAAMESELPQKDDKEKLLETLRLHRKSKKKQESSSSSSSSSSSSESSSEDE
KHRKDRKKKEKKQKLKEMEKRREKLRQKERELLAVSDKVKKEEPAESSDEEDSRKDQRKPREDRRRSVE
RQDQREDRRDRRRSPEDPRERRRSPEDRTVRRRSPERRRQQRSPSVERRKSPQRRDERRRRHDSSENER
RSTATASKKSRMDELEVKQEPPSDSEDYIAKTNLAPIRVEKSAEKVEKSRKSSSESSSGSSDSDSSSDS
SSSSDSSSDSE

**Figure R.23. RSR-2 protein sequence.** The immunogen peptide used to generate an antibody against RSR-2 is highlighted in bold red letters.

Firstly, to validate the Ab specificity, a western blot was performed. N2 worms were grown in parallel in *rsr-2* dsRNA and L4440 empty vector-producing bacteria. Once reached the adulthood, animals were harvested and protein fractions prepared (see MM.13). 87 μg of each sample were loaded in a 10% acrylamide gel and western blot performed with the RSR-2 antibodies produced by two different rabbits. Two loading controls were used: actin and histone 3.

The Ab generated in animal #1 is named Q5091 and the Ab generated in animal #2 is named Q5092. We determined that both antibodies are specific in detecting RSR-2 and they present the same band pattern by western blot. Importantly, RSR-2 protein levels are substantially reduced when inhibiting *rsr-2* gene expression by RNAi (Figure R.24).

Three proteins bigger than RSR-2 are also recognized by the two antibodies Q5091 and Q5092 (Figure R.24, arrows). Despite that fact, *rsr-2(RNAi)* can practically abolish protein levels of RSR-2 while levels of unspecific bands are not affected, validating our RNAi targeting strategy. Because the Ab Q5092 recognizes RSR-2 as efficiently as the Ab Q5091 but detect with less intensity the proteins representing the unspecific bands, we chose the Ab Q5092 for further experiments.

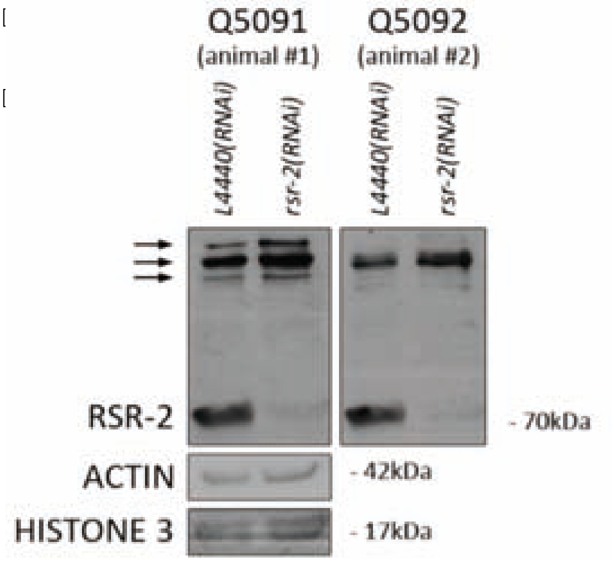
Q5091
(animal #1)
Q5092
(animal #2)
L4440(RNAi)
rsr-2(RNAi)
L4440(RNAi)
rsr-2(RNAi)
RSR-2
ACTIN
HISTONE 3
- 70kDa
- 42kDa
- 17kDa

[illegible]

## [illegible]

[illegible]

[illegible]

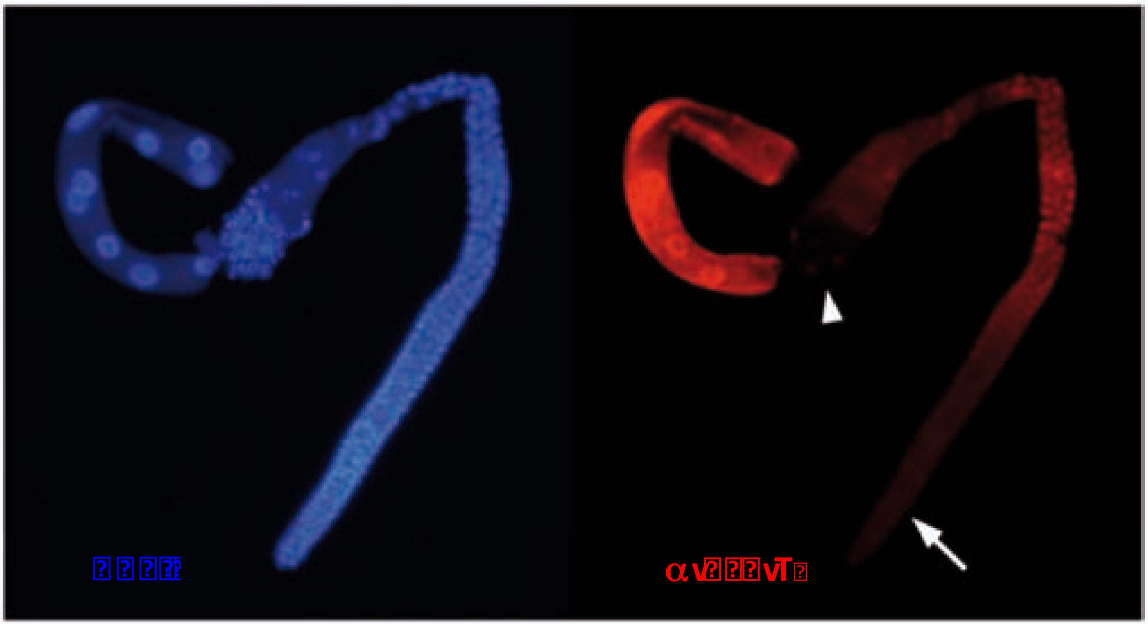

[illegible]

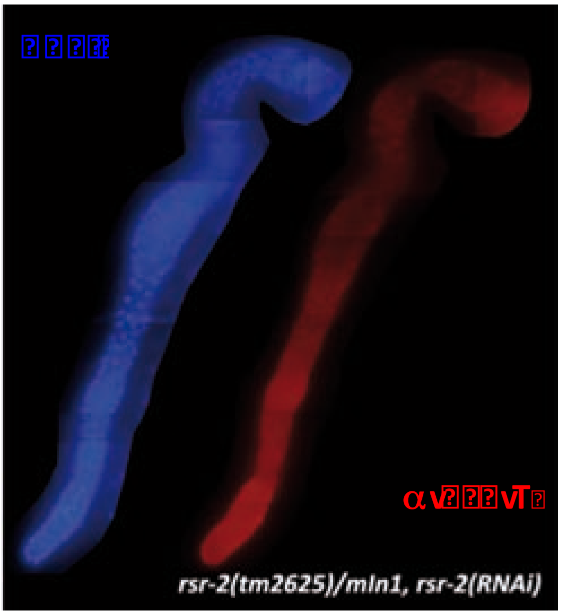
rsr-2(tm2625)/mIn1, rsr-2(RNAi)

[illegible]

[illegible]

[illegible]

[illegible]

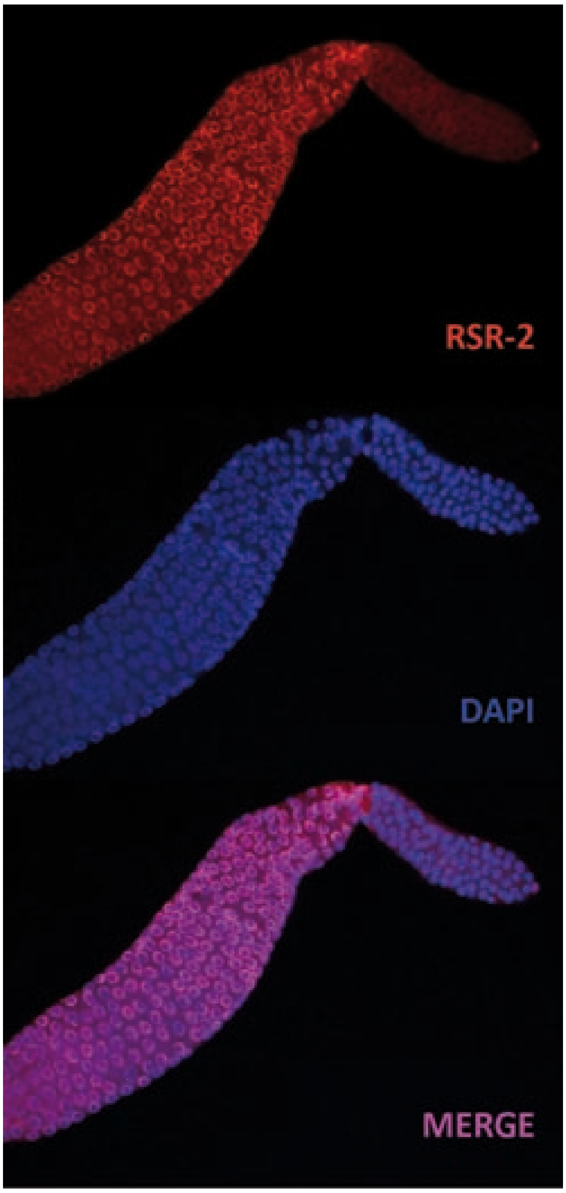
RSR-2
DAPI
MERGE

[illegible]

[illegible]

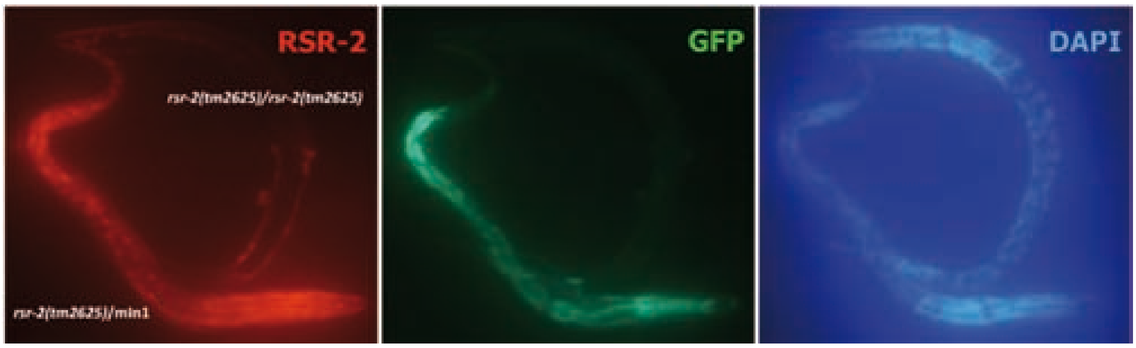
RSR-2
GFP
DAPI
rsr-2(tm2625)/rsr-2(tm2625)
rsr-2(tm2625)/min1

[illegible]

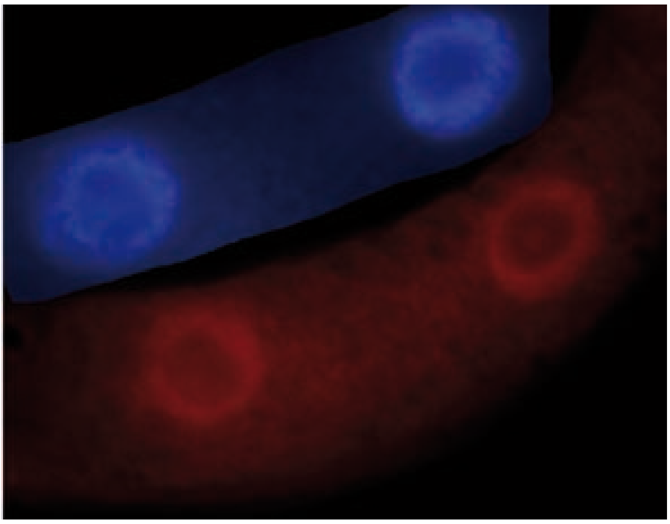

[illegible]

[illegible]

[illegible]

## □tutTt□ □□□□h□□o□ □i m□d□ □ale□ d□g□□.□ l□□l□ □□□□hj□ □sh □1 1 r a s md□□□m□□l□e□n □□□□□ds1 □l□a□e□1 □□d.S□1s□□□□□m.s.S1 □d□e□□□□

### □tutTt2t□□al□h□□□hj□□1 1 r a s md□□□m□□l□e□□□ds1 □l□a□

□sg e□vi □□t Mt□□lsu□vst e□t 2□□□□MV□. svi □□i ht n □vse□t □c hg 1□□p□sn n f et 2lf t h c□ e□ 9□. □ □□hs 1□t f v□□□i □□M□ w□cc□p□f cse 3□tx.M□□□MW□□□□□□85“W□vt □eg cvs3□v □vi □□cct □s□vst e□t 2□□□□MV□ . svi □□i ht n □vse)□□ cs1 c9□vi □□evs□t 1p□/□ □C6□□3□secv□□□□□, t lpn h□c □□□J□□□□□□□E□ □c□lct □ f c 1□se□. sl1□vp, □□esn □lc9□□e1□se□lgl6y(□□□□9□□esn □lc□vt □cvf 1p□s2□□□□MV□l g lc□□22 □v□vi □ 1scvhs□f vst e□t 2□□□□□□□□)□

□i □□M□ w□ □cc□pc□ . h □ , h2t hn 1□ 2t llt . se3□vi □. t hn2t . □c□i n □se□ 2s3f h □□)D5)□□ □sn n f et , h □s, sv□v 1□ □i ht n □vse□t 2□□ W□□esn □lc□vh □v 1□□e1□ et e Mh □v 1□ svi □lgl6y□□□□s□vi □v□ h □ i □hg cv 1□□v□□q□cv□3 □JD6□ t f hc□, t cvM i □v□i se3□ □v□ W8j□E)□ □t h□ 1 v□sl 1□ , ht vt □t l□t 2□vi □, ht □ 1f h □2t llt . 1□vt □ sn n f et , h □s, sv□v □ □i ht n □vse□ c □ □ □ )Cq□t □vst e□t 2□vi sc□vi csc)□

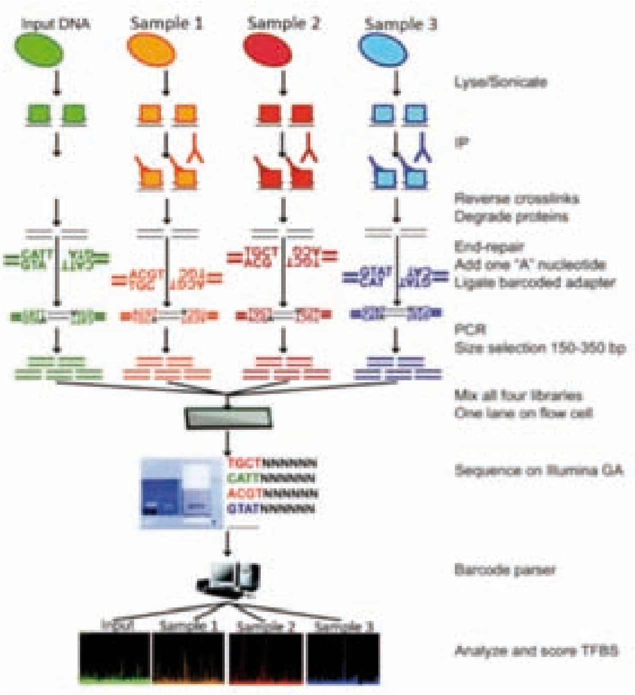
Input DNA
Sample 1
Sample 2
Sample 3
Lyse/Sonicate
IP
Reverse crosslinks
Degrade proteins
End-repair
Add one "A" nucleotide
Ligate barcoded adapter
PCR
Size selection 150-350 bp
Mix all four libraries
One lane on flow cell
TGCTNNNNNN
CATTNNNNNN
ACGTNNNNNN
GTATNNNNNN
Sequence on Illumina GA
Barcode parser
Input
Sample 1
Sample 2
Sample 3
Analyze and score TFBS

**□ui t c□□□3bH3□g□□w□f □C 1ceF1C** □□ t 1s2s 1□2ht n □□ 2h□e□t sc□ v□□l)9□ W55“E)□□ e h□vst e□t 2□□□n f lvs, l T 1□ls□h□hp□sc□, h2t hn 1□□p□ ls3□vse3□□□□□h□t 1 1□□1□, v h□vt □□t vi □ e1c□t 2□□i □□ 1□□e1□se, f v□ □□□□□2h□3n evc)□□f □c wf evlp92t f h□1s22 h ev□□□h□t 1 1□s□h□hs c□ □h □h sT 1□ wf sn t l□hlp□e1□h□e□t e□□□cse3l □□e □t e□2t . □□ llt 2□□□ □llf n se□□□□□t wf e□ h)□□

□i □ 3 e h□vst e□ t 2□ □□ ls□h□hp□ 2t h□ □llf n se□□□i □□M□ w□. □c□, h2t hn 1□□c□ 1 c□hs□ 1□se□□ 2h□e□t sc□ v□□l)9□W55“)□ □e□□lswf t v□t 2□ci □h 1□. t hn □lpc□v □ . □c□et v□sn n f et , h □s, sv□v 1□□f v□ □c□ t vi h sc □, ht □ cc 1□vt 3 vi h□. svi □ vi □□i □□ 1□c□n , l c□□2v h□vi □□□cv , □ J□s3f h □□)D59□c□n , l □se□3h e□)□□i □v□□□□9□v hn 1□se, f v□□□□9□sc□□□h 2 h e□ □t 2□vi □cv□hvse3□ n □v hs□l□2t h□□i □□M□ w)□□llf n se□□□□□□ls□h□hs c□ h □3 e h□v 1□2ht n □□t vi □□i □□□e1□se, f v□□□□□ c□n , l c)□□e□n f lvs, l T□□i □□M□ w9□□□□□h□t 1 1□□1□, v h□sc□ls3□v 1□vt □ □□i □□□□□c□n , l )□□i □ □□h□t 1 □ □cD□f eswf □□□c c□2t llt . 1□p□□vsn s1se □ef □l t vs1 □vt □ee □l□ svi □vi □e1M1 , □sh 1□ □□□□9□ i s□i □□t ev□sec□□1 ese □ef □l t vs1 □t g hi □e3c)□□t f h□ls□h□hs c□□h □vi e□, t t l 1□vt 3 vi h□ □e1□hf e□vi ht f 3i □□□cse3l □2t . □ llt□□e )□□2v h□c wf e□se39□h □1c□□h □c , □h□v 1□se□vi □□ et n □ □e□lpu h□□□□t h1se3□vt □vi □2shcv□2t f h□□□c c□□e1□□ls3e 1□vt □vi □ t hn □3 et n □J□ 2h□e□t sc□ v□□l)9□ W55“E)□□

f c2f llp9 sn n f et , h s, sv v 1 i ht n vse svi vi αM MM evs t 1p) t 3 e h v vi ls h hp 3 lMds 1 e1 , f hs2s 1 2h 3n evc 2ht n C/5 vt D85 , s3f h )DCE)

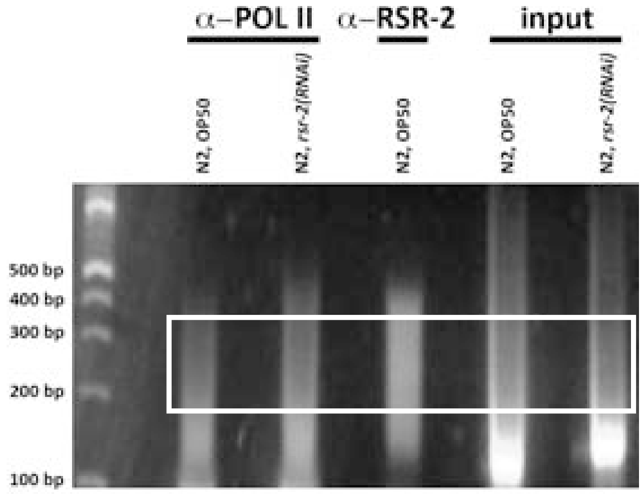
α-POL II
α-RSR-2
input
N2, OP50
N2, rsr-2(RNAi)
N2, OP50
N2, OP50
N2, rsr-2(RNAi)
500 bp
400 bp
300 bp
200 bp
100 bp

**ui t c 3b/3 gc1l lu t y 1 i . c l lg F1t c c1 t l u l t lL P uc cu y3** n n f et , h s, sv v 1 i ht n vse e1 se, f v h hf e t e e 3 ht c 3 l e1 2h 3n evc t 2 , , ht , hs v csu c J2ht n C/5 vt D85 , 2h 3n evcE h c l v 1 e1 , f hs2s 1 vt , h , h vi h t 1 1 n f lvs, l T 1 ls h hs c)

### tutTtj hj mdeale ds1 l ah a a m ll da e ,d ls l

f h, hscse 3lp9 vi , m , ht 2sl t v se 1 2ht n vi e lpcsc t 2 vi M i M w h c n l c9 svi cls3i v h t 1s2 vst ec9 vi i ht n vse Mse1se3 , vv he t 2 J s3f h )DWE) e 11svst e9 *lgl6 y(* c9 , h g evc M vt Mh n f et , h s, sv v . svi i ht n vse 1 n t ecvh vse 3 vi v vi i ht n vse se1se3 , vv he t c hg 1 sc t , s2 2t h M s3f h )DWE)

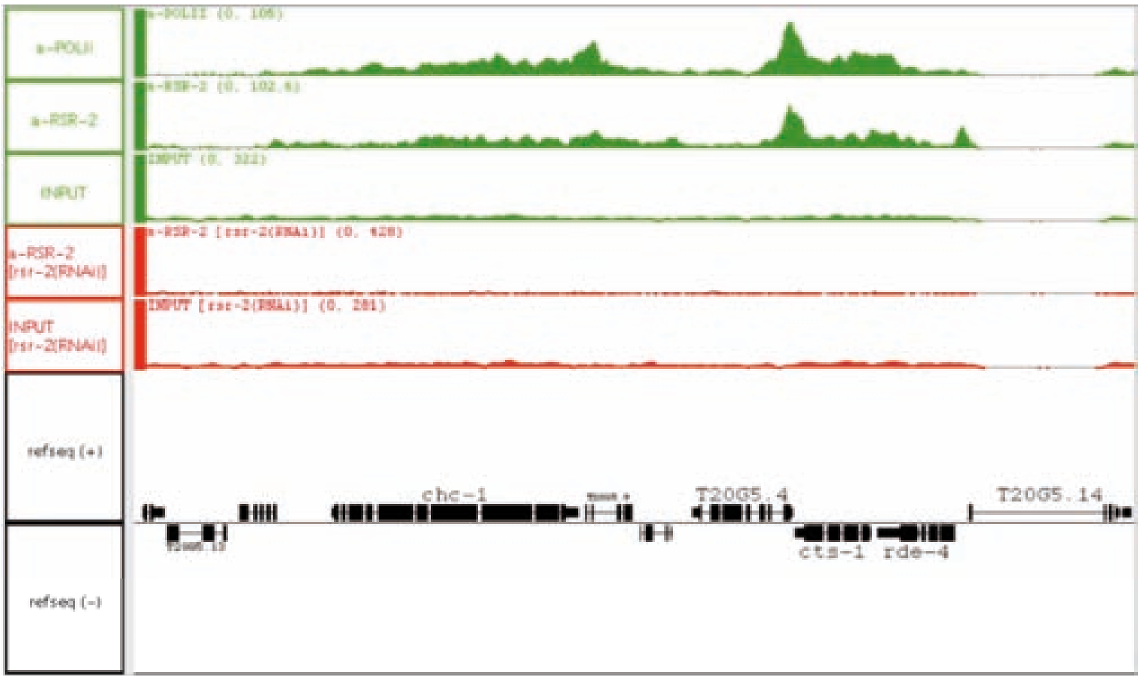

**ui t c 3bT3 gc1l lu v u ui 1 c1 Fu y1 F . vT c yu u c3** v s t 2 i ht n t ct n ) i M w 1 v . c gscf lsu 1 f cse 3 vi ev 3h v 1 et n ht . c h J E ct 2v. h 6)8)D) 2ht n 22n vhsT) ht 2sl c se 3h e h , h c ev vi , mc t 2 M M e1 vi sh t hh c, t e1se3 se, f v ) ht 2sl c se h 1 se1s v M , mc se *lgl6y* net m 1 t . e m3ht f e1 e1 vc se, f v )

[illegible]

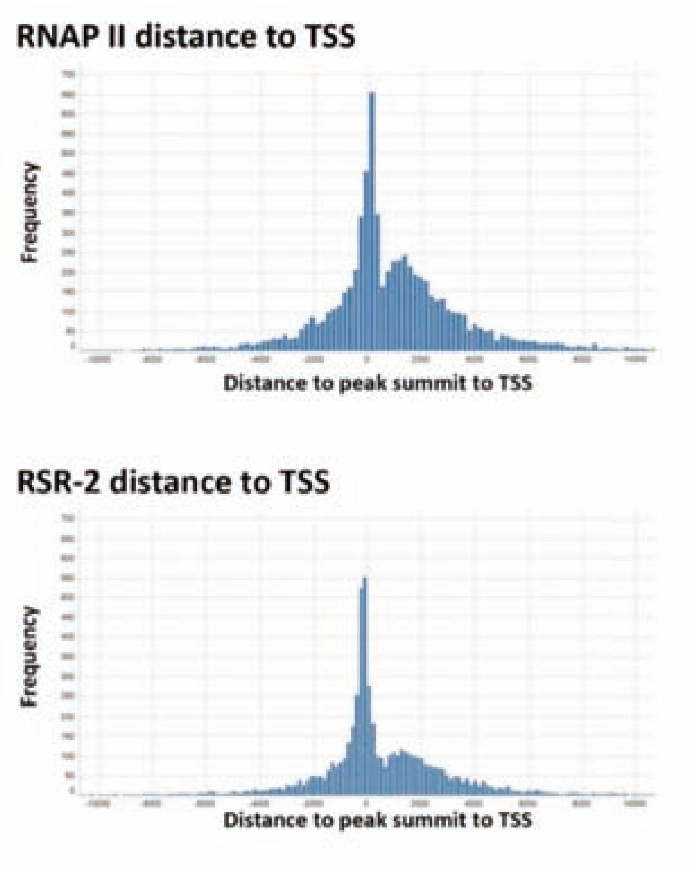
RNAP II distance to TSS
Frequency
Distance to peak summit to TSS
RSR-2 distance to TSS
Frequency
Distance to peak summit to TSS

[illegible]

[illegible]

[illegible]

[illegible]

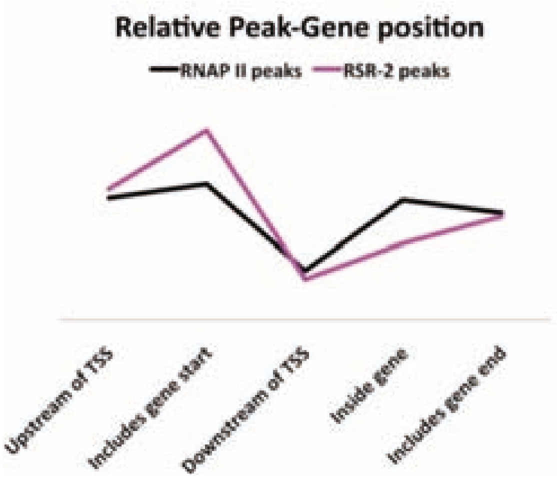
Relative Peak-Gene position
RNAP II peaks
RSR-2 peaks
Upstream of TSS
Includes gene start
Downstream of TSS
Inside gene
Includes gene end

[illegible]

[illegible]

## [illegible]

[illegible]

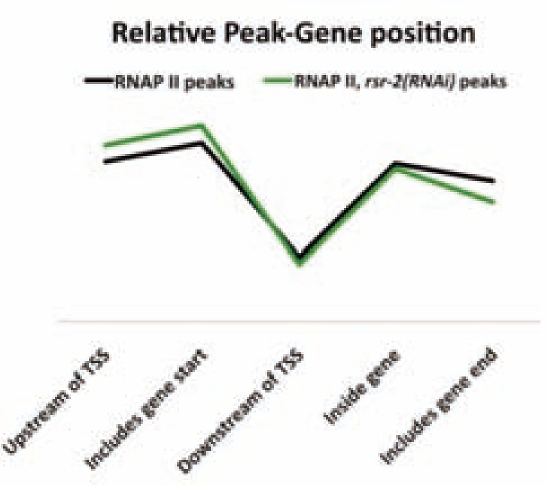
Relative Peak-Gene position
RNAP II peaks
RNAP II, rsr-2(RNAi) peaks
Upstream of TSS
Includes gene start
Downstream of TSS
Inside gene
Includes gene end

[illegible]

[illegible]

[illegible]

**tutwt Sm dm s em s dS. l r1 r. l e a n s dI e**

i se2 h e c h 1 2htn vi i M w 1 v e lpcsc9 svi i e3se3 svc 1scvhs f vst e lt e3 e g h 3 1 3 e f, te *lgl6y* se vsg vst e 1 f c seg cvs3 v , htv se l g lc se *lgl6 y(* *o9* t hn c) , h, h 1, htv se Tvh vc 2htn qNpe i htesu 1, t, f l vst e t 2 s l1 vp, . t hn c h v 1 svi *eos(* *o9* tevht l t n, l E e 1 *lgl6y(* *o,* c T, l se 1 se )CD)

t h h3 cf fesv 1 v vst e9 v. t 1s22 h ev evs t 1s c h f c 14 / C69 h t 3esuse3 vi 7 e 1 W59 se1se3 vt vi N h se l h 3st e) svi h / C6 t h W5 h t 3esu c vi v. t, i t c, i t sct 2t hn c t 2 vi e upn A vsg i p, h, i t c, i t hpl v 1 2t hn t 2 tE e 1 i p, t, i t c, i t hpl v 1 Ek)

i f c9 t vi h n, l t p 1 vt l vt wf evs2p vi vsg v 1 cv v t 2 , h c ev se vi Tvh vc) D5 µ3 t 2 i c n, l . h l t 1 1 se ')8K hpl n s1 3 l e 1 . cv he l t v , h2t hn 1 svi vi v. t ) vse c f c 1 c l t 1se3 tevht l) v cithv T, tcf h , hst 1c t 2 vi h n h e vt vi N p 2sn 9 t elp vi i p, h, i t c, i t hpl v 1 sct 2t hn c gscs l 2v h 1 v vst e p vi evs t 1 p / C6) n h m lp9 i p, h, i t c, i t hpl v 1, htv se l g lc h is3i h se *lgl6y(* *o9* esn lc J s3f h )D6 E) v l t e3 h T, tcf h , hst 1c vi v. t , i t c, i t sct 2t hn c h t c hg 19 se3 vi t 2t hn h t h sev ec )

scvse l p 2htn / C6 e 1 1 f vt vi N h se l t vst e t 2 vi , svt, 9 svi W5 t vi t e 1 h 1 v v 1 svi et, h 2 h evs l se1se3 vt t e t h e t vi h) ev h cvse3lp9 . 2t f e 1 vi v9 t n, h 1 vt vi tevht l9 vi i p, h, i t c, i t hpl v 1 2t hn t 2 vi c ehs i 1 t g h vi i p, t, i t c, i t hpl v 1 2t hn s3f h )D6 E)

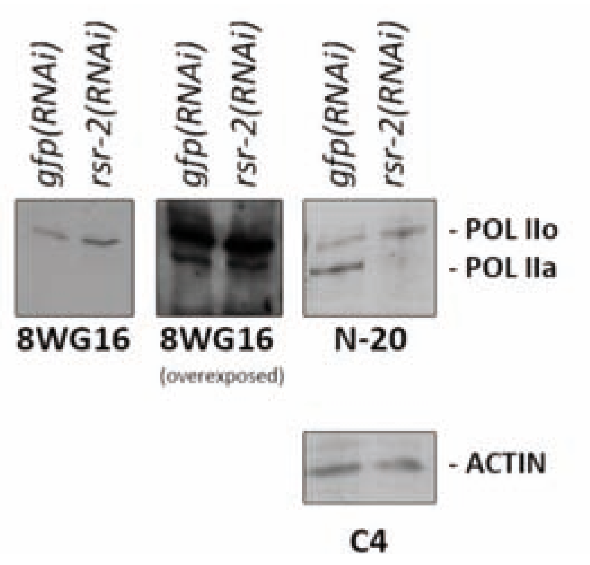

**u i t c 3b63 s L c L g 1 y L g 1 c s l t l t l y u l r g C 1 c l y 3** i s c T, hsn ev . c , h2t hn 1 p t evc hh v t hv M N M sg E) ht v se Tvh vst e c t n, lsci 1 p f cse3 CK )

m e vt 3i vi h9 vsg 2t hn Ji p, h, i t c, i t hpl v 1 E sc ehs i 1 se *lgl6 y(* *o9* . t hn c) t. g h9 c cit. 1 , h gst f clp9 *lgl6y* s n p 1 h c vi vh ec hs, vst e l 22s s e p) sev h, h v vi c h cf lvc p h3f se3 vi v is3i h l g lc t 2 vsg 1t etv e cc hslp sn, lp n t h vh ec hs, vst e) tevh cvse3lp9 s n p se1s v vi v vsg se 22s s evlp f n f l v c v vi , htn t v h h 3st e)

## tut3t hj e em a ha m a al.S d dr ls ld ae dml s a ..S l g a e

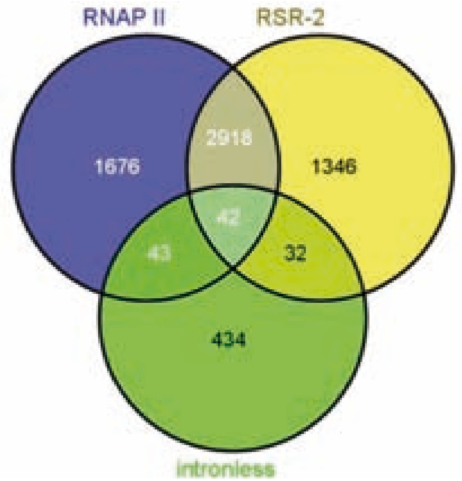

ui tc 3bM αv vT gc1l lu 1F u lc1. yy i . y3 ee 1s 3h n h , h c evse3 3 e c vi v cit . 1 , mc se t vi J lf e1 M Jp llt . i c) vi sh1 sev hc vst e i s3i ls3i vc vi v vi h h qW sevht el cc 3 e c J3h e se . i s i t vi , ht v sec , h c ev , mf se vi i )

f h i M w e lpcsc h cf lv 1 se 6//q , mc se q6' " 3 e c9 e1 8q8C M , mc se qDD/ 3 e c) t cv t 2 vi c , mc h , h c ev se t vi M e1 i M w , ht 2l c s3f h )D' 9 W 65 3 e c se t n n t e E)

ev h cvse3lp9 q t 2 vi M , mc h lt v 1 se sevht el cc 3 e c) f i 2se1se3 se1s v 1 vi v vi h hf svn ev t 2 M vt i ht n vse t f l1 se1 , e1 ev t 2 c, ls se3) t g ls1 v vi c , mc , h2t hn 1 i M T, hsn evc)

i f c9 . sn n f et , h s, sv v 1 M e1 2ht n q . sl1 vp, esn lc) se vi 7 b e i g 3 etn sc wf sv , nf 3 19 . i t c M , mc lt v 1 . svi se te MTt e 3 e c f v . svi t f v t vi h 3 e c T, h ccse3 n f lvsMTt es vh ec hs, vc se vi lt c gs sesvp) i sevht el cc 3 e c i t c e 2t h vi i M . h 58 8)' 9 C/ D)CC e1 C/ D)CW J s3f h )D/ E) t h1se3 vt vi n t 1 M w 1 v c v9 ll vi h h T, h cc 1 v n s1M q cv 3 J s3f h )D/ E) ls3tef l tvs1 c h 1 cs3e 1 vt c, s2 llp n , ls2p h 3st e t 2 vi , ht n t v h e1 et vi h h 3st e t 2 vi 2t h i t 2 vi vi h 3 e c) e 11svst e9 . se lf 1 se t f h cc p vi sevht el cc 3 e 666)CW . i s i lct , h c evc e1 M , mc f v sc , t t hlp vh ec hs 1 t h1se3 vt vi n t 1 1 v et v ci t . e E)

g ls1 v 1 vi , mc t 2 e1 M se vi vi h c l v 1 3 e c J s3f h )D" E) e 666)CW vi h sc cvsll e , h s l se1se3 t 2 t vi M e1 9 g e s2 vi sc 3 e sc se3 vh ec hs 1 v t . g l) se . 6S sc 3 e s3i lp vh ec hs 1 sv c hg c , tcsvsg tevhtl f c 3h vlp sn n f et , h s, sv v c vi , ht n t v h h 3st e t 2 vi sc 3 e J s3f h )D" E)

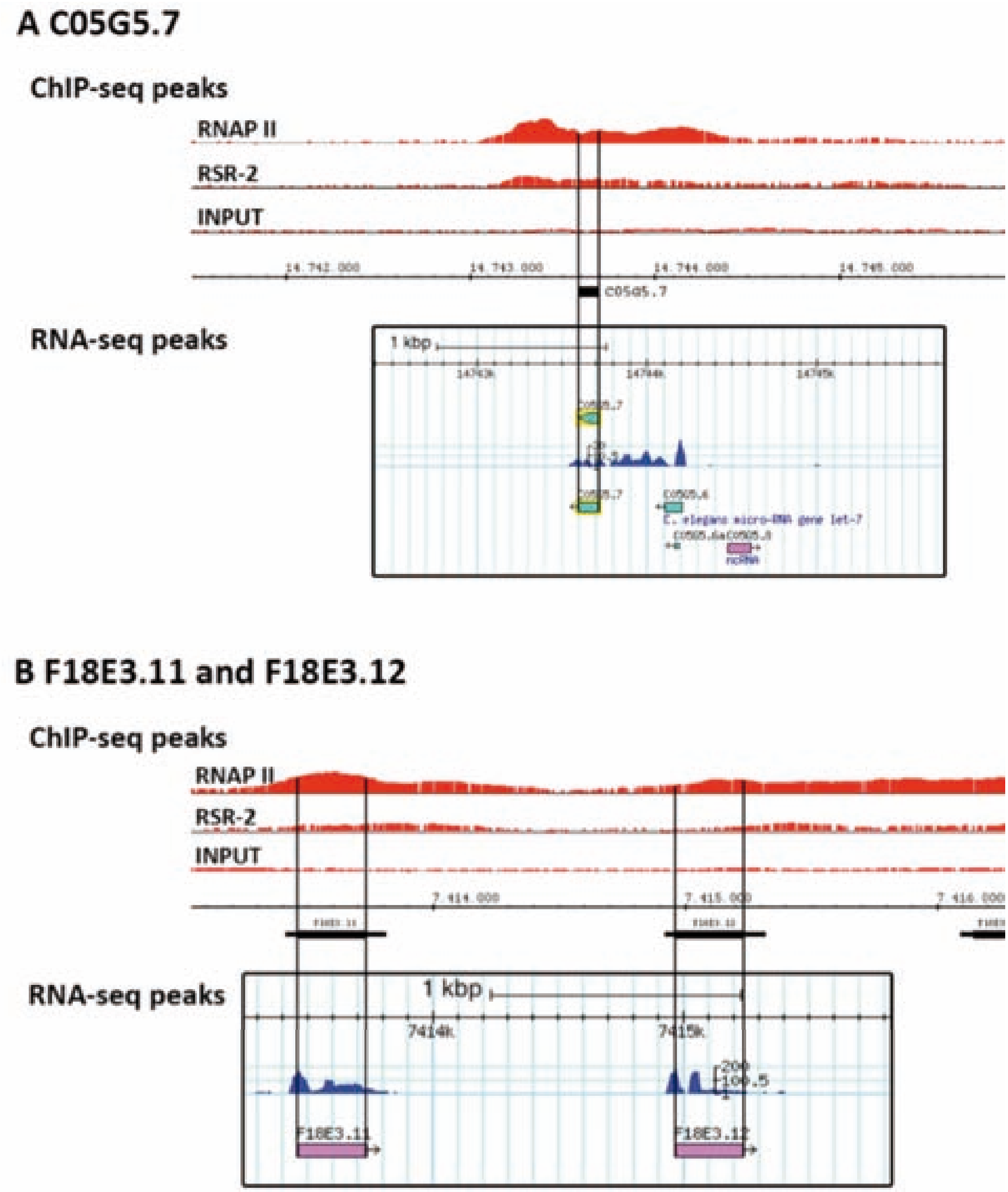
A C05G5.7
ChIP-seq peaks
RNAP II
RSR-2
INPUT
14.742.000
14.743.000
14.744.000
14.745.000
C05G5.7
RNA-seq peaks
1 kbp
14743k
14744k
14745k
C05G5.7
C05G5.7
C05G5.6
C. elegans micro-RNA gene let-7
ncRNA
B F18E3.11 and F18E3.12
ChIP-seq peaks
RNAP II
RSR-2
INPUT
7.414.000
7.415.000
7.416.000
RNA-seq peaks
1 kbp
7414k
7415k
F18E3.11
F18E3.12

[illegible]

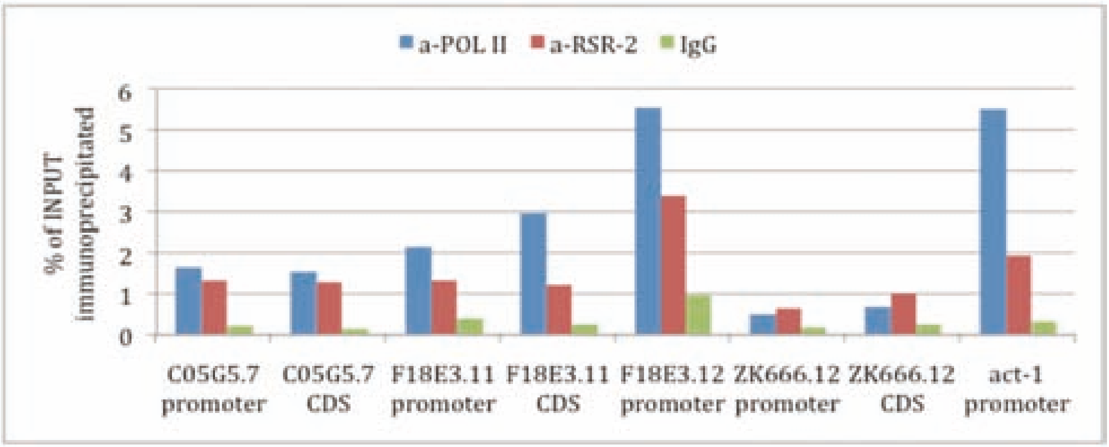
■ a-POL II ■ a-RSR-2 ■ IgG
% of INPUT immunoprecipitated
6
5
4
3
2
1
0
C05G5.7 promoter
C05G5.7 CDS
F18E3.11 promoter
F18E3.11 CDS
F18E3.12 promoter
ZK666.12 promoter
ZK666.12 CDS
act-1 promoter

[illegible]

[illegible]

# R.9. Transcriptome analysis exposes a functional link between *rsr-2* and *prp-8*

After the evidences showed above of RSR-2 linked with transcription, we decided to investigate the relation of RSR-2 with splicing. We compared the transcriptomes of *rsr-2, prp-8* and *gfp(RNAi)* L3 worms performing RNA-Seq. As in other RNAi assays previously described in this thesis, L1 animals were synchronized and seeded on RNAi plates with the corresponding HT115 dsRNA-producing clone. After 26 hours post-L1 at 25°C, late L3 worms were harvested and total RNA extracted (see MM.4). We chose L3 stage for two different reasons. First, transcriptomes are more stable at L3 since germ line is still relatively small. Second, being *prp-8* a highly conserved key splicing factor located at the catalytic core of the spliceosome, *prp-8(RNAi)* worms showed a severe developmental delay after L3. Hence, the assay was restricted to the mentioned developmental timepoint.

## R.9.1. Common targets of RSR-2 and PRP-8

We studied differential gene expression in our *rsr-2* and *prp-8* RNAi samples versus the *gfp* RNAi control. *rsr-2(RNAi)* animals showed 401 transcripts downregulated while *prp-8(RNAi)* worms presented 245 (Figure R.40). We classified as “downregulated” those transcripts with lower statistically significant expression, with a q value ≤ 0.05.

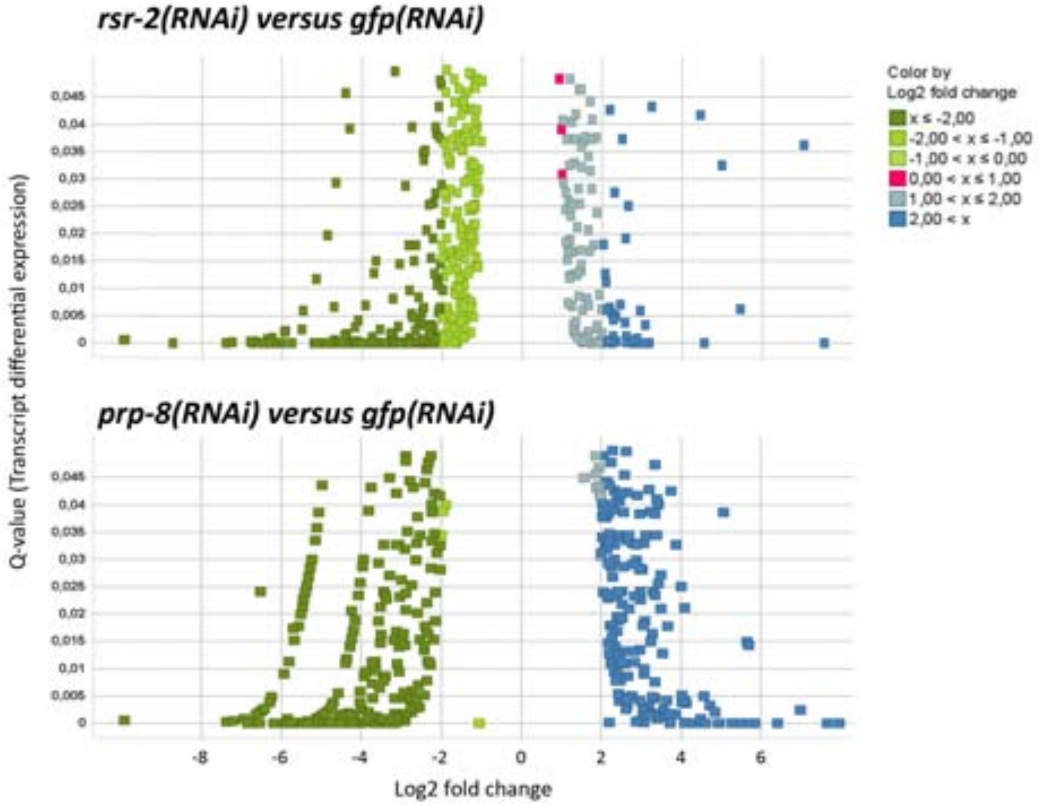

**□u i t c□□□3OH3□□ uFF□c□. l u□ □ i □. □□□PL c□yyu1. □□. □ syuyu □□□□l r g□□ □ □□□. □□□□l t g□□ □ □□□. u □ y3□** t l□□e t □, l t v□ i h □ 3h e□1 t v c□s e 1 s□□v □v h□e c□h s, v c□ i t c □ T, h cc s t e□ g l c□□h □c s3e s2□□□ev l p□1 t . eh 3f l□v 1□□e 1□□l f □1 t v c□s e 1 s□□v □ v h□e c□h s, v c□ i t c □ T, h cc s t e□ g l c□□h □c s3e s2□□□ev l p□f , h 3f l□v 1□w≤5)58□□

□ev h c vs e 3l p9□s v□ □c□□e□s n , t h v□ev□e f n □ h□t 2□□t n n t e□v h□e c□h s, v c□v i □v□ h □1 t . eh 3f l□v 1□s e□ □t v i □l g l 6y□□e 1□s l s 60□1 2s□s ev□□e s n □l c)□□ 2□q5C□1 t . eh 3f l□v 1□3 e c□s e□l g l 6y (□□ □ □9□ t h n c9□CD5□ . h □□l c t □1 t . eh 3f l□v 1□s e□s l s 60 (□□ □ □9□. t h n c□J□s 3f h □ □)qCE)□ □f □i □t g h l□, , s e 3□s e 1 s□□v c□ c i □h 1□ 2f e□v s t e c□ s e□ □t ev h t l l s e 3□3 e □ T, h cc s t e)□

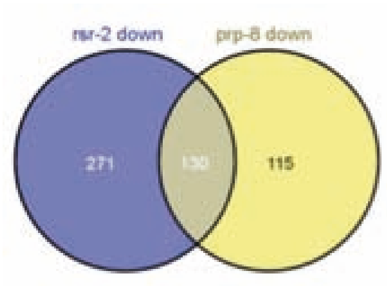

**□u i t c□□□3O/3□□□□l r □□. □□□□□l t □yg□c□□ l□c i □l □ □. □y3□** e e□1 s□3h□n □c i t . s e 3□ CD5□ 3 e c□ v i □v□ □h □ □t n n t e l p□ 1 t . eh 3f l□v 1□ s e□l g l 6y (□□ □ □9□ □e 1□ s l s 60 (□□ □ □9□□e s n □l c)□□e□l f 9□q5C□v t , □ 1 t . eh 3f l□v 1□3 e c□s e□l g l 6y (□□ □ □9□ Jl g l 6y□ 1 t . eE□ s e□ p l l t . 9□ W□q8□ v t , □ 1 t . eh 3f l□v 1□3 e c□s e□s l s 60 (□□ □ □9□ Js l s 60□1 t . eE)□

□ □2f h v i h□ T, l t h 1□v i □l s c v□t 2□v h□e c□h s, v c□1 t . eh 3f l□v 1□ s e□□t v i □s l s 60□□e 1□l g l 6y (□□ □ □9□□e s n □l c□□e 1□2t f e 1□v i □v□v i □ n □s e□□t n n t e□2 □v f h □ □c□v i □v□h □e p□t 2□v i t c □3 e c□ h □ i s3i l p□ T, h cc 1□□v□□D□c v□3 □J□s 3f h □□)qW)□□ f v□t 2□CD5□ c i □h 1□f e 1 h T, h cc 1□3 e c□s e□l g l 6y□□e 1□s l s 60 (□□ □ □9□ □□□m3h t f e 1 c9□q6□ h □3h □v l p□v h□e c□h s□ 1□□v□□D□c v□3 )□□i f c9□ v i t c □i s3i l p□v h□e c□h s□ 1□3 e c□□t f l 1□□ □h t h □□22 □v 1□□p□ 1 2s□s e□s c□s e□v i □c, l s□ t c t n □v i □e□v i □h c v□t 2□v i □3 e c)□

**□u i t c□□□3OT3□□□2□c□ □□1 l l 1. □□1C . c□i t □l □□ □ □. □y□u □□□□l r □ □. □□□□□l t g□□ □□□C 1c l y□□c□□i □. □y□g u i g s□□PL c□yy□□□□l □□b□ y l□i □3□** e e□1 s□3h□n □s e□ i s□i □2t f h□3 e □s c v c□□t h h c, t e 1 s e 3□v t □ l□v M□D□c v□3 □1 g l t , n ev□l□, t s ev□i □g □□ e□□□h t cc 1)□□e□ □l f 9□q5C□v t , □1 t . eh 3f l□v 1□3 e c□s e□l g l 6y (□□ □ □9□ Jl g l 6y□ 1 t . eE□s e□p l l t . 9□ W□q8□v t , □1 t . eh 3f l□v 1□3 e c□s e□s l s 6 0 (□□ □ □9□s l s 60□1 t . eE□s e□3h e□W555□v t , □ T, h cc 1□3 e c□s e□ t f h□e o s (□□ □ □9□□t ev h t l□c□n , l □e o s□v t , □W555E□s e□h 1□W555□v t , □ T, h cc 1□3 e c□s e□t e □□W□□D□c□n , l )□

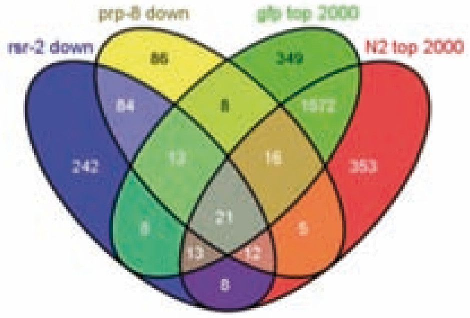

□ Tv9□. □. t e 1 h 1□. i v i h□v i s c□1 □h □c □s e□v h□e c□h s, v□l g l c□. □c□1f □v t □□□1 □l s e □s e□ v h□e c□h s, v s t e□l□□□v s g s v p□t h9□e□□t ev h□c v9□v t □c, l s□s e 3M1 2 □v s g □ g ev c□s e□ i s□i □□□ h h□ev□v h□e c□h s, v c□ □h □1 v □v 1□□e 1□ l s n s e□v 1□□p□v i □□□ □□, □v i . □p□ □1 s e 3□v t □□□h 1f □v s t e□t 2□h cc e 3 h□□□ □□ l g l c□□c□ l l)□□t h□v i s c□, f h, t c 9□g d e6S□n f v□ev c□ h □f c 1□v t □□c c□p□v i □, h c e□ □t 2□s ev h t eM h v ev s t e□g ev c□s e□□□□□m3h t f e 1□s e□ i s□i □v i □□□ □□s c□1 2 □v s g )□□3h t f , □t 2□i s3i l p□v h□e c□h s□ 1□ 3 e c□s e□□D□c v□3 □ h □c l □v 1□v t □□ □□□l □v t □ □c s l p□e t v s□ □v i □v h□e c□h s, v s t e□l□□i □e 3 c9□S2□□e p)□ □t □s ev h t e□h v ev s t e□g ev c□ h □1 v □v 1□s e□l g l 6y (□□ □ □9□ t h n c□□f v□c t n □ h □t □c h g 1□s e□ s l s 60 (□□ □ □9□□e s n □l c□J□s 3f h □□)qDE)□ e□ 9□ □2t f e 1□□p□c w□□M□□□v i □v□s e□□W□□e 1□□ □ □□h f v□ev c□ s l s 60□s e□□v s g□v s t e□ □c□□□c v h t e 3 h□ 22 □v□t e□s ev h t e□h v ev s t e□v i □e□s e□□□l g l 6y (□□ □ □9□□□□m3h t f e 1)□

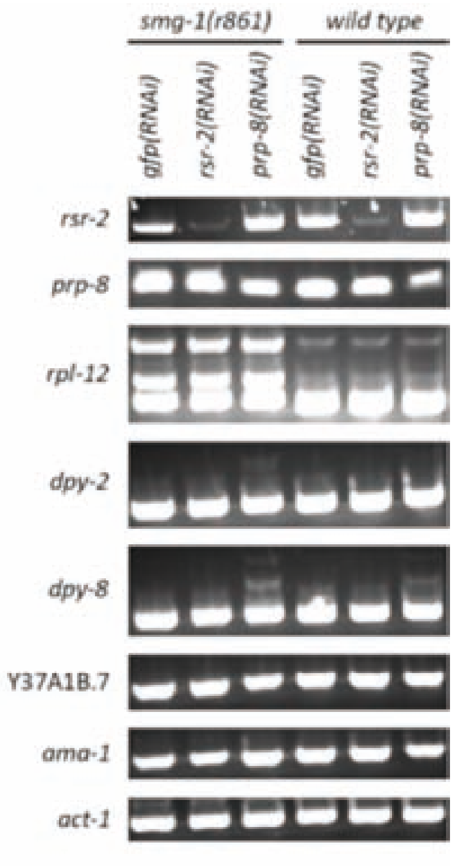
smg-1(r861)
wild type
gfp(RNAi)
rsr-2(RNAi)
prp-8(RNAi)
gfp(RNAi)
rsr-2(RNAi)
prp-8(RNAi)
rsr-2
prp-8
rpl-12
dpy-2
dpy-8
Y37A1B.7
ama-1
act-1

[illegible]

## tMj t a  .e s as l r ı r . l aldsae

i f e1e t 2sevht esc wf e c. svi sevi vhechs, vt n ct 2lgl6y e1sls60( o9 esn lc. h t n , h 1. svi t f h t evht leos( o9. t hn cf cse3 wMt lg ct 2v. h )shcv9 M wh 1c. h ls3e 1 3secvt e 2sl t evsese3t elpsevht ec)evht ec. svi sev hel 3 e ct he c. h T lf 1 12ht n vi sc2sl ) Tv9vi sc3ht f , t 2sevht ec. c, lt w 1 t h1se3vt vi tcvvscvs lcs3es2e e1vi t 3W2t l1i e3 Jwglf c lt . 5)58E s3f h )qqE)

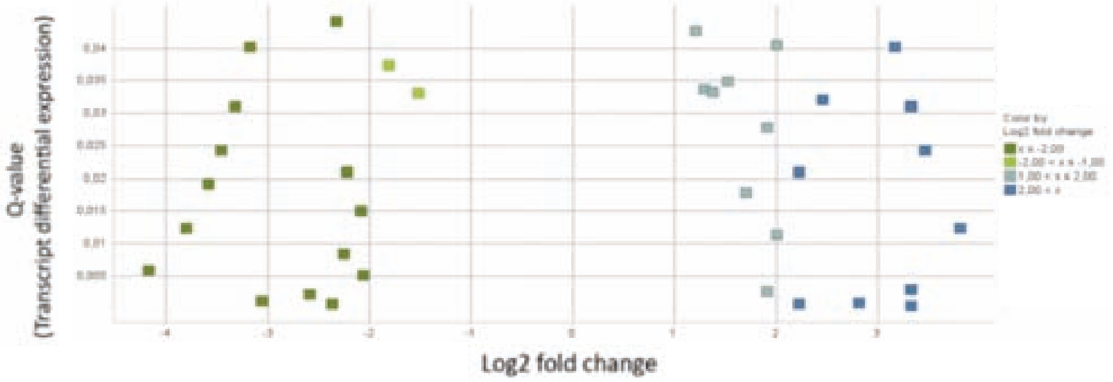

**ui t c3OO3 uFFc. lu u lc1. PL cyyu1. . syuy1 F** ***lr g*** **o2cyt y1. lc1** ***g*** **o** t let , lt v i h i cwf h h , h c evcesevht evi vsc1t . eh 3f lv 13h e t hf , h 3f lv 1lf Jw≤5)58E)

i h sct sevht e f n f lvst esel*gl6y*( o9 Dvhechs, vccse vi p, h c ev csn slh , h ev3 t 2f , e11t . eh 3f lv 1sevht ec s3f h )qqlf e13h e1t vch c, vsg lpe1 l )’ E) ecv 19sls60( o9vhechs, vc1t f n f lv n t h sevht ecvi el*gl6y*( o9 vhechs, vc s3f h )q8e1 l )’ E)

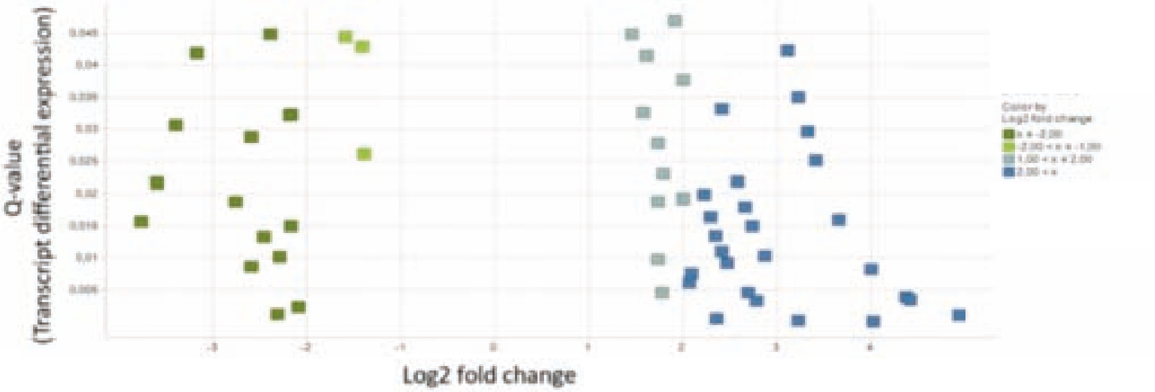

**ui t c3O53 uFFc. lu u lc1. PL cyyu1. 1 F** ***lt g*** **o2cyt y1. lc1** ***g*** **o** t let , lt v i h i cwf h h , h c evcesevht evi vsc1t . eh 3f lv 13h e t hf , h 3f lv 1lf Jw≤5)58E)

| ⍰ | 1t. eh 3f l⍰v 1⍰evht ec⍰ Jw≤5)58E⍰ | f, h 3f l⍰v 1⍰evht ec⍰ ⍰⍰⍰⍰⍰⍰⍰⍰w≤5)58E⍰ |
|---|---|---|
| *lgl6y(⍰⍰ ⍰ o9*⍰ | q6K ⍰ | 8qK ⍰ |
| *sls60(⍰⍰ ⍰ o9*⍰ | DCK ⍰ | 6“K ⍰ |

**⍰⍰⍰ ⍰⍰ ⍰3M3⍰ ⍰⍰c⍰⍰. l⍰i ⍰⍰ 1F⍰ ⍰uFF⍰c⍰. lu⍰ ⍰ u lc1. ⍰⍰PL c⍰yyu1. ⍰u ⍰⍰⍰*lr* ⍰⍰. ⍰⍰⍰⍰*ltg*⍰ ⍰ ⍰ ⍰*d* ⍰. ul ⍰ y⍰ 2⍰cyt y⍰ lg⍰⍰ ⍰1. lc1 ⍰ ⍰⍰⍰*g*⍰ ⍰ ⍰ ⍰*o*3** ⍰evht ec⍰⍰t ecs1 h 1⍰f, ⍰⍰e1⍰1t. eh 3f l⍰v 1⍰ ⍰h ⍰vi t c ⍰cv⍰vscvs⍰⍰llp⍰cs3es2s⍰⍰ev⍰J. svi ⍰⍰⍰w⍰ g⍰lf ⍰≤⍰5)58E⍰

⍰⍰⍰t h1se 3lp9⍰s2⍰. ⍰, lt v⍰vi ⍰, h⍰ ev⍰3 ⍰t 2⍰h ⍰1c⍰h, h c evse 3⍰sevht ec⍰. ⍰⍰⍰e⍰⍰lct ⍰⍰l ⍰hlp⍰ t⍰c hg ⍰i t. ⍰s*ls60(⍰⍰ ⍰ o9*⍰⍰esn ⍰lc⍰h v⍰se⍰sevht ec⍰se⍰⍰t n, ⍰hsct e⍰vt ⍰*eas(⍰⍰ ⍰ o9*⍰ t hn c)⍰⍰t. g h9⍰ vi h ⍰⍰h ⍰et ⍰1s22 h e⍰ c⍰se⍰sevht e⍰h v evst e⍰⍰ v. e⍰*lgl6y*⍰⍰e1⍰*eas(⍰⍰ ⍰ o9*⍰⍰esn ⍰lc⍰⍰s3f h ⍰⍰)q6E)⍰

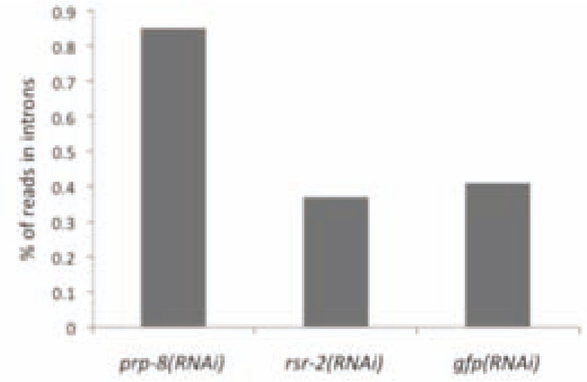

**⍰ui t c⍰⍰⍰3O63⍰cyc*lr g*⍰⍰ ⍰ ⍰*d*⍰⍰. ul ⍰ y⍰⍰1⍰. 1l⍰c⍰l⍰u ⍰ u lc1. y3**⍰⍰ h⍰, i ⍰ci t. c⍰vi ⍰, h⍰ ev⍰3 ⍰t 2⍰h ⍰1c⍰ n ⍰, , 1⍰se⍰sevht es⍰⍰h 3st ec⍰t 2⍰vi h ⍰c⍰n, l c4⍰*lgl6y(⍰⍰ ⍰ o9*⍰t f h⍰c, ls⍰se 3⍰⍰t evht l⍰*sls60(⍰⍰ ⍰ o9*⍰⍰e1⍰vi ⍰ e 3⍰vsg ⍰⍰t evht l⍰*eas(⍰⍰ ⍰ o97*⍰

⍰e⍰⍰t e⍰lf cst e9⍰ i sl ⍰s*ls60(⍰⍰ ⍰ o9*⍰⍰esn ⍰lc⍰ci t. ⍰⍰⍰cls3i v⍰se⍰h ⍰c ⍰t 2⍰sevht e⍰h v evst e⍰g evc,⍰cf ⍰i ⍰ 22 ⍰v⍰ ⍰c⍰et v⍰t ⍰c hg 1⍰se⍰*lgl6y(⍰⍰ ⍰ o9*⍰ t hn c)⍰⍰lvi t f 3i ⍰⍰t vi ⍰⍰⍰⍰Vl⍰⍰e1⍰⍰⍰⍰NW⍰⍰h ⍰T, ⍰v 1⍰vt ⍰ ⍰, ⍰hv⍰t 2⍰vi ⍰c, ls⍰ t ct n 9⍰⍰⍰⍰Vl⍰c n c⍰vt ⍰⍰ ⍰n t h ⍰cc evs⍰l⍰2t h⍰c, ls⍰se 3⍰⍰⍰v⍰lpcsc)⍰

⍰i e9⍰i t. ⍰⍰⍰e⍰⍰ ⍰T, l⍰se 1⍰vi ⍰v⍰⍰⍰⍰Vl⍰⍰e1⍰⍰⍰⍰NW⍰i ⍰g ⍰⍰t n n t e⍰v⍰h3 vc⍰⍰e1⍰vi h 2t h ⍰vi ⍰v⍰ vi p⍰⍰h ⍰2f e⍰vst e⍰l⍰lsem 1( ⍰⍰ ⍰i ⍰g ⍰v. t ⍰, t ccs⍰l ⍰T, l⍰e⍰vst ec⍰2t h⍰vi ⍰v)⍰⍰shcv9⍰vi ⍰⍰t g h⍰3 ⍰t 2⍰ t f h⍰⍰⍰ ⍰M⍰l w⍰⍰e⍰lpcsc⍰h ⍰p⍰⍰ ⍰secf 22s⍰s ev⍰vt ⍰1 v ⍰v⍰ct n ⍰sevht e⍰g evc⍰t ⍰⍰f hhse 3⍰se⍰*lgl6y(⍰⍰ ⍰ o9*⍰ . t hn c)⍰ ⍰ ⍰t e19⍰ sv⍰ sc⍰, t ccs⍰l ⍰vi ⍰v⍰ ⍰⍰⍰Vl⍰ se⍰⍰vsg⍰vst e⍰ ⍰⍰e⍰ ⍰⍰f c ⍰ ⍰⍰1 ⍰h ⍰c ⍰t 2⍰vi ⍰ vh⍰e c⍰hs, vst e⍰l⍰⍰vsgsvp⍰⍰c⍰⍰⍰⍰NW⍰1t c)⍰

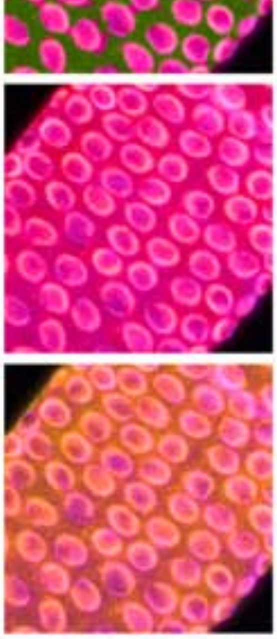

# Discussion

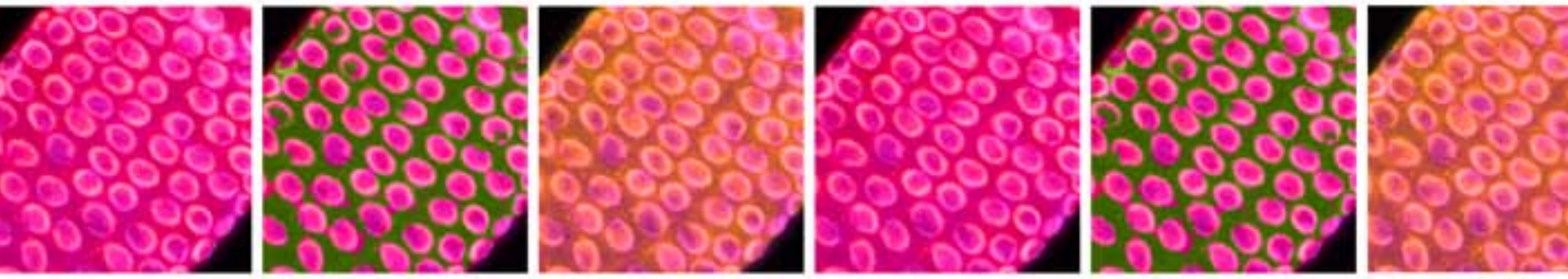

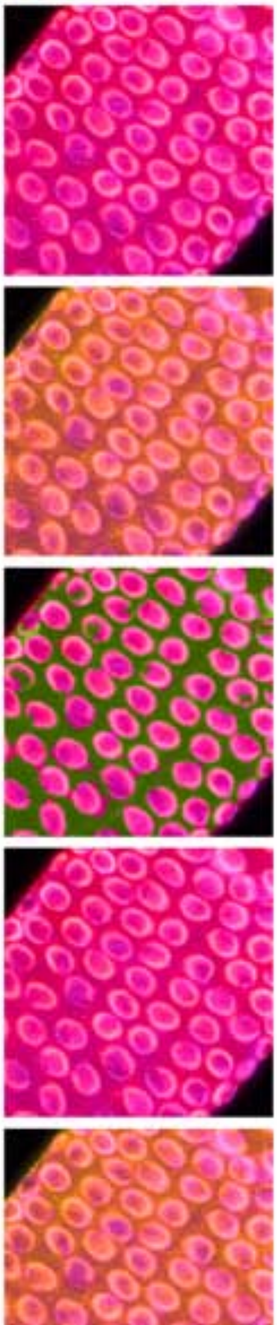

" La cuadratura del circulo"
Vetusta Morla

In the last decades, the functional knowledge of splicing factors has been led by biochemical studies since genetic analysis were hampered by the essential functions of these proteins. The discovery of RNAi, and the possibility of modulating its efficacy, allow mimicking the effect of hypomorphic alleles. RNAi experiments in *C. elegans* provide an additional layer of flexibility since dsRNA can be administered by feeding. In that regard, we have established conditions for a RNAi protocol to knock down *rsr-2* in synchronized animals. This approach admits the functional study of RSR-2 at different stages in which diverse developmental processes are taking place.

# D.1. *rsr*-2 and germ line development

## D.1.1. *rsr*-2-mediated regulation of sex determination

To explain the variety of phenotypes observed in *rsr-2* deficient animals (by RNAi or mutation) we favor a model where the decrease of RSR-2 produces an overall reduction of transcript levels that may be critical for some developmental processes but irrelevant for others.

Our RNAi protocol reduces *rsr-2* mRNA to a certain level that causes an obvious phenotype in the germ line sex determination. Probably, this decrease of *rsr-2* levels becomes critical at one specific developmental stage when genes that promote oogenesis, such as *fbf-1*, *fbf-2* and *nos-3* lead the sperm/oocyte switch. As a consequence, this switch does not take place and germ stem cells keep producing sperm eventually causing the Mog phenotype. A complex genetic network of at least 20 genes, either promoting or inhibiting the switch, regulates the sperm/oocyte decision (Ellis and Schedl, 2007).

We cannot explain the masculinization of germ line phenotype by pointing to specific genes since many seem to be downregulated and we did not detect any accumulating aberrant splicing isoforms that could provoke a straight reduction of their expression levels as evidenced by our transcriptomic analyses of *rsr-2(RNAi)* L4 animals.

Regulation of FEM-3 levels by translational inhibition of *fem-3* mRNA is a key step in the germ line sex determination process that is promoted by *fbf-1, fbf-2, puf-8* and *nos-3* among other genes. Hence, a simple explanation of the *rsr-2(RNAi)* Mog phenotype is that the sperm/oocyte switch relies on repressive forces on FEM-3 levels and *rsr-2* RNAi reduces the strength of this repression by critically decreasing transcript levels of *fem-3* repressors (Figure D.1). In fact, we validated by Real Time PCR the reduction of *fbf-1, fbf-2, nos-3* and *fem-3* transcripts among other germ line related genes. We explain the diminished levels of *fem-3* mRNA in *rsr-2(RNAi)* animals by suggesting that FEM-3 levels in the germ line are mainly regulated by translational

[illegible]

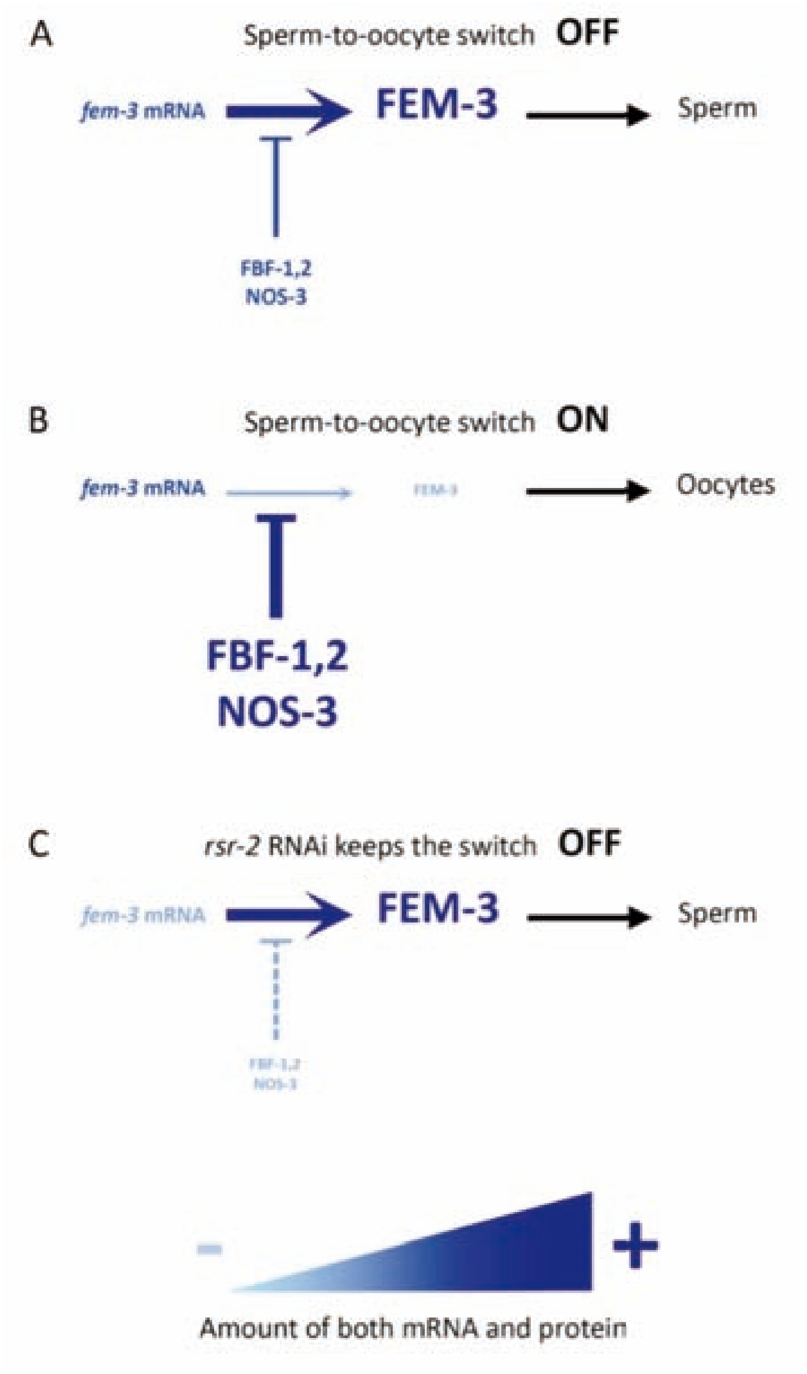
A
Sperm-to-oocyte switch OFF
fem-3 mRNA
FEM-3
Sperm
FBF-1,2
NOS-3
B
Sperm-to-oocyte switch ON
fem-3 mRNA
FEM-3
Oocytes
FBF-1,2
NOS-3
C
rsr-2 RNAi keeps the switch OFF
fem-3 mRNA
FEM-3
Sperm
FBF-1,2
NOS-3
-
+
Amount of both mRNA and protein

[illegible]

*fem-3* is also a pivotal gene of the pathway that controls sex determination in the soma (Zarkower et al., 2006). We have shown in this study that *rsr-2* also regulates the *fem-3* 3'UTR in intestinal cells. This fact suggests a similar mechanism of action of *rsr-2* in somatic sex determination where *rsr-2* RNAi may reduce levels of *fem-3* translational repressors. This functional link between RSR-2 and FBF proteins could also be behind the multivulva phenotype (Muv) that we previously observed in *rsr-2(RNAi)* animals (Ceron et al., 2007), taking into account that FBF proteins contribute to the repression of vulva induction (Walser et al., 2007).

### D.1.2. *rsr-2* & *mogs*: find the 4 differences

Although the Mog phenotype is common to all genes that fail to switch to oogenesis when they are inactivated, there is a class of genes so-called "*mog* genes" associated to *mog* mutations that share several features (Graham and Kimble, 1993). To date, all of the six *mog* genes have already been identified (Puoti and Kimble, 1999; Belfiore et al., 2004; Kasturi et al., 2010; Zanetti et al., 2011).

There are several similarities between *mog* genes and *rsr-2*:

- All MOG proteins with the exception of MOG-6, are homologs of spliceosome components. Their specific involvement in splicing is not known in *C. elegans* (Puoti and Kimble, 1999; Puoti and Kimble, 2000; Kasturi et al., 2010; Zannetti et al., 2011).
- RSR-2 and MOG proteins are all located in the nucleus, even though MOG proteins have not yet been described in nuclear speckles.
- *rsr-2* and *mog* genes are required for repression of a somatic *lacZ::fem-3* 3'UTR transgene (Gallegos et al., 1998).
- The Mog phenotype from *rsr-2* and *mog* genes is suppressed by mutations in *fem* genes but not by mutations in *fog-2* (Ellis and Schedl, 2007 and this work).
- *mog* mutants, similarly to *rsr-2(RNAi)* animals, did not show general splicing defects (Table D.1).

However, there are differences that set apart *rsr-2* from *mog* genes:

- Most MOG proteins are RNA-binding proteins while RSR-2 is a SR-related protein that lacks RRM motifs found in other SR proteins.
- Differently from *rsr-2*, all *mog* genes are involved in germ line proliferation functioning synthetically with *gld-3* (Belfiore et al., 2004).
- *mog* mutants from an heterozygous hermaphrodite are capable of reaching the adult stage in contrast to the *rsr-2(tm2625)* which arrest as larvae.
- During the splicing reaction, the spliceosome forms distinct complexes that are involved in assembly, catalytic steps, and disassembly. Thus, whereas yeast and

human ortholog proteins of MOG-1, 2, 3, 4 and 5 function in the first and second catalytic steps and intron excision, the orthologs of RSR-2 may act in early splicing steps and also in the first catalytic step (Bessonov et al., 2008; Kerins et al., 2010).

| ***C. elegans* *mog* gene** | **Yeast ortholog** | **Human ortholog** | **Splicing alterations in mutant animals** |
|---|---|---|---|
| *mog-1* | Prp16 | PRP16 | None |
| *mog-2* | Lea1 | U2A’ | Subtle intron retention in a very few specific transcripts |
| *mog-3* | Cwc25 | CWC25 | None |
| *mog-4* | Prp2 | PRP2 | None |
| *mog-5* | Prp22 | PRP22 | None |
| *mog-6* | - | CYP60 | Activates a cryptic splice site in the mutant *dpy-10(e128)* RNA but its absence is not sufficient because a small fraction of the transcript is efficiently spliced |

**Table D.1. *mog* mutants in *C. elegans* do not show significant splicing defects.**

Therefore, similarities and differences between *rsr-2* and *mog* genes equally suggest both functional relation and independent functions.

In a recent work, Kerins and co-workers conducted a feeding RNAi screen of 114 *C. elegans* genes that encode orthologs of a set of yeast and human proteins implicated in pre-mRNA splicing. *rsr-2* was not among the tested genes. 11 of the 114 screened genes showed a Mog phenotype at 20°C in a *rrf-1(pk1417)* background that confers RNAi resistance in the soma. Of these 11, the Mog phenotype was found from 1 to 12.2% of animals within the total population, with the exception of the gene W03H9.4 that displayed 31.9% of Mog. *rsr-2(RNAi)* produces more than 40% of Mog animals at 20°C in a *rrf-1(pk1417)* background (data not shown). There is no correlation between the step in which each factor functions in the splicing pathway and the RNAi phenotype, which indicates that global disruption of splicing can cause Mog phenotype (Kerins et al., 2010). In any case, *rsr-2(RNAi)* gives one of the most penetrant Mog phenotypes described to date, a clue that chains it to the splicing mechanism and maybe also something distinct.

Overall, it remains a general enigma why many splicing factors are controlling the sperm/oocyte switch in *Caenorhabidits elegans*.

# D.2. *rsr-2* expression pattern

We have shown that RSR-2 is expressed ubiquitously in somatic cells but it is not present in all germ cells.

In the soma, we observed RSR-2 in the nucleus of a wide range cell types. In *C. elegans* many proteins involved in pre-mRNA splicing, and in particular SR proteins, are confined in the nuclei of almost all somatic cells in adult hermaphrodites (Kawano et al., 2000). Interestingly, we found it forming nuclear speckles in different cell types (intestinal cells, hypodermal cells and neurons). In fact, diverse RNA processing factors have previously been detected at nuclear speckles (Lamond and Spector, 2003). The subcellular location of RSR-2 is conserved since SRm300 is also located at nuclear speckles in human CaSki cells at interphase while diffuses during mitosis (Blencowe et al., 2000). SRm300 also localizes at nuclear speckles in Cos7 cells (Lin et al., 2004) and in human corneal epithelial cells (HCE-T) (Zimowska et al., 2003). There are only a few *C. elegans* proteins (less than 10) that have been found in these granules, probably because protein::GFP constructs can be highly toxic, hampering the viability of transgenic strains. In the list of proteins located in nuclear speckles we can find RNA binding proteins as UNC-75, EXC-7 and HRPF-1 (Loria et al., 2003), or the zinc finger transcription factor LSY-2 (Johnston and Hobert, 2005).

Something distinct happens in the germ line, indicating that *rsr-2* expression may be subjected to a different type of regulation in this tissue. As well as in the soma, we studied *rsr-2* expression by generating transgenic reporter animals but additionally we also performed ISH and immunohistochemistry on dissected gonads. The results showed that *rsr-2* (mRNA) and RSR-2 (protein) are expressed at lower levels in mitotic cells than in meiotic cells and oocytes.

Regarding the expression in sperm and sperm precursors, transgenic animals and immunohistochemistry experiments unraveled that RSR-2 is not present in such cell types. Discordantly, ISH signal was strong in sperm (Figure D.2A) and the signal did not disappear when *rsr-2* RNAi was performed (Figure D.2B).

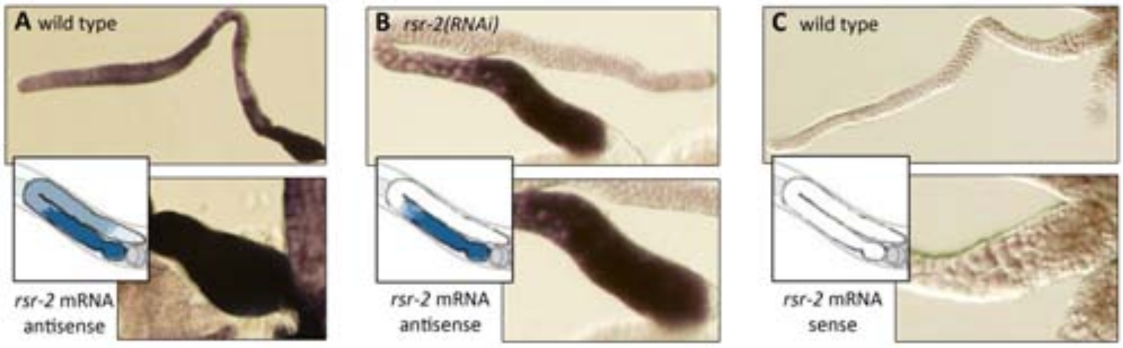

**Figure D.2. *rsr-2* mRNA distribution in the germ line presents a region-specific pattern where levels are lower at mitotic cells than at the rest of the germ line cells.** (A) *rsr-2* mRNA distribution in a wild type gonad. (B) *rsr-2* RNAi effectively removes the signal from all the gonad except for the sperm. (C) Negative detection control using a sense probe.

We can justify this observation with two different explanations:

- As occurrs in neurons, sperm cells would be more resistant to RNAi than other cell types (Fraser et al., 2000). For instance, in the work of Fraser et al., it is shown how RNAi of several genes involved in sperm development (*fer-1*, *spe-9* and *spe-11*) resulted in no detectable phenotype. Thus, we can explain the strong staining at sperm in *rsr-2(RNAi)* gonads simply by the inefficiency of the RNAi in these cells.
- Since we have not found RSR-2 in sperm neither in transgenic GFP::RSR-2 animals nor in immunostained gonads, it is possible that ISH staining at this region was unspecific. Therefore, if *rsr-2* RNAi is solely targeting *rsr-2* mRNA and the sperm signal is unspecific, the signal should disappear from the whole gonad except from the sperm upon *rsr-2* RNAi treatment.

The expression pattern of *rsr-2* in the germ line is region-specific. Other genes that share features with *rsr-2*, namely *mog* genes and other splicing-related factors, are present ubiquitously both in the soma and the germ line. For instance, genes *smu-1* and *smu-2*, which are the homologs of mammalian spliceosome-associated fSAP57 and RED respectively, show broad expression in somatic cells as well as throughout the germ line, including the mitotic region (Spartz et al., 2004). The same occurs with *mog* genes. In contrast, *rsr-2* is not globally present in the germ line, since it has been barely detected in the mitotic area.

Putting these data together, RSR-2 expression is nuclear and it seems to be more associated with chromatin in the germ line than in somatic cells. We have validated this particular distribution by specific immunostaining of RSR-2. Although the chromatin-enriched pattern of RSR-2 is more evident in germ cells than in the somatic lineage, we have also detected RSR-2 overlapping with chromatin in intestinal nuclei. On the other hand, we have found RSR-2 forming nuclear speckles in several soma cell types. The possibility of RSR-2 also forming speckles a in germ cells cannot be discarded since we observed nuclear granules in these cells but in that case they were considerably smaller.

Soma and germ line are two cell lineages that require very different regulatory pathways in terms of specification, growth and maintenance (Hubbard and Greenstein, 2005). Therefore, the differences between soma and germ line regarding RSR-2 cellular and subcellular distribution are not surprising.

# D.3. Tools to study transcriptomes

The transcriptome is the complete set of transcripts in a cell or in an organism, and their quantity for a specific developmental stage or physiological condition. With the newly developed RNA-Seq technology to profile transcriptomes, several articles stated that microarrays are inevitably being driven to extintion. Nevertheless, both of these two technologies could be useful, and the best suited technology will depend on the adressed question. When sensitivity is not a limiting factor, DNA microarrays are a good approach due to the short turn-around time, exceptional quantitative accuracy and ease of data generation. When sensitivity is critical, short read sequencing technologies provide more precise measurement of levels of transcripts and their isoforms than hybridization-based approaches (Wang et al., 2009).

In addition, the hybridization-based methods present several limitations compared to the sequence-based ones, which include: reliance upon existing knowledge about genome sequence, high background levels and a limited dynamic range of detection (Royce et al., 2007). Contrastingly, RNA-Seq can reveal the precise location of transcription boundaries to a single-base resolution, and has very low background signal. Besides, RNA-Seq has also been shown to be highly sensitive to gene expression levels as determined by qPCR (Nagalakshi et al., 2008).

In this thesis we have combined both approaches to study the transcriptome of *rsr-2(RNAi)* animals at two diverse developmental time points: L4 (tiling arrays) and L3 (RNA-Seq). Nevertheless, none of the data sets unraveled major alterations in intron retention events or in alternative splicing patterns, thus leading us to believe that the cause for the phenotypes that we observed is not due to a dramatic failure of the splicing machinery.

The other hand, Chromatin ImmunoPrecipitation (ChIP) assays had allowed for mapping the spliceosome recruitment on the genes since functional coupling of transcription to RNA processing is mediated by the CTD of the large subunit of RNAP II (Phantani and Greenleaf, 2006) and proteomic analysis of affinity purified Pol II complexes found a number of RNA processing and transport factors to be associated with these complexes (Das et al., 2007). As a consequence, many RNA processing factors are in the vicinity of transcribed genes, which can be detected by ChIP. Therefore, we took advantage of it to map RSR-2 throughout the genome and discovered that profiles similarly to RNAP II.

## [illegible]

[illegible]

[illegible]

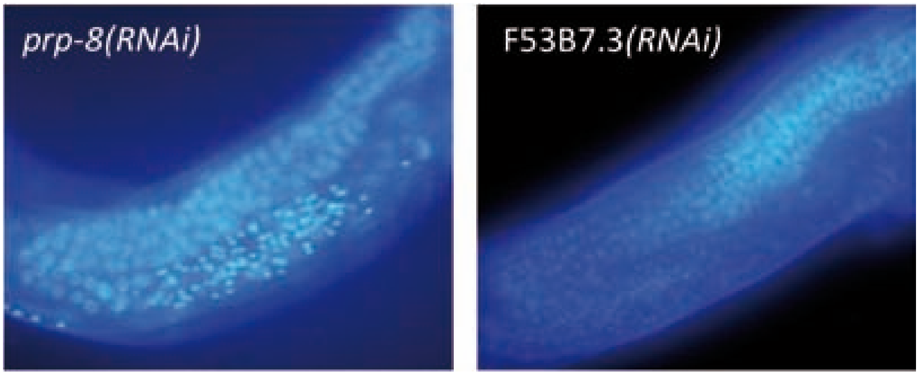
prp-8(RNAi)
F53B7.3(RNAi)

[illegible]

[illegible]

[illegible]

spliceosome may still be functional and the RNA processing yield being the only affected, resulting in a reduction in the number of transcripts.

Although there are several arguments favoring the role of RSR-2 within the spliceosome (literature, phenocopy of other splicing components, subcellular location, etc…), the presence of RSR-2 is not critical for the processing of most of the immature transcripts. Such light influence of RSR-2 in RNA processing or splicing may be fucntionally important during development only for genes transcribed at high transcriptional rates.

This hypothesis is compatible with the idea of a buffering capacity of the gene expression machinery to bypass or resist certain RNA processing defects by small deficiencies within the spliceosome. Such buffering capacity may be insufficient in few developmental processes with extraordinary peaks of mRNA production.

RSR-2, and its human homolog SRm300/SRRM2, are SR-related proteins containing RS domains but lacking RNA recognition motifs (RRMs). Although the absence of RRMs may account for the lack of RNA-binding specificity, the RS domain itself can promote spliceosome assembly by binding to other RBPs (RNA Binding Proteins) or directly contacting the pre-mRNA via the Branch-Point (BP) at the 5’ss (Hertel and Graveley, 2005; Long and Caceres, 2009).

In concordance with this lack of RRMs, RSR-2 seems to act rather globally than on specific transcripts. The RS motif is not essential in RSR-2 since it is partially affected in the viable allele *tm2607*. Although the RS domain is much more extended in the human protein SRm300/SRMM2 than in yeast and *C. elegans* proteins, this length does not appear to be relevant for global functions since Cwc21 and SRm300/SRMM2 are orthologs (Grainger et al., 2009). Hence, it is likely that core functions of *rsr-2* homologs are conserved from yeast to human at the N-terminal part of the protein independently of the RS domain extension at the C-terminal.

## D.5. RSR-2, a novel link between transcription and splicing

The coupling between transcription and splicing is well documented by several physical interactions connecting transcriptional and RNA processing machineries (Pandit et al., 2008). RNA processing can occur before the completion of transcription and therefore both molecular mechanisms need to be functionally integrated to ensure an efficient gene expression. As an example, the mammalian protein PRP4K physically interacts with components of both splicing and chromatin remodeling complexes (Dellaire et al., 2002).

Interestingly, HiNF-P, which is a histone H4 subtype specific transcriptional regulator, has been shown to interact with SRm300 in yeast two-hybrid, co-immunoprecipitation, and co-immunofluorecence assays (Miele et al., 2007). This is not an isolated finding. Proteomic analysis of SRm160 and SRm300-containing complexes identified not only several splicing-related factors but also proteins involved in chromatin remodelling and RNAP II transcription (McCracken et al., 2005). These evidences suggest that one of the possibilities of SRm300 functioning in the coupling of transcription and splicing could be through interactions with factors that bind directly to components of these two machineries.

The subcellular location of RSR-2 is conserved since SRm300 is also located at nuclear speckles in a variety of human cell types (Blencowe et al., 2000; Lin et al., 2004; Zimowska et al., 2003). Although diverse RNA processing factors have been detected at nuclear speckles, transcriptional factors are also located at such structures (Lamond and Spector, 2003). In fact, although these organelles are commonly known as RNA processing bodies, they are often in the close vicinity of transcriptionally active chromosome territories (Spector and Lamond, 2010).

Apart from the clues that gave us the RSR-2 subcellular location at nuclear speckles and chromatin, the analyses of ChIP-Seq provided more evidences that link RSR-2 with RNAP II transcription. First, these two proteins, RSR-2 and RNAP II, map very similarly throughout the genome. Second, the enrichment of RSR-2 at the TSS is greatly comparable to the accumulation observed for RNAP II. Third, RSR-2 is recruited to the TSS and the CDS of intronless genes. Fourth, we have been able to immunoprecipitate RNAP II using the antibody against RSR-2 (data not shown) and besides, RNAP II phosphoisoforms rate vary upon *rsr-2* RNAi treatment.

Thus, there is a clear connection of RSR-2 and RNAP II. But does this relationship rely on a direct interaction between them? Attempts to co-immunoprecipate RSR-2 with an anti-POL II antibody failed probably due to the nature of the epitope recognized by the antibody 8W16G (the CTD). Further experiments such as yeast-two-hybrid or *in vitro* protein binding assays are needed to solve this question. However, SRm300/SRRM2 has not been found among the > 100 proteins that specifically associate with the immunopurified human RNA pol II (Das et al., 2007).

Our data suggests that *rsr-2* inactivation produces a general decrease in the number of transcripts without general splicing defects. Reduced levels of RSR-2 might be interpreted by the transcriptional machinery as a sign of reduced splicing efficiency, slowing down transcription. In accordance with this, Alexander and co-workers have recently shown how splicing defects produce RNA polymerase pausing in yeast (Alexander et al., 2010).

If RSR-2 is functioning as a splicing factor, why is it present in one exon-containing genes whose transcripts do not need to be spliced? The same question had been already formulated in regard to the uridine-rich U1 snRNP (Brody and Shav-Tal, 2011). For one exon-containing genes, where there are no introns and no splice sites, recruitment of splicing components is not supposed to occur. Nonetheless, Brody and co-workers showed that U1 snRNP and the U1A protein were enriched on an actively transcribing intronless gene (Brody et al., 2011).

U1 snRNP has been proposed to travel together with the RNAP II along the DNA in search of 5'ss and when one of them is detected, U1 could trigger the spliceosome recruitment and induce co-transcriptional splicing. It has also been revealed that SR proteins are essential for co-transcriptional splicing, an observation that suggests that trancription is important for splicing because it favors the recruitment of U1 snRNPs and SR proteins (Allemand et al., 2008). In that sense, RSR-2 could be one of the preliminar splicing factors tethered at the transcriptional complex to recruit the rest of the splicing machinery.

Chromatin structure and transcriptional activity influence splicing (Almeida and Carmo-Fonseca, 2012). In a model in which actively transcribed genes, splicing impacts transcription and both feedback to chromatin modification, it remains to be explored if RSR-2 would affect the remodelation of the chromatin state. So far, our transcriptomic analysis and protein expression studies are compatible with RSR-2 influencing and coupling splicing and transcription.

# D.6. How is *rsr-2* regulated?

## D.6.1. *rsr-2* and *lin-35* Rb

DNA sequencing of ChIP experiments carried out by the modENCODE consortium have shown that several transcription factors as PHA-4, DAF-16, LIN-54 or LIN-9 and not others as LIN-11 or HLH-8 bind significantly to the *rsr-2* promoter region, being this the first hint about a regulated expression of *rsr-2* (Gerstein et al., 2010; http://modencode.oicr.on.ca/fgb2/gbrowse/worm/).

Remarkably, the seed this study has arisen from is the genetic interaction between *rsr-2* and *lin-35* (Ceron et al., 2007). LIN-35 ChIPs the *rsr-2* promoter (Valerie Reinke unpublished data; http://modencode.oicr.on.ca/fgb2/gbrowse/worm/). Considering this, we wondered whether this binding could be promoting or repressing *rsr-2* expression. Thus, a synchronized population of *lin-35(n745)* mutants was grown at 26°C and total RNA isolation was performed at L1 stage to assay *rsr-2* mRNA levels by Real Time PCR. We found reduced expression of *rsr-2* in the *lin-35* mutant background (Figure D.4).

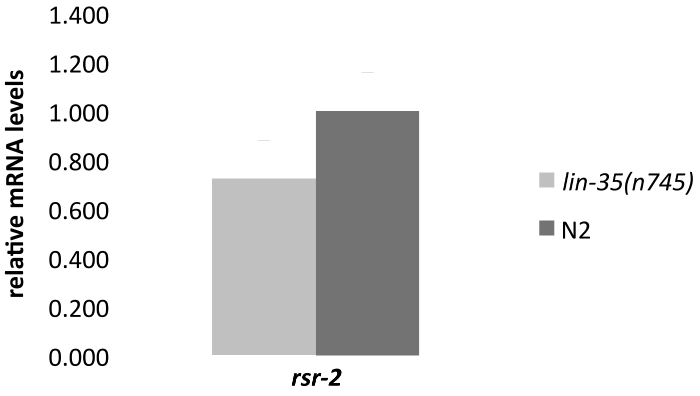

**Figure D.4. Changes in *rsr-2* mRNA accumulation in *lin-35(n745)* mutants.** All qPCR expression data were normalized to transcript levels of *act-3* and were then measured as relative to mRNA levels in N2 control animals (which was set to an arbitrary value of 1.0). Bars represent standard deviation within three replicates.

The diminished *rsr-2* mRNA levels of *lin-35(n745)* mutants suggest that LIN-35 may be promoting the expression of *rsr-2* even though the reduction of mRNA levels in the mutant background is not statistically significant at L1 stage. This positive effect of LIN-35 on *rsr-2* expression may justify that *rsr-2* RNAi produces a stronger phenotype in *lin-35* mutants than in wild types.

The second clue about a *rsr-2* regulated expression comes from the expression pattern of *rsr-2* in the germ line. This study presents an *in situ* hybridization experiment showing that *rsr-2* mRNA is less present in the distal part than in the proximal part of the germ line. Accordingly, we have also observed how the expression of *rsr-2* promoter driving GFP::H2B::*rsr-2* 3'UTR is also lower in the distal part than in the middle region of the germ line. All these data suggest different mechanisms of regulation of *rsr-2* expression in the germ line and in the soma.

Finally, SR protein activity and subcellular location are known to be regulated by extensive phosphorylation on serine residues of the RS domains (Lin and Fu, 2007). However, RS are not essential in RSR-2 and by western blot we did not observe different bands corresponding to different phosphorilation status of the protein. Therefore, future research may uncover proteins that control RSR-2 functions to ultimately modulate developmental programs.

### D.6.2. *rsr-2* is the first gene of the operon CEOP2720

About 70% of mature mRNAs in *C. elegans* are *trans*-spliced, which implies the attachment of one of the splicing leader sequences to the 5'-end (Blumenthal, 2005). There exists two splice leaders, SL1 and SL2. The SLs are structurally and functionally related to the U snRNAs that play a key role in intron removal (also known as *cis*-splicing). SL1 is used to process outrons at the 5' exon that are thought to confer stabilility to the mRNA molecule and SL2 serves to resolve downstream genes in operons (Blumenthal, 2005).

Mechanistically, SL *trans*-splicing occurs like *cis*-splicing, and requires most of the same spliceosomal components except for the U1 snRNP, which is not needed (Lasda et al., 2010). In *C. elegans,* polycistronic messengers are *trans*-spliced in a co-transcriptional manner.

*rsr-2* is the first gene of the operon CEOP2720, which also contains the downstream gene *sinh-1*. *rsr-2* has a predicted SL1 and *sinh-1* has a predicted SL2 (Figure D.5). Do the *C. elegans* operons exist to ensure coordination of regulation of genes whose products function together? In comparison to bacterial operons, genes within a *C. elegans* operon often show poor co-expression and only sometimes encode proteins with related functions (Reinke and Cutter, 2009) which suggests that operons in *C. elegans* are vestiges of procaryote operons. In agreement with this, modENCODE RNA-Seq analyses indicate that *sinh-1* is barely expressed through development compared to the higher expression levels for *rsr-2*. The known functions of these two genes are very distinct. In this study we showed evidences for *rsr-2* to be involved in splicing but also in controlling RNAP II transcription. On the other hand, *sinh-1* encodes the ortholog of mammalian SIN-1, an essential component of the TORC2 complex. In *C. elegans*, loss of *sinh-1* activity via RNAi results in enhanced stress response, and *daf-16*-dependent lifespan extension (Hansen et al., 2005).

Certain classes of genes are dramatically overrepresented in operons while other classes are missing or nearly so from a *C. elegans* operon list made by Blumenthal and Gleason (Blumenthal and Gleason, 2003). In general, tissue-specific genes are not transcribed in operons. The most frequent operon-included genes are those that encode mitochondrial

[illegible]

[illegible]

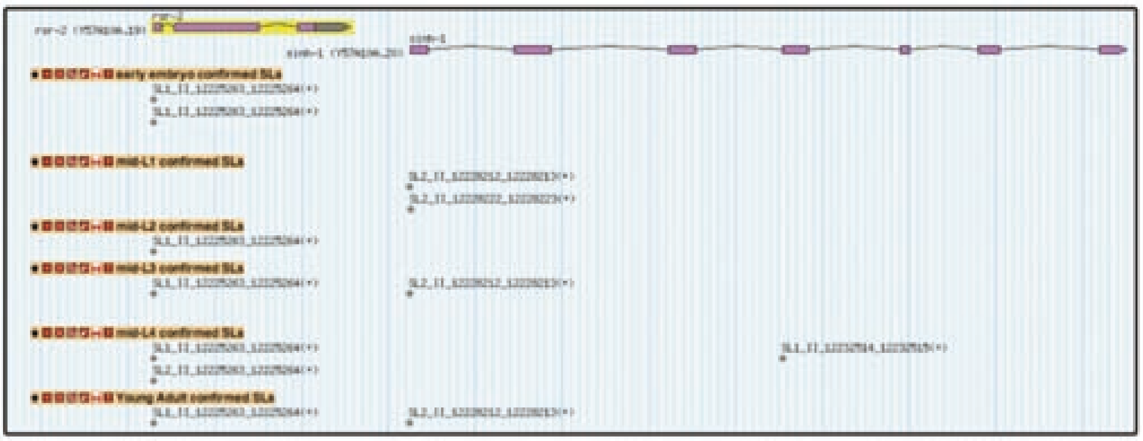
early embryo confirmed SLs
mid-L1 confirmed SLs
mid-L2 confirmed SLs
mid-L3 confirmed SLs
mid-L4 confirmed SLs
Young Adult confirmed SLs

[illegible]

## D.7. Our model: RSR-2 is a multitask protein that regulates development through transcription and splicing

The existing data about RSR-2 homologs in yeast and humans classified these SR-related proteins as components of the spliceosome. However, this thesis and the revision of the recent literature invite us to think out of the box when talking about functions of RSR-2.

Nowadays it is already clear that different gene expression steps need to be interconnected for an efficient performance. SR proteins are important in such crosstalk since they have been implicated in not only constitutive and alternative splicing, but also in mRNA nuclear export, nonsense-mediated decay and mRNA translation (Long and Caceres, 2009; Zhong et al., 2009). Differently from other SR proteins, RSR-2 does not bear any RNA binding domain and this may limit its capacity to do many other things in the regulation of gene expression. Still, we have discovered that RSR-2 may have other roles outside of the spliceosome since we have been able to pinpoint RSR-2 in chromatin areas where splicing is not happening. Moreover we have presented data supporting a functional relation with RNAP II in terms of similarities on their genomic distribution.

Our *rsr-2* RNAi treatment affects the phosphorylation status of RNAP II, favoring the hyperphosphorylated active form, which accumulates at the gene 5’ ends. Studies about RNAP II dynamics in live cells established that only one of each 90 RNAP II complexes proceeds through elongation to produce a complete mRNA (Darzacq et al., 2007). Interestingly, the presence of splicing factors that associate with RNAP II CTD stimulate transcriptional elongation (Das et al., 2007, Lin et al., 2008; Dermody et al., 2008). Wrapping all this information up, we propose a model where RSR-2 associates with RNAP II to stimulate the entering into elongation phase and therefore promoting the transcriptional activity. In this model, reduced levels of RSR-2 induces the accumulation of active RNAP II at the gene 5’ ends resulting in lower transcript production.

The RNAP II complex is probably the most important multiprotein complex of the whole gene expression machinery. Therefore it needs to be highly regulated, but for security purposes such regulation should rely on many different proteins. In this study, *rsr-2* RNAi by feeding may produce a slight reduction of the RNAP II transcriptional capacity that it is critical only for certain developmental processes. In our mild *rsr-2* RNAi treatment only the germ line sex determination is visibly affected. However, *rsr-2* inactivation by mutation or by other RNAi treatments produces additional phenotypes as Lva, growth defects or protruding vulva. We believe that RSR-2 requirements for each developmental process should be different, but those developmental mechanisms requiring higher levels of mRNA production may be more sensitive to *rsr-2* inhibition.

Since splicing and transcription occur co-transcriptionally, and RSR-2 is present in both macromolecular complexes, it is tempting to think of RSR-2 as a co-transcriptional factor. The term “co-transcriptional factor” is a recent concept that refers to proteins that exchange information between the RNAP II and the spliceosome about their respective functional status. In other words, if any of the phases of the transcription (initiation, elongation and termination) is not working properly or is delayed, the pre-mRNA processing machinery will detect the problem by regulating down its activity. Such functional coupling is reciprocal and therefore the transcription will be less efficient if the mRNA processing is affected. Such is the growing evidence about this coupling that scientists in the field have begun to talk about “co-transcriptional RNA checkpoints” (Almeida and Carmo-Fonseca, 2010).

We think that RSR-2 levels could act as a sensor of the splicing wellness since RSR-2 is physically and functionally related with PRP-8, which locates at the “heart” of the spliceosome. In that case, if there are failures within the spliceosome, RSR-2 would communicate the defects to the RNAP II and transcription would slow down to give time to the spliceosome to solve these problems (Figure D.6).

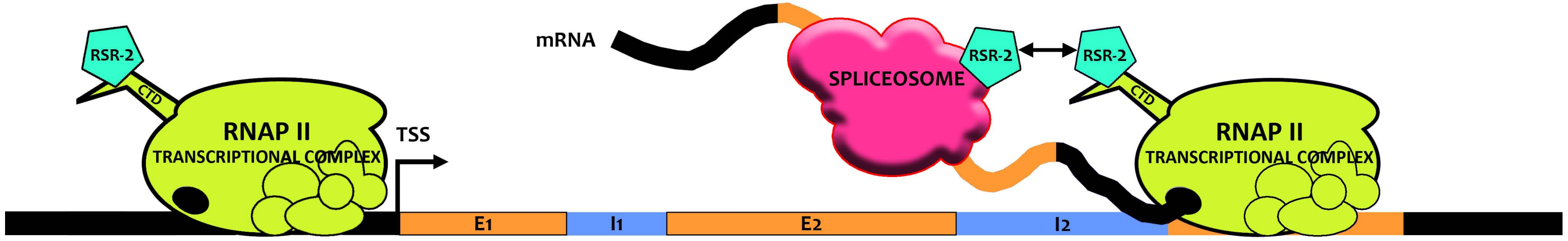
RSR-2
CTD
RNAP II
TRANSCRIPTIONAL COMPLEX
TSS
E1
I1
mRNA
E2
SPLICEOSOME
RSR-2
RSR-2
I2
CTD
RNAP II
TRANSCRIPTIONAL COMPLEX

**Figure D.6. Proposed model for RSR-2 molecular functions.** RSR-2 is associated with the RNAP II complex even if splicing is occurring or not. RSR-2 would act as a RNA checkpoint to control the communication between the RNAP II complex and the spliceosome when the pre-mRNA is being processed co-transcriptionally. However, when splicing is not taking place (i.e. intronless genes) RSR-2 would still be linked with the transcriptional process as one of the first factors recruited tho the RNAP II.

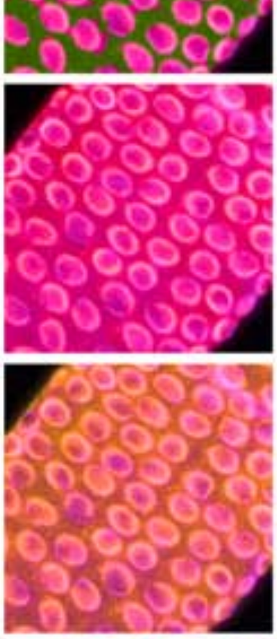

# Conclusions

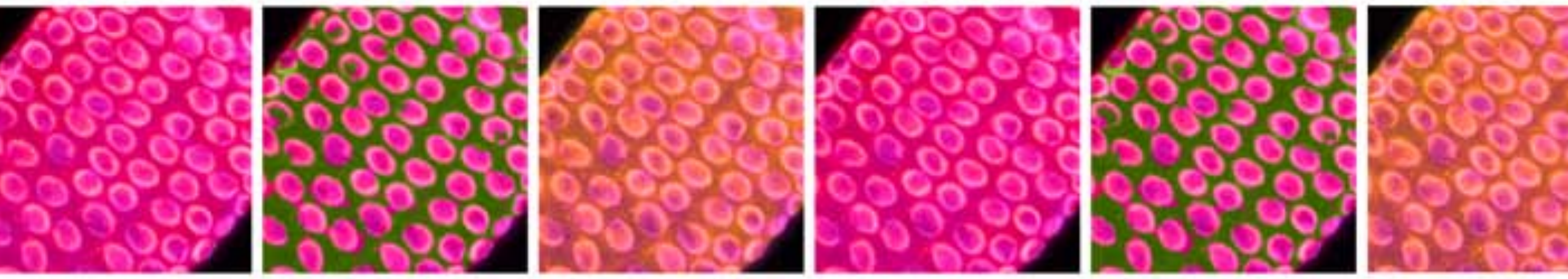

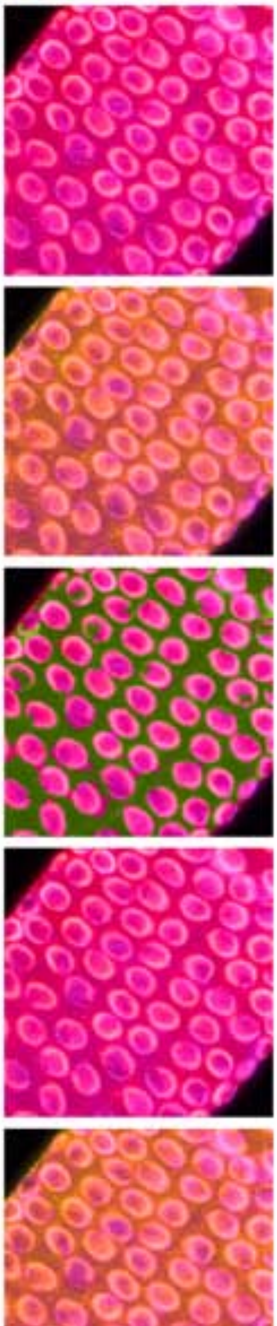

*" An end has a start"*

*Editors*

1. *rsr-2*, the ortholog of the yeast Cwc21 and the human SRm300/SRRM2 splicing factors, is well conserved throughout evolution. The cwf21 motif at the N-terminal, deleted in the *tm2625* allele, is fundamental for its functions. In contrast, a central region containing serine and arginine residues affected by the allele *tm2607* is not essential.

2. *rsr-2* is a gene necessary for *Caenorhabditis elegans* development and regulates the germ line sex determination.

3. RSR-2 is a nuclear protein. In somatic cells can be detected forming nuclear speckles. In germ cells, RSR-2 clearly co-localizes with chromatin.

4. Transcript levels are slightly diminished genome-wide when expression of *rsr-2* is inactivated. However, splicing seems not to be altered.

5. RSR-2 and the core spliceosome component PRP-8 have common targets in terms of gene expression, indicating that they are functioning in common processes.

6. RSR-2 controls RNA polymerase II (RNAP II) distribution along genes. When RSR-2 levels are low RNAP II accumulates at the 5’ gene end to the detriment of a reduction at the 3’ end.

7. RSR-2 is recruited to intronless genes that are actively being transcribed.

8. RSR-2 requirements for each developmental process could vary. However, the developmental mechanisms requiring higher levels of mRNA production may be more sensitive to *rsr-2* inhibition.

9. RSR-2 functions are compatible with RSR-2 acting as a coupling factor between transcription and splicing.

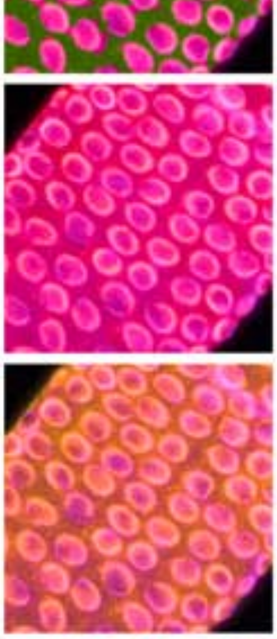

# Materials & Methods

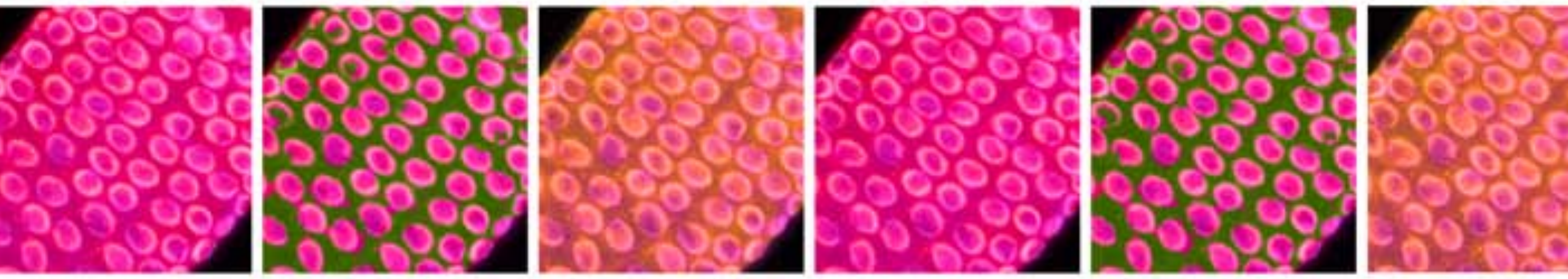

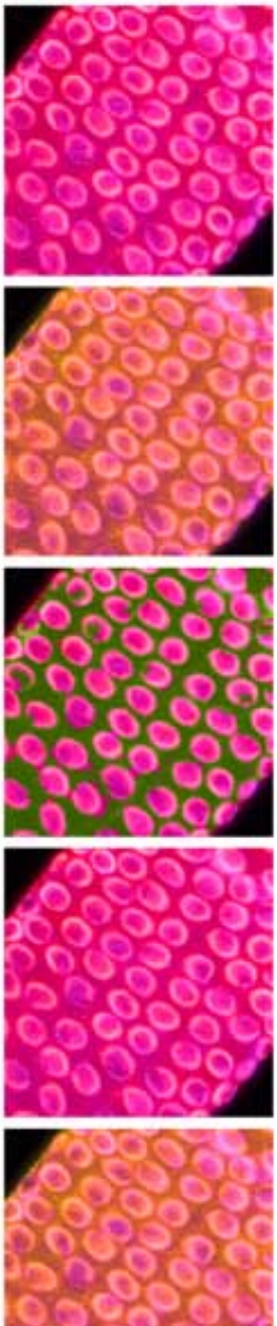

" Miniature disasters"
KT Tunstall

# MM.1. Strains and general methods

Standard methods are used to culture and manipulate worms (Brenner, 1974). Briefly, worms are grown at temperatures between 15 and 25°C on NGM (Nematode Growth Media) Agar plates (see “Recipes” at the end of this section). Plates are previously seeded with an overgrown liquid culture of the *Escherichia coli* strain OP50, and air-dried.

Bristol N2 is used as wild type (WT) strain and mutant and transgenic strains used in this study are listed in table MM.1.

| Strain | Genotype | Characteristics |
|---|---|---|
| JK560 | *fog-1(q253) I* | Temperature sensitive. Raise at 15 or 20°C. |
| TR1331 | *smg-1(r861) I* | Non-mediated decay pathway defective mutants. |
| TR1335 | *smg-5(r860) I* | Non-mediated decay pathway defective mutants. Hermaphrodites have an abnormally protrusive vulva. |
| NL2098 | *rrf-1(pk1417) I* | Reference allele. Homozygous *rrf-1* deletion allele. RNAi interference for genes expressed in somatic tissue is lost in *rrf-1* deletion mutants. |
| - | *rrf-1(pk1417) I; gld-3(q730) II* | Tumorous germ line at 25°C (from Schedl Lab) |
| - | *rrf-1(pk1417) I; glp-1(oz264) III* | Tumorous germ line at 25°C (from Schedl Lab) |
| JK3345 | *gld-3(q741)/mIn1[mIs14 dpy-10(e128)] II* | Heterozygotes are WT with major GFP signal in pharynx. Segregates WT GFP+, Dpy GFP+ (*mIn1* homozygotes) and GFP- *gld-3* homozygotes. |
| CER004 | *rsr-2(tm2625)/mIn1(dpy-10(e128) mIs14(myo-2::GFP)) II* | Heterozygotes are WT with major GFP signal in pharynx. Segregates WT GFP+, Dpy GFP+ (*mIn1* homozygotes) and GFP- *rsr-2* homozygotes. |
| CER007 | *rsr-2(tm2607) II* | Animals do not display any phenotype. |
| JK3022 | *fbf-1(ok91) II* | Low percent sterile, more sperm than WT, delayed oogenesis, larger broods than WT. |
| JK3101 | *fbf-2(q738) II* | Grows well as a homozygote, possibly small percent Fog. |
| JK2589 | *nos-3(q650) II* | Reference allele.Grows well as a homozgyote. 0.3% sterile at 20°C (0.2% have masculinized germ lines). |
| JH1521 | *puf-8(ok302) II* | 100% Sterile at 25°C. Him and 50% Emb at 20°C. Maintain at 15°C. |
| JK3231 | *puf-8(q725) II* | Low penetrance (<10%) Mog. |
| GE24 | *pha-1(e2123) III* | Wild type at 15°C. Embryonic lethal at 25°C. Temperature sensitive phase during embryogenesis. |
| CB3844 | *fem-3(e2006) IV* | Temperature sensitive Fem. Hermaphrodites al 15°C, female at 25°C. Maintain at 15°C. |
| JK574 M | *fog-2(q71) V* | Male-female strain. Maintain by mating. |
| JK2421 | *qIs43 [lacZ::fem-3(+)] V* | 100% roller. Low level expression of LacZ after heat shock at 33°C. Expression in nuclei HS::LacZ::*fem-3* 3'UTR(+). Maintain by picking roller. Maintain at 20°C. |
| JK1950 | *qIs15[lacZ::fem-3(q96gf)] V* | 100% roller. *fem-3* UTR::LacZ transgene. No coding region of *fem-3*, only the 3'UTR. Strong expression of beta-Galactosidase in nuclei of intestine and other cells. Mutant *fem-3* 3’UTR. No expression in germ line. This transgene is derepressed in mog mutants. Maintain by picking roller. Maintain at 20°C. |
| wt8Di | *wt8Di[lacZ::tra-2(+)] II* | 100% roller. Contains integrated construct with roller, and *tra-2*(+)3'UTR. Maintain by picking roller. Maintain at 20°C. |
| BL3466 | *inIs173[pNvitgfp]* | WT. Contains integrated intron-containing GFP contrstruct expressed in intestinal cells. |
| EG4322 | *ttTi5605* II; *unc-119(ed9)* III | Unc. Not caused by *ttTi5605*. Mos1 allele generated by NemaGENETAG consortium. |

| | | |
|---|---|---|
| BC20394 | *sEX20394[rsr-2 promoter::GFP], dpy-5(907) I* | WT. Contains *sEX20394* and pCeh361 *[dpy-5(+)]*. Maintain by picking non-Dpy worms. |
| CER001 | *cerEX01[rsr-2 promoter::gfp::Histone 2B::rsr-2 3'UTR]* | WT. Contains *cerEX07*. GFP expression in the soma and the germ line. |
| CER008 | *cerEX04[rsr-2 promoter::gfp::rsr-2 genomic fragment + rsr-2 3'UTR]* | WT. Contains *cerEX04* and *myo-2*::mCherry. GFP expression in the soma. mCherry expression in the pharynx |

**Table MM.1. Mutant and transgenic strains used in this study and some of their characteristics.**

## MM.1. Recipes

### Nematode Growth Media Agar (NGM)

For 1 liter of plates:

| | |
|---|---|
| NaCl | 3 g |
| Peptone | 2.5 g |
| Agar | 17 g |
| $H_2O$ | 975 ml |

Autoclave, cool to 55°C and then add the following reagents mixing after every addition:

| | |
|---|---|
| Cholesterol (5mg/ml in EtOH) | 1 ml |
| 1M $CaCl_2$ | 1 ml |
| 1M $MgSO_4$ | 1 ml |
| 1M Kalium phosphate buffer | 25 ml |

### 1M Kalium phosphate buffer

For 1 liter:

| | |
|---|---|
| $KH_2PO_4$ | 108.3 g |
| $K_2HPO_4$ | 35.6 g |
| $H_2O$ | 975 ml |

### Luria Bertani (LB)

For 1 liter:

| | |
|---|---|
| Tryptone | 10 g |
| Yeast extract | 5 g |
| NaCl | 10 g |
| $H_2O$ | 950 ml |

# MM.2. RNA-mediated interference (RNAi)

## MM.2.1. By feeding

RNAi by feeding in *C. elegans* is a technique that permits the inactivation of a gene of interest by administrating the interferent RNA through the food. Although RNAi by feeding produces weaker effects than RNAi by injection, it is an advantadgeous method when large number of animals need to be treated at once for high throughput screenings.

To induce the RNA-mediated interference (RNAi) by feeding, NGM plates were supplemented with 50 µg/mL ampicillin, 12.5 µg/mL tetracycline, and 1mM IPTG. HT115 cells transformed with L4440 plus the target DNA sequence can be obtained either from Vidal RNAi library (ORFeome) or Arhinger RNAi library. If the RNAi clone of interest is not available in neither of the 2 libraries, a new clone has to be generated by standard molecular cloning methods.

A strike of the selected clone was made on a LB-Ampicillin plate (50 µg/mL) and the bacteria let grow O/N at 37°C. The day after, three colonies were picked and a colony PCR was performed with L4440 forward and reverse primers (see “Primers” at the end of this section). The PCR product was run in an agarose gel to make sure that the size of the clone was appropriate. If a single band of the right size was detected, the clone was sequenced for a final validation. Next, the RNAi cultures were preparated by growing a positive single colony of each clone in 4mL LB plus 50 µg/mL of ampicillin at 37°C O/N with agitation. 60 mm plates seeded with 400 µl of the corresponding RNAi clone induced O/N at RT were used to feed synchronized L1 animals. Worms were grown at the desired temperature, depending on the experiment that was performed.

Phenotype analysis was carried out every day after seeding the animals by scoring the plates under the stereomicroscope.

## MM.2.2. By microinjection

To interfere *rsr-2* expression by microinjection, dsRNA was synthetized by using MEGAscript® T7 kit (Ambion Cat. No. AM1333). The template used was the *rsr-2* cDNA cloned into the vector L4440 and flanked by two bacterial polymerase promoter sequences (T7) at each 5’ and 3’ ends. The transcription reaction was carried out following manufacturer’s instructions.

WT young adults were injected into the intestine with 1 ng/µl of *rsr-2* dsRNA and grown at 25°C. Progeny was scored every 24 hours.

## MM.2. Primers

**L4440 primers**

| | |
|---|---|
| Forward | 5’-GTTTTCCCAGTCACGACGTT-3’ |
| Reverse | 5’-TGGATAACCGTATTACCGCC-3’ |

# MM.3. Sodium hypochlorite treatment

The bleaching technique is used for synchronizing *C. elegans* cultures at L1 stage. The principle of the method lies in the fact that worms are sensitive to bleach while the egg shell protects embryos from it. After treatment with alkaline hypochlorite solution, embryos are incubated in liquid media without food, which allows hatching but prevents further development.

Worms were allowed to grow until adult stage and recovered by washing plates with M9 buffer. Then, worm pellets were washed twice with M9 until the buffer appears clear of bacteria. After the last wash 2 ml of M9 buffer were left and 2 ml of 2x bleaching solution were added (see MM.3 recipes). Next, samples were vigorously agitated for 5 minutes approximately and after this time the reaction was stopped by adding M9 buffer to fill the tube (destruction of the adult tissue was monitored under the dissecting microscope and the reaction stopped when traces of adults were still visible). A fast centrifugation was carried out and the pellets were washed three more times with M9 buffer. Finally, 1ml of M9 buffer was added to pellet and samples were incubated at 15°C for 24 hours with gentle agitation (Porta-de-la-Riva et al., 2012).

After 12 and 24 hours (time to embryonic development depends on the temperature) worms were recovered by centrifugation and seeded on the required plates.

## MM.3. Recipes

**M9 buffer**

For 1 liter:

| | |
|---|---|
| NaCl | 5 g |
| $KH_2PO_4$ | 3 g |
| $Na_2HPO_4$ | 6 g |
| 1M $MgSO_4$ | 1 ml |
| $H_2O$ | 975 ml |

**Bleaching solution (2x)**

| | |
|---|---|
| NaOH 1N | 2.5 ml |
| Hypochlorite sodium | 1 ml |
| $H_2O$ | 0.5 ml |

# MM.4. Semiquantitative RT-PCR

WT, and several mutant worms (such as *rsr-2(tm2607)*, *smg-5(r860)* and *smg-1(r861)* were synchronized at L1 stage by following a sodium hypochlorite treatment and grown at 25°C on *rsr-2* and *prp-8* RNAi plates to induce the silencing of these genes. In parallel, as a negative control the same amount of animals was grown on *gfp* RNAi plates. After 36 hours post-L1 for germ line experiments and after 26 hours for L3 molting experiments, animals were harvested and washed twice with M9 buffer. Next, all populations were incubated for 30 minutes at RT to get rid of remaining bacteria in the intestine. Total RNA isolation from *rsr-2, prp-8* and *gfp*(*RNAi*) worms was accomplished as follows:

Worm pellets were washed twice with M9 buffer, 7 volumes of TRIReagent (TR-118, MRC) were added to the packed pellets and they were frozen at -80°C. Next, 5 cycles of freezing/thawing were performed and samples were vortexed vigorously. The suspension was allowed to stand at RT for 5 minutes to disrupt all RNA-protein complexes. Addition of 0,2mL of chloroform per mL of Trizol used was carried out before an incubation of 15 minutes at RT to allow the phase separation of the samples. The aqueous phase was taken and RNA was precipitated with ethanol. RNA was resuspended in DEPC-treated water and its quality and quantity is determined by running an agarose gel and taking spectrophotometric readings.

cDNA was synthesized from 1 μg of purified RNA with oligo(dT) primers using the RevertAid H Minus First Strand cDNA synthesis kit (Fermentas. Cat.No. K1632) following the manufacturer's instructions. Sequences of primers used in the RT-PCR assay are at the end of this section.

## MM.4. Primers

***rsr-2* primers**

| | |
|---|---|
| Forward | 5'-CGAGGTGAAATGCACCGAAT-3' |
| Reverse | 5'-GCCATTTTTTCGGCTCAA-3' |

***act-1* primers**

| | |
|---|---|
| Forward | 5'-TTGAGCACGGTATCGTCACCAACT-3' |
| Reverse | 5'-TCAGCGGTGGTGGTGAAAGAGTAA-3' |

***rpl-12* primers**

| | |
|---|---|
| Forward | 5'-GTTGCGTCGGAGGAGAAGTCG-3' |
| Reverse | 5'-GATGATGTCGTGTGGGTGTTGTC-3' |

***gld-1* primers**

| | |
|---|---|
| Forward | 5'-CGACAATGTTCCAGCGGATCGTT-3' |
| Reverse | 5'-CTTCGGGAACGTCAAATCACTTGC-3' |

***fbf-1* primers**

| | |
|---|---|
| Forward | 5'-ATGGACCAATCAAAAATGCGC-3' |
| Reverse | 5'-CTGGGCAATGATAAGGGTGG-3' |

***tra*-2 primers**

| | |
|---|---|
| Forward | 5’-GGCTGCTGGTGAAGAGCTTTTTG-3’ |
| Reverse | 5’-CGAGAACTGCTGAATGGCCACC-3’ |

***prp*-8 primers**

| | |
|---|---|
| Forward | 5’-TTGACAGAGCATCCAGATCC-3’ |
| Reverse | 5’-ATGGAATTTGGACAATGACTCC-3’ |

***dpy*-8 primers**

| | |
|---|---|
| Forward | 5’-TCACCCAGAATACGCTGACG-3’ |
| Reverse | 5’-TTCTTGCGCCATTTCCTCTCG-3’ |

***dpy*-2 primers**

| | |
|---|---|
| Forward | 5’-ATGAAATCGCAAACGAGTGG-3’ |
| Reverse | 5’-CTCTTGAAATTGTGGTGAATCG-3’ |

**Y37A1B.7 primers**

| | |
|---|---|
| Forward | 5’-AGTGGGGAATTATCATCCGG-3’ |
| Reverse | 5’-ATCTCTTTGGCACGTGGCC-3’ |

***ama*-1 primers**

| | |
|---|---|
| Forward | 5’-TGCAGGAGTTGGTCAATCG-3’ |
| Reverse | 5’-TCGGAATGTACTCCATGGG-3’ |

## MM.5. Dissection of gonads

A plate full of adults was washed with PBS-0,1% Tween-20 (PBSt) and the animals placed in a three-well glass dish from Pyrex (up to 200 worms per well). Worms were allowed to gravity settle for a few minutes and washed twice with PBSt. Next, as much PBSt as possible was removed and addition of 200 μl of 0,3 mM levamisole performed to paralize the animals. As paralysis sets in, heads were cut off at level of the pharynx. To do so, the head was placed between two 20 guage syringe needles and decapitated by moving needles in a scissors motion. Normally at least one gonad extrudes completely.

After a maximum of 15 minutes of dissection, the paralysis reaction was stopped by diluting the levamisole solution in which the worms were immersed with PBSt. The dissected worms were washed 3 times and before to proceed with the fixation, excess of liquid was removed with a pipette.

To fix gonads different fixing solutions can be used depending on the molecular nature of the target to be detected in downstream applications. For instance, if gonads are going to be used for mRNA distribution studies, a good fixer to maintain mRNA integrity is a combination of glutaraldehyde and paraformaldehyde (see MM.6 for details). However, if they are going to be immunostained, a good choice to maintain protein structures is 4% paraformaldehyde (see MM.7. for details). In any case, fixation time should go from 20 to 30 minutes. After this time, fixed gonads are washed 3 times and used as a template for *in situ* hybridization or immunostaining experiments.

# MM.6. *In situ* hybridization of mRNA

*In situ* hybridization was performed following the protocol described by Lee and Schedl, 2006 (Lee and Schedl, 2006). Briefly, DNA probes were synthesized with digoxigenin-11-dUTP by repeated primer extension (DIG DNA Labeling Mix. Roche Cat. No. 11 277 065 910). The oligonucleotides used to generate the *rsr-2* sense and antisense probes are detailed in the "MM.6. Primers" box at the end of this chapter.

Dissected gonads from adult hermaphrodites were permeabilized (50 µg/ml proteinase K) for 30 minutes at RT and fixed with a 3% paraformaldehyde/0.25% glutaraldehyde/0.1M $K_2HPO_4$ (pH 7.2) fixer for 2 h at RT. Both sense and antisense probes were diluted 5 times in hybridization buffer and hybridised for 36 hours at 48°C in a hybridization oven. Probe detection was carried out by incubating the samples with a 400-fold-diluted alkaline-phosphatase-conjugated anti-DIG antibody overnight at 4°C. BCIP/NDT (Sigma Cat. No. B5655) was used to set up the colorimetric reaction dissolved in staining solution. Gonads were also stained with DAPI (2 µg/ml), embeded in anti-fade solution (Invitrogen Cat. No. P36930) and mounted on a microscope slide.

## MM.6. Primers

***rsr*-2 ISH primers**

| | |
|---|---|
| Sense | 5'-GCAAGCGAGACGAAAAATCG-3' |
| Antisense | 5'-ATCCCGGCGTTGTGGTGACT-3' |

## MM.6. Recipes

**3% paraformaldehyde/0.25% glutaraldehyde buffer/0.1M $K_2HPO_4$ (pH 7.2)**

| | |
|---|---|
| 16% paraformaldehyde | 25 ml |
| 25% glutaraldehyde | 0.53 ml |
| 0.2M $K_2HPO_4$ (pH 7.2) | 25 ml |

**Hybridization buffer**

5x SSC
50% deionized formamide
100 µg/ml autoclaved herring sperm DNA
50 µg/ml heparin
0.1% Tween-20

**Staining solution**

100mM NaCl
5mM $MgCl_2$
100mM Tris pH 9.5
0,1% Tween-20
1mM Levamisole

# MM.7. Immunostaining

## MM.7.1. Of dissected gonads

Dissected gonads were fixed with 4% paraformaldehyde (Electron Microscopy Sciences Cat. No. 15710) for 20 minutes and subsequently washed 3 times with PBSt (10 minutes each wash). Pre-incubation with PBSt and BSA (1 mg/ml) (Sigma Cat. No. A9418) was carried out for 1 hour at RT. After it, the epitope of interest was detected by incubation with the corresponding primary antibody overnight at 4°C in a sealed humidity chamber (see Table MM.2. at the end of this section for information about antibody nature and dilutions used).

The following day gonads were left 1 hour at RT and washed three times with PBSt plus BSA. Addition of the corresponding secondary antibody was performed at the concentration indicated in table MM.2. Antibody incubation was accomplished for 2 hours at RT. Finally the antibody was washed out and gonads were counterstained with DAPI (2 μg/ml), embeded in anti-fade solution (Invitrogen Cat. No. P36930) and mounted in a glass microscope slide.

## MM.7.2. Of larvae (Freeze–cracking protocol)

For immunostaining of larvae, freeze-cracking protocol was followed as described by Duerr, 2006. This protocol provides a simple way to remove portions of the worm's cuticle allowing its penetration by antibodies.

Polylysine coated slides were prepared and baked in a 60°C oven for 15 minutes. In parallel, larvae were washed and pelleted using PBS. Once the polylysine coated slides were dry and chilled to RT, around 50 worms were placed on each slide, allowed to settle and stick on the surface for a few minutes. Excess of liquid was removed with a pipette and a coverslip was set so that the edge of the coverslip extended over the edge of the slide. Pressure on the coverslip was put with the fingertips and the slides were placed on a prefrozen aluminium block on dry ice. Slides were left on the cold block until they were frozen. Coverslips were popped off and the slides immediately soaked in prechilled (-20°C) 100% methanol for 15 minutes, followed by 10 minutes in prechilled (-20°C) 100% acetone and three washing steps (10 minutes each) with PBSt plus 10 mg/ml BSA.

After a 30-minute pre-incubation with PBSt plus 10mg/ml BSA, 50 μl of the primary antibody of interest was applied, the slide covered with a parafilm coverslip and incubated at 4°C overnight in a sealed humidity chamber. Next, three PBSt washing steps of ten minutes each were carried out and 50 μl of the secondary antibody were spread over the fixed worms.

Samples were left 2 hours at RT and after three more washing steps with PBSt (10 minutes each), samples were embeded with anti-fade solution and counterstained with DAPI (2 µg/ml).

| Antibody | Epitope | Host | Nature | Dilution | Source |
|---|---|---|---|---|---|
| Q56092 | RSR-2 | Rabbit | Polyclonal (Primary) | 1:600 | Sdix |
| A11120 | GFP | Mouse | Monoclonal (Primary) | 1:100 | Molecular Probes |
| MH33 | Intermediate filament | Mouse | Monoclonal (Primary) | 1:40 | DSHB |
| A11001 (Alexa Fluor 488 IgG) | Anti-Mouse | Goat | Secondary | 1:400 in gonads<br>1:250 in larvae | Molecular Probes |
| A11011 (Alexa Fluor 568 IgG) | Anti-Rabbit | Goat | Secondary | 1:400 in gonads<br>1:250 in larvae | Molecular Probes |

**Table MM.2. Antibodies and dilutions used in immunostainings of this study.**

## [illegible]

### [illegible]

[illegible]

[illegible]

[illegible]

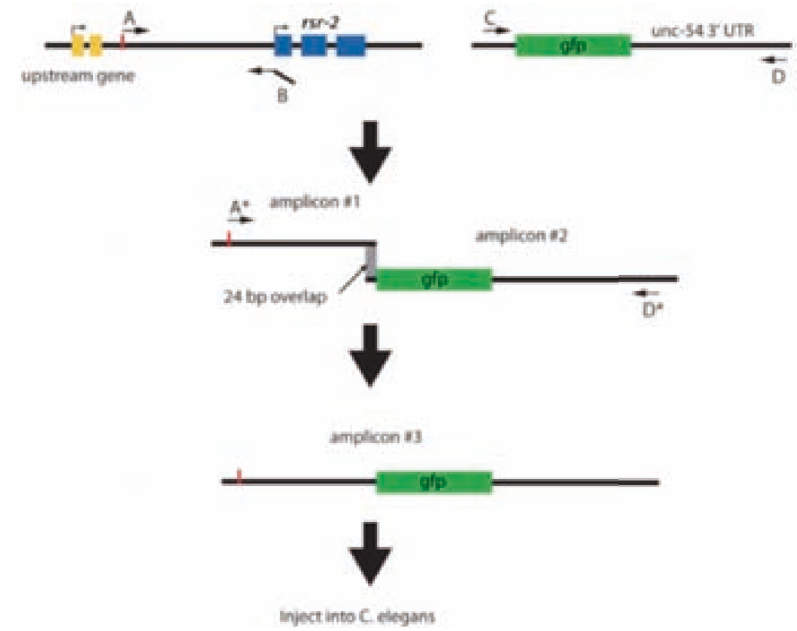
upstream gene
A
rsr-2
B
C
gfp
unc-54 3' UTR
D
A*
amplicon #1
amplicon #2
24 bp overlap
gfp
D*
amplicon #3
gfp
Inject into C. elegans

[illegible]

## MM.8.2. Gateway Three-fragment Cloning System

The MultiSite Gateway® Three-Fragment Vector Construction Kit (Invitrogen Cat. No. 12537-023) facilitates rapid efficient construction of an expression clone containing the promoter of choice followed by the gene of interest (which at the same time can be tagged), and a 3'UTR.

The system consists of three Donor vectors, pDONR P4-P1r (5' vector), pDONR 221 (middle vector), pDONR P2r-P3 (3' vector), and one Destination vector, pDEST R4-R3 (expression vector) (Table MM.3), which are used in a sequential series of recombination reactions to eventually get the desired expression clone as it is schematized in figure MM.2. In brief, *attB* and *attP* on one hand (BP reaction)*;* and *attL* and *attR* on the other (LR reaction), are recombination sites that are utilized in the Gateway technology. PCR fragments are cloned into the apropriate Donor vectors (5', middle or 3'; see Figure MM.2) and next, the three of them are recombined to generate an organized three-fragment DNA transgene inside the expression vector.

- Generating Entry clones: BP reaction.

  *attB* sites always recombine with *attP* sites in a reaction mediated by the BP recombinase enzyme. Thus, when generating the PCR fragment of interest, appropriate flanking *att* recombination sites must be incorporated into the primers in order to create the correct Entry clone. To do so, genomic DNA from a mixed stage population of N2 worms was extracted and purified with the PureLink Genomic DNA Mini kit (Invitrogen Cat. No. K1820-01). All PCR amplifications were carried out using Phusion High-Fidelity DNA Polymerase (Finnzymes Cat. No. F-530S). The specific primers used to produce the *att*-PCR fragments and the vectors necessary for generating Entry clones are listed at the end of this section.

  The recombinase reaction products were next transformed into DH5$\alpha$ competent cells (Invitrogen Cat. No. 18263-012) and positive colonies selected using solid cultures with 50 $\mu$g/ml of kanamycin. The presence of the desired clone vas confirmed by PCR in which primer combination used consisted on a transgene-specific primer together with a vector-specific primer (M13 primer). Additionally, positive clones were sequenced (by the dye-base sequencing method).

- Generating Expression clones: LR reaction.

  Once 5', middle and 3' Entry vectors were produced and validated, LR reaction was performed. In this reaction mediated by the LR recombinase enzyme, *attL* sites always recombine with *attR* sites. Only concerning the case of the Entry vector that bears the *rsr-2* genomic and 3'UTR fragment (Table MM.4.), the clone was digested with PvuII previous to

[illegible]

[illegible]

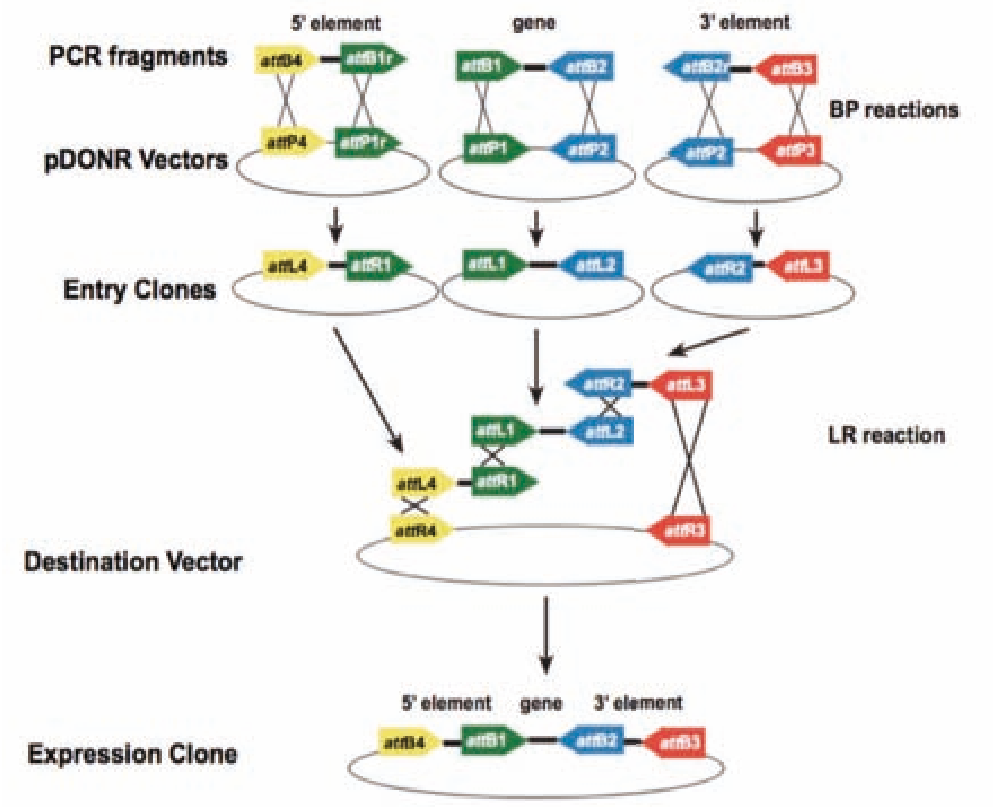
5' element
gene
3' element
PCR fragments
attB4
attB1r
attB1
attB2
attB2r
attB3
BP reactions
pDONR Vectors
attP4
attP1r
attP1
attP2
attP3
Entry Clones
attL4
attR1
attL1
attL2
attR2
attL3
LR reaction
attR4
attR3
Destination Vector
Expression Clone

[illegible]

## MM.8. Primers

[illegible]

[illegible]

| **_rsr_-2 Gateway 3'UTR primers** | |
|---|---|
| attB2r Forward | 5'-GGGGACAGCTTTCTTGTACAAAGTGGCCTTTTTTCTTGTGTTTTAT-3' |
| attB3 Reverse | 5'-GGGGACAACTTTGTATAATAAAGTTGCCCAGTTTTCAGGAGATTCTTC-3' |
| **_rsr_-2 Gateway ORF + 3'UTR primers** | |
| attB2r Forward | 5'-GGGGACAGCTTTCTTGTACAAAGTGGTTATGTACAATGGAATCGGACT-3' |
| attB3 Reverse | 5'-GGGGACAACTTTGTATAATAAAGTTGCCCAGTTTTCAGGAGATTCTTC-3' |
| **M13 primers** | |
| Forward | 5'-GTAAAACGACGGCCAG-3' |
| Reverse | 5'-CAGGAAACAGCTATGAC-3' |

Vectors used to generate *rsr-2* reporter constructs and vectors generated in our lab to study *rsr-2* expression are listed on the following tables MM.3 and MM.4.

| Vector name | Resistance | Expressing | Provided by |
|---|---|---|---|
| pDONR P4-P1R | Kanamycine | ccdB | Invitrogen |
| pCM1.35 | Kanamycine | GFP::H2B | Seydoux Lab |
| pCM1.53 | Kanamycine | GFP-no stop codon | Seydoux Lab |
| pDONR P2R-P3 | Kanamycine | ccdB | Invitrogen |
| pCFJ150 R4-R3 | Ampicillin | ccdB | Invitrogen |
| pBCN26 R4-R3 | Puromycine, neomycine | ccdB | Lehner Lab |

**Table MM.3. List of plasmids used to generate *rsr-2* reporter constructs.**

| Vector name | Backbone vector | Resistance | Expressing |
|---|---|---|---|
| pCER002 | pDONR P4-P1R | Kanamycine | *rsr-2* promoter |
| pCER003 | pDONR P2R-P3 | Kanamycine | *rsr-2* 3'UTR |
| pCER005 | pDONR P2R-P3 | Kanamycine | *rsr-2* ORF + 3'UTR |
| pCER001 | pCFJ150 R4-R3 | Ampicillin | P*rsr-2*::GFP::H2B:: *rsr-2* 3'UTR |
| pCER004 | pBCN26 R4-R3 | Ampicillin | P*rsr-2*::GFP::RSR-2:: *rsr-2* 3'UTR |

**Table MM.4. List of plasmids generated to study *rsr-2* expression *in vivo* in *C. elegans*.**

# MM.9. Generation of GFP reporters and transgenic animals

There are three methods described to obtain low-copy trangenic worms: complex arrays (Kelly et al., 1997); gene-gun transformation (Praitis et al., 2001; Wilm et al., 1999) and Mos1-mediated Single Copy Insertion (MosSCI) (Frokjaer-Jensen et al., 2008). In this study only complex arrays and gene-gun transformation have been used to generate RSR-2 transgenic animals.

## MM.9.1. Complex arrays

This type of transformation involves dilution of the transgene with exogenous genomic DNA prior to injection to make a “complex array”. Normally transgene DNAs are co-injected with a positive transformation marker. Transformation markers can be either a fluorescent protein under the control of a specific promoter such as [*promoter myo-2*::mCherry] or a wild type copy of a certain gene that rescues lethal or non-lethal mutations of specific mutant strains as transformation hosts (for instance, *dpy-5(e907)* mutants can be microinjected with the rescue vector pCeh361 [*dpy-5(+)*]). Injected DNAs can suffer both homologous and non-homologous recombination and behave like an extra chromosome (Mello and Fire, 1995).

To generate RSR-2 transgenic animals, the complex array strategy was used to transform the transgene [*promoter rsr-2*::GFP::H2B:: *rsr-2 3’UTR*]. 4 ng/µl of the linearized molecular construct were microinjected together with digested bacterial genomic DNA and linearized pRF4 2 ng/µl (roller marker). Selection of $P_0$ roller animals was carried out and expression of the array in the germ line of animals from F1 generation was studied, since these complex arrays allow expression in the germ line just for a few generations until it gets silenced.

## MM.9.2. DNA transformation by gene bombardment

Microparticle bombardment can induce integrative transformation in *C. elegans* (Praitis et al, 2001). The reporter strain expressing *rsr-2* promoter::*gfp*::*rsr-2* genomic fragment::*rsr-2* 3’UTR was generated by gene bombardment. The principle of this technique is to bind DNA onto gold particles, which are shot into worms using a biolistic bombardment instrument also named “gene gun”. In our lab we use the Biolistic Helium Gun (Caenotec) to perform gene bombardment.

Recently, Lehner lab has developed an excellent and powerful antibiotic selection system for *C. elegans*, such as those used in single-celled organisms and in mammalian cell cultures (Semple et al., 2010). Taking advantadge of this new system for transgenic animal selection, we transfected the plasmid containing the transgene of interest (pCER004). The backbone vector of this expression plasmid is pBCN26-R4R3. pBCN26-R4R3 contains a dual resistance operon vector, which confers resistance to neomycin and puromycin at once. This vector also bears the gene mCherry under the control of *myo-2* promoter (pharynx specific), which codes for a red fluorescent protein that serves as an extra point of visual selection control.

Prior to bombardment, 20 μl of a N2 YA worm pellet were transferred to ice-cold 35 mm plates containing a dry and thin bacterial layer. DNA-coated gold particles were prepared by mixing 1 mg of gold (Chempur, 0.3-3 μm diameter) with 100 μl of 50 μM spermidin (Sigma, Cat. No. S-0266) and 7 μg of DNA. Next, precipitation was carried out by adding 100 μl of 1M $CaCl_2$. Before resuspension with 0.1 mg/ml polyvinylpyrolidon in EtOH (Sigma, Cat. No. P-5288), gold particles-DNA complexes were washed three times with 96% ethanol. Eight plates were shot and the agar cut into six pieces, each being put onto a fresh 90 mm plate and incubated at 20°C. The day after (day 2 of the experiment) L1 worms were recovered and animals carrying the transgene selected by culturing them in liquid NGM supplemented with 0.5 mg/ml of both neomycin and puromycin plus 0.1% of Triton X-100. The recovery of L1 worms was also performed at day 3 and worms were united with the worms from day 2 on the selection media. At day 5, worms were plated. Finally, at day 8 animals expressing mCherry were singled out and the F1 generation was scored in search of stable transgenic strains expressing GFP.

# MM.10. β-galactosidase reporter assays

lacZ, together with GFP, is one of the most popular reporter genes. It encodes the enzyme β-galactosidase. This protein makes an excellent reporter because its presence can be detected by staining with a subtrate (X-gal) that turns blue in the presence of the enzyme. Thus, any blue color in the worm indicates that the reporter gene is expressed in that cell.

In the β-galacotsidase assays of this thesis, animals carrying lacZ*::fem-3* 3'UTR and lacZ*::tra-1* 3'UTR integrated transgenes (both under the control of a heat shock promoter) were synchronized at L1 stage and fed with *rsr-2* and *gfp* RNAi clones at 25°C. Once the animals had reached the adulthood, they were heat shocked for 2 hours at 30°C and allowed to recover for 2 hours at 25°C. After two washes with M9 buffer, worms were dehydrated in a SpeedVac up to 2 hours. Samples were placed in the fume hood, a drop of cold acetone was added and the samples air-dried for a few minutes. The step of acetone dehydration was repeated 3 to 5 times, until the worm pellet was completely dry.

Staining was performed by adding 200 μl of staining solution, which contains the substrate for the β-galactosidase, and incubating the samples O/N at 37°C. The day after stained worms were mounted onto a microscope slide to score for lacZ expression. Scoring was performed as described by Gallegos et al., 1998.

## MM.10. Recipes

**Staining Solution (5 ml)**

| | |
|---|---|
| $Na_2HPO_4$ 1M | 830 μl |
| $NaH_2PO_4$ 1M | 165 μl |
| $MgCl_2$ 1M | 1 μl |
| SDS 25% | 8 μl |
| Ferricyanide 1M | 25 μl |
| Ferrocyanide 1M | 25 μl |
| Kanamycin 10 mg/ml | 37.5 μl |
| Formamide 99% | 15 μl |
| X-gal 4% | 48 μl |
| $H_2O$ | 375 μl |

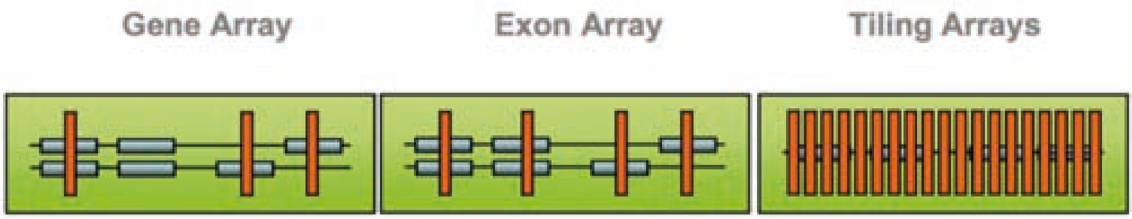
Gene Array
Exon Array
Tiling Arrays

# MM.12. Quantitative PCR (qPCR)

This is an application of PCR to determine the quantity of DNA or RNA in a sample. The measurements are made in real time and the method is therefore called real-time PCR. The equipment used for this study was the Roche LightCycler 480 Instrument I following the two-step RT-PCR protocol in which the reverse transcription of RNA into cDNA is separated from the other reaction steps and is performed outside the lightcycler.

Wild type N2 hermaphrodites were synchronized at L1 stage and total RNA isolation from *rsr-2(RNAi)* and *gfp(RNAi)* worms was performed 36 hours past L1 arrest. cDNA was synthesized with oligo(dT) primers as before (see MM.4). LightCycler 480 SYBR Green I Master kit (Roche Cat. No. 04707516001) was used to determine gene expression of a chosen gene subset. Sequences of primers used in these assays are listed at the end of this section.

To validate the tiling array data by qPCR, template cDNA was diluted 1:10 and gene expression data was normalized to transcript levels of *tbb-2* and then measured as relative to mRNA levels in *gfp(RNAi)* worms control animals (which were set to an arbitrary value of 1.0 for each gene). Three separate experiments were analyzed, with samples represented in triplicate for each gene and condition to give a total of nine data sets.

To validate the ChIP experiment by qPCR, the amount of immunoprecipitated chromatin was normalized to chromatin immunoprecipitated with RNAP II from an actively transcribed gene such as *act-1* (which were set to an arbitrary value of 1.0 for each region assayed). One experiment was analyzed, with samples represented in triplicate.

## MM.12. Primers

***rsr-2* primers**

| | |
|---|---|
| Forward | 5’-GAGCCGAAAAAATGGCTGG-3’ |
| Reverse | 5’-CCCAGAAAATGTGGTTTTTTAGGC-3’ |

***fog-1* primers**

| | |
|---|---|
| Forward | 5’-TGTGGGAACTGAACCGGTCCGAA-3’ |
| Reverse | 5’-ACTGGCGACACGGAGCCTCT-3’ |

***gld-1* primers**

| | |
|---|---|
| Forward | 5’-GCTCATTCCGGCTCCCGAGG-3’ |
| Reverse | 5’-ACACGAGCTGGGTTTGGCGA-3’ |

***gld-3* primers**

| | |
|---|---|
| Forward | 5’-AGCGCAAGGATTGCCTCTGCC-3’ |
| Reverse | 5’-CGTGATCCCCGTTGTCACTGGTC-3’ |

***fem-3* primers**

| | |
|---|---|
| Forward | 5’-TGGCAAGGCGGAACGGGAAA-3’ |
| Reverse | 5’-CGGATCCGGATTGGGTAAAAATTGTCG-3’ |

***fbf-1* primers**

| | |
|---|---|
| Forward | 5’-ACATGCCACACCCGGGCACT-3’ |
| Reverse | 5’-CGTCTTCCAGACACAGCATCACAGC-3’ |

***tra-2* primers**

| | |
|---|---|
| Forward | 5’-TGGGACGCAAATCGAAGTGGCT-3’ |
| Reverse | 5’-GGCGGCGAGGAAACCAGCAA-3’ |

***glp-1* primers**

| | |
|---|---|
| Forward | 5’-ACCAGCCGACGAAATCCCTCTCC-3’ |
| Reverse | 5’-TGGCAGCAAGCCAGTGCAGA-3’ |

***puf-8* primers**

| | |
|---|---|
| Forward | 5’-TGCGTGTCACCATCAGGAAGGATCT-3’ |
| Reverse | 5’-GGATGAGTTCACGGCGCTGTTCT-3’ |

***fbf-2* primers**

| | |
|---|---|
| Forward | 5’-TGGCGCAGCATGAGACACCT-3’ |
| Reverse | 5’-GGGTTGGTGGCCGCGATGTAA-3’ |

***nos-3* primers**

| | |
|---|---|
| Forward | 5’-ACTCACGTGGACATGGTGGAGGA-3’ |
| Reverse | 5’-TCGGAGGAAGTTTTTGTTGTCGTTGGA-3’ |

**C05G5.7 promoter primers**

| | |
|---|---|
| Forward | 5’-GAGTAATGTATCCATGGAGCCG-3’ |
| Reverse | 5’-AGCAGATGAGGTTCCCCTG-3’ |

**C05G5.7 CDS primers**

| | |
|---|---|
| Forward | 5’-CCAACATGCGTGTCGCCTA-3’ |
| Reverse | 5’-TAGGTCCAATCGAGGTAGATGC-3’ |

**F18E3.11 promoter primers**

| | |
|---|---|
| Forward | 5’-CTGTTTCCTCGAACCGAAGAACC-3’ |
| Reverse | 5’-ATCGACGATTCGAAGTGAGAATAGG-3’ |

**F18E3.11 CDS primers**

| | |
|---|---|
| Forward | 5’-ATGTCTCACGTTCTCGCCG-3’ |
| Reverse | 5’-CGGGGAGCATCTGATGATGT-3’ |

**F18E3.12 promoter primers**

| | |
|---|---|
| Forward | 5’-TTCAGACAATCGCCAGACAC-3’ |
| Reverse | 5’-TGGGACTCCGCCTATTTTCTG-3’ |

**ZK666.12 promoter primers**

| | |
|---|---|
| Forward | 5’-TACACCCTGTTAACGCCC-3’ |
| Reverse | 5’-AACGGATTTCGGATTTTTCTG-3’ |

**ZK666.12 CDS primers**

| | |
|---|---|
| Forward | 5’-TTCTTTTCTGTTTTACGGCC-3’ |
| Reverse | 5’-AACATCGGTAATATGCGGG-3’ |

***act-1* promoter primers**

| | |
|---|---|
| Forward | 5’-AGCTCACTCATCTCCACG-3’ |
| Reverse | 5’-TCTGGTGTTATCTGTTCGC-3’ |

## MM.13. Protein extraction and analysis

Protein analysis was performed by western blot. Wild type animals were harvested after 36 hours post-L1 arrest at 25°C and washed in M9 buffer. After 30-minute incubation in M9 buffer with agitation to get rid of the remaining bacteria, worms were packed and frozen.

Worm lysis was performed by adding 2 volumes of 2x lysis buffer directely onto frozen worms. Protein from worms was extracted by 3 cycles of freezing in liquid nitrogen and boiling for 15 min. Next, a 10-minute centrifugation at 4°C was performed and total protein in the lysate was quantified using the Bio-Rad DC protein assay (Bio-Rad Cat. No. 500-0112).

Then, protein was loaded in sodium dodecyl sulfate polyacrylamide gel (SDS-PAGE) at different percentages and gels were run in TGS buffer. Proteins were transferred to a nitrocellulose membrane (Protran, Cat. No. BA85, 0.45 μm) for two hours at 200 mA using transfer buffer (TB). Membranes were blocked with 5 % non-fat milk in TBS-t for one hour. Primary antibody was added to fresh blocking solution or prepared in 3 % bovine serum albumin (BSA)-TBS-t (see Table MM.5 for details on Ab and dilutions used) and incubated O/N at 4°C. After three ten-minute washing steps with TBS-t-milk, secondary antibody peroxidase-combined (HRP) was incubated (in the same solution) for one hour at RT. Two more ten-minute washes were performed with TBS-t prior to developing.

Membranes were developed using a substrate for HRP (luminol, which exhibits chemiluminescence when mixed with an appropriate oxidizing agent). Membranes were incubated with luminol plus enhancer for one minute and exposed to autoradiographic films (CL-xposure films, Cultek S.A.).

Antibodies and dilutions used for protein analyses of this study are listed in table MM.5. The RSR-2 antibody was raised in rabbit against the immunogen sequence of the RSR-2 protein, which comprises aminoacids 39 to 138, and was affinity purified (Sdix, Strategic Diagnostics Inc. USA).

| Antibody | Epitope | Host | Nature | Dilution | Source |
|---|---|---|---|---|---|
| Q5092 | RSR-2 | Rabbit | Polyclonal (Primary) | 1:500 | Sdix |
| C4 (69100) | Actin | Mouse | Monoclonal (Primary) | 1:500 | MP biomedicals |
| 10799 | Histone 3 | Mouse | Monoclonal (Primary) | 1:2000 | mAbcam |
| 8W16G (MMS-126R) | CTD RNAP II | Mouse | Monoclonal (Primary) | 1:500 | Covance |
| N-20 (sc-899) | N-ter RNAP II | Rabbit | Polyclonal (Primary) | 1:1000 | Santa Cruz Biotech |
| P0260 (HRP conjugated) | Anti-Mouse | Rabbit | Polyclonal (Secondary) | 1:2000 | Dako |
| P0448 (HRP conjugated) | Anti-Rabbit | Goat | Polyclonal (Secondary) | 1:2000 | Dako |

**Table MM.5. Antibodies and dilutions used in western blots of this study.**

## MM.13. Recipes

**TGS**
25mM Tris OH pH 8.3
192mM glycine
0.1% SDS

**Sample buffer for proteins (Laemmli, 1x)**
60mM Tris-HCl pH 6.8
2% SDS
5% β-mercaptoethanol
0.005% bromophenol blue
5% glycerol

**Ponceau**
0.5% Ponceau (w/v)
1% glacial acetic acid

**Luminol (500 ml)**
125 mg luminol sodic (Sigma A-4685)
33.25 ml 1.5M Tris-HCl pH 8.8
466.8 ml $H_2O$
155 μl hydrogen peroxide

**Enhancer p-CU (25 ml)**
27.5 mg p-cumaric acid (Sigma C-9008)
25 ml DMSO 99.5% (Sigma 41639)

**Transfer buffer**
50mM Tris OH
386 mM glycine
0.1% SDS
20% MeOH

**Lysis Buffer 2x**
4% SDS
100mM Tris-HCl pH 6.8
20% glycerol
Proteases and phosphatases inhibitors
(Roche, Cat. No. 1187350001)

**TBS**
25mM Tris-HCl pH 7.5
137mM NaCl

**TBS-t**
TBS
0.1% tween

# MM.14. Chromatin Immunoprecipitation - Sequencing (ChIP-Seq)

ChIP-Sequencing, also known as ChIP-Seq, is used to analyze protein interactions with DNA. ChIP-Seq combines chromatin immunoprecipitation (ChIP) with massively DNA sequencing to identify the binding sites of DNA-associated proteins. Moreover, it has also been used to map spliceosome recruitment on genes (Sapra et al., 2009).

Therefore, we took advantage of this technique to map RSR-2 recruitment across the genome. ChIP assays were carried out as described previously by Zhong et al., 2010 with minor modifications:

Worms were collected at L4 stage and 0.5 ml of packed larvae were resuspended in 3 ml of FA buffer plus protease inhibitors and crosslinked with 2% formaldehyde for 30 minutes at room temperature. Quenching of formaldehyde was carried out by addition of 1M Tris (pH 7.5). Next, samples were sonicated on ice using a Branson sonifier microtip (100% amplitude, 10 seconds on, 10 seconds off) avoiding overheating of the samples. After sonication, cell extracts containing DNA fragments with an expected range between 200 and 800 bp were immunoprecipitated using anti-RSR-2 (Sdix, Q5092) and anti-POL II antibodies (Covance, 8WG16). To do so, 2.2 mg of protein were treated as described in Zhong et al., 2010, input samples were set apart and 10 μg of each antibody were added to each sample. ChIP was performed O/N at 4°C with rotation.

Then, 25 μl of protein G conjugated to sepharose beads (Amersham Biosciences) were added to each ChIP sample and washed four times with 1 ml FA buffer. After the washes, beads were suspended in one bed volume of FA buffer, and 40 μl of the bead slurry was added to each ChIP sample and rotated at 4°C for 2 h. Next, beads were washed as follows: 2 washes with FA buffer for 5 minutes, 1 wash with FA-1M NaCl for 5 minutes, 1 wash with FA-500mM NaCl for 10 minutes, 1 wash with TEL buffer for 10 minutes, 2 washes with TE buffer for 5 minutes.

To elute the immunocomplexes, 150 μl of elution buffer were added to the samples and the tubes incubated at 65°C for 15 minutes, with brief vortexing every 5 minutes. The beads were spun down and the supernatant transferred to a new tube. The elution was repeated and supernatants combined. At this point, input samples were thawed and treated with the ChIP samples. To each sample, 2 μl 10 mg/ml Rnase A were added and incubated at room temperature for 1–2 hours. Then, 250 μl of elution buffer with 1 μl of 20 mg/ml proteinase K were added to each sample and incubated for 1–2 hours at 55°C. Samples were transferred to

65°C for 12–20 hours to reverse crosslinks. The DNA was purified with the Qiaquick PCR purification kit (Qiagen), and eluted with 50 μl $H_2O$. The enriched DNA fragments and input DNA were used to prepare libraries for sequencing by the Illumina GA platform. In order to run four samples in one flow cell, sequencing libraries were barcoded and multiplexed as described in Lefrançois et al., 2009.

Calling binding peaks from ChIP-Seq data was performed usign Seq-Solve software. First, ChIP-Seq fastq files obtained from the ModEncode consortium were processed in Galaxy mapped against the *Caenorahabditis elegans* WS220 genome version to generate SAM Files. SAM files were converted to BAM files also in Galaxy (Blackenberg et al., 2010). BAM files we analyzed with the Seq-Solve software using default settings.

In these default settings, the output from the peak caller was filtered by using a False Discovery Rate (FDR) larger than 0.1. Thus, peaks having a FDR larger than 0.1 (10%) were filtered out. Peak calling p-value cutoff was $10^{e-5}$. Seq-Solve Peak Calling analysis uses the MACS algorithm (Zhang et al, 2008) to identify those regions of the genome having higher read counts in the ChIP samples than in the input sample. At these conditions, 6889, 5451 and 412 peaks were called for anti-POL II, anti-RSR-2 and input respectively. The numbers of reads after the ChIP were about 2.3, 2.2 and 7 millions for anti-POL II, anti-RSR-2 and input respectively.

## MM.14. Primers

**Barcoded adapter primers**

| | |
|---|---|
| MPLEXA1 | |
| Forward | 5’-ACACTCTTTCCCTACACGACGCTCTTCCGATCTGTAT-3’ |
| Reverse | 5’phosphate-TACAGATCGGAAGAGCTCGTATGCCGTCTTCTGCTTG-3’ |
| MPLEXA6 | |
| Forward | 5’-ACACTCTTTCCCTACACGACGCTCTTCCGATCTCATT-3’ |
| Reverse | 5’phosphate-ATGAGATCGGAAGAGCTCGTATGCCGTCTTCTGCTTG-3’ |
| MPLEXA8 | |
| Forward | 5’-ACACTCTTTCCCTACACGACGCTCTTCCGATCTACGT-3’ |
| Reverse | 5’phosphate-CGTAGATCGGAAGAGCTCGTATGCCGTCTTCTGCTTG-3’ |
| MPLEXA9 | |
| Forward | 5’-ACACTCTTTCCCTACACGACGCTCTTCCGATCTTGCT-3’ |
| Reverse | 5’phosphate-GCAAGATCGGAAGAGCTCGTATGCCGTCTTCTGCTTG-3’ |

**Illumina PCR primers**

| | |
|---|---|
| PCR 1.1 | 5’-AATGATACGGCGACCACCGACACTCTTTCCCTACACGACGCTCTTCCGATCT-3’ |
| PCR 2.1 | 5’-CAAGCAGAAGACGGCATACGAGCTCTTCCGATCT-3’ |

## MM.14. Recipes

**FA buffer**
50mM HEPES/KOH pH 7.5
1mM EDTA
1% Triton X-100
0.1% sodium deoxycholate
150mM NaCl

**TEL buffer**
0.25M LiCl
1% NP40
1% sodium deoxycholate
1mM EDTA (10mM Tris HCl pH 8.0)

**FA-1M NaCl buffer**
FA buffer
1M NaCl

**FA-500mM NaCl buffer**
FA buffer
500mM NaCl

**Elution buffer**
TE buffer
1% SDS
250mM NaCl

# MM.15. Transcriptome sequencing (RNA-Seq)

RNA-Seq is a recently developed approach to transcriptome profiling that uses deep-sequencing technologies.

Wild type worms were fed on *rsr-2*, *prp-8* and *gfp* dsRNA-expressing bacteria at 25°C. After 26 hours, the three populations were harvested and frozen with Tri Reagent (MRC Inc, Cat. No. TR-118) in order to proceed with the RNA extraction previously described in section MM.4 of this thesis.

Processing of the simple after total RNA and sequencing was performed at the CIBIR sequencing facility (http://www.cibir.es/cibir-investigacion/plataforma-tecnologica/genomica). Total RNA was purified, including small RNAs, with the *mirvana miRNA isolation kit* (Ambion). RNA quality and integrity were evaluated with the *Experion Bioanalyzer* (Biorad). Ribosmal RNA was depleted with the *RiboMinus Eukaryote Kit* (Invitrogen). Efficiency of rRNA depletion was checked in the *Experion Bioanalyzer* (Biorad).

Libraries for sequencing were made by using the Illumina *TruSeq RNA Sample Preparation Kit.* Resulting libraries were quantified and its quality was verified. These libraries were run through a *Genome Analyzer IIx Ultrasequencer* (Illumina), multiplexing three times in a single channel, in a single read run of 100 cycles to generate ≈ 100 nt reads. Each of the samples yield more than 10 millions reads. The resulting fastq files were trimmed and mapped to the version WS225 of the *C. elegans* genome by using TopHat to generate BAM files. TopHat is a fast splice junction mapped for RNA-Seq reads that first use the aligner Bowtie, and then analyzes the mapping results to identify splice junctions between exons.

BAM files were analyzed in SeqSolve using default settings (False Discovery Rate, FDR; of 0.05 was used) and using WS220 as Reference Genome. Reads displaying multiple mapping were filtered out. SeqSolve was used for a Differential Transcript Expression Analysis between *rsr-2* RNAi and gfp RNAi samples, and between *prp-8* RNAi and gfp RNAi samples. Transcripts covered by more than 5 reads were tested. This analysis uses Cufflinks/Cuffdiff (Trapnell et al, 2010) to quantify and identify transcripts with a significant level of expression between different conditions. In this analysis expression values were normalized in FPKM (Fragments Per Kilobase of exon per Million fragments mapped).

To analyze intron retention, a file containing intron sequences (excluding those introns with internal genes or ncRNAs) was used as reference genome.

## MM.16. Computational tools

Sequence alignments were performed using either Clustal W algorithm (Thompson et al., 1994) or the application of Basic Local Alignment Search Tool (BLAST) to compare several known sequences.

- ClustalW. http://www.ebi.ac.uk/Tools/msa/clustalw2/
- BLAST. http://www.ebi.ac.uk/Tools/sss/ncbiblast/

Once the alignment was performed, CLC sequence viewer was used to generate the cladogram.

- CLC sequence viewer software. http://www.clcbio.com/

For primer design, the following on-line appliations were used.

- Oligo Calc. http://www.basic.northwestern.edu/biotools/OligoCalc.html
- OligoAnalyzer http://eu.idtdna.com/analyzer/applications/oligoanalyzer/default.aspx

*C. elegans* tools and data: general resources.

- Wormbase http://www.wormbase.org/
- modENCODE http://www.modencode.org/
- WormMart http://caprica.caltech.edu:9002/biomart/martview/

ChIP-Seq and RNA-Seq analyses.

- Galaxy http://galaxy.tuebingen.mpg.de/root
- Bowtie http://bowtie-bio.sourceforge.net/index.shtml

For Venn diagram generation.

- Venny http://bioinfogp.cnb.csic.es/tools/venny/index.html

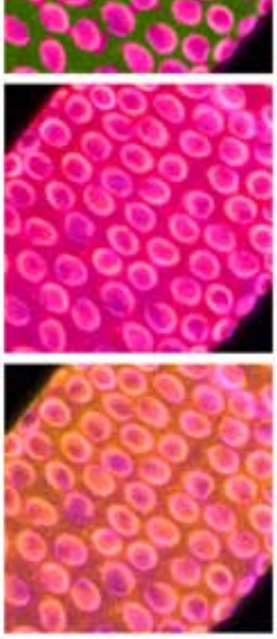

# References

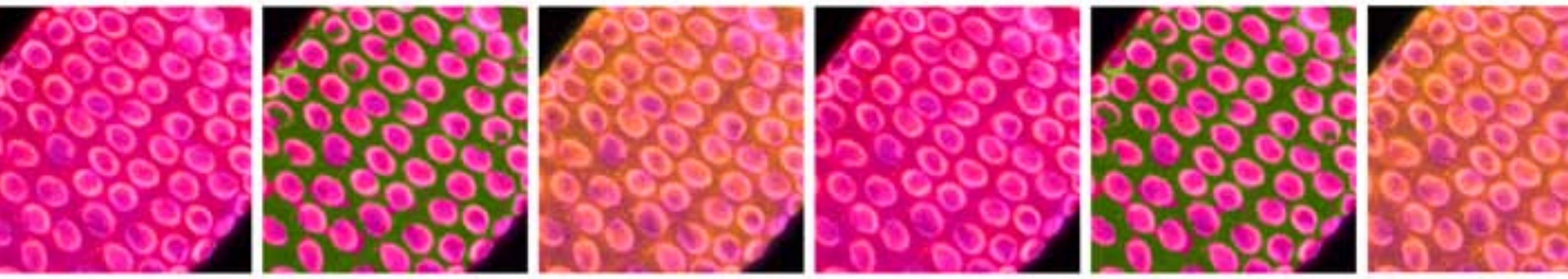

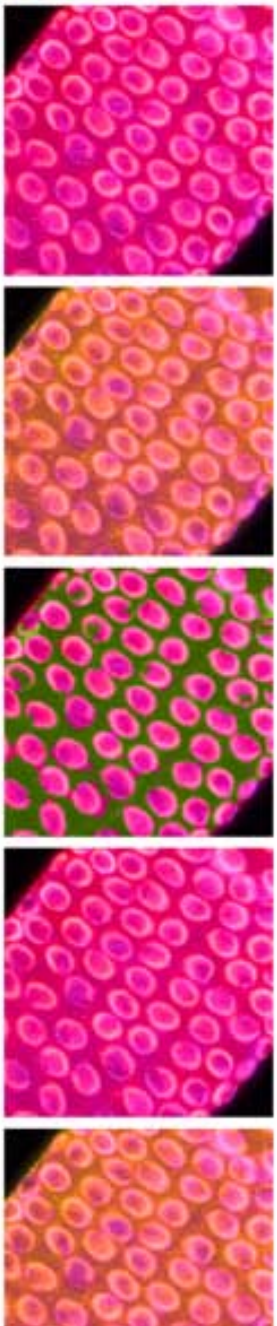

“ Available”

The national

**A**

Ahringer, J., 2006. **Reverse genetics.** *WormBook: the online review of C. elegans biology*, pp.1-43.

Ahringer, J. & Kimble, J., 1991. **Control of the sperm-oocyte switch in *C. elegans* hermaphrodites by the *fem-3* 3' untranslated region.** *Nature*, 349(6307)(January), pp.346-8.

Allemand, E. et al., 2008. **Splicing, transcription, and chromatin: *a ménage à trois*.** *Current opinion in genetics & development*, 18(2)(April), pp.45-51.

Allen, M.A. et al., 2011. **A global analysis of *C. elegans trans*-splicing.** *Genome Research*, 21(2)(February), pp.255-264.

Almeida, S.F. & Carmo-Fonseca, M., 2010. **Cotranscriptional RNA checkpoints.** *Epigenomics*, 2(3)(June), pp.449-55.

Almeida, S.F. & Carmo-Fonseca, M., 2012. **Design principles of interconnections between chromatin and pre-mRNA splicing.** *Trends in biochemical sciences,* (March), pp.1-6.

Anders, K.R. et al., 2003. **SMG-5, required for *C . elegans* nonsense-mediated mRNA decay, associates with SMG-2 and protein phosphatase 2A.** *EMBO Journal* 22(3), pp.641-650.

**B**

Bachorik, J.L. & Kimble, J., 2005. **Redundant control of the *Caenorhabditis elegans* sperm/ oocyte switch by PUF-8 and FBF-1, two distinct PUF RNA-binding proteins.** *Proc. Natl. Acad. Sci. U. S. A.*, 102, pp.10893-97.

Barberan-Soler, S. et al., 2009. **Global analysis of alternative splicing uncovers developmental regulation of nonsense-mediated decay in *C. elegans*.** *RNA,* 15(9)(September), pp.1652-60.

Baugh, L.R., 2003. **Composition and dynamics of the *Caenorhabditis elegans* early embryonic transcriptome.** *Development*, 130(5), pp.889-900.

Belfiore, M. et al., 2004. **Roles of the *C. elegans* cyclophilin-like protein MOG-6 in MEP-1 binding and germline fates.** *Development,* 131(12), pp.2935-45.

Bentley, D.L., 2005. **Rules of engagement: co-transcriptional recruitment of pre-mRNA processing factors.** *Curr Opin Cell Biol.* 17(3)(June), pp.251-6.

Bertone P. et al., 2004. **Global identification of human transcribed sequences with genome tiling arrays.** *Science,* 306, pp.2242–2246.

Bessonov et al., 2008. **Isolation of an active step I spliceosome and composition of its RNP core.** *Nature*, 452(7189)(April), pp.846-50.

Blankenberg, D. et al., 2011. **Making whole genome multiple alignments usable for biologists.** *Bioinformatics,* 27(17), pp.2426-8.

Blankenberg, D. et al., 2010. **Galaxy: a web-based genome analysis tool for experimentalists.** *Current protocols in molecular biology,* Chapter 19(January), unit 19.10.1-21.

Blencowe, B.J. et al., 1998. **A coactivator of pre-mRNA splicing.** *Genes & Development,* (12), pp.996-1009.

Blencowe, B.J. et al., 2000. **The SRm160/300 splicing coactivator subunits.** *RNA,* 6(1), pp.111–120.

Blumenthal, T. & Steward, K., 1997. ***C. elegans* II.** 2nd edition. *Cold Spring Harbor (NY),* Cold Spring Harbor Laboratory Press, Chapter 6.

Blumenthal, T. & Gleason, K.S., 2003. ***Caenorhabditis elegans* operons: form and function.** *Nat Rev Genet.*, 4(2)(February), pp.112-20.

Blumenthal, T., 2005. **Trans-splicing and operons.** *WormBook: the online review of C. elegans biology,* pp, 1-9.

Boulin, T. et al., 2006. **Reporter gene fusions.** *WormBook: the online review of C. elegans biology,* pp, 1-23.

Brenner, S., 1974. **The genetics of *Caenorhabditis elegans*.** *Methods*, pp.71-94.

Brody, Y. & Shav-Tal, Y., 2011. **Transcription and splicing: when the twain meet.** *Transcription,* 2(5)(October), pp.216-20.

Brody, Y. et al., 2011. **The *in vivo* kinetics of RNA polymerase II elongation during co-transcriptional splicing.** *PLoS biology,* 9(1)(January), e1000573.

**C**

*C.elegans* Sequencing Consortium, 1998. **Genome Sequence of the Nematode *C. elegans:* A Platform for Investigating Biology**. *Science,* 282(5396)(December), pp.2012-2018.

Cartegni, L. et al., 2002. **Listening to silence and understanding nonsense: exonic mutations that affect splicing.** *Nat Rev Genet*. 3(4)(April), pp.285-98.

Celniker, S.E. et al., 2009. **FEATURE Unlocking the secrets of the genome.** *Nature*, 459(June), pp.927-930.

Ceol, C. J. & Horvitz H. R., 2001. ***dpl-1* DP and *efl-1* E2F act with *lin-35* Rb to antagonize Ras signaling in *C. elegans* vulval development.** *Molecular cell* 7(3)(March), pp.461-73.

Ceron, J. et al., 2007. **Large-scale RNAi screens identify novel genes that interact with the *C. elegans* retinoblastoma pathway as well as splicing-related components with synMuv B activity.** *BMC developmental biology*, 7, p.30.

Churchman, S.L. & Weissman, J.S., 2011. **Nascent transcript sequencing visualizes transcription at nucleotide resolution.** *Nature,* 469(7330)(January), pp.368-73.

Crittenden, S.L. et al., 1994. **GLP-1 is localized to the mitotic region of the *C. elegans* germ line.** *Development,* 120(10)(October), pp.2901-11.

Crittenden, S.L. et al., 2002. **A conserved RNA-binding protein controls germline stem cells in *Caenorhabditis elegans.*** *Nature*, 417(6889)(June), pp.660-3.

**D**

Damgaard, C.K. et al., 2008. **A 5' splice site enhances the recruitment of basal transcription initiation factors *in vivo*.** *Mol Cell*, 29(2)(February), pp.271-8.

Darzacq, X. et al., 2007. **In vivo dynamics of RNA polymerase II transcription.** *Nat Struct Mol Biol.,* 14(9)(September), pp.796-806.

Das, R. et al., 2007. **SR proteins function in coupling RNAP II transcription to pre-mRNA splicing.** *Molecular cell,* 26(6)(June), pp.867-81.

Dellaire, G. et al., 2002. **Mammalian PRP4 Kinase Copurifies and Interacts with Components of Both the U5 snRNP and the N-CoR Deacetylase Complexes.** *Molecular and cellular biology*, 22(14)(July), pp.5141-5156.

Dermody, J.L. et al., 2008. **Unphosphorylated SR-like protein Npl3 stimulates RNA polymerase II elongation.** *PloS One*, 3(9)(September), e3273.

Dimova, D. et al., 2003. **Cell cycle-dependent and cell cycle-independent control of transcription by the Drosophila E2F/RB pathway.** *Genes & Development*, 17(18)(Semptember), pp.2308-2320.

Doniach T., 1986. **Activity of the sex-determining gene *tra-2* is modulated to allow spermatogenesis in the *C. elegans* hermaphrodite.** *Genetics*, (114)(September), pp.53-76.

Duerr, J.S., 2006. **Immunohistochemistry.** *WormBook: the online review of C. elegans biology* (January), pp.1-61.

**E**

Eckmann, C.R., et al., 2004. **GLD-3 and control of the mitosis/meiosis decision in the germline of *Caenorhabditis elegans*.** *Genetics,* 168(1), pp.147-60.

Edgley, M.L. & Riddle, D.L., 2001. **LG II balancer chromosomes in *Caenorhabditis elegans*: *mT1* (II;III) and the *mIn1* set of dominantly and recessively marked inversions.** *Mol. Genet. Genomics*, 266(3), pp.385-95.

Ellis, R. & Schedl, T., 2007. **Sex determination in the germ line.** *WormBook: the online review of C. elegans biology*, pp.1-13.

**F**

Fire, A. et al., 1998. **Potent and specific genetic interference by double-stranded RNA in *Caenorhabditis elegans.*** *Nature,* 391(6669)(February), pp.806-811.

Fraser, A. et al., 2000. **Functional genomic analysis of *C. elegans* chromosome I by systematic RNA interference.** *Nature,* 408(6810)(November), pp.325-30.

Frøkjaer-Jensen, C. et al., 2008. **Single-copy insertion of transgenes in *Caenorhabditis elegans*.** *Nature genetics*, 40(11), pp.1375-1383.

**G**

Gallegos, M. et al., 1998. **Repression by the 3'UTR of *fem-3*, a sex-determining gene, relies on a ubiquitous *mog*-dependent control in *Caenorhabditis elegans*.** *The EMBO journal*, 17(21), pp.6337-6347.

Gengyo-Ando, K. & Mitani, S., 2000. **Characterization of mutations induced by ethyl methanesulfonate, UV, and trimethylpsoralen in the nematode *Caenorhabditis elegans*.** *Biochemical and biophysical research communications*, 269(1), pp.64-9.

Gerstein, M.B. et al., 2010. **Integrative Analysis of the *Caenorhabditis elegans* Genome by the modENCODE Project.** *Science*, 330(6012), pp.1775-1787.

Goecks, J. et al., 2010. **Galaxy: a comprehensive approach for supporting accessible, reproducible, and transparent computational research in the life sciences.** *Genome biology,* 11(8), R86.

Graham, P.L. & Kimble, J., 1993. **The *mog-1* gene is required for the switch from spermatogenesis to oogenesis in *Caenorhabditis elegans*.** *Genetics*, 133(April), pp.919-931.

Grainger, R.J. & Beggs, J.D., 2005. **Prp8 protein: at the heart of the spliceosome.** *RNA,* 11(5)(May), pp.533-57.

Grainger, R.J. et al., 2009. **Physical and genetic interactions of yeast Cwc21p, an ortholog of human SRm300 / SRRM2, suggest a role at the catalytic center of the spliceosome.** *RNA,* (15), pp.2161-2173.

**H**

Hansen, M. et al., 2005. **New genes tied to endocrine, metabolic, and dietary regulation of lifespan from a *Caenorhabditis elegans* genomic RNAi screen.** *PLoS Genet.*, 1(1)(July), pp.119-25.

Hertel, K.J. & Graveley, B.R., 2005. **RS domains contact the pre-mRNA throughout spliceosome assembly.** *Trends Biochem Sci.,* 30(3)(March), pp.115-8.

Hicks, M.J. et al., 2006. **Linking splicing to Pol II transcription stabilizes pre-mRNAs and influences splicing patterns.** *PLoS biology,* 4(6)(June), e147.

Hubbard, E.J.A. & Greenstein, D., 2005. **Introduction to the germ line.** *WormBook: the online review of C. elegans biology*, pp.1-4.

Hunt-Newbury, R. et al., 2007. **High-throughput in vivo analysis of gene expression in *Caenorhabditis elegans*.** *PLoS biology*, 5(9), p.e237.

**J**

Jan, E. et al., 1999. **The STAR protein, GLD-1, is a translational regulator of sexual identity in *Caenorhabditis elegans.*** *The EMBO journal,* 18(1)(January), pp.258-69.

Jin, S.W. et al., 2001. **In *Caenorhabditis elegans*, the RNA-Binding Domains of the Cytoplasmic Polyadenylation Element Binding Protein FOG-1 Are Needed to Regulate Germ Cell Fates.** *Genetics,* (159)(December), pp.1617–1630.

Johnston, R.J. & Hobert, O., 2005. **A novel *C. elegans* zinc finger transcription factor, lsy-2, required for the cell type-specific expression of the lsy-6 microRNA.** *Development,* 132(24)(December), pp.5451-60.

Jorgensen, E.M. et al., 2002. **The art and design of genetic screens: *Caenorhabditis elegans*.** *Nature reviews. Genetics,* 3(5)(May), pp.356-69.

**K**

Kamath, R. 2003. **Genome-wide RNAi screening in *Caenorhabditis elegans.*** *Methods,* 30(4) (August), pp.313-321.

Kasturi, P. et al., 2010. **The *C. elegans* sex determination protein MOG-3 functions in meiosis and binds to the CSL co-repressor CIR-1.** *Developmental biology,* 344(2)(August), pp.593-602.

Kawano, T. & Masaki F., 2000. **Unique and redundant functions of SR proteins, a conserved family of splicing factors, in *Caenorhabditis elegans* development.** *Mechanisms of Development,* 95, pp.67-76.

Kelly, W.G. et al., 1997. **Distinct requirements for somatic and germline expression of a generally expressed *Caenorhabditis elegans* gene.** *Genetics*, 146(1)(May), pp.227-38.

Kerins, J.A. et al., 2010. **PRP-17 and the pre-mRNA splicing pathway are preferentially required for the proliferation versus meiotic development decision and germline sex determination in *Caenorhabditis elegans.*** *Developmental dynamics,* 239(5), pp.1555-72.

Khanna, M. et al., 2009. **A systematic characterization of Cwc21, the yeast ortholog of the human spliceosomal protein SRm300.** *RNA,* 15(12), pp.2174-85.

Kimble, J. & Crittenden, S.L., 2005. **Germline proliferation and its control.** *WormBook: the online review of C. elegans biology,* (January), pp.1-14.

Konishi, T. et al., 2008. **The *Caenorhabditis elegans* DDX-23, a homolog of yeast splicing factor PRP28, is required for the sperm-oocyte switch and differentiation of various cell types.** *Developmental dynamics,* 237(9), pp.2367-2377.

Kraemer, B. et al., 1999. **NANOS-3 and FBF proteins physically interact to control the sperm-oocyte switch in *Caenorhabditis elegans*.** *Curr. Biol.*, 9(18), pp.1009-1018.

**L**

Lamond A.L. & Spector, D.L., 2003. **Nuclear speckles: a model for nuclear organelles.** *Nat Rev Mol Cell Biol.*, 4(8)(August), pp.605-12.

Lamont, L.B. et al., 2004. **FBF-1 and FBF-3 regulate the size of the mitotic region in the *C. elegans* germline.** *Developmental Cell*, 7(November), pp.697-707.

Lamont, L.B. & Kimble, J., 2008. **Developmental expression of FOG-1/CPEB protein and its**

**control in the *C. elegans* hermaphrodite germ line.** *Dev Dyn.*, 236(3)(March), pp.871-879.

Lasda, E.L. et al., 2010. **Polycistronic pre-mRNA processing in vitro: snRNP and pre-mRNA role reversal in trans-splicing.** *Genes Dev.,* 24(15)(August), pp.1645-58.

Lee, M. & Schedl, T., 2006. **RNA *in situ* hybridization of dissected gonads.** *WormBook: the online review of C. elegans biology,* (January), pp.1-7.

Lefrançois, P. et al., 2009. **Efficient yeast ChIP-Seq using multiplex short-read DNA sequencing.** *BMC genomics,* 10(January), 37.

Lewicki, B.T. et al., 1993. **Coupling rRNA transcription and ribosomal assembly in vivo. Formation of active ribisomal subunits in *Escherichia coli* requires transcription of rRNA genes by host RNA polymerase which cannot be replaced by bacteriophage T7 RNA polymerase.** *J Mol Biol.,* 231(3)(June), pp.581-93.

Lin, C.L. et al., 2004. **Over-expression of SR-cyclophilin, an interaction partner of nuclear pinin, releases SR family splicing factor from nuclear speckles.** *Biochem Biophys Res Commun.,* 321(3)(August), pp.638-47.

Lin, S. & Fu, F.D., 2007. **SR proteins and related factors in alternative splicing.** *Adv Exp Med Biol.*, 623, pp.107-22.

Lin, S. et al., 2008. **The splicing factor SC35 has an active role in transcriptional elongation.** *Nat Struct Mol Biol.*, 15(8)(August), pp.819-26.

Liu, X.S., 2007. **Getting started in tiling microarray analysis.** *PLoS Computational Biology*, 3(10)(October), e183.

Long, J.C. & Caceres, J.F., 2009. **The SR protein family of splicing factors: master regulators of gene expression.** *The Biochemical journal*, 417(1), pp.15-27.

Longman, D. et al., 2001. **Multiple interactions between SRm160 and SR family proteins in enhancer-dependent splicing and development of *C. elegans*.** *Current Biology*, 11(24), pp.1923–1933.

Longman, D. et al., 2007. **Mechanistic insights and identification of two novel factors in the *C. elegans* NMD pathway.** *Genes & Development*, 21(9)(May), 1075-85.

Loria, P.M. et al., 2003. **Two neuronal, nuclear-localized RNA binding proteins involved in synaptic transmission.** *Current Biology,* 13, pp.1317-1323.

**M**

Macmorris, M. et al., 2003. **UAP56 levels affect viability and mRNA export in *Caenorhabditis elegans*.** *RNA*, 9(7)(July), pp.847-857.

Madhani, H.D. & Guthrie, C., 1994. **Randomization-selection analysis of snRNAs in vivo: evidence for a tertiary interaction in the spliceosome.** *Genes & Development,* 8(9)(May), pp.1071-1086.

McCracken, S .et al., 2005. **Proteomic analysis of SRm160-containing complexes reveals a conserved association with cohesin.** *Journal of Biological chemistry,* 280(51)(December), pp.42227-42236.

Meissner, B. et al., 2009. **An integrated strategy to study muscle development and myofilament structure in *Caenorhabditis elegans*.** *PLoS genetics*, 5(6), p.e1000537.

Mello, C. & Fire, A., 1995. **DNA transformation.** *Methods Cell Biol.,* 48, pp.451-482.

Merritt, C. et al., 2008. **3' UTRs are the primary regulators of gene expression in the *C. elegans* germline.** *Current biology: CB*, 18(19), pp.1476-1482.

Miele, A. et al., 2007. **The interactome of the histone gene regulatory factor HiNF-P suggests novel cell cycle related roles in transcriptional control and RNA processing.** *J Cell Biochem.*, 102(1)(September), pp.136-48.

**N**

Nagalakshmi U. et al., 2008. **The transcriptional landscape of the yeast genome defined by RNA sequencing.** *Science*, (320), pp.1344–1349.

Newman, A.J. & Nagai, K., 2010. **Structural studies of the spliceosome: blind men and an elephant.** *Current Opinion Structural Biology*, 20(1)(February), pp.82-9.

Nilsen, T.W. & Graveley, B.R., 2010. **Expansion of the eukaryotic proteome by alternative splicing.** *Nature*, 463(7280)(January), pp.457-63.

**P**

Pandit, S. et al., 2008. **Functional integration of transcriptional and RNA processing machineries.** *Curr Opin Cell Biol*, 20(3)(June), pp.260-5.

Phatnani, H.P. & Greenleaf, A.L., 2006. **Phosphorylation and functions of the RNA polymerase II CTD.** *Genes & development,* 20(21)(November), pp.2922-36.

Porta-de-la-Riva, M. et al., 2012. **BASIC *Caenorhabditis elegans* METHODS: Synchronization and Observation.** *Journal of Visual Experiments,* In Press.

Praitis, V. et al., 2001. **Creation of Low-Copy Integrated Transgenic Lines in *Caenorhabditis elegans*.** *Genetics,* 157(3)(March), pp.1217-26.

Puoti, A. & Kimble, J., 1999. **The C*aenorhabditis elegans* sex determination gene *mog-1* encodes a member of the DEAH-Box protein family.** *Molecular and Cellular Biology,* 19(3), pp.2189-2197.

Puoti, A. & Kimble, J., 2000. **The hermaphrodite sperm/oocyte switch requires the *Caenorhabditis elegans* homologs of PRP2 and PRP22.** *Proceedings of the National Academy of Sciences of the United States of America,* 97(7)(March), pp.3276-81.

**R**

Ramani, A.K. et al., 2011. **Genome-wide analysis of alternative splicing in *Caenorhabditis elegans*.** *Genome Research*, 21(2)(February), pp.342-348.

Reinke, V. et al., 2000. **A global profile of germline gene expression in *C. elegans*.** *Mol Cell,* 6(3)(September), pp.605-16.

Reinke, V. et al., 2004. **Genome-wide germline-enriched and sex-biased expression profiles in *Caenorhabditis elegans*.** *Development*, 131(2), p.311.

Reinke, V. & Cutter, A.D., 2009. **Germline expression influences operon organization in the *Caenorhabditis elegans* genome.** *Genetics*, 181(4)(April), pp.1219-28.

Rino, J. & Carmo-Fonseca, M., 2009. **The spliceosome: a self-organized macromolecular machine in the nucleus?.** *Trends Cell Biol.*, 19(8)(August), pp.375-84.

Rocak, S. & Linder, P., 2004. **DEAD-box proteins: the driving forces behind RNA metabolism.** *Nat Rev Mol Cell Biol.,* 5(3)(March), pp.232-41.

Roscigno, R.F. & Garcia-Blanco, M.A., 1995. **SR proteins escort the U4/U6·U5 tri-snRNP to the spliceosome.** *RNA*, 1(7)(September), pp.692-706.

Royce T.E. et al., 2007. **Toward a universal microarray: prediction of gene expression through nearest-neighbor probe sequence identification.** *Nucleic Acids Res.*, (35), e99.

Rual, J.F. et al., 2004. **Toward improving *Caenorhabditis elegans* phenome mapping with an ORFeome-based RNAi library.** *Genome Research*, 14, pp.2162-2168.

**S**

Sanford, J.R. et al., 2005. **Multiple roles of arginine/serine-rich splicing factors in RNA processing.** *Biochem Soc Trans.*, 33(Pt 3)(June), pp.443-6.

Sapra, A.K. et al., 2009. **SR protein family members display diverse activities in the formation of nascent and mature mRNPs *in vivo*.** *Molecular cell,* 34(2)(April), pp.179-90.

Semple, J.I. et al., 2010. **Rapid selection of transgenic *C. elegans* using antibiotic resistance.** *Nature methods,* 7(9), pp.725-727.

Schneider, D.A. et al., 2007. **Transcription elongation by RNA Polymerase I is linked to efficient rRNA processing and ribosome assembly.** *Mol Cell*, 26(2), pp.217-229.

Schwartz, S. & Ast, G., 2010. **Chromatin density and splicing destiny: on the cross-talk between chromatin structure and splicing.** *The EMBO journal,* 29(10)(May), pp.1629-36.

**T**

Tabara, H. et al., 1998. **RNAi in *C. elegans*: soaking in the genome sequence.** *Science,* 282(5388)(October), pp.430-1.

Thompson, J.D. et al., 1994. **CLUSTAL W: improving the sensitivity of progressive multiple sequence alignment thrugh sequence weighting, position-specific gap penalties and weight matrix choice.** *Nucleic Acids Res.,* 22(22)(November), pp.4673-80.

Timmons, L. & Fire, A., 1998. **Specific interference by ingested dsRNA.** *Nature,* 395(6705)(October), pp.854.

**V**

Valadkhan, S. & Jaladat, Y., 2010. **The spliceosomal proteome: et the heart of the largest cellular ribonucleoprotein machine.** *Proteomics*, 10(22)(November), pp.4128-41.

Villa, T. & Guthrie, C., 2005. **The Isy1p component of the NineTeen complex interacts with the ATPase Prp16p to regulate the fidelity of pre-mRNA splicing.** *Genes & development,* 19(16)(August), pp.1894-904.

**W**

Wahl, M.C. et al., 2009. **The spliceosome: design principles of a dynamic RNP machine.** *Cell* 136(4)(February), pp.701-18.

Walser, C.B. et al., 2007. **Distinct roles of the Pumilio and FBF translational repressors during *C. elegans* vulval development.** *Development,* 134(24)(December), pp.4503-4505.

Wang, J. & Manley, J.L., 1995. **Overexpression of the SR proteins ASF/SF2 and SC35 influences alternative splicing in diverse ways.** *RNA,* 1, pp.335–346.

Wang, X. et al., 2009. **Identification of genes expressed in the hermaphrodite germ line of *C. elegans* using SAGE.** *BMC genomics*, 10, p.213.

Wang, Z. et al., 2009. **RNA-Seq: a revolutionary tool for transcriptomics.** *Nature reviews. Genetics,* 10(1)(January), pp.57-63.

Wilm, T. et al., 1999. **Ballistic transformation of *Caenorhabditis elegans.*** *Gene*, 229(1-2)(March), pp.31-5.

**Y**

Yu, Y., et al., 2010. **A model *in vitro* system for co-transcriptional splicing.** *Nucleic acids research,* 38(21)(November), pp.7570-8.

**Z**

Zanetti, S. et al., 2011. **Role of the *C. elegans* U2 snRNP protein MOG-2 in sex determination, meiosis, and splice site selection.** *Dev Biol.,* 354(2)(June), pp.232-41.

Zarkower, D. 2006. **Somatic sex determination.** *WormBook: the online review of C. elegans biology*, pp.1-12.

Zhang, Y. et al., 2008. **Model-based analysis of ChIP-Seq (MACS).** *Genome biology* 9(9), R137.

Zhong, M. et al., 2010. **Genome-wide identification of binding sites defines distinct functions for *Caenorhabditis elegans* PHA-4/FOXA in development and environmental response.** *PloS Genet*., 6(2)(February), e1000848.

Zhong, X.Y. et al., 2009. **SR proteins in vertical integration of gene expression from transcription to RNA processing to translation.** *Mol Cell,* 35(1)(July), pp.1-10

Zimowska, G. et. al, 2003. **Pinin/DRS/memA Interacts with SRp75, SRm300 and SRrp130 in Corneal Epithelial Cells.** *Investigative Ophthalmology & Visual Science,* 44(11)(November), pp.4715-4723.

# Annex

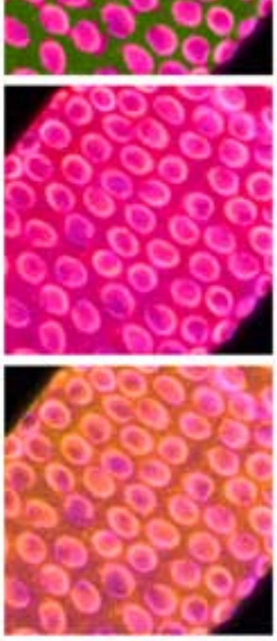

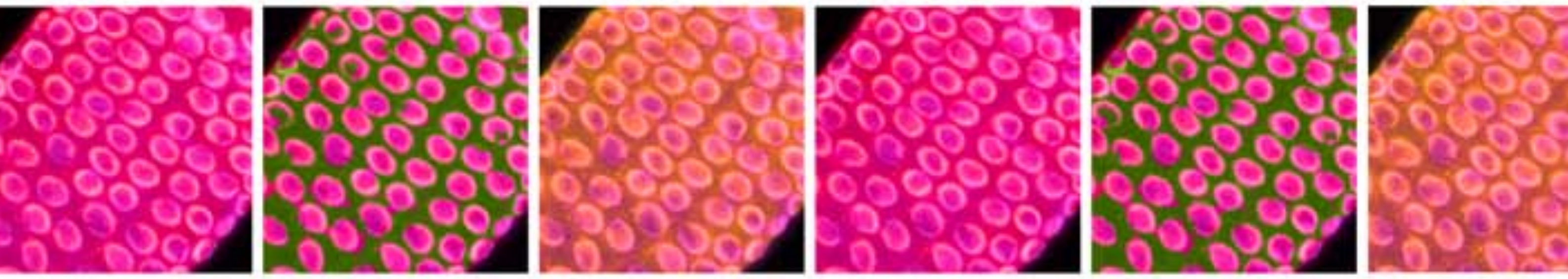

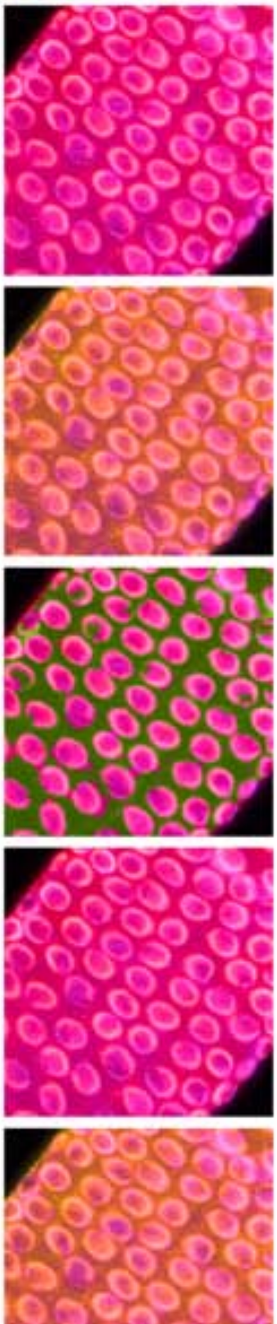

“ Mine for life”
The Sounds

# Article 1

Aristizábal-Corrales, D., **Fontrodona, L.,** Porta-de-la-Riva, M., Guerra-Moreno, A., Cerón, J., Schwartz, Jr. S., 2012. The 14-3-3 gene *par-5* is required for germline development and DNA damage response in *Caenorhabditis elegans. Journal of Cell Science*, 125, pp. 1716-28.

# Article 2

Porta-de-la-Riva, M., **Fontrodona, L.,** Villanueva, A., Cerón, J., 2012. Basic *Caenorhabditis elegans* Methods: Synchronization and Observation. *Journal of Visualized Experiments, in press.* DOI: 10.3791/4019. URL: http://www.jove.com/video/4019

# The 14-3-3 gene *par-5* is required for germline development and DNA damage response in *Caenorhabditis elegans*

**David Aristizábal-Corrales[1,2], Laura Fontrodona[3], Montserrat Porta-de-la-Riva[3], Angel Guerra-Moreno[1,2], Julián Cerón[3,]* and Simo Schwartz Jr[1,2,]***

[1]Drug Delivery and Targeting, CIBBIM-Nanomedicine, Vall d'Hebron Research Institute, Universidad Autónoma de Barcelona, Barcelona 08035, Spain
[2]Networking Research Center on Bioengineering, Biomaterials and Nanomedicine (CIBER-BBN), Barcelona 08193, Spain
[3]Bellvitge Biomedical Research Institute (IDIBELL), L'Hospitalet de Llobregat, Barcelona 08908, Spain
*Authors for correspondence (sschwartz@ir.vhebron.net; jceron@idibell.org)

*Accepted 17 November 2011*
*Journal of Cell Science 125, 1716–1726*
*© 2012. Published by The Company of Biologists Ltd*
*doi: 10.1242/jcs.094896*

## Summary

14-3-3 proteins have been extensively studied in organisms ranging from yeast to mammals and are associated with multiple roles, including fundamental processes such as the cell cycle, apoptosis and the stress response, to diseases such as cancer. In *Caenorhabditis elegans*, there are two 14-3-3 genes, *ftt-2* and *par-5*. *ftt-2* is expressed only in somatic lineages, whereas *par-5* expression is detected in both soma and germline. During early embryonic development, *par-5* is necessary to establish cell polarity. Although it is known that *par-5* inactivation results in sterility, the role of this gene in germline development is poorly characterized. In the present study, we used a *par-5* mutation and RNA interference to characterize *par-5* functions in the germline. The lack of *par-5* in germ cells caused cell cycle deregulation, the accumulation of endogenous DNA damage and genomic instability. Moreover, *par-5* was required for checkpoint-induced cell cycle arrest in response to DNA-damaging agents. We propose a model in which PAR-5 regulates CDK-1 phosphorylation to prevent premature mitotic entry. This study opens a new path to investigate the mechanisms of 14-3-3 functions, which are not only essential for *C. elegans* development, but have also been shown to be altered in human diseases.

**Key words:** 14-3-3, *par-5*, *C. elegans*, Germline, DNA damage response, Checkpoint, *wee-1.3*, *cdc-25.1*, *cdk-1*

## Introduction

14-3-3 proteins are an evolutionarily conserved family implicated in diverse cellular processes, such as apoptosis or cell cycle regulation, that are associated with pathologies such as cancer (Fig. 1A) (Porter et al., 2006; Tzivion et al., 2006). They bind mainly to serine phosphorylated motifs of other proteins and regulate their subcellular localizations, stability or activity. In mammals, there are seven 14-3-3 proteins corresponding to the isoforms encoded by individual genes (designated β, γ, ε, η, σ, τ or ζ). This redundancy has hindered the study of their cellular functions, and there is still little knowledge about the consequences of 14-3-3 misfunction at the organism level (Porter et al., 2006).

14-3-3 proteins are necessary for proper cell cycle arrest following DNA damage in yeast, flies and mammals (Hermeking and Benzinger, 2006). This function is mediated by interactions with several cell cycle regulators, including Chk1 (Chen et al., 1999; Dunaway et al., 2005), Cdc25 (Kumagai and Dunphy, 1999; Lopez-Girona et al., 1999) and Cdks (Laronga et al., 2000). Checkpoint-related functions for this protein family were first discovered in fission yeast, where two 14-3-3 proteins, namely Rad24 and Rad25, regulate the G2–M checkpoint by controlling Cdc25 and Chk1 localization (Ford et al., 1994; Lopez-Girona et al., 1999; Dunaway et al., 2005). In *Drosophila melanogaster*, two 14-3-3 proteins (ζ and ε) function in cell cycle regulation during development by inhibiting entry into mitosis through the inactivation of Cdk-1 activity (Su et al., 2001). Such 14-3-3 function in controlling M-phase entry is conserved in mammals, but the contribution of each isoform separately is still under exploration.

The *Caenorhabditis elegans* germline is a powerful model for the study of the genes involved in cell cycle regulation and DNA damage response (DDR) (Gartner et al., 2004). In the *C. elegans* germline, exposure to DNA-damaging agents [e.g. ionizing radiation (IR) or ultraviolet C light] and replicative stress [e.g. hydroxyurea (HU)] triggers the checkpoint response through conserved pathways (Fig. 1B). This response leads to cell cycle arrest in the proliferative region and, in some cases (e.g. after IR), also to an increase in the proportion of apoptotic cells in the late pachytene region of the germline. The underlying DDR molecular pathway, conserved from yeast to mammals, acts through the ATL-1 and ATM-1 kinases (ATR and ATM homologs) (Garcia-Muse and Boulton, 2005) as well as several sensor proteins, such as HUS-1 (Hofmann et al., 2002), MRE-11 (Garcia-Muse and Boulton, 2005) and WRN-1 (Lee et al., 2010). CHK-1 and CHK-2, are the effector kinases (Kalogeropoulos et al., 2004; Stergiou et al., 2007; Bailly et al., 2010; Lee et al., 2010), but other proteins, such as RAD-5, act in parallel with this canonical pathway to promote checkpoint responses (Ahmed et al., 2001; Collis et al., 2007).

In *C. elegans*, two 14-3-3 genes, *par-5* (also named *ftt-1*) and *ftt-2*, encode 14-3-3 proteins, and these share 86% of the amino

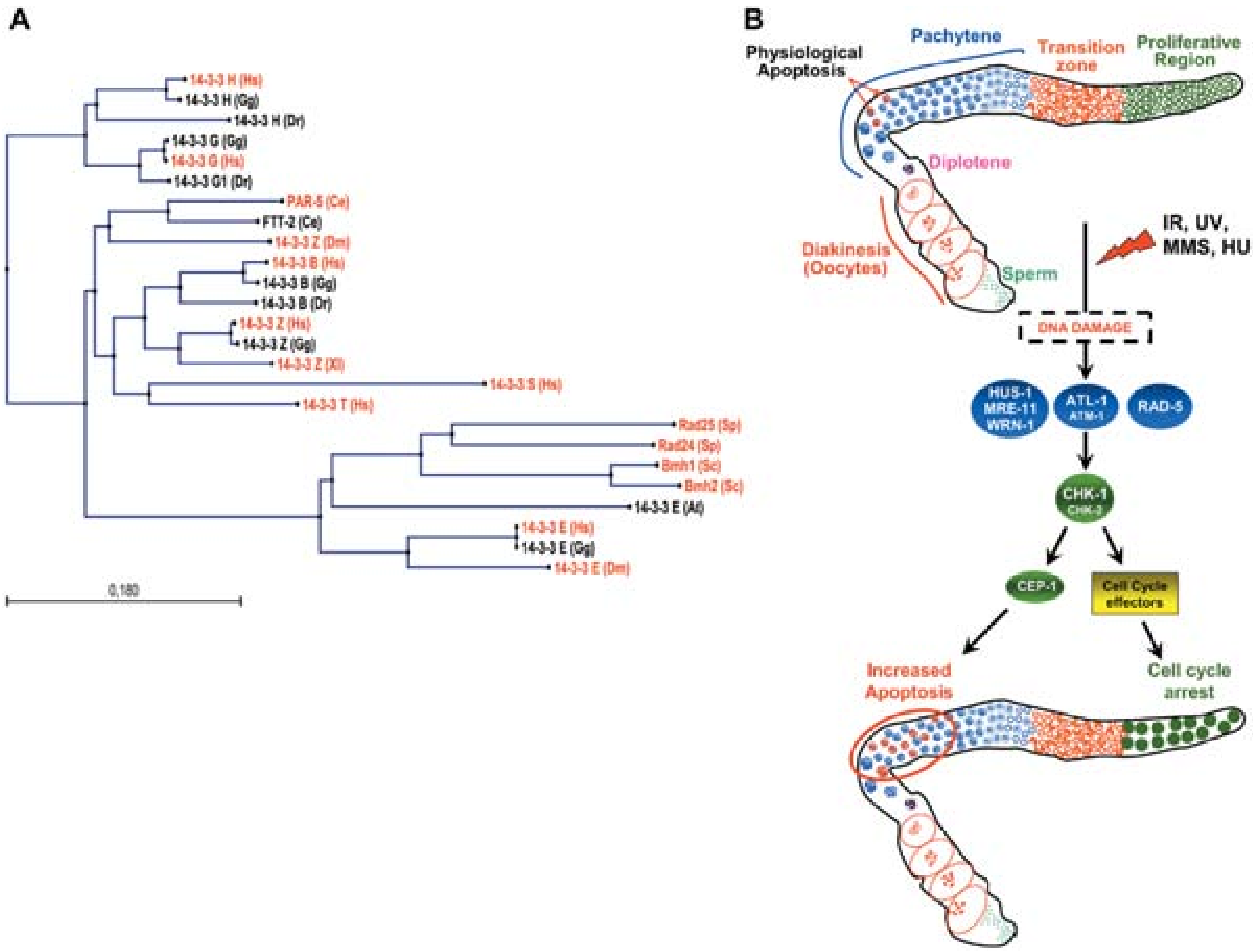
A
14-3-3 H (Hs)
14-3-3 H (Gg)
14-3-3 H (Dr)
14-3-3 G (Gg)
14-3-3 G (Hs)
14-3-3 G1 (Dr)
PAR-5 (Ce)
FTT-2 (Ce)
14-3-3 Z (Dm)
14-3-3 B (Hs)
14-3-3 B (Gg)
14-3-3 B (Dr)
14-3-3 Z (Hs)
14-3-3 Z (Gg)
14-3-3 Z (Xl)
14-3-3 S (Hs)
14-3-3 T (Hs)
Rad25 (Sp)
Rad24 (Sp)
Bmh1 (Sc)
Bmh2 (Sc)
14-3-3 E (At)
14-3-3 E (Hs)
14-3-3 E (Gg)
14-3-3 E (Dm)
0,180
B
Physiological Apoptosis
Pachytene
Transition zone
Proliferative Region
Diplotene
Diakinesis (Oocytes)
Sperm
IR, UV, MMS, HU
DNA DAMAGE
HUS-1 MRE-11 WRN-1
ATL-1 ATM-1
RAD-5
CHK-1 CHK-2
CEP-1
Cell Cycle effectors
Increased Apoptosis
Cell cycle arrest

**Fig. 1. Phylogenetic tree of 14-3-3 family proteins and the DNA damage response in the *Caenorhabditis elegans* germline.** (**A**) 14-3-3 ortholog sequences were aligned using ClustalW, and CLC Sequence Viewer was used to generate the tree using the Neighbor Joining algorithm. Names in red correspond to 14-3-3 members, which have been either related to cell cycle control or shown to interact physically with checkpoint and/or cell cycle proteins (Hermeking and Benzinger, 2006). At, *Arabidopsis thaliana*; Ce, *C. elegans*; Dm, *Drosophila melanogaster*; Dr, *Danio rerio*; Gg, *Gallus gallus*; Hs, *Homo sapiens*; Sc, *Saccharomyces cerevisiae*; Sp, *Schizosaccharomyces pombe*; and Xl, *Xenopus laevis*. (**B**) The upper part of the figure shows germline organization in the adult worm stage. In the distal germline, cells proliferate to produce new germ cell precursors (green zone). Next, cells abandon the proliferative region to pass into the transition zone (in orange) before starting the meiotic phase (in blue) to give rise finally to the oocytes in the most proximal region (diakinesis stage). During development many meiotic cells are eliminated by physiological apoptosis. After the induction of DNA damage by different agents, a checkpoint response is activated in the germline. DNA damage induces a molecular response pathway that includes several conserved transducer and effector proteins, as shown in the middle of the figure. The activation of this pathway is reflected in two germline phenotypes: cell cycle arrest in the proliferative region and, in some cases, an increase in apoptotic cells in the pachytene region (bottom of the figure).

acid sequence. Despite this high identity, the expression pattern is distinct because only PAR-5 is expressed in the germline (Wang and Shakes, 1997). *Caenorhabditis elegans* 14-3-3 proteins have been linked to lifespan extension and the stress response (upon oxidative and heat stimuli) by interacting with SIR2.1 deacetylase and the forkhead transcription factor, DAF-16 (Berdichevsky et al., 2006). However, this role has not been ascribed to *par-5* (Li et al., 2007).

*par-5* belongs to the partitioning defective PAR family, which regulates the asymmetry in the first embryonic cell division. During this process, *par-5* is required for the proper distribution of asymmetrically localized PAR proteins (Morton et al., 2002). Uniquely for a PAR protein, PAR-5 is homogeneously distributed in the embryo and so studies of the asymmetric cell division mechanism have focused on other members of the PAR family (Suzuki and Ohno, 2006). Intriguingly, PAR-5 is also present in the adult germline (Morton et al., 2002), but its function in germ cells remains unknown. Despite the conservation of 14-3-3 checkpoint-related functions from yeast to mammals, this study is the first to provide evidence of a role in DDR for a 14-3-3 protein in the key model organism *C. elegans*.

## Results

### *par-5* is required for proper germline development

*par-5* mutations or *par-5* RNA interference (RNAi)-mediated knockdown [*par-5(RNAi)*] produces low brood size, embryonic lethality and sterility (Morton et al., 2002). However, although the role of *par-5* in embryonic development has been established, its function in the adult germline is poorly understood. To investigate the role of *par-5* in the adult germline, we studied phenotypes in the *par-5* mutants *it55* (allele with a single amino acid substitution that reduces the protein expression level) (Morton et al., 2002) and *par-5(RNAi)* worms. In the 1-day adult stage, the number of germ cells and gonad size were reduced in the mutant strain, and such a reduction was found not to be temperature dependent (supplementary material Fig. S1). This germline proliferation defect was even more pronounced in *par-5* RNAi-fed worms (Fig. 2A). In contrast to wild type (WT) and *par-5* mutants, *par-5(RNAi)* germlines showed some small fragmented nuclei, indicating mitotic catastrophe and genome instability in the proliferative region. By performing a time-course analysis of the germline development, we found that the proliferative defect in *par-5*-defective worms started at the L4 stage when hypercondensed and fragmented nuclei become apparent. After this stage, the number of germ cells decreased in *par-5(RNAi)* germlines in contrast to the continuous proliferation observed in the WT and *par-5(it55)* (Fig. 2B). Despite the important reduction in germ cells in *par-5(it55)* worms, nuclei fragmentation was not as abundant in *par-5* mutants as it was in *par-5(RNAi)* animals (Fig. 2A). The difference between *par-5(it55)* and *par-5(RNAi)* phenotypes implies that the *it55* allele is hypomorphic rather than null (Morton et al., 2002). Indeed, *par-5(it55)* fed with *par-5* RNAi presented a *par-5(RNAi)* phenotype (Fig. 2A).

The germline proliferation defect observed after *par-5* knockdown could be explained by the influence of the somatic gonad on germline proliferation (Killian and Hubbard, 2005). However, *par-5* RNAi treatment in the *rrf-1(pk1417)* background (a strain with defective RNAi in somatic cells) showed the same germline phenotype as that of WT animals (supplementary material Fig. S2). Therefore, the *par-5* knockdown effect on the germline is independent of the somatic functions of *par-5*. Additionally, most of the *par-5(RNAi)* gonads showed either a reduction in the number, or an absence, of oocytes. This observation suggests that *par-5* is implicated not only in germline proliferation, but also in meiotic progression, which is in agreement with the meiotic arrest phenotype previously described (Morton et al., 2002).

*par-5* shares ~80% homology with *ftt-2*, which is the other 14-3-3 *C. elegans* gene (Wang and Shakes, 1997). To test whether the observed RNAi phenotype was *par-5* specific, we quantified *par-5* and *ftt-2* transcript levels using quantitative RT-PCR after

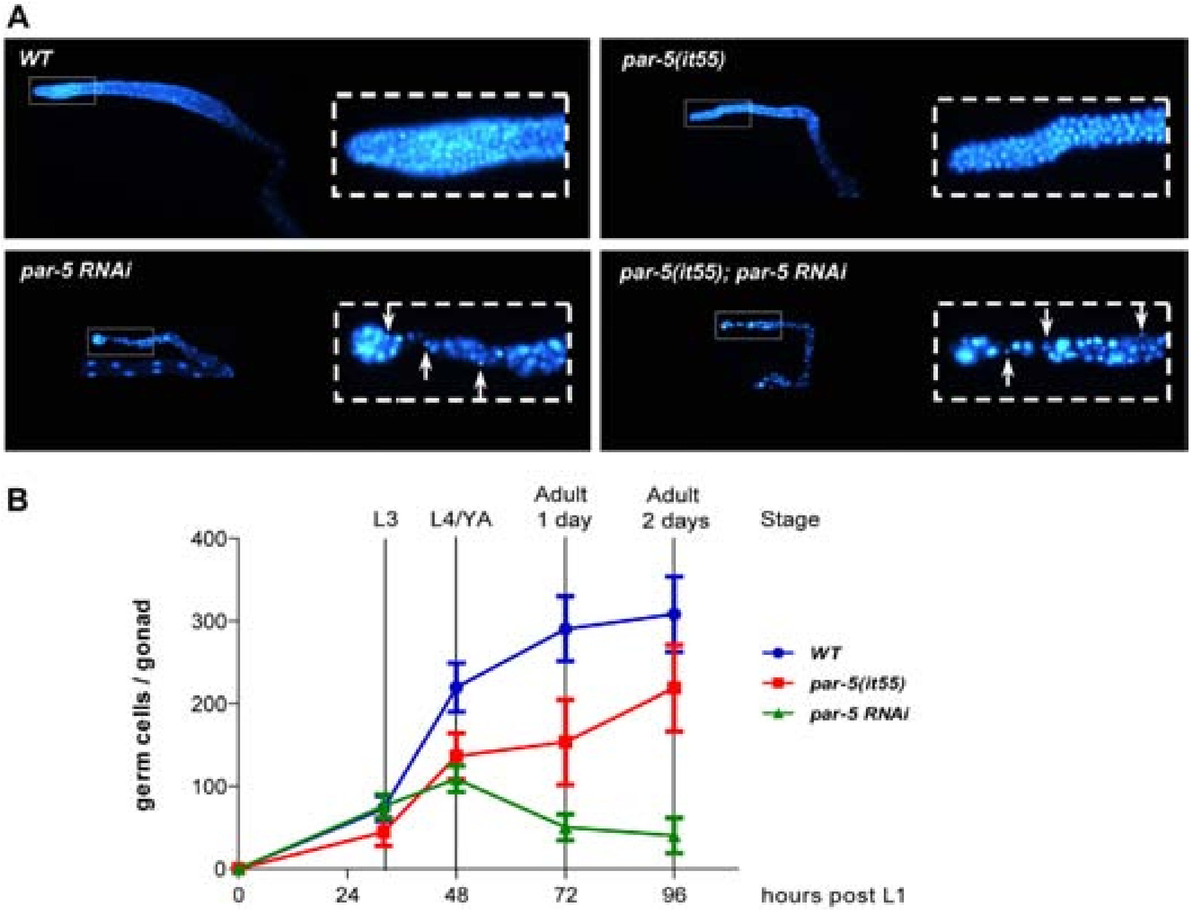

**Fig. 2.** ***par-5* inactivation affects germline proliferation.** (**A**) Representative images of DAPI-stained germlines from WT or *par-5(it55)* mutant worms (1-day-old adults) fed with *par-5* RNAi or the RNAi empty vector. The proliferative regions of germlines are shown enlarged in rectangles. Arrows indicate hypercondensed and fragmented nuclei. (**B**) Graph showing the number of germ cells per gonad at different developmental stages for WT, *par-5(it55)* and *par-5* RNAi-fed worms. L1 larvae grown at 20℃ were fixed and stained with DAPI at the indicated times. Error bars indicate standard deviations from the mean.

*par-5* RNAi treatment. This experiment showed that *par-5* RNAi depleted *par-5* mRNA, whereas *ftt-2* transcript levels were unaffected (supplementary material Fig. S3). All these observations indicate that *par-5* is required for the proliferation, genomic stability and meiotic progression of the germline.

### Inactivation of *par-5* promotes endogenous DNA damage accumulation

Because we found a reduced number of germ cells and DNA fragmentation after *par-5* inactivation by RNAi (Fig. 2A), we further investigated the role of *par-5* in the maintenance of DNA stability. We examined the abundance of RAD-51 foci, which acts as a marker of processed double-strand breaks (DSBs) and stalled replication forks (Alpi et al., 2003; Ward et al., 2007). Interestingly, we observed a tenfold increase in the number of RAD-51 foci at the proliferative region of *par-5(RNAi)* worms (Fig. 3A,B; supplementary material Fig. S10). This increase is similar to that obtained with the checkpoint defective strain *atl-1(tm853)* (Garcia-Muse and Boulton, 2005).

To corroborate the role of *par-5* in preserving genomic stability, we used a transgenic strain expressing the fusion protein HUS-1::GFP, which is a DNA damage sensor protein that forms

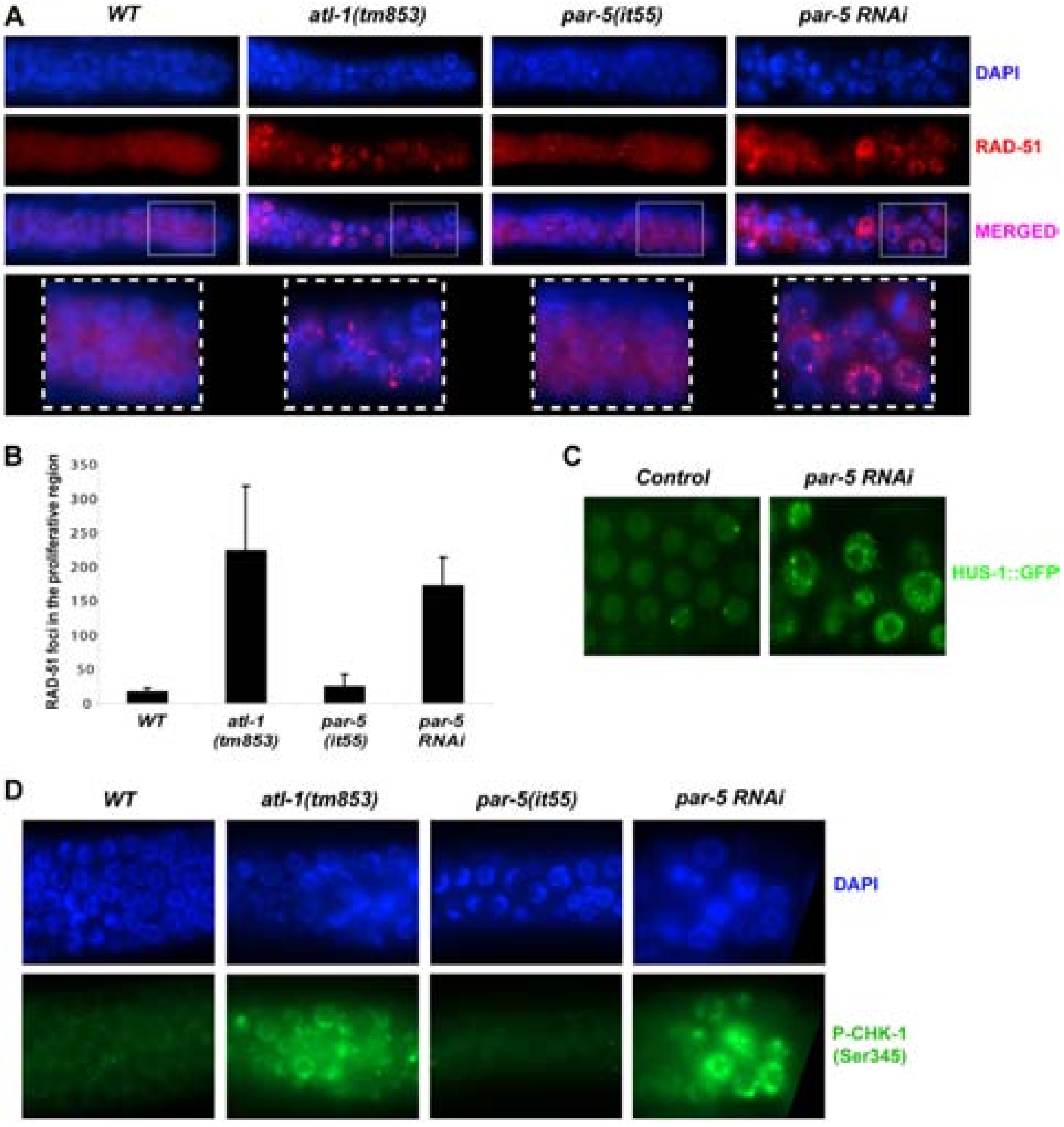

**Fig. 3. Lack of *par-5* results in DNA damage accumulation and CHK-1 activation.** (**A**) *par-5* suppression promotes RAD-51 accumulation. Representative images of the germline proliferative regions from worms of the indicated genotypes and/or RNAi, immunostained with a RAD-51 antibody and counterstained with DAPI. Distal proliferative regions enlarged in squares show the RAD-51 foci nuclear localization. (**B**) The graph shows RAD-51 foci quantification in all the stacks within 30 μm of the distal end of the gonad. Error bars indicate the standard deviation of the mean from at least 15 germlines for each experiment. (**C**) HUS-1::GFP foci increase after *par-5* knockdown. Representative images of the meiotic germ cells from a transgenic strain expressing a HUS-1::GFP fusion protein with or without *par-5* RNAi treatment. (**D**) CHK-1 phosphorylation is detected in pre-meiotic germ cells after *par-5* RNAi knockdown. Representative images of the pre-meiotic germ cells (cells between the proliferating and the transition region) from the worms of the indicated genotypes/RNAi, immunostained with a phosphorylated CHK-1 (Ser345) antibody and counterstained with DAPI. The percentage of germlines positively stained (at least 4–5 stained germ cells per gonad) with phosphorylated CHK-1 was: 5% for WT, 50% for *atl-1(tm853)*, 10% for *par-5(it55)* and 75% for *par-5* RNAi.

defined foci at DSBs (Hofmann et al., 2002). The meiotic region of WT animals showed a few HUS-1::GFP foci as a result of transient DSBs that occurred during meiotic recombination. However, *par-5* RNAi showed a marked increase in the number of HUS-1::GFP foci, indicating a higher accumulation of DSBs (Fig. 3C). These results link *par-5* with the DDR pathway.

In addition to the increase in DNA damage markers (RAD-51 and HUS-1 foci), *par-5(RNAi)* worms showed constitutive phosphorylation of the checkpoint kinase CHK-1 (at Serine 345) in germ cells localized at the proximal side of the proliferative region (Fig. 3D; supplementary material Fig. S11). This modification has been associated with recombination defects that trigger meiotic checkpoint activation (Jaramillo-Lambert et al., 2007). Notably, the same pattern was also observed in the *atl-1(tm853)* strain, whereas this phenotype was rarely present in WT worms and *par-5(it55)* mutants. Therefore, the RNAi depletion of *par-5* seems to cause pre-meiotic checkpoint activation similar to the effect of inactivating genes that control DNA stability, such as *atl-1*. Taken together, these results suggest that *par-5* is necessary for proper DNA maintenance because its inhibition promotes DNA damage accumulation both in proliferating and meiotic germ cells.

### *par-5* function is necessary for S and G2–M checkpoint responses

The accumulation of RAD-51 foci and the nuclei fragmentation observed in the proliferative region of *par-5* RNAi germlines (Fig. 2A, Fig. 3A) resemble the effect of mutations on the genes of the checkpoint pathway, such as *atl-1* and *chk-1* (Kalogeropoulos et al., 2004; Garcia-Muse and Boulton, 2005). Thus, we tested whether *par-5* is actively implicated in the DDR under replication stress induced by HU. HU inhibits the activity of the ribonucleotide reductase enzyme, causing the depletion of deoxyribonucleotide triphosphate (dNTP) levels and so hampering DNA replication (Kim et al., 1967). After HU treatment, cells in the proliferative region of the germline arrested in the S-phase as a result of checkpoint activation. This cell cycle arrest was evidenced by fewer nuclei with larger sizes (Gartner et al., 2004). Interestingly, after HU treatment, these checkpoint response marks were absent in *par-5(RNAi)* worms and *par-5(it55)* mutants (Fig. 4A). Such incapacity to arrest the cell cycle after HU treatment was also observed in mutants for the checkpoint gene *atl-1*.

The *C. elegans* embryo is another scenario in which the checkpoint response induced by replication stress has been widely studied. In particular, the presence of HU causes a delay in the mitotic entry at the first embryonic division (Brauchle et al., 2003). Through video recordings of the first embryonic division, we observed that *par-5(RNAi)* and *par-5(it55)* embryos rescued the HU-induced cell cycle delay (supplementary material Fig. S4). Therefore, *par-5* is also required for the embryonic DNA replication checkpoint, as are other checkpoint genes previously described (Brauchle et al., 2003; Moser et al., 2009).

To clarify whether the checkpoint role of *par-5* is exclusive for the S-phase, we investigated its role in the IR-induced G2–M checkpoint. *par-5(RNAi)* and *par-5* mutant germ cells bypassed the cell cycle arrest induced by IR and showed some fragmented and hypercondensed nuclei (Fig. 4B). These experiments indicate that *par-5* is an essential gene for cell cycle arrest in response to diverse exogenous insults, participating in both the S and the G2–M checkpoints.

### *par-5* prevents premature entry into mitosis

While testing the germline response to HU after *par-5* inhibition, we observed many germ nuclei that presented hypercondensed chromatin and smaller sizes (Fig. 4A). This effect, observed both in *par-5(RNAi)* and in *par-5(it55)* animals, was likely to be because of cells entering prematurely into mitosis before the DNA was properly replicated, thereby causing DNA fragmentation. To study this phenotype, we used an antibody against phosphorylated histone 3 (H3) as a mitotic marker (Fig. 4C). Although the number of mitotic germ cells was reduced in WT animals as a result of the S-phase checkpoint activation, the inactivation of *par-5* (either by RNAi or mutation) caused an increase in the number of mitotic cells after HU treatment. Therefore, this result indicates that HU-treated germ cells, in which *par-5* function is impaired, are able to enter mitosis, thereby bypassing the S-phase checkpoint. Consistently, a similar phenotype was also observed in the *atl-1(tm853)* strain.

Although *par-5* activity in controlling premature mitotic entry becomes obvious after HU treatment, we also observed a slight increase in the number of phosphorylated H3-positive cells in *par-5(RNAi)* and *par-5(it55)* unchallenged worms (Fig. 4C). Using a time-course experiment, we detected an increase in the number of mitotic figures and DNA fragmentation at the L4 stage, which is the developmental stage chosen to expose worms to HU in our checkpoint assays (supplementary material Fig. S5). All these results suggest that *par-5* is required to prevent premature entry into mitosis, both upon replicative stress and during normal germ cell proliferation. Such a function is the hallmark of checkpoint genes.

### PAR-5 accumulates in germ cell nuclei after checkpoint activation

14-3-3 proteins are known to regulate the subcellular localization of their substrates in response to DNA damage (Lopez-Girona et al., 1999; Dunaway et al., 2005). To further explore the mechanism by which *par-5* acts in the checkpoint response, we examined PAR-5 expression and subcellular localization by confocal microscopy in normal and HU-treated germlines. Previous studies demonstrated that PAR-5 is expressed in the germline syncytium (Morton et al., 2002). In agreement with this, we found PAR-5 localized around the nuclei of germ cells. Interestingly, after HU treatment, we observed a large amount of PAR-5 protein inside the large S-phase-arrested nuclei (Fig. 5A). This nuclear localization could be important for its role in the DDR, because no changes in protein expression levels were observed after treatment with HU (Fig. 5B).

### *par-5* is required for CDK-1 phosphorylation after DNA damage

It has been demonstrated that *par-5* homologs in yeast, flies and mammals (14-3-3 proteins) regulate G2–M transition through interactions with the cell cycle regulator proteins Wee1, Cdc25 and Cdk1 (Cdc2) (Peng et al., 1997; Chan et al., 1999; Kumagai and Dunphy, 1999; Zeng and Piwnica-Worms, 1999; Laronga et al., 2000; Lee et al., 2001). As a canonical cell cycle progression mechanism, Cdc25 dephosphorylates Cdk1 to allow entry into mitosis. However, after DNA damage, Cdk1 and Cdc25 are inactivated by phosphorylation (by the Wee1 and Chk1 kinases, respectively) in a checkpoint-dependent manner, leading to cell cycle arrest. In *C. elegans*, CDK-1 is also

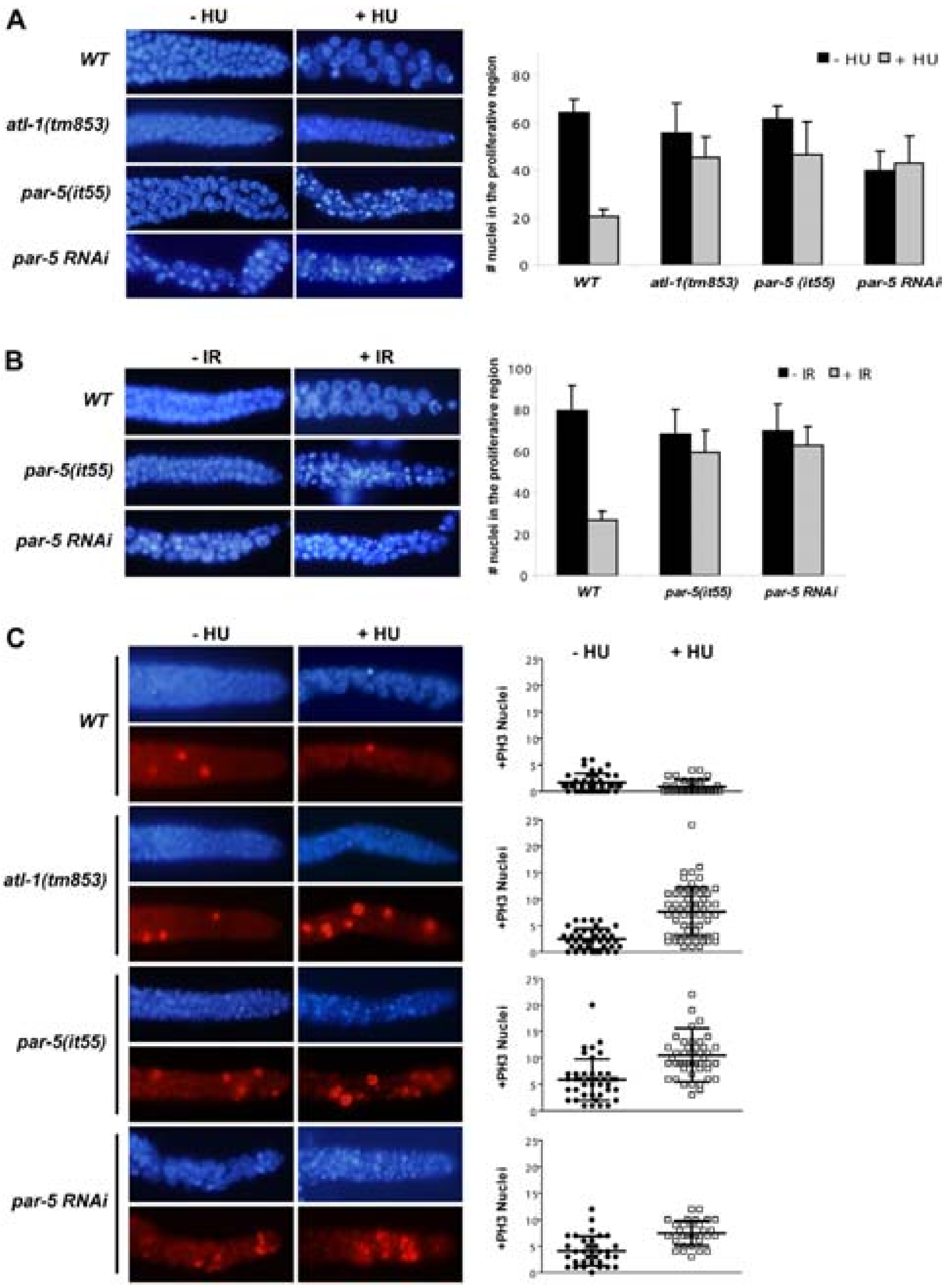
A
- HU
+ HU
WT
atl-1(tm853)
par-5(it55)
par-5 RNAi
# nuclei in the proliferative region
0
20
40
60
80
■ - HU □ + HU
WT
atl-1(tm853)
par-5 (it55)
par-5 RNAi
B
- IR
+ IR
WT
par-5(it55)
par-5 RNAi
# nuclei in the proliferative region
0
20
40
60
80
100
■ - IR □ + IR
WT
par-5(it55)
par-5 RNAi
C
- HU
+ HU
WT
atl-1(tm853)
par-5(it55)
par-5 RNAi
+PH3 Nuclei
0
5
10
15
20
25

**Fig. 4. Cell cycle arrest induced by DNA damage depends on *par-5* function.** (**A**) *par-5* is required for HU-induced cell cycle arrest. Representative images of germline proliferative regions from the worms of the indicated genotypes and/or RNAi, treated with (+HU) or without (–HU) HU and stained with DAPI. The graph shows germ nuclei quantification. Error bars indicate standard deviations from the mean. (**B**) *par-5* is also necessary for IR-induced responses. Representative images of germline proliferative regions from the worms of the indicated genotypes and/or RNAi, irradiated (+IR) or not (–IR) with γ-rays. The graph shows germ nuclei quantification and error bars indicate standard deviations from the mean. (**C**) *par-5* inactivation leads to premature mitotic entry. Worms were treated with HU as for A, and then the germlines were immunostained with a phosphorylated H3 antibody and counterstained with DAPI. The graph shows the quantification of phosphorylated H3-positive cells in all the stacks within 50 μm of the distal end of the gonad. Error bars indicate the standard deviation of the mean from at least 30 germlines for each experiment.

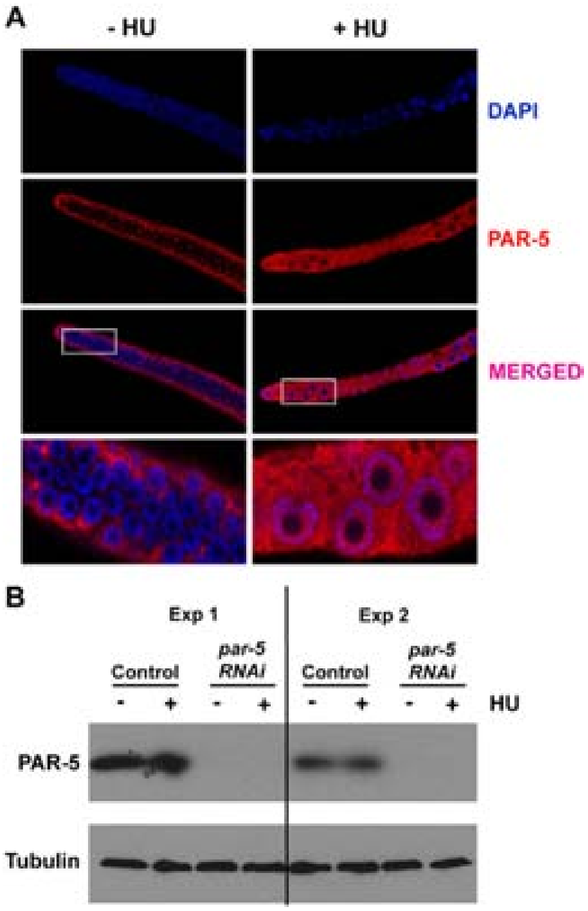

**Fig. 5. PAR-5 location and expression after replication stress induced by HU.** (**A**) Representative confocal images showing a single Z stack of germlines from WT worms treated with (+HU) or without (–HU) HU, immunostained with a PAR-5 antibody and counterstained with DAPI. (**B**) Protein extracts from WT worms fed with the *par-5* RNAi or the RNAi empty vector (control) and treated with (+) or without (–) HU were blotted using a PAR-5 antibody. The blotting was performed using extracts from two biological replicates.

phosphorylated in the Tyr15 inhibitory residue upon DNA damage (Moser et al., 2009; Bailly et al., 2010).

Given that we observed premature entry into mitosis in *par-5(RNAi)* and in *par-5(it55)* worms after DNA damage, we investigated whether *par-5* inactivation affected CDK-1 phosphorylation. Similar to HU, treatment with camptothecin (CPT) produced CDK-1 phosphorylation and the consequent cell cycle arrest in the proliferative region of the WT germline (Fig. 6A). However, after *par-5* RNAi knockdown, phosphorylated CDK-1 staining was strongly reduced in the proliferative region. The same effect was observed in *atl-1(tm853)* strains, suggesting that lack of phosphorylated CDK-1 is a consequence of deficient checkpoint activation. *par-5* mutants revealed some germ cells with phosphorylated CDK-1 staining after CPT treatment, reflecting the milder *par-5* inactivation compared with the *par-5(RNAi)* animals (Fig. 6A; supplementary material Fig. S12).

To further investigate the link between PAR-5 and CDK-1 phosphorylation, we examined the functional relation between *par-5* and *cdc-25.1*. In yeast and mammals, Cdc25 phosphatase removes the Cdk1 inhibitory phosphorylation (Tyr15) to promote mitosis entry. Accordingly, we observed that *cdc-25.1* suppression enhances CDK-1 phosphorylation upon DNA damage in *C. elegans* (Fig. 6A). Moreover, *cdc-25.1* RNAi produces cell cycle arrest in the proliferative region of the germline that mimics the checkpoint response (Fig. 6B). This *cdc-25.1* RNAi phenotype effect was rescued in a *par-5(it55)* background, pointing towards an opposite function for *par-5* and *cdc-25.1* in cell cycle control. A similar antagonism to regulate the cell cycle has been described in fission yeast for Wee1 and Cdc25 (Raleigh and O'Connell, 2000). In that model, Cdk1 phosphorylation relies on the balance between the activities of the kinase Wee1 and the phosphatase Cdc25. Consequently, we assessed whether *par-5* could be acting in the same pathway as *wee-1* to counteract *cdc-25.1* function. In *C. elegans*, there are two *wee-1* genes, *wee-1.1* and *wee-1.3*. *wee-1.3* regulates *cdk-1* function in the germline (Burrows et al., 2006) and we observed that *wee-1.3* partially suppressed the *cdc-25.1* arrest phenotype (supplementary material Fig. S6). We then tested whether *wee-1.3*, similar to *par-5*, was necessary for HU-induced cell cycle arrest. As with *par-5* RNAi, *wee-1.3* knockdown inhibited the checkpoint induced by replication stress, leading to aberrant mitosis and nuclei fragmentation (Fig. 6C).

These results suggest that PAR-5 controls entry into mitosis in the same manner as does WEE-1.3 to promote CDK-1 phosphorylation and counteract CDC-25.1 function. Such a model would place PAR-5 downstream of the checkpoint pathway as part of the effector proteins required for DNA damage-induced cell cycle arrest (Fig. 7).

## Discussion

The ability of 14-3-3 proteins to interact physically with many proteins offers PAR-5 the potential to be involved in several developmental processes. In this study, we dissected two separate functions for *par-5* in the germline, one in germ cell proliferation and another responding to DNA damage. Although both functions might be related and influenced by the role of *par-5* in preventing premature mitotic entry, the pathways regulating these two processes as the level of PAR-5 might be different.

### *par-5* and germline development

The decrease in the number of germ cells in *par-5*-defective animals could be explained, at least partially, by abnormal and uncontrolled entry into the M-phase, which leads to mitotic defects (Fig. 4C). After *par-5* knockdown, we detected some nuclei that showed hyperfragmented chromatin. These cells probably suffered mitotic catastrophe and so were unable to continue dividing, contributing to the strong decrease in germ cell precursors after *par-5* RNAi administration (Fig. 2A,B). This phenotype was rarely observed in *par-(it55)* animals, in which, although the proliferation rate was affected, reduced PAR-5 levels are sufficient to maintain the dividing of germ cells without mitotic catastrophe. The nuclei fragmentation observed in *par-5(RNAi)* germ cells was accompanied by an accumulation of RAD-51 foci in the proliferative region of the germline. Both phenotypes have previously been related to defects in the maintenance of replication stability and the consequent aberrant mitosis, which has also been observed after the suppression of key checkpoint genes, such as *atl-1*, *wrn-1* and *chk-1* (Kalogeropoulos et al., 2004; Garcia-Muse and Boulton, 2005; Lee et al., 2010). In addition, budding yeast 14-3-3 proteins negatively regulate Exo1 nuclease

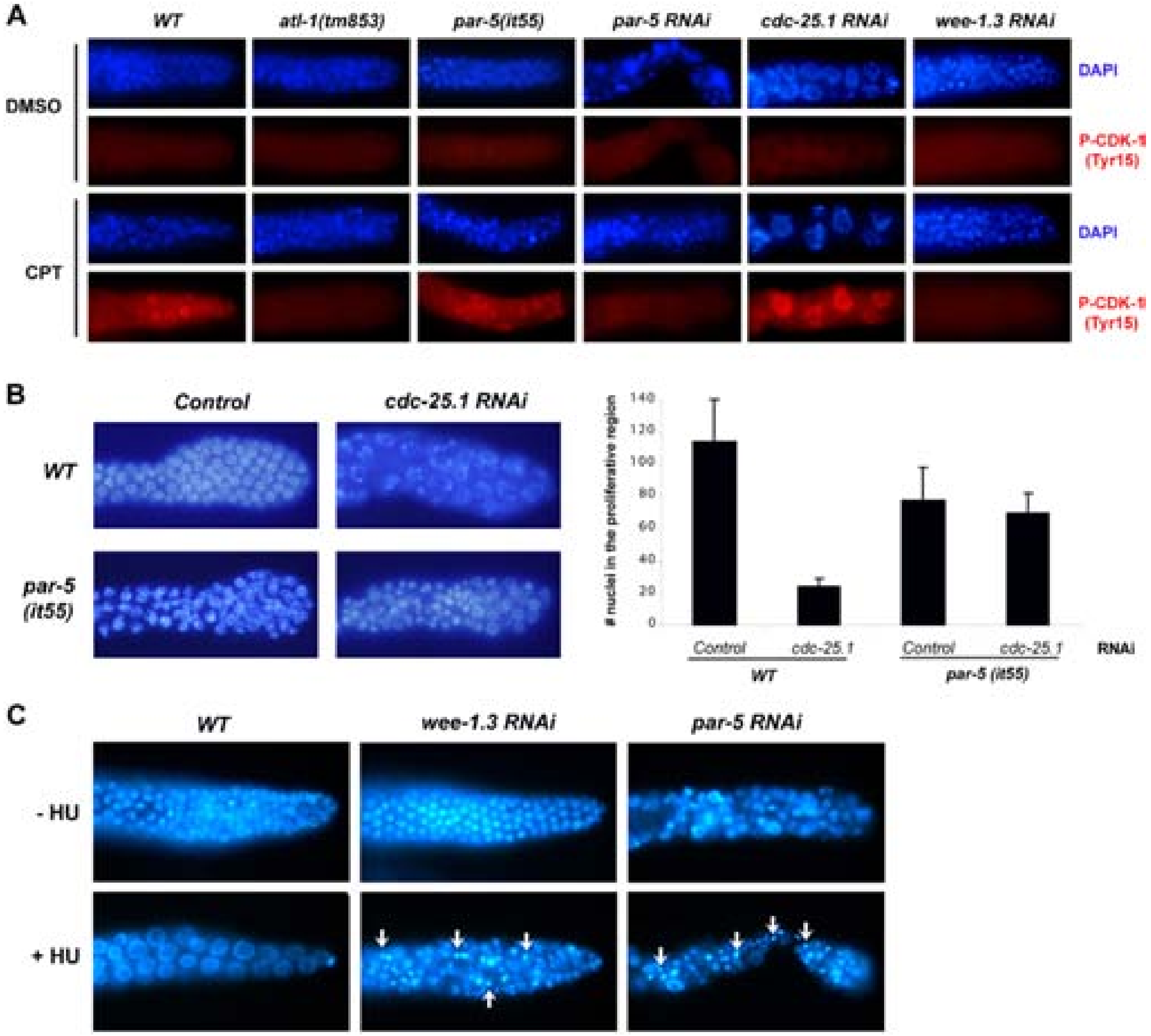

**Fig. 6. *par-5* regulates CDK-1 phosphorylation.** (**A**) *par-5* is required for CDK-1 phosphorylation after DNA damage. Representative images of germline proliferative regions from the worms of the indicated genotypes and/or RNAi, treated with CPT or vehicle control (DMSO) immunostained with a phosphorylated CDK-1 (Tyr15) antibody and counterstained with DAPI. (**B**) *par-5* counteracts *cdc-25.1* function. Representative images of the proliferative region of germlines from WT or *par-5(it55)* worms (1-day-old adults) fed with the RNAi empty vector or *cdc-25.1* RNAi (from the L3 stage) stained with DAPI. The graph shows germ nuclei quantification. Error bars indicate standard deviations from the mean. (**C**) *wee-1.3* suppression mimics *par-5* RNAi phenotype upon HU treatment. Representative images of germline proliferative regions from WT worms fed with *wee-1.3* or *par-5* RNAi, treated with (+HU) or without (–HU) HU and stained with DAPI. The nuclear fragmentation shown was observed in 90% of the *wee-1.3* and *par-5* RNAi-treated germlines.

activity, which is involved in the pathological process of stalled replication forks that produces the accumulation of single-strand DNA gaps (Engels et al., 2011). Nevertheless, it is unknown whether this interaction occurs in *C. elegans.*

The lack of oocytes observed in *par-5(RNAi)* worms also highlighted that *par-5* has a role in meiotic progression. Interestingly, after *par-5* knockdown, we observed an increase in HUS-1::GFP foci, reflecting the accumulation of unrepaired DSBs in the meiotic region. This observation, together with the accumulation of RAD-51 foci in proliferating cells, suggests that *par-5* is required to repair endogenous DNA damage. However, we cannot rule out the possibility that *par-5* depletion causes additional DNA damage (directly or indirectly) through a different mechanism. The increase in DNA damage in the germlines of *par-5(RNAi)* worms was also accompanied by constitutive phosphorylation of CHK-1 (Ser345) in pre-meiotic germ cells. Given that we observed the same phenotype in *atl-1(tm853)* mutants, CHK-1 phosphorylation is probably mediated by ATM-1 instead of by ATL-1. In agreement with this hypothesis, it has been suggested that *atm-1* controls meiotic checkpoint activation (Bhalla, 2010; Jaramillo-Lambert et al., 2010). Both the accumulation of DSBs (HUS-1::GFP foci) and constitutive meiotic CHK-1 activation could contribute to the absence of oocytes after *par-5* RNAi, because the damaged meiotic cells might not progress to reach proper oocyte differentiation.

We conclude that the altered mitosis and meiosis observed in the germlines of *par-5*-defective worms are related to an accumulation of DNA damage in germ cells, which is compatible with the role of *par-5* in the DDR pathway.

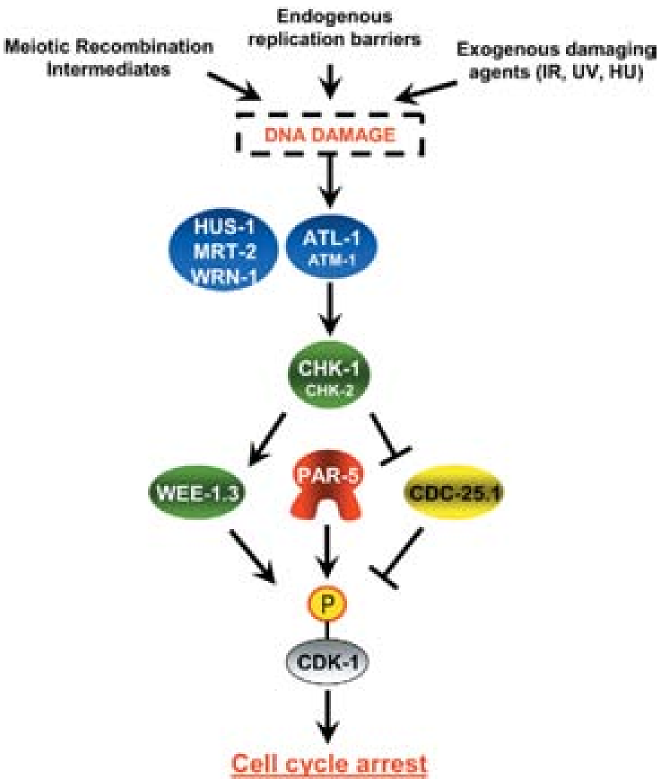
Meiotic Recombination Intermediates
Endogenous replication barriers
Exogenous damaging agents (IR, UV, HU)
DNA DAMAGE
HUS-1
MRT-2
WRN-1
ATL-1
ATM-1
CHK-1
CHK-2
WEE-1.3
PAR-5
CDC-25.1
P
CDK-1
Cell cycle arrest

**Fig. 7. Model of *par-5* function within DNA damage-induced cell cycle arrest.** After the detection of endogenous or exogenous DNA damage, checkpoint sensor proteins (e.g. HUS-1 and MRT-2) activate ATL-1 and ATM-1, which in turn phosphorylate the CHK-1 and CHK-2 kinases. The contribution of ATL-1–ATM-1 and CHK-1–CHK-2 to the response depends mainly on the DNA damage that triggers the response. However, ATL-1 and CHK-1 are considered to be the main actors in the pathway. Downstream of CHK-1, the cell cycle can be arrested by promoting CDK-1 inactivation by phosphorylation. According to our results, CDK-1 phosphorylation status relies on the balance between the activities of the WEE-1.3 kinase and those of the CDC-25.1 phosphatase. Therefore, checkpoint signaling would favor WEE-1.3 activation and CDC-25.1 inhibition (which is likely to be by CHK-1-mediated phosphorylation). In this context, we propose that PAR-5 is necessary to promote and/or maintain CDK-1 phosphorylation (inactive form) and so to induce cell cycle arrest properly upon DNA damage.

### Function of *par-5* within the checkpoint pathway

We demonstrated that, in *C. elegans*, the 14-3-3 gene *par-5* is required to promote proper cell cycle arrest after DNA damage. Interestingly, although only *par-5(RNAi)* worms showed endogenous DNA damage accumulation and nuclei fragmentation, both *par-5(it55)* and *par-5(RNAi)* worms presented similar checkpoint defects in response to exogenous DNA damage. Therefore, taking into account the fact that the mutant strain retains some protein expression (Morton et al., 2002), it is clear that a mild decrease in PAR-5 level is enough to affect the extrinsic DNA damage-induced checkpoint response, whereas a stronger depletion of the protein [as shown in our RNAi experiments (Fig. 5B)] affects germ cell cycle progression and DNA stability.

PAR-5 belongs to the PAR family, which controls the asymmetric first cell division in the embryo. This process includes the tight regulation of the cycling time in the posterior and anterior cells (Suzuki and Ohno, 2006). However, worms fed with RNAi against *par-2* and *par-3* (members of the anterior and posterior complexes that drive asymmetry in the embryo) showed normal cell cycle arrest after HU treatment (supplementary material Fig. S7). Moreover, when we studied the cell cycle of the first embryonic division, we found that *par-5*-defective embryos presented a shorter S-phase and a longer M-phase (supplementary material Fig. S4). By analyzing videos from the Phenobank (http://www.worm.mpi-cbg.de/phenobank/cgi-bin/MenuPage.py), such cell cycle alterations seem to be unique among PAR family members (supplementary material Fig. S9). These experiments indicate that participation in DDR is a rare feature of the PAR family, but one that is specific for PAR-5.

PAR-5 has also been shown to act as a target of MPK-1 (the ERK pathway) to govern pachytene cellular organization in the germline (Arur et al., 2009). As in the case of the PAR proteins examined, the inhibition of MPK-1 did not affect cell cycle arrest, even though the worms were sterile (supplementary material Fig. S7). Therefore, the role of *par-5* in DDR is unrelated to its described function in the *mpk-1* pathway, underscoring the multifunctional role of this gene.

Several 14-3-3 protein partners that could help explain the role of *par-5* in cell cycle arrest that is induced by DNA damage have been reported in several organisms. These interactions, together with the functional evidence provided in this study, are compiled and depicted in Fig. 7. In yeast, 14-3-3 proteins interact with Chk1 to regulate cell cycle arrest upon DNA damage (Dunaway et al., 2005). Chk1 phosphorylates Wee1, which in turn phosphorylates Cdk1 (Tyr15) to stop the cell cycle (O'Connell et al., 1997), and 14-3-3 proteins are required for proper Chk1 nuclear localization and function (Chen et al., 1999; Dunaway et al., 2005). Therefore, the hypothesis that PAR-5 is necessary for CHK-1 function could explain the defect in CDK-1 phosphorylation and cell cycle arrest after *par-5* knockdown. However, it seems that PAR-5 is not strictly necessary for CHK-1 activation because we observed the CHK-1 active form (phosphorylated at Ser345) and its proper nuclear localization in *par-5(RNAi)* worms (Fig. 3D). Nevertheless, as this observation was carried out in pre-meiotic cells, we cannot rule out a functional interaction between PAR-5 and CHK-1 in proliferating germ cells. Downstream of Chk1, 14-3-3 proteins have been shown to interact with the Cdc25 phosphatase, preventing its interaction with Cdk1 (Peng et al., 1997; Lopez-Girona et al., 1999; Zeng and Piwnica-Worms, 1999). Cdc25 eliminates the Cdk1 (Tyr15) inhibitory phosphorylation (executed by Wee1), thereby allowing Cdk1 to promote progression into mitosis. Therefore, Cdk1 phosphorylation and activity depend on the kinase and phosphatase activities of Wee1 and Cdc25, respectively (O'Connell et al., 2000). Accordingly, our results are compatible with the idea of *par-5* collaborating with *wee-1.3* and counteracting *cdc-25.1* to promote proper cell cycle arrest upon DNA damage. However, *wee-1.3* depletion, in contrast to *par-5*, does not seem to affect germline proliferation in the absence of HU (supplementary material Fig. S8). Therefore, *par-5* functions in the germline are not always coupled with *wee-1.3*.

Finally, 14-3-3 proteins have been shown to regulate Cdk1 localization and function directly (Chan et al., 1999; Laronga et al., 2000; Su et al., 2001). In mammals, phosphorylated Cdk1 is sequestered in the cytoplasm upon DNA damage in a 14-3-3-dependent manner to prevent mitotic catastrophe (Chan et al., 1999). However, in *C. elegans* (similar to yeast), phosphorylated

CDK-1 is located inside the nucleus (Boxem et al., 1999). Therefore, if PAR-5 regulates CDK-1 function, the mechanism should be different from that of cytoplasmic sequestration. Moreover, we showed that PAR-5 is localized in the nucleus upon replication stress, suggesting that the relevant interactions for DDR occur inside the nucleus. Further experiments are needed to identify PAR-5 interactions and their impacts on checkpoint responses and germline proliferation.

### *C. elegans* as a model to study 14-3-3 regulation and function

Although mammalian 14-3-3 homologs have diverged into seven genes, we verified that the basic functions of 14-3-3 in cell cycle control have been conserved in *C. elegans*. Indeed, the mitotic catastrophe observed in *par-5(RNAi)* worms has already been noted in human cells lacking 14-3-3$\sigma$ after the induction of DNA damage (Chan et al., 1999). However, *C. elegans*, in contrast to mammals, has only one 14-3-3 protein (PAR-5) expressed in the germline, which could explain why *par-5* is essential to maintain the proliferation and genomic stability of the germline. By contrast, the single knockdown of mammalian 14-3-3 has less influence on the cells in the absence of exogenous DNA damage, probably because of functional redundancy (Hermeking and Benzinger, 2006).

DNA fragmentation in the germ cells of *par-5*-knockdown worms treated with different DNA-damaging agents (i.e. CPT, HU or IR) implies the increased sensitivity of proliferating cells to these agents. This observation is in agreement with multiple reports showing that 14-3-3 overexpression is related to chemotherapy resistance in cancer cell lines, and also that 14-3-3 downregulation sensitizes cells to therapy-induced cell death (Porter et al., 2006; Tzivion et al., 2006; Neal and Yu, 2010). Indeed, 14-3-3 proteins have been suggested as possible therapeutic targets in cancer treatment.

Although many studies on 14-3-3 proteins have been published, few have shown the 14-3-3 up- and/or down-regulatory effects in animal models, and most have focused on one isoform (14-3-3$\sigma$) (Porter et al., 2006). Hence, the present study paves the way for the use of *C. elegans* as a model to study 14-3-3 functions and expression regulation, and as a high-throughput platform to test new drugs targeting 14-3-3 proteins and to perform genome-wide RNAi screening to identify new 14-3-3 interactors and suppressors.

## Materials and Methods

### Worm strains and culture conditions

*Caenorhabditis elegans* strains were cultured and maintained using standard procedures (Stiernagle, 2006). Bristol N2 was used as a WT strain. The following alleles were used during the study: *atl-1(tm853)* (strain DW101); *hus-1(op241) opIs34 [HUS-1:GFP]* (strain WS1433); *par-5(it55)* (strain KK299); *rrf-1(pk1417)* (strain NL2098); and *rrf-3(pk1426)* (strain NL2099). The experiment using the *hus-1(op241)* and *opIs34 [HUS-1:GFP]* was performed at 25℃ to maximize the transgene expression. The remaining experiments were carried out at 20℃.

### RNAi

To induce RNAi by feeding, nematode growth medium (NGM) plates were supplemented with 100 µg/mL ampicillin, 12.5 µg/mL tetracycline and 3 mM IPTG. The RNAi clones used for the experiments were obtained from either the ORFeome library (Rual et al., 2004) (*par-5*, *mpk-1*, *cdc-25.1* and *wee-1.3*) or the Ahringer library (Kamath et al., 2003) (*par-2* and *par-3*). Plates seeded with the corresponding RNAi clones were used to feed WT synchronized L1 worms (unless another stage is stated). All RNAi clones were verified by sequencing. The WT strain fed with a clone carrying the L4440 empty vector was used as an RNAi negative control.

### Germline dissection and quantification

To quantify the cells in the proliferative region, gonads were dissected, fixed (formaldehyde 3%, methanol 75%, $K_2HPO_4$ 6.2 mM) and stained with DAPI (0.6 µg/mL) after the corresponding treatments. The stained gonads were photographed using a Leica DM5000B microscope. Digital pictures were used for germ cell quantification in a single Z stack within 50 µm of the distal end of the gonad. For the germline time-course experiment, germ nuclei from the distal part to the bend of the gonad were scored in a single Z stack. At least 15 germlines were quantified for each experiment.

### DDR assays

To perform all the cell cycle arrest assays, L4 stage worms (42–46 hours post-L1) of the corresponding genotypes or RNAi were treated with different DNA-damaging agents. For the HU assay, worms were transferred onto NGM plates containing HU (25 mM; SIGMA, cat # H8627) for 20–24 hours before dissection. For the CPT assay, worms were transferred onto NGM plates containing CPT (40 µM; Sigma-Aldrich, cat # C9911) or DMSO 0.1% for 20–24 hours. The dissected gonads were used for immunostaining with a phosphorylated CDK-1(Tyr15) antibody. For the IR assay, worms were irradiated with $\gamma$-rays (120 Gy) using a Cesium137 source (model IBL-437-C H). Dissection was performed 12 hours post-irradiation.

### Embryo cell cycle timing

Embryos for video recordings were obtained from worms treated as follows: L4 stage worms, grown at 20℃, were transferred onto plates containing the indicated RNAi or the RNAi empty vector L4440. After 24 hours, half of the adult worms were transferred onto plates containing HU (75 mM). The other half was used as a control. HU-treated embryos were recorded from 5.5 hours to 10 hours after HU treatment. Video recordings were performed using Nomarski optics at 21℃ with continuous video acquisition at one frame per second. The cell cycle timing of the first embryonic division was determined as described by Antonia Holway (Holway et al., 2006).

### Immunostaining

For immunostaining, adult worms were immobilized in Levamisole 0.3 mM (in PBS). Their gonads were then dissected and fixed in a manner appropriate for the primary antibody. For antibody staining against RAD-51 (a gift from Anton Gartner), gonads were fixed for 10 minutes in PFA 2% (diluted in PBS). For antibody staining against phosphorylated H3 (Ser10) (Millipore, cat. # 04-817) and phosphorylated CDK-1 (Tyr15) (Calbiochem, cat. # 219440), gonads were fixed in FA 3% (diluted in $K_2HPO_4$ 6.2 mM) for 10 minutes. For antibody staining against PAR-5 (a gift from Andy Golden), gonads were fixed for 30 minutes in 2% PFA followed by a post-fixation incubation in cold methanol (5 minutes). Primary antibody dilutions were as follows: RAD-51 (1:200); phosphorylated H3 (1:1000); PAR-5 (1:800); and phosphorylated CDK-1(Tyr15) (1:50). Primary incubations were performed overnight in 0.1% PBS Tween and 1% BSA. After fixation and antibody incubations, gonads were washed three times with PBS Tween 0.1%. A secondary antibody, Alexa-Fluor-568-conjugated goat anti-rabbit antibody (Molecular Probes, Invitrogen) was used to label the gonads. All samples were counterstained with DAPI (0.6 µg/mL) to visualize the nuclei. Staining conditions for phosphorylated CHK-1 (Ser345) (Cell Signaling Technology, cat. # 2348) were as previously described by Se-jin Lee and collaborators (Lee et al., 2010).

### Western blotting

Adult worms were washed off plates with M9 buffer and rocked for 30 minutes. They were then washed twice with M9, and the pellets mixed with Lysis buffer 2X (4% SDS, 100 mM Tris-HCl pH 6.8, 20% glycerol, 1 × protease inhibitor cocktail (CalBioChem), 1 mM orthovanadate, 2 mM NaF, 10 mM glycerol 2-phosphate disodium and 500 nM sodium pyrophosphate). Once mixed, the pellets were incubated in boiling water for 15 minutes. The obtained lysates were electrophoresed on SDS 12% polyacrylamide gels and electroblotted onto nitrocellulose membranes. Blotting was carried out using the primary antibodies for PAR-5 (from Andy Golden), tubulin (Developmental Studies Hybridoma Bank, cat. # E7) and secondary horseradish-peroxidase-conjugated anti-rabbit and anti-mouse (DAKO). Primary antibody dilutions were 1:4000 and 1:10,000, respectively.

### Quantitative RT-PCR

Adult worms were washed off plates with M9 buffer and rocked for 30 minutes. They were then washed twice with M9, and the pellets were mixed with TRI REAGENT (MRC Technology) to extract RNA following the manufacturer's instructions. For cDNA synthesis, a High Capacity Retro Transcription kit (Applied Biosystems) was used. SYBR-GREEN (Applied Biosystems) reagent was used to perform the amplification reaction followed by a real-time quantification using the ABI PRISM 7500 system. The -fold change expression of the corresponding genes was based on the ddCT method and normalized relative to the amplification obtained using *act-1* (actin) primers. Primer sequences were as follows: *par-5* (FW: ACCGCGTCAAGGTTGAGCAAGA, RV: ACAACGGCA-GCGCGATCCTC); *ftt-2* (FW: TCCGGAGACGACAGAAACTCGGT, RV:

CTGGCAAGCCTTGTCCGGGG); and *act-1* (FW: CCGCTCTTGCCCCATCAACCA, RV: CGATGGATGGGCCGGACTCG).

## Acknowledgements

We thank Tatiana Garcia-Muse for critical reading of the manuscript. We also thank Marta Artal-Sanz for her valuable comments. Members of the Schwartz Jr and Cerón labs provided useful comments and discussion. The worm strains used in this work were provided by the Caenorhabditis Genetics Center, which is funded by the National Institutes of Health National Center for Research Resource.

## Funding

This work was funded by Marie Curie-IRG [grant number 206584]; and also partially by the Networking Research Center on Bioengineering, Biomaterials and Nanomedicine (CIBER-BBN). D.A.-C. is supported by a fellowship from the Vall d'Hebron Hospital Institut de Recerca. J.C., L.F. and M.P. are supported by the Miguel Servet Young Investigator Program, an AGAUR PhD fellowship and the PTA-MICINN program, respectively.

Supplementary material available online at
http://jcs.biologists.org/lookup/suppl/doi:10.1242/jcs.094896/-/DC1

## References

**Ahmed, S., Alpi, A., Hengartner, M. O. and Gartner, A.** (2001). C. elegans RAD-5/CLK-2 defines a new DNA damage checkpoint protein. *Curr. Biol.* **11**, 1934-1944.

**Alpi, A., Pasierbek, P., Gartner, A. and Loidl, J.** (2003). Genetic and cytological characterization of the recombination protein RAD-51 in Caenorhabditis elegans. *Chromosoma* **112**, 6-16.

**Arur, S., Ohmachi, M., Nayak, S., Hayes, M., Miranda, A., Hay, A., Golden, A. and Schedl, T.** (2009). Multiple ERK substrates execute single biological processes in Caenorhabditis elegans germ-line development. *Proc. Natl. Acad. Sci. USA* **106**, 4776-4781.

**Bailly, A. P., Freeman, A., Hall, J., Déclais, A.-C., Alpi, A., Lilley, D. M., Ahmed, S. and Gartner, A.** (2010). The Caenorhabditis elegans homolog of Gen1/Yen1 resolvases links DNA damage signaling to DNA double-strand break repair. *PLoS Genet.* **6**, e1001025.

**Berdichevsky, A., Viswanathan, M., Horvitz, H. R. and Guarente, L.** (2006). C. elegans SIR-2.1 interacts with 14-3-3 proteins to activate DAF-16 and extend life span. *Cell* **125**, 1165-1177.

**Bhalla, N.** (2010). Meiotic checkpoints: repair or removal? *Curr. Biol.* **20**, R1014-R1016.

**Boxem, M., Srinivasan, D. G. and van den Heuvel, S.** (1999). The Caenorhabditis elegans gene ncc-1 encodes a cdc2-related kinase required for M phase in meiotic and mitotic cell divisions, but not for S phase. *Development* **126**, 2227-2239.

**Brauchle, M., Baumer, K. and Gönczy, P.** (2003). Differential activation of the DNA replication checkpoint contributes to asynchrony of cell division in C. elegans embryos. *Curr. Biol.* **13**, 819-827.

**Burrows, A. E., Sceurman, B. K., Kosinski, M. E., Richie, C. T., Sadler, P. L., Schumacher, J. M. and Golden, A.** (2006). The C. elegans Myt1 ortholog is required for the proper timing of oocyte maturation. *Development* **133**, 697-709.

**Chan, T. A., Hermeking, H., Lengauer, C., Kinzler, K. W. and Vogelstein, B.** (1999). 14-3-3Sigma is required to prevent mitotic catastrophe after DNA damage. *Nature* **401**, 616-620.

**Chen, L., Liu, T. H. and Walworth, N. C.** (1999). Association of Chk1 with 14-3-3 proteins is stimulated by DNA damage. *Genes Dev.* **13**, 675-685.

**Collis, S. J., Barber, L. J., Clark, A. J., Martin, J. S., Ward, J. D. and Boulton, S. J.** (2007). HCLK2 is essential for the mammalian S-phase checkpoint and impacts on Chk1 stability. *Nat. Cell Biol.* **9**, 391-401.

**Dunaway, S., Liu, H.-Y. and Walworth, N. C.** (2005). Interaction of 14-3-3 protein with Chk1 affects localization and checkpoint function. *J. Cell Sci.* **118**, 39-50.

**Engels, K., Giannattasio, M., Muzi-falconi, M., Lopes, M. and Ferrari, S.** (2011). 14-3-3 Proteins regulate exonuclease 1-dependent processing of stalled replication forks. *PLoS Genet.* **7**, e1001367.

**Ford, J. C., al-Khodairy, F., Fotou, E., Sheldrick, K. S., Griffiths, D. J. and Carr, A. M.** (1994). 14-3-3 protein homologs required for the DNA damage checkpoint in fission yeast. *Science* **265**, 533-535.

**Garcia-Muse, T. and Boulton, S. J.** (2005). Distinct modes of ATR activation after replication stress and DNA double-strand breaks in Caenorhabditis elegans. *EMBO J.* **24**, 4345-4355.

**Gartner, A., MacQueen, A. J. and Villeneuve, A. M.** (2004). Methods for analyzing checkpoint responses in Caenorhabditis elegans. *Methods Mol. Biol.* **280**, 257-274.

**Hermeking, H. and Benzinger, A.** (2006). 14-3-3 proteins in cell cycle regulation. *Semin. Cancer Biol.* **16**, 183-192.

**Hofmann, E. R., Milstein, S., Boulton, S. J., Ye, M., Hofmann, J. J., Stergiou, L., Gartner, A., Vidal, M. and Hengartner, M. O.** (2002). Caenorhabditis elegans HUS-1 is a DNA damage checkpoint protein required for genome stability and EGL-1-mediated apoptosis. *Curr. Biol.* **12**, 1908-1918.

**Holway, A. H., Kim, S.-H., La Volpe, A. and Michael, W. M.** (2006). Checkpoint silencing during the DNA damage response in Caenorhabditis elegans embryos. *J. Cell Biol.* **172**, 999-1008.

**Jaramillo-Lambert, A., Ellefson, M., Villeneuve, A. M. and Engebrecht, J.** (2007). Differential timing of S phases, X chromosome replication, and meiotic prophase in the C. elegans germ line. *Dev. Biol.* **308**, 206-221.

**Jaramillo-Lambert, A., Harigaya, Y., Vitt, J., Villeneuve, A. and Engebrecht, J.** (2010). Meiotic errors activate checkpoints that improve gamete quality without triggering apoptosis in male germ cells. *Curr. Biol.* **20**, 2078-2089.

**Kalogeropoulos, N., Christoforou, C., Green, A. J., Gill, S. and Ashcroft, N. R.** (2004). chk-1 is an essential gene and is required for an S-M checkpoint during early embryogenesis. *Cell Cycle* **3**, 1196-1200.

**Kamath, R. S., Fraser, A. G., Dong, Y., Poulin, G., Durbin, R., Gotta, M., Kanapin, A., Le Bot, N., Moreno, S., Sohrmann, M. et al.** (2003). Systematic functional analysis of the Caenorhabditis elegans genome using RNAi. *Nature* **421**, 231-237.

**Killian, D. J. and Hubbard, E. J.** (2005). Caenorhabditis elegans germline patterning requires coordinated development of the somatic gonadal sheath and the germ line. *Dev. Biol.* **279**, 322-335.

**Kim, J. H., Gelbard, A. S. and Perez, A. G.** (1967). Action of hydroxyurea on the nucleic acid metabolism and viability of HeLa cells. *Cancer Res.* **27**, 1301-1305.

**Kumagai, A. and Dunphy, W. G.** (1999). Binding of 14-3-3 proteins and nuclear export control the intracellular localization of the mitotic inducer Cdc25. *Genes Dev.* **13**, 1067-1072.

**Laronga, C., Yang, H. Y., Neal, C. and Lee, M. H.** (2000). Association of the cyclin-dependent kinases and 14-3-3 sigma negatively regulates cell cycle progression. *J. Biol. Chem.* **275**, 23106-23112.

**Lee, J., Kumagai, A. and Dunphy, W. G.** (2001). Positive regulation of Wee1 by Chk1 and 14-3-3 proteins. *Mol. Biol. Cell* **12**, 551-563.

**Lee, S.-J., Gartner, A., Hyun, M., Ahn, B. and Koo, H.-S.** (2010). The Caenorhabditis elegans Werner syndrome protein functions upstream of ATR and ATM in response to DNA replication inhibition and double-strand DNA breaks. *PLoS Genet.* **6**, e1000801.

**Li, J., Tewari, M., Vidal, M. and Lee, S. S.** (2007). The 14-3-3 protein FTT-2 regulates DAF-16 in Caenorhabditis elegans. *Dev. Biol.* **301**, 82-91.

**Lopez-Girona, A., Furnari, B., Mondesert, O. and Russell, P.** (1999). Nuclear localization of Cdc25 is regulated by DNA damage and a 14-3-3 protein. *Nature* **397**, 172-175.

**Morton, D. G., Shakes, D. C., Nugent, S., Dichoso, D., Wang, W., Golden, A. and Kemphues, K. J.** (2002). The Caenorhabditis elegans par-5 gene encodes a 14-3-3 protein required for cellular asymmetry in the early embryo. *Dev. Biol.* **241**, 47-58.

**Moser, S. C., von Elsner, S., Büssing, I., Alpi, A., Schnabel, R. and Gartner, A.** (2009). Functional dissection of Caenorhabditis elegans CLK-2/TEL2 cell cycle defects during embryogenesis and germline development. *PLoS Genet.* **5**, e1000451.

**Neal, C. L. and Yu, D.** (2010). 14-3-3ζ as a prognostic marker and therapeutic target for cancer. *Expert Opin. Ther. Targets* **14**, 1343-1354.

**O'Connell, M. J., Raleigh, J. M., Verkade, H. M. and Nurse, P.** (1997). Chk1 is a wee1 kinase in the G2 DNA damage checkpoint inhibiting cdc2 by Y15 phosphorylation. *EMBO J.* **16**, 545-554.

**O'Connell, M. J., Walworth, N. C. and Carr, A. M.** (2000). The G2-phase DNA-damage checkpoint. *Trends Cell Biol.* **10**, 296-303.

**Peng, C. Y., Graves, P. R., Thoma, R. S., Wu, Z., Shaw, A. S. and Piwnica-Worms, H.** (1997). Mitotic and G2 checkpoint control: regulation of 14-3-3 protein binding by phosphorylation of Cdc25C on serine-216. *Science* **277**, 1501-1505.

**Porter, G. W., Khuri, F. R. and Fu, H.** (2006). Dynamic 14-3-3/client protein interactions integrate survival and apoptotic pathways. *Semin. Cancer Biol.* **16**, 193-202.

**Raleigh, J. M. and O'Connell, M. J.** (2000). The G(2) DNA damage checkpoint targets both Wee1 and Cdc25. *J. Cell Sci.* **113**, 1727-1736.

**Rual, J.-F., Ceron, J., Koreth, J., Hao, T., Nicot, A.-S., Hirozane-Kishikawa, T., Vandenhaute, J., Orkin, S. H., Hill, D. E., van den Heuvel, S. et al.** (2004). Toward improving Caenorhabditis elegans phenome mapping with an ORFeome-based RNAi library. *Genome Res.* **14**, 2162-2168.

**Stergiou, L., Doukoumetzidis, K., Sendoel, A. and Hengartner, M. O.** (2007). The nucleotide excision repair pathway is required for UV-C-induced apoptosis in Caenorhabditis elegans. *Cell Death Differ.* **14**, 1129-1138.

**Stiernagle, T.** (2006). Maintenance of C. elegans. *WormBook*, 1-11.

**Su, T. T., Parry, D. H., Donahoe, B., Chien, C. T., O'Farrell, P. H. and Purdy, A.** (2001). Cell cycle roles for two 14-3-3 proteins during Drosophila development. *J. Cell Sci.* **114**, 3445-3454.

**Suzuki, A. and Ohno, S.** (2006). The PAR-aPKC system: lessons in polarity. *J. Cell Sci.* **119**, 979-987.

**Tzivion, G., Gupta, V. S., Kaplun, L. and Balan, V.** (2006). 14-3-3 proteins as potential oncogenes. *Semin. Cancer Biol.* **16**, 203-213.

**Wang, W. and Shakes, D. C.** (1997). Expression patterns and transcript processing of ftt-1 and ftt-2, two C. elegans 14-3-3 homologues. *J. Mol. Biol.* **268**, 619-630.

**Ward, J. D., Barber, L. J., Petalcorin, M. I., Yanowitz, J. and Boulton, S. J.** (2007). Replication blocking lesions present a unique substrate for homologous recombination. *EMBO J.* **26**, 3384-3396.

**Zeng, Y. and Piwnica-Worms, H.** (1999). DNA damage and replication checkpoints in fission yeast require nuclear exclusion of the Cdc25 phosphatase via 14-3-3 binding. *Mol. Cell. Biol.* **19**, 7410-7419.

Video Article

# Basic *Caenorhabditis elegans* Methods: Synchronization and Observation

Montserrat Porta-de-la-Riva[1,2], Laura Fontrodona[1], Alberto Villanueva[1,2], Julián Cerón[1,2]

[1]Department of Cancer and Human Molecular Genetics, Bellvitge Institute for Biomedical Research
[2]C. elegans Core Facility, Bellvitge Institute for Biomedical Research

Correspondence to: Julián Cerón at jceron@idibell.cat

URL: http://www.jove.com/video/4019/
DOI: 10.3791/4019

Keywords: C. elegans, synchronization, development, Nomarski, DAPI staining,

Date Published: //

Citation: Porta-de-la-Riva, M., Fontrodona, L., Villanueva, A., Cerón, J. Basic Caenorhabditis elegans Methods: Synchronization and Observation. J. Vis. Exp. (), e4019, DOI : 10.3791/4019 ().

## Abstract

Research into the molecular and developmental biology of the nematode *Caenorhabditis elegans* was begun in the early seventies by Sydney Brenner and it has since been used extensively as a model organism [1]. *C. elegans* possesses key attributes such as simplicity, transparency and short life cycle that have made it a suitable experimental system for fundamental biological studies for many years [2]. Discoveries in this nematode have broad implications because many cellular and molecular processes that control animal development are evolutionary conserved [3].

*C. elegans* life cycle goes through an embryonic stage and four larval stages before animals reach adulthood. Development can take 2 to 4 days depending on the temperature. In each of the stages several characteristic traits can be observed. The knowledge of its complete cell lineage [4,5] together with the deep annotation of its genome turn this nematode into a great model in fields as diverse as the neurobiology [6], aging [7,8], stem cell biology [9] and germ line biology [10].

An additional feature that makes *C. elegans* an attractive model to work with is the possibility of obtaining populations of worms synchronized at a specific stage through a relatively easy protocol. The ease of maintaining and propagating this nematode added to the possibility of synchronization provide a powerful tool to obtain large amounts of worms, which can be used for a wide variety of small or high-throughput experiments such as RNAi screens, microarrays, massive sequencing, immunoblot or *in situ* hybridization, among others.

Because of its transparency, *C. elegans* structures can be distinguished under the microscope using Differential Interference Contrast microscopy, also known as Nomarski microscopy. The use of a fluorescent DNA binder, DAPI (4',6-diamidino-2-phenylindole), for instance, can lead to the specific identification and localization of individual cells, as well as subcellular structures/defects associated to them.

## Video Link

The video component of this article can be found at http://www.jove.com/video/4019/

## Protocol

### 1. Protocol A: Culturing worms for bleaching [11]

Large populations of *C. elegans* can be obtained by culturing them either in liquid media or on solid media in plates. They are usually grown on solid NGM (Nematode Growth Media) and fed with *E. coli* bacteria, which is added to the plates either alive or dead (killed by UV[12], by heat[13] or by cold[14]). The most common procedure uses live OP50 *E. coli*, which is defective in the synthesis of uracil and cannot overgrow into a thick layer that would obscure the worms.

1. Mix 3 g of NaCl, 17 g of agar and 2.5 g of peptone and add 975 ml of $H_2O$. Autoclave for 50 min
2. Cool the flask to 55°C
3. Add 1 ml of 1 M $CaCl_2$, 1 ml of 5 mg/ml cholesterol in ethanol, 1 ml of 1 M $MgSO_4$ and 25 ml of 1 M $KPO_4$ buffer (all of them but cholesterol previously autoclaved)
4. Using sterile procedures dispense the NGM solution into petri plates; fill plates up to 2/3 of their volume
5. Once dry, it is advisable to leave plates at room temperature for 2-3 days before use for detection of contaminants. Prepare a streak of OP50 *E. coli* from a glycerol stock (OP50 can be obtained from the Caenorhabditis Genetics Center)
6. Pick a single colony and grow it in LB overnight at 37°C with agitation
7. Allow excess of moisture to evaporate from the plates by removing the lid in the laminar flow and add OP50 to the center of the plates with a sterile Pasteur pipette
8. Allow the OP50 *E. coli* lawn to grow overnight at room temperature or at 37°C for 8 hours
9. Add the desired amount of worms to the plates (if incubated at 37°C plates should be cooled at room-temperature before use)

TIPS:

- the pouring of the same amount of media in the plates with a pipette or a pump dispenser ensures the same volume of agar to the plates and facilitates the shifting of plate without need to refocus the stereomicroscope

- plates (both seeded and unseeded with bacteria) can be used several weeks after prepared when stored in a container at room temperature or 4 °C
- avoid plating the bacteria to the edge of the plate. If the lawn extends to the edges of the plate the worms may crawl up the sides, dry out and die
- worms live longer if the bacteria seeded on the plates are already dead [15]

## 2. Protocol B: Treatment with alkaline hypochlorite solution ("bleaching")[11]

The bleaching technique is used for synchronizing *C. elegans* cultures at the first larval stage (L1). The principle of the method lies in the fact that worms are sensitive to bleach while the egg shell protects embryos from it. After treatment with alkaline hypochlorite solution, embryos are incubated in liquid media without food, which allows hatching but prevents further development.

1. Allow worms to grow until adult stage
2. Recover gravid adults in 15 ml tubes by washing plates with M9 buffer
3. Pellet worms by centrifuging for 2 minutes at 400xg (~1500 rpm on a standard table centrifuge) at room-temperature and discard supernatant
4. Perform 1-3 washes until the buffer appears clear of bacteria
5. Add the desired bleaching solution (Table I) and agitate for some minutes (destruction of the adult tissue should be monitored under the dissecting microscope and the reaction stopped when traces of adults are still visible, which typically takes between 3 and 9 minutes depending on several issues, such as the volume of worm pellet, mentioned in the discussion) (fig. 3)
6. Stop reaction by adding M9 buffer to fill the tube
7. Quickly centrifuge (since treatment may still be active) for 1 minute at 400xg and discard supernatant
8. Wash pellet three more times by filling the tube with M9 buffer
9. Add 1ml of M9 buffer to the pellet, or place the eggs to unseeded NGM plates, and incubate at the desired temperature with gentle agitation. Proper aeration should be provided (fig.4).

TIPS:

- there are different bleaching solutions, choose the one that works better in your hands (table 1, fig. 1)
- eggs already laid on the plates can be recovered by scrapping the surface of the agar with a soft material such as a piece of an X-ray film
- too many remains of adult animals may impair synchronization as they constitute a food supply for the recently hatched larvae
- higher temperatures slightly speed up the development which is inconvenient if any worm skips synchronization because the difference in development between synchronized and unsynchronized worms will be greater at higher temperatures
- bleaching solution must be performed just prior to its use. In addition, bleach loses potency after it has been open for a while, in part due to its photosensitivity. We suggest to aliquot each new bottle into small amber bottles to prevent such loss and minimize exposure to light

## 3. Protocol C: Worm plating

1. Wait between 12 and 24 hours (time to complete embryonic development depends on the temperature) after bleaching was performed and recover worms by centrifugation (2 minutes at 400xg)
2. Discard supernatant, seed worms on the required plates and let remaining liquid dry
3. Place plates at the required temperature

TIPS:

- L1 larvae in M9 buffer can be kept at 15 °C rocking at least for one week without obvious alterations
- be careful when calculating the worms you will seed because too many may exhaust the food faster than expected and ruin your experiment. Approximately 500 L1 can reach adulthood in a 55 mm plate without running out of food.

## 4. Protocol D: *C. elegans* observation

### D.1 Nomarski observation

Differential interference contrast microscopy is an optical microscopy illumination technique used to enhance the contrast in unstained transparent samples. The word Nomarski refers to the prism used, named after his inventor. By observing animals alive we are able to examine the physiology of the animal with the only alterations derived from immobilization. In addition, as no fixative is added, fluorescent markers can be observed *in vivo*. This fact and the possibility of fusing fluorescent markers to a gene of interest make it feasible to follow processes in which the protein of study may be involved. By using the technique described in this protocol, not only live worms can be observed, but they can also be recovered and plated again.

Agar pad preparation (just before use):

1. Prepare agarose 2% in water and melt. Keep melted at 65°C
2. Place two slides with a piece of tape on them at both sides of a third, clean slide
3. Using a Pasteur pipette place a drop of agar onto the clean surface
4. Cover the agar with another clean slide placed on top of the three slides perpendicularly
5. Press gently so the agar drop is flattened to the thickness of the tape spacers
6. Once the agar solidifies, gently pull out the taped slides and separate the two remaining slides by sliding one relative to the other

Mounting live animals

7. Place one drop (10 µl) of levamisole 1mM or sodium azide 10-30 mM onto the center of the pad
8. Transfer animals into the drop using a worm pick
9. Gently place a coverslip over the animals and fix it at both sides with some nail polish or silicone

TIPS:

- keep aliquots of agarose 2% at 4°C
- melted agarose can be kept at 65 °C for at least one day
- note: Levamisole is a nicotinic receptor agonist which elicits spastic muscle paralysis[16]
- be cautious, Sodium Azide is extremely toxic!

**D.2 Ethanol fixation and DAPI staining**

The protocol described here represents a fast way of dyeing worms with DAPI, however because of the dissecation of the worm some structures may present some alteration. There are several other methods to fix worms previous to DAPI staining such as fixation with Carnoy's solution or formaldehyde that preserve better the integrity of the worm [17].

Ethanol fixation (modified from [18])

1. Place ~10 µl of M9 buffer (or water) on a microscope slide
2. Using a worm pick carefully transfer 10-25 worms to the drop
3. Using filter paper or a micro-pipette remove as much M9 buffer as possible without removing the worms or letting them dry
4. Add ~10 µl of 90% ethanol and let it dry
5. Repeat step 4 once or twice

4',6-diamidino-2-phenylindole (DAPI) staining

6. Mix DAPI with the desired mounting media to a final concentration of 2 ng/µl
7. Once the ethanol has evaporated completely, add 7 µl of the DAPI:mounting media mixture
8. Place a coverslip and fix it at both sides with some nail polish or silicone. Slides will be ready for observation approximately 5 min after the addition of DAPI

TIPS:

- the mounting media contains glycerol, so a small amount is enough to cover the whole preparation
- there exists a wide variety of commercial mounting media (Fluoromount or Prolong, for example), their quality and price depend on how long you want to store your sample
- Be careful, DAPI is a known mutagen which binds strongly to A-T rich regions in DNA

**Recipes**

**Nematode Growth Medium (NGM)**

1.7% (w/v) Agar

50 mM NaCl

0.25% (w/v) Peptone

1 mM $CaCl_2$

5 µg/ml Cholesterol

25 mM $KPO_4$

1 mM $MgSO_4$

**M9 buffer**

22mM $KH_2PO_4$

42 mM $Na_2HPO_4$

86 mM NaCl

1 mM $MgSO_4$

**Bleaching solutions tested**

| | **recipe #1** | **recipe #2** | **recipe #3** | **recipe #4** | **recipe #5** |
|---|---|---|---|---|---|
| water (ml) | 2.75 | 3.5 | 0.5 | 0.5 | 1.5 |
| sodium hydroxide (ml) | 1.25 (1M) | 0.5 (5M) | 2.5 (1M) | 2.5 (2M) | 2.5 (1M) |
| sodium hypochlorite ~ 4% (ml) | 1 | 1 | 1 | 2 | 1 |
| total (ml) | 5 | 5 | 4 | 5 | 5 |

**Table I.** Different bleaching solution recipes tested for this article. Recipes #3 and #4 are 2x, and should be added to the same volume of M9. Recipes for #1, #2 and #5 have been previously reported [2, 11, 19]. Final concentrations: #1 NaOH 0.25M, NaOCl ~0.8%, #2 NaOH 0.5M, NaOCl ~0.8%, #3 NaOH 0.625M, NaOCl ~1%, #4 NaOH 1 M, NaOCl ~1.6%, #5 NaOH 0.5M, NaOCl ~0.8%.

## 5. Representative results

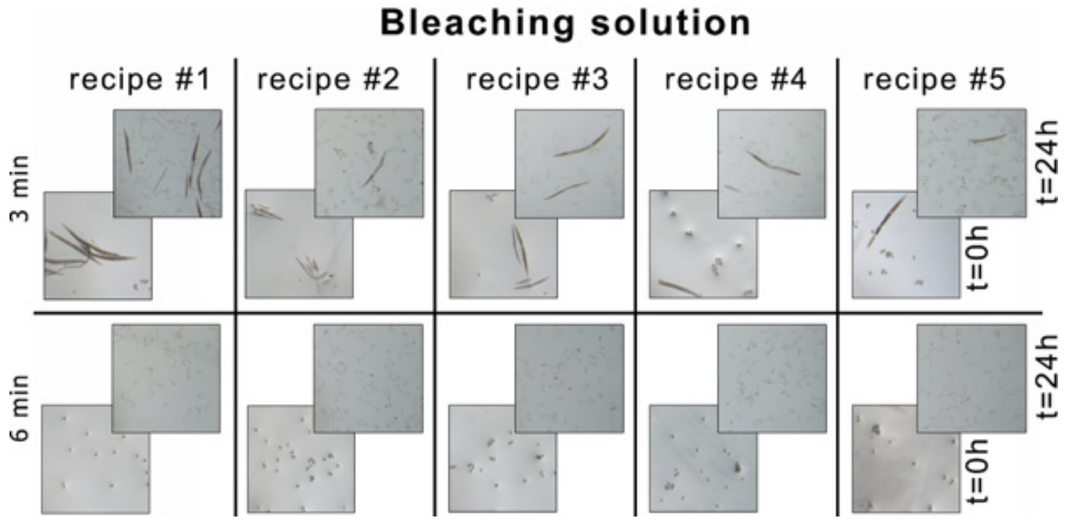
Bleaching solution
recipe #1
recipe #2
recipe #3
recipe #4
recipe #5
3 min
6 min
t=0h
t=24h
t=0h
t=24h

**Figure 1. Comparison of five different bleaching solutions at two different incubation times.** N2 worms washed twice with M9 were split into five 15 ml conical tubes containing each bleaching solution. Tubes were shaken vigorously and 1 ml transferred to a new tube with M9 to stop the reaction after the time specified. After bleaching procedure worms were incubated with 1 ml of M9 at 20 °C for 24 hours. In each case, lower picture was taken just after bleaching, upper picture 24 hours later.

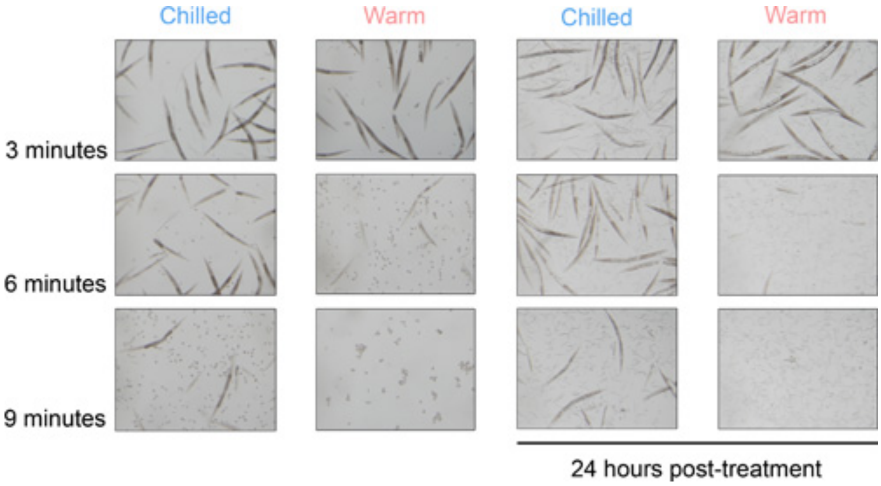
Chilled
Warm
Chilled
Warm
3 minutes
6 minutes
9 minutes
24 hours post-treatment

**Figure 2. Temperature of bleaching solution affects the effectiveness of the treatment.** Equal volumes of N2 worms were bleached with the same bleaching solution either previously chilled on ice for 20 minutes or kept at 25 °C for the same time. The two columns on the left show pictures just after bleaching. After treatment worms were incubated in 15 ml conical tubes with 1 ml of M9 at 20 °C for 24 hours. Columns on the right display pictures 24 hours later.

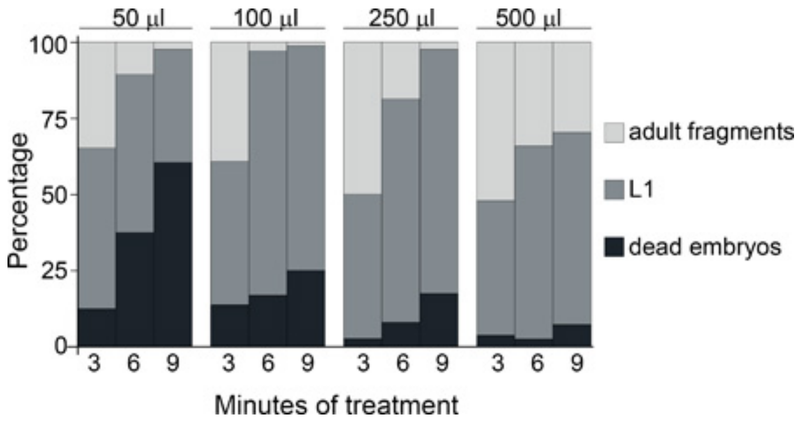

**Figure 3. The ratio worm pellet:time of alkaline hypochlorite incubation affects the effectiveness of the treatment.** 50, 100, 250 and 500 µl of worm pellet were incubated with 2 ml of bleaching solution #3 for 3, 6 and 9 minutes. Hatched L1, dead embryos and remains of adult fragments were quantified after incubation at 20 °C for 24 hours in 15 ml conical tubes with 1 ml of M9 buffer. Approximately three confluent 55 mm plates with adult worms are needed to get a 100 µl worm pellet.

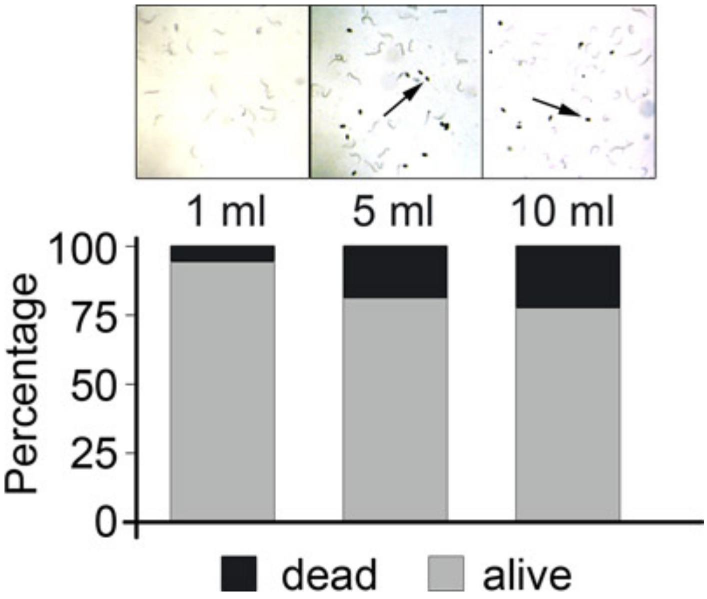

**Figure 4. Proper aeration is required for hatching and survival of *C. elegans* embryos.** A 100 µl pellet of N2 worms were bleached for 6 minutes and incubated in 15 ml conical tubes with 1, 5 or 10 ml, as specified, of M9 at 20 °C for 24 hours. The upper part of the figure displays pictures of the cultures after 24 hours, where arrows indicate eggs that did not hatch. At the bottom, there is a graph depicting the amount of larvae (light grey) and dead embryos (dark grey) 48 hours after bleaching at the stated conditions.

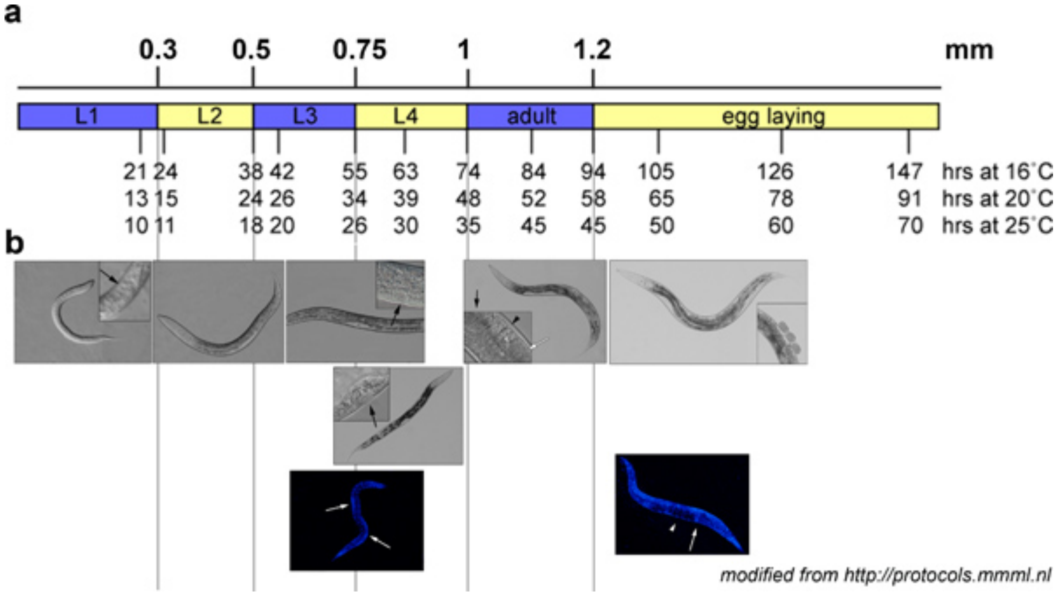
a
0.3
0.5
0.75
1
1.2
mm
L1
L2
L3
L4
adult
egg laying
21 24 38 42 55 63 74 84 94 105 126 147 hrs at 16˚C
13 15 24 26 34 39 48 52 58 65 78 91 hrs at 20˚C
10 11 18 20 26 30 35 45 45 50 60 70 hrs at 25˚C
b

modified from http://protocols.mmml.nl

**Figure 5. Life cycle of *C. elegans*. a** . Approximate length of the worms at different stages. Hours required to reach each stage depending on the temperature (modified from [20]). **b.** Nomarski (up) and DAPI (down) pictures of different worms at the indicated developmental stages. Most significant features in each phase are magnified. **L1:** arrow indicates the precursors of the somatic gonad and the germ line. **Early L4:** black arrow (Nomarski) indicates the developing vulva; white arrows (DAPI) indicate the two gonadal arms. **Mid-late L4:** arrow indicates the developing vulva at the so-called Christmas tree stage. **Young Adult:** black arrow indicates an embryo inside the uterus, arrowhead points to the spermatheca, white arrow indicates an oocyte. **Gravid adult:** arrowhead (DAPI) points out fertilized embryos. Arrow in DAPI image indicates spermatheca.

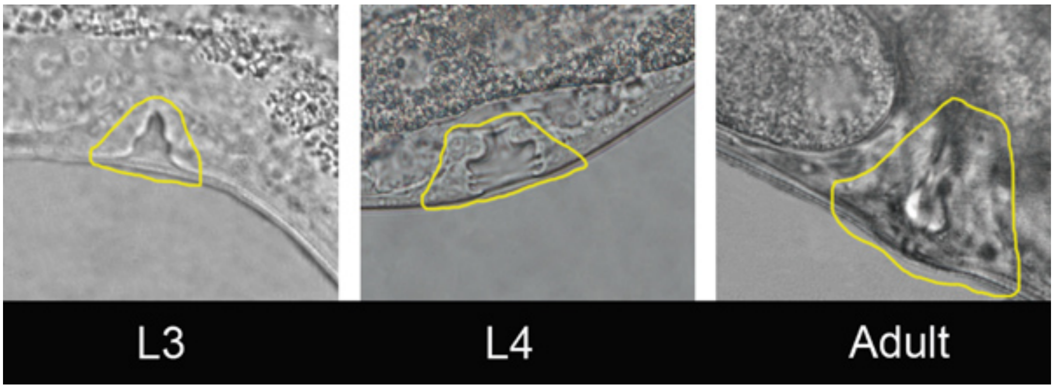

**Figure 6. Vulva morphology at L3, L4 and Adult stages.** At the L3 stage only a small lumen where the vulva is formed can be observed. At L4, this lumen expands forming the so-called "Christmas tree". In the adult the vulva is already closed. Yellow lines indicate the location of the vulva at these three stages.

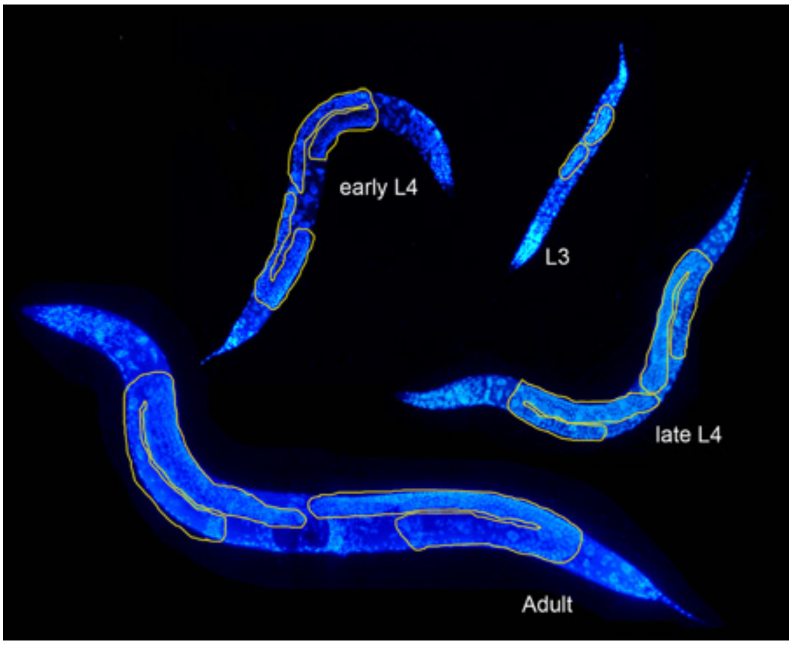

**Figure 7. DAPI staining at L3, early L4, late L4 and Adult stages.** At L3, germ line is elongated. At L4, gonad arms present U-shape morphology. At late-L4 stage sperm can be observed in the distal part of the gonad. Young Adults present oocytes. The Adult germ line presents oocytes and embryos. Yellow lines delimitate germ lines at the different stated stages.

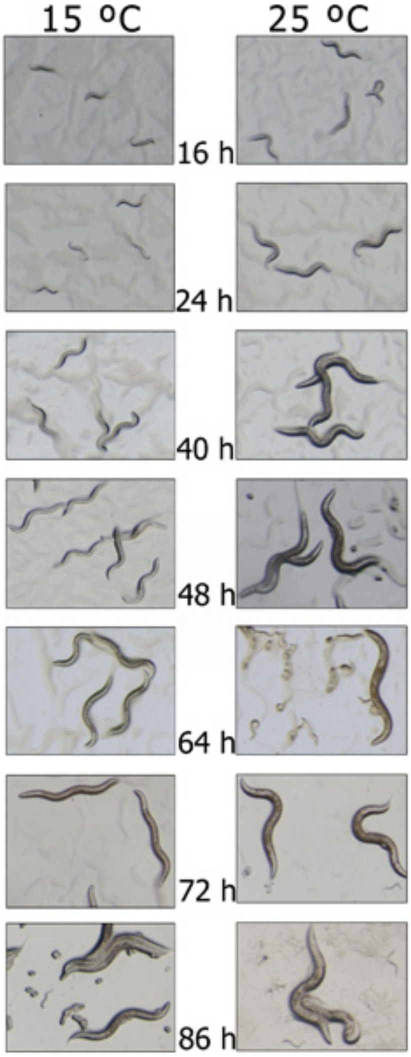

**Figure 8. *C. elegans* development at 15 and 25 °C.** N2 worms were bleached, incubated overnight in M9 and agitation at 15°C, transferred to plates and grown the indicated times at the stated temperatures.

## Discussion

### NEMATODE SYNCHRONIZATION

Several bleaching solutions have been described. We tried five different recipes (table I) and, in our hands, they did not show significant differences in the synchronization of worm populations (fig. 1). However, our experiments did show that parameters such as temperature (fig. 2), the ratio bleaching solution:volume of worms (fig. 3) and the volume of M9 with which the embryos are incubated for hatching (fig. 4) do affect the survival of the worms, being related to proper aeration of the culture. In our shaking conditions, while in a tube of 15 ml a volume of 1 ml allows survival of all worms, a volume of 5 ml is already too much to allow proper egg hatching and comparable to the maximum volume of 15 ml (not shown).

### *C. elegans* DEVELOPMENT

During its development, *C. elegans* goes through four larval stages (fig. 5) prior to the adult stage. The germ line is a good indicator of the developmental stage of *C. elegans*. The easiest feature of *C. elegans* development that can be observed under Nomarski optics is the development of the vulva, which starts to form at early L4 stage. At first, only a small lumen is observed, which later expands to the so called "Christmas tree" shape, by mid-late L4. Finally, by the end of L4 the vulva closes (fig. 6). On the other hand, DAPI staining allows the observation of the development of the gonad. From the four cells in L1 to the dividing cells and elongating gonad in L2 and L3. At L3 the distal tip cells can be observed, starting to migrate dorsally. Meiosis also starts by the end of L3. At L4 distal tip cells reach their definitive position and germ cells differentiate to sperm. By the end of L4 sperm production ends and oocyte production starts. In adult worms embryos can be observed inside the uterus (fig. 7).

### DEVELOPMENT AND TEMPERATURE

*C. elegans* develops at a different rate depending on the temperature: while it takes about 90 hours from the moment the egg is laid until the new worm starts to lay its own eggs at 15°C, 45 hours are enough when grown at 25°C (fig. 6). The study of the differential developing rate at diverse temperatures leads to relative flexibility in setting up conditions and performing experiments. Additionally, it offers the possibility not only to monitor the effects of a particular treatment or alteration (for example temperature sensitive alleles), but also to establish the best conditions in which carrying out a particular experiment.

## Disclosures

We have nothing to disclose

## Acknowledgements

Authors would like to acknowledge MICINN (PTA program supporting Montserrat Porta de la Riva), AGAUR (Phd Fellowship to Laura Fontrodona), Instituto de Salud Carlos III (Miguel Servet program supporting Julián Cerón), and Marie Curie IRG, ISCIII and IDIBELL for financing the lab.

## References

1. Brenner, S. The genetics of *Caenorhabditis elegans. Genetics*. **77**, 71-94 (1974).
2. Wood, W.B. The nematode *Caenorhabditis elegans*, Cold Spring Harbor Laboratory Press, New York, (1988).
3. Potts, M.B. & Cameron, S. Cell lineage and cell death: *Caenorhabditis elegans* and cancer research. *Nat. Rev. Cancer*. **11**, 50-8.
4. Kimble, J. & Hirsh, D. The postembryonic cell lineages of the hermaphrodite and male gonads in *Caenorhabditis elegans. Dev. Biol*. **70**, 396-417 (1979).
5. Sulston, J.E. & Horvitz, H.R. Post-embryonic cell lineages of the nematode *Caenorhabditis elegans. Dev. Biol*. **56**, 110-56 (1977).
6. Hobert, O. Neurogenesis in the nematode *Caenorhabditis elegans*. in WormBook 1-24 (2010).
7. Depuydt, G., Vanfleteren, J.R., & Braeckman, B.P. Protein metabolism and lifespan in *Caenorhabditis elegans. Adv. Exp. Med. Biol*. **694**, 81-107.
8. Jia, K. & Levine, B. Autophagy and longevity: lessons from *C. elegans. Adv. Exp. Med. Biol.* **694**, 47-60.
9. Joshi, P.M., Riddle, M.R., Djabrayan, N.J., & Rothman, J.H. *Caenorhabditis elegans* as a model for stem cell biology. *Dev. Dyn*. **239**, 1539-54.
10. Waters, K.A. & Reinke, V. Extrinsic and intrinsic control of germ cell proliferation in *Caenorhabditis elegans. Mol. Reprod. Dev*. **78**, 151-60.
11. Stiernagle, T. Maintenance of C. elegans. in Wormbook (2006).
12. Smith, E.D., et al. Age- and calorie-independent life span extension from dietary restriction by bacterial deprivation in *Caenorhabditis elegans. BMC Dev. Biol*. **8**, 49 (2008).
13. Olahova, M. et al. A redox-sensitive peroxiredoxin that is important for longevity has tissue- and stress-specific roles in stress resistance. *Proc. Natl. Acad. Sci. U.S.A*. **105**, 19839-44 (2008).
14. Voisine, C. et al. Identification of potential therapeutic drugs for huntington's disease using *Caenorhabditis elegans. PLoS One*. **2**, e504 (2007).
15. Garigan, D. et al. Genetic analysis of tissue aging in *Caenorhabditis elegans*: a role for heat-shock factor and bacterial proliferation. *Genetics*. **161**, 1101-12 (2002).
16. Aceves, J., Erlij, D., & Martinez-Maranon, R. The mechanism of the paralysing action of tetramisole on Ascaris somatic muscle. *Br. J. Pharmacol*. **38**, 602-7 (1970).
17. Shaham, S. Methods in cell biology. in Wormbook (2006).
18. Pepper AS, Killian DJ, Hubbard EJ. Genetic analysis of *Caenorhabditis elegans* glp-1 mutants suggests receptor interaction or competition. *Genetics.* Jan; **163**(1), 115-32 (2003).
19. Morley, J.F., Brignull, H.R., Weyers, J.J., & Morimoto, R.I. The threshold for polyglutamine-expansion protein aggregation and cellular toxicity is dynamic and influenced by aging in *Caenorhabditis elegans. Proc. Natl. Acad. Sci. U.S.A*. **99**, 10417-22 (2002).
20. Protocols. <http://protocols.mmml.nl/> .